Investigation of DNA repair gene expression and protein function in human oocytes and preimplantation embryos

by

Pinar Tulay

Thesis submitted for the degree of Doctor of Philosophy at University College London

June 2013

Supervisors: Dr. Sioban SenGupta
Dr. Joyce Harper

UCL Centre for PGD
Institute for Women's Health
University College London

I, Pinar Tulay, confirm that the work presented in this thesis is my own. Where information has been derived from other sources, I confirm that this has been indicated in the thesis.

ACKNOWLEDGEMENTS

It is my pleasure to thank to those who made this project possible and helped through my PhD. First of all, I would like to thank my dear supervisor, Sioban SenGupta. Sioban, you have helped and guided me throughout my PhD and PGD training. You have patiently listened to me several times to talk about how things with the experimental work are not progressing as I wanted. You always supported me. It was a great pleasure to be your PhD student. Without your help, guidance and continuous support, I wouldn't have been at this stage now. I have already missed our 3-hour PGD and PhD meetings. Thank you very much for making me a better scientist.

I would like to thank to my secondary supervisor, Dr. Joyce Harper. Joyce, you were the first person who introduced me to preimplantation genetics during my Master's degree. Your passion in this field made me grow a great interest in preimplantation genetics and embryology. I would like to thank you for your warm welcoming to this field and all your support and guidance throughout my PhD. I would also like to thank to Professor Joy Delhanty for her expert advice and guidance through my PhD and PGD training. I would like to thank to the whole PGD team; Seema Dhanjal, Thalia Mamas, Leoni Xanthopoulou and Harita Gheveria. Seema, you have helped me though my PGD training. I have learned so much from you. Thank you for being patient with me and being there to support both the experimental side of things and personal things. Thank you very much for reading this thesis- your comments were very much appreciated. I miss our tube rides to Waterloo. Thalia, you were the first person at the UCL (starting from my Master's) to help me. You were extremely patient with me. I have learned what I know about aCGH from you. It was very nice to know that I could turn to you when I felt down. Leoni, thank you very much for helping me with the FISH work-ups. I am very glad that you were there with me at CM during long hours at the weekends- it was very nice to come to the office in between running around in the lab to have lunch with you and take short breaks. Harita, thank you for your help in FISH work-ups and being a friend. I

will miss going to conferences with you. Roy, thank you for all your guidance and statistical advice for my expression study. You have been always a good friend and supported me when I felt down- thank you very much. I also would like to thank to the rest of the group members; Aisha, Razan and Amanthi- it was nice working with you all. Razan, thank you for helping me sort out lab things after I left London.

I also would like to thank to my friends outside the lab for all their support and motivation- Didem, Melek and Acelya. Didem, you are one of my best friends. You were always there to support me and calm me when I felt much stressed. It was very comforting to know that I could turn to you when I needed.

I also would like to acknowledge all the patients who made this project possible by giving consent to use their samples.

Finally and most importantly, I would like to thank to my family. My dear sister, Bahar, I am extremely lucky to have you as a sister. You always supported me. No matter what time I needed you, you were there to keep me motivated and cheer me up. My brother in law, Necati, thank you for cheering me up when I thought the end would never come. My little niece, Melisa, even though you are very little to know that you were a great courage to me, you have motivated me and kept me going by saying: “auntie finish school and come home”. My grandmother, Fikriye, and my aunt, Semral, thank you very much to you both. You have called me and checked on me constantly to keep me company while I was far away from home.

And finally, my parents, Muyesser and Erdal, there are not enough words to explain how grateful I am to you. You have supported me until this age without thinking twice. You stood by all my decisions. You encouraged me to start my PhD and complete it. You have motivated me all the time. I hope in return I had made you proud. I could not have accomplished any of this without you. Thank you for loving me and supporting me.

I am dedicating this PhD to my parents, Muyesser and Erdal.

Abstract

This study investigated microRNA and mRNA expression and protein function associated with DNA repair in human oocytes and embryos.

MicroRNAs have been shown to down-regulate and in some cases to stabilise the expression of several genes including repair genes. The first aim of this study was to analyse the differences in the expression of microRNAs and their target mRNAs involved in repair. This study showed that the levels of expression of most of the repair gene mRNAs were higher in oocytes than blastocysts and this was also the case for many of the miRNAs. The correlation analysis of the miRNA and their target expression levels in the oocyte and blastocyst samples were restricted by the limited size and number of available samples, but indicated no clear cut pattern of differences in relative expression.

Differential methylation of parental genomes that may lead to differential parental gene expression had been observed previously in mouse embryos. The second aim of this study was to investigate differential parental expression of *BRCA1* in human embryos. This study showed that differential paternal *BRCA1* expression exists in the early developing embryos. Moreover, embryos with paternally inherited *BRCA* mutations were shown to develop more slowly compared to embryos with maternally inherited *BRCA1* mutations. Both differential expression and the developmental delay may be associated with differential methylation of parental genomes.

Expression analyses are crucial to investigate the potential function of genes. However these analyses do not provide information on the functionality of biological processes. Therefore, the final part of this study aimed to develop a sensitive functional assay detecting mismatch repair efficiency in preimplantation embryos. In this study a unique assay was developed to detect mismatch repair efficiency using small amounts of nuclear/whole cell extracts and experiments demonstrated that mismatch repair is active in mouse and human blastocysts.

Table of Contents

List of Figures

List of Tables

Abbreviations

ºC	degrees Celsius
β-Me	beta-mercaptoethanol
µ	micro
5mC	5-methyl cytosine
A	adenine nucleotide base
A549	lung adenocarcinoma cell line
aCGH	array comparative genomic hybridisation
ACTB	Beta actin
ADO	allele drop out
AGO/ Ago	Argonaute *gene*/ protein
AID	activation induced cytidine deaminase
AP	Apurinic/apyrimidinic
APE1	Apurinic endonuclease 1
APTX	*aprataxin*
ATM	*ataxia-telangiectasia-mutated*
ATP	adenosine triphosphate
BER	base excision repair
BLAST	basic local alignment search tool
bp	base pair
BRCA1	*breast cancer gene 1*
BTR	Bloom's syndrome complex
C	cytosine nucleotide base
C. Elegans	*Caenorhabditis elegans*
CDK	cyclin-dependent kinase
cDNA	complementary deoxyribonucleic acid
ceRNA	competitive endogenous RNA
COS	CV-1 in Origin and carrying the SV40 genetic material cell line
Cq	cycle of quantification

CRGH	Centre for Reproductive and Genetic Health
ddNTP	dideoxynucleotide triphosphate
DGCR8	DiGeorge syndrome critical region gene 8
DNA	deoxyribonucleic acid
DNA-PKcs	DNA-dependent protein kinase, catalytic subunit
DNMT1	DNA methyltransferase 1
dNTP	deoxynucleotide triphosphate
DS	dextran sulphate
DSB	double strand break
DSBR	double strand break repair
E. coli	*Escherichia coli*
EDTA	ethylenediaminotetra acetic acid
EGA	embryonic genome activation
EGFP	enhanced green fluorescent protein
Exo I	Exonuclease I
Exp5	exportin-5
FA	Fanconi anemia
FANCM	*Fanconi anemia complementation group M*
g	gram
G	guanine nucleotide base
G1/2	gap 1/2 of cell cycle
GGR	global genomic repair
GV	germinal vesicle
HCl	hydrochloric acid
Hct	human colon carcinoma cell line
HEK	human embryonic kidney
HFEA	Human Fertilisation and Embryology Authority
HR	homologous recombination
ICM	inner cell mass
ICSI	intracytoplasmic sperm injection
IVF	*in vitro* fertilisation
Kb	kilobase

kDa	kiloDalton
KSRP	KH-type splicing regulatory protein
l	litre
LIG4	DNA ligase 4
m	milli
M	mitosis
MI	Meiosis I
MII	Meiosis II
miRNA	micro ribonucleic acid
miRNP	micro-ribonucleoprotein
MLH1/3	*MutL* homologous gene 1/3
MMR	mismatch repair
MRE	miRNA response element
mRNA	messenger ribonucleic acid
MSH2/3/6	*MutS* homologous gene 2/3/6
MSI	microsatellite instability
MutS/*H*/*L*	Mutator genes S/H/L
n	nano
NaCl	sodium chloride
NaOH	sodium hydroxide
NER	nucleotide excision repair
NHEJ	non-homologous end joining
NRES	National Research Ethics Service
nt	nucleotide
ORF	open reading frame
PARP1	*poly (ADP-ribose) polymerase 1*
PBS	phosphate buffered saline
PCNA	proliferating cell nuclear antigen
PCR	polymerase chain reaction
PGC	primordial germ cell
PGD	preimplantation genetic diagnosis
PK	proteinase K

Pol β	Polymerase β
pri-miRNA	primary miRNA
PVA	polyvinyl alcohol
RAN	Ras-related nuclear protein
Rec	Research ethics committee
RISC	RNA-induced silencing complex
RNA	ribonucleic acid
Rnase	Ribonuclease
RPA	replication protein A
rpm	revolutions per minute
RT	room temperature
S	synthesis of cell cycle
SAP	shrimp alkaline phosphatise
SCID	severe combined immunodeficiency
SD	standard deviation
SELDI-TOF-MS	Surface enhanced laser desorption/ionization time-of-flight mass spectrometry
SNP	single nucleotide polymorphism
SSC	saline sodium citrate
STR	short tandem repeat
T	thymine nucleotide base
TBE	tris-borate-EDTA
TCR	transcription-coupled repair
TE	trophectoderm
TET3	tet-eleven translocation3
TLS	translesion synthesis
tRNA	transfer RNA
U/µl	units per micro litre
UTR	3’ untranslated region
UV	Ultraviolet
V	volts
WCE	whole cell extract

WGA	whole genome amplification

1. Introduction

1.1. DNA repair in human oocytes and preimplantation embryos

Normal development of preimplantation embryos involves complex mechanisms. Determining the expression of repair genes and their possible regulatory factors provide a better understanding of the embryo's capacity to perform repair and therefore verify the survival ability of the embryo. This thesis focuses on the expression of DNA repair genes and the functional activity of these genes in preimplantation human embryos. Possible correlation between expression of miRNAs and mRNAs involved in DNA repair was investigated. It was hypothesised that an inverse correlation between miRNAs and their target mRNAs would be observed. Differential expression of parental genes may be observed in embryos due to differential demethylation of parental genomes at the early stages of preimplantation embryos in mouse. Therefore, further analysis focused on investigation of possible differential expression of four genes (*ACTB*, *SNRPN*, *H19* and *BRCA1*) in human embryos. It was hypothesised that differential gene expression was present at the early stages of cleavage stage human embryos. Although expression studies provide information on genes present in the embryos, these analyses cannot establish the functional activity of these genes. Therefore, a functional assay was developed to evaluate the mismatch repair efficiency in mouse and human oocytes and blastocysts, respectively. It was hypothesised that since the expression of mismatch repair genes are detected, mismatch repair is functionally active in human oocytes and blastocysts.

1.2. Gametogenesis and preimplantation embryo development

Mammalian preimplantation embryo development follows a series of critical events. These events start at gametogenesis and last until parturition. Male and female gametes are derived from primordial germ cells (PGCs) by the processes of spermatogenesis and oogenesis, respectively. In mice once the primordial germ cells undergo mitosis, spermatogenesis and oogenesis progress differently. In spermatogenesis, spermatogonia undergo mitosis starting at puberty until death and each primary spermatocyte produces four spermatids at the end of meiosis. In mouse oogenesis, primordial germ cells differentiate into oogenia and they enter meiosis. Unlike meiosis in spermatogenesis, primary oocyte arrests at prophase I until puberty. At puberty a single oocyte completes meiosis I forming the secondary oocyte. Oocytes arrest in metaphase II and at this stage transcription stops and translation of mRNAs reduces (Bachvarova, 1992). After fertilisation, meiosis II is completed and each oocyte produces a single viable oocyte forming the maternal pronucleus (Figure 1.1) (Dean *et al.*, 2003, Jaroudi and SenGupta, 2007).

After fertilisation oocyte and sperm nuclei fuse resulting in syngamy (Figure 1.2). The one-cell mammalian embryo contains one haploid paternal and one haploid maternal pronucleus from the sperm and oocyte, respectively (Zheng *et al.*, 2005). DNA from each pronucleus is replicated prior to mitosis. The two-cell embryo is produced in the first cleavage division consisting of two diploid nuclei with one set of maternal and one set of paternal chromosomes (Figure 1.2). In mammals, during the cleavage stage divisions programming of maternal and paternal chromosomes takes place to create the embryonic genome (embryonic genome activation, EGA) and to start the preimplantation embryo development.

Figure 1-1 Schematic diagram of spermatogenesis and oogenesis.

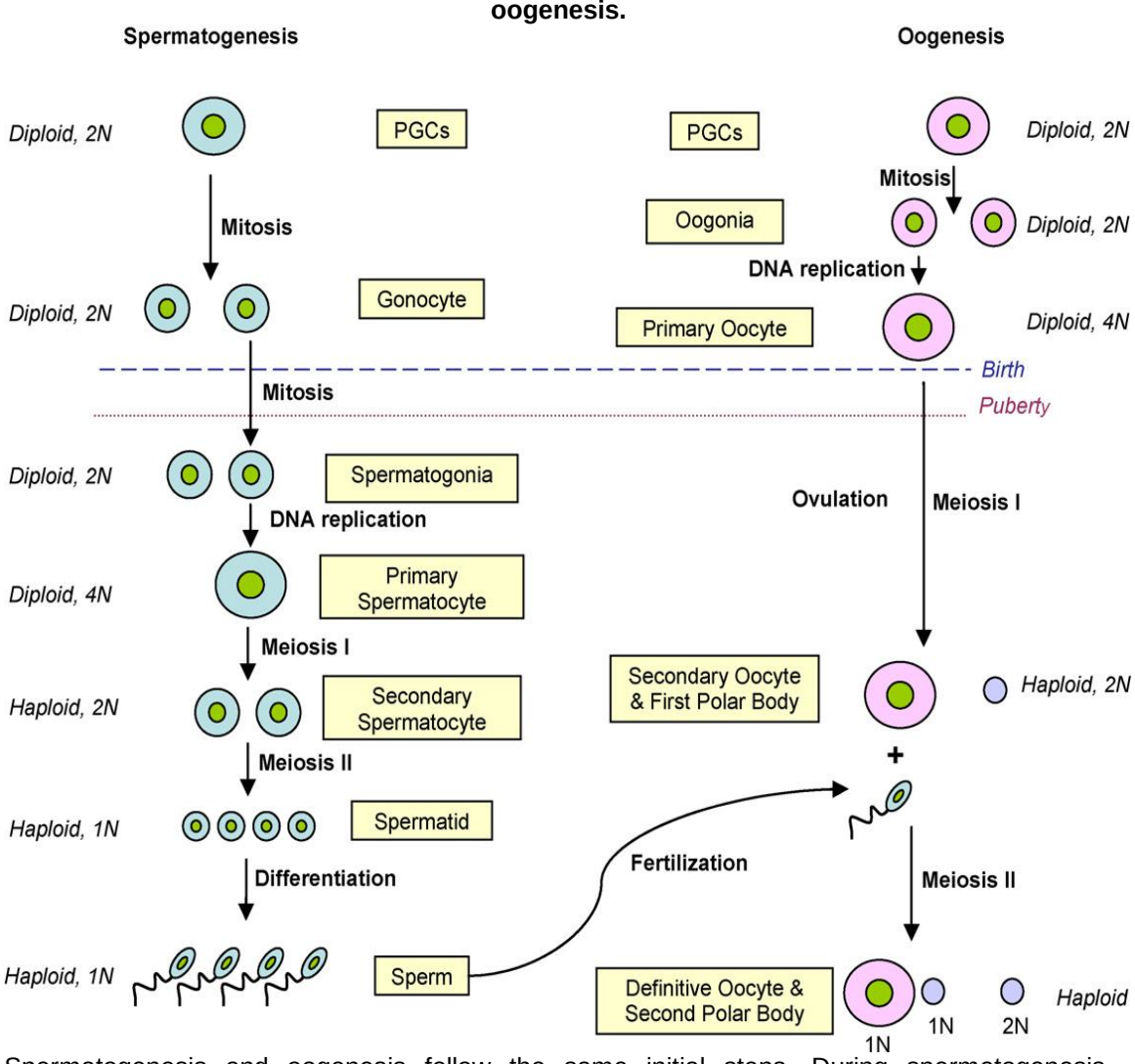

Spermatogenesis and oogenesis follow the same initial steps. During spermatogenesis, spermatogonia undergo mitosis starting at puberty until death and each primary spermatocyte produces four spermatids at the end of meiosis. During oogenesis DNA replication occurs and primary oocyte arrests at birth. Each oogonium produces a single viable oocyte following fertilisation. N represent the amount of DNA in a haploid chromosome set (Jaroudi and SenGupta, 2007). Copyright (2009), Oxford University Press.

The embryonic genome is suggested to be activated at the 2-cell and 4- to 8-cell stages in mouse and human embryos, respectively (Wang *et al.*, 2004, Flach *et al.*, 1982, Telford *et al.*, 1990). This activation is initiated by degradation of maternal nucleic acids, specific RNAs stored in human oocytes, proteins and other macromolecules (Moore, 1998, Tesarik et al., 1988, Braude et al., 1988). Upon embryonic genome activation, remarkable reprogramming of expression occurs in the preimplantation embryo. In mammals, these

reprogramming events are controlled by DNA methylation, histone acetylation, transcription, translation and microRNA (miRNA) regulation (Bell *et al.*, 2008).

DNA replication and cell proliferation is fast in rat preimplantation embryo development. However as the cell cycle is short, this increases the risk of genetic errors, in replication or segregation (Mac Auley *et al.*, 1993). These errors may damage the DNA and to preserve the genomic integrity detection of DNA damage is crucial in preimplantation embryos. Once the DNA damage is detected, cells may undergo apoptosis, or different DNA repair mechanisms; base excision repair (BER), nucleotide excision repair (NER), double strand break repair (DSBR) and mismatch repair (MMR) (Haber, 2000, Johnson and Jasin, 2000, Cromie *et al.*, 2001); may be activated (Vinson and Hales, 2002).

Figure 1-2 Schematic diagram outlining the main stages of preimplantation embryo development.

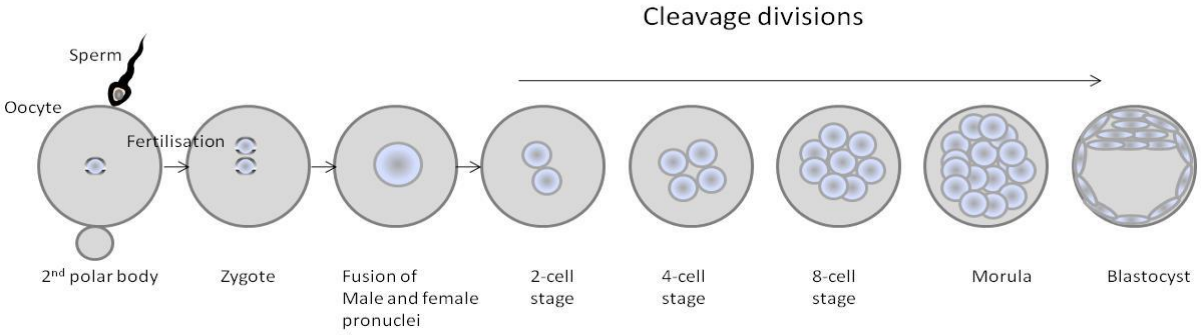

Zygote is formed following fertilisation. Fusion of male and female pronuclei takes place. DNA replication occurs and the 2-cell stage embryo forms. Cleavage divisions result in 2, 3, 4 etc. cell embryos which eventually form the morula and the blastocyst.

1.3. Origin of DNA damage and DNA repair in gametes and preimplantation embryos

In mammals DNA damage can rise from exogenous genotoxic chemical modifications, such as ultraviolet (UV) light and chemicals, and from endogenous chemical modifications, such as reactive oxygen species (Jackson and Bartek, 2009). Different types of lesions may be observed in the genome, such as mismatches, crosslinks and insertion/deletion of loops due to DNA replication and recombination errors. In mammals, the cell may naturally experience DNA depurination by non-enzymatic hydrolytic cleavage of glycosyl bonds and lose between 9000 to 10000 nucleotides per day (Nakamura *et al.*, 1998, Lindahl and Nyberg, 1972, Lindahl and Barnes, 2000).

In oocytes, damage can occur because of the long duration of meiosis. Although mouse oocytes have been shown to express genes and enzymes involved in DNA repair, many oocytes at the germinal vesicle stage have been shown to enter the meiotic divisions even in the presence of DNA damage (Marangos and Carroll, 2012). In human sperm, damage is more common than in oocytes and this can be due to mutagenic events during spermatogenesis (Drost and Lee, 1995, Huttley *et al.*, 2000). One of the main reasons for this greater damage could be the high number of pre-meiotic divisions in mammalian sperm at spermatogenesis that can be more than 1000, whereas there are only about twenty mitotic divisions in oogenesis (Hurst and Ellegren, 1998, Baarends *et al.*, 2001). Although the mouse sperm have a higher occurrence of mutation compared to oocytes, male germ cells have lower risk of spontaneous mutation rate compared to the somatic tissues (Walter *et al.*, 1998). Studies in mice show that the mutation frequency is reduced in younger males and as the mice grow older this frequency is increased in post-replicative meiotic cells (Walter *et al.*, 1998).

In mammalian preimplantation embryo development, DNA damage detection and coordination of the cell cycle is crucial. Cell cycle arrest occurs during

replication and at G1/S (first gap phase/ DNA synthesis phase) or G2/M (second gap phase/ mitosis) checkpoints to activate the correct repair pathway (Lukas *et al.*, 2004). If the repair mechanisms are unable to repair the damage, which can be due to inactive DNA repair mechanisms, apoptosis of an embryonic cell may be detrimental to the early developing embryo. Therefore correct activation of genes and proteins is critical for fully functioning DNA repair pathways.

1.3.1. Current knowledge on the techniques used for investigating the activity of repair pathways in oocytes and preimplantation embryos

1.3.1.1. Functional studies

Functional studies are the most informative analysis of DNA repair activity. Transfection of cells with plasmid/bacteriophage circular DNA substrates is widely used to assess the efficiency of repair *in vivo* or *in vitro* by exposure to nuclear or whole cell extracts. These techniques have been applied to repair deficient *Escherichia coli* (*E. coli*) (Waters and Akman, 2001, Zhang and Dianov, 2005, Fang and Modrich, 1993, Matheson and Hall, 2003, Feldmann *et al.*, 2000, Riis *et al.*, 2002, Dyrkheeva *et al.*, 2008, Kadyrov *et al.*, 2009, Littman *et al.*, 1999, McCulloch *et al.*, 2003, Wang and Hays, 2002), mouse embryonic stem cells (Dronkert *et al.*, 2000) and primate cells (Susse *et al.*, 2004). Mismatch repair in live cells has also been assessed using a plasmid enhanced green fluorescent protein (EGFP) reporter system (Folger *et al.*, 1985, Lei *et al.*, 2004).

A large amount of protein is required for these assays and they can be expensive (Tsai-Wu *et al.*, 1999, Lei *et al.*, 2004). One of the main difficulties in assessing the repair in human oocytes and embryos is the small amount of protein present in these samples, such as 122ng to 0.1µg in cattle oocytes and 162ng to 50µg in cattle preimplantation embryos (Grealy *et al.*, 1996, Thompson *et al.*, 1998). There have been a few studies assessing mismatch repair efficiency in Xenopus oocytes using two different methods; egg extracts were

used to measure the mismatch repair activity in cell free assays or mismatched DNA constructs were microinjected into the oocytes to detect the mismatch repair functionality (Maryon and Carroll, 1989, Oda *et al.*, 1996, Petranovic *et al.*, 2000, Varlet *et al.*, 1996, Labhart, 1999). All these techniques require construction of plasmids which is technically demanding and also time consuming. The basis of an aspect of this study was built on the importance of functional assay development and therefore one of the projects aimed to develop a sensitive *in vitro* functional assay for mismatch repair that could be applied to nuclear and whole cell extracts from human oocytes and embryos.

1.3.1.2. Proteomic studies

Several techniques have been used to detect proteins present in oocytes and embryos. Human, rat and mouse proteins involved in DNA repair have been localised by immunofluorescence analysis in oocytes and embryos (Barton *et al.*, 2007, Adiga *et al.*, 2007, Fernandez-Gonzalez *et al.*, 2008, Roig *et al.*, 2004, Wirthner *et al.*, 2008). The presence of proteins in pooled mouse embryos has also been studied by two-dimensional gel electrophoresis (Latham *et al.*, 1992, Shi *et al.*, 1994). Surface-enhanced laser desorption/ionisation coupled to time-of-flight mass spectrometry (SELDI-TOF-MS) in addition to western blotting and bioinformatics analyses have been used for the detection levels of particular proteins in human embryos (Katz-Jaffe *et al.*, 2009, Dominguez *et al.*, 2008, Brison *et al.*, 2007). Genome wide proteomic analysis has been performed using capillary liquid chromatography-tandem mass spectrometry (CapLC–MS/MS) in zebrafish embryos (Lin *et al.*, 2009).

1.3.1.3. Gene expression studies

Genome wide gene expression in bovine, mouse and human studies are generally performed by microarray analysis when the starting material is large (Fair *et al.*, 2007, Jaroudi *et al.*, 2009, Xie *et al.*, 2010). However the main difficulty of the genome wide expression studies in oocytes and preimplantation embryos is the small amount of material obtained from these samples. This has been overcome by pooling and/or amplifying rhesus monkey, mouse and human embryonic samples prior to the analysis (Mamo *et al.*, 2007, May *et al.*,

2009, Wells *et al.*, 2005, Zheng *et al.*, 2005, Xu *et al.*, 2011). However, both pooling and amplification has disadvantages; such that analysis of gene expression in individual samples is not possible and amplification bias may be introduced, respectively (Duftner *et al.*, 2008, Patel *et al.*, 2005). Although microarray analysis provides a large expression profile of genes from a single experiment, it is still not as sensitive as real time polymerase chain reaction (PCR) (Wong and Medrano, 2005). Gene expression in a single human oocyte and human embryo has been examined using real time PCR without any requirement of a pre-amplification step (McCallie *et al.*, 2009, Kakourou *et al.*, 2012).

Many cell cycle checkpoint and DNA repair genes have been shown to be expressed in rhesus monkey, mouse and human oocytes and blastocysts by both real time PCR and microarray analyses (Zheng *et al.*, 2005, Jaroudi *et al.*, 2009, Menezo *et al.*, 2007, Wells *et al.*, 2005, Tominaga *et al.*, 2006).

1.3.1.3.1. Expression of DNA damage sensor genes and cell cycle checkpoint genes in oocytes and preimplantation embryos

Several DNA damage sensor genes with different expression levels (*ATR*, *BLM*, *RFC*, *CHEK1*, *CHEK2 and TOPBP1*, *PCNA* proliferating cell nuclear antigen, *ATM ataxia-telangiectasia-mutated*) have been detected in rhesus monkey oocytes and blastocysts (Zheng *et al.*, 2005). *ATR*, *CHEK2* and *BUB1* were detected in human oocytes (Menezo *et al.*, 2007, Wells *et al.*, 2005). Expression of multiple genes, such as *BUB1*, *APC*, *MAD2*, *TP53* and *RB1*, were detected in human blastocysts (Wells *et al.*, 2005). Some of these genes, such as *Chek1* (Takai *et al.*, 2000) and *Wee1* were detected in mouse preimplantation embryos (Tominaga *et al.*, 2006).

Cell cycle checkpoint genes and polo-like kinases functioning at the G2/M phase (*CDKN1B*, *MDM2*, *MTBP*, *PLK1*, *PLK3* and *TP53*) were shown to be expressed only at low levels in rhesus monkey oocytes and blastocysts. Since these genes are expressed at low levels in oocytes, this may indicate reduced

repair efficiency at G2/M check point in rhesus monkey (Zheng *et al.*, 2005, Jurisicova *et al.*, 1998).

1.3.1.3.2. Expression of base excision repair genes in gametes and preimplantation embryos

Base excision repair is involved in repairing damaged bases occurring due to inflammatory responses and exposure to reactive oxygen species and exogenous agents including radiation. Base excision repair pathway repairs the damaged DNA in two pathways, short-patch and long-patch (Figure 1.3). In mammalian cell extracts, it was shown that the long-patch base excision repair constitutes 25% of all base excision repair events and the repair frequency *via* long-patch base excision repair may be higher upon DNA damage (Sung *et al.*, 2005, Dianov *et al.*, 1998).

In mammalian cells, the initial steps of the short-patch and long-patch base excision repair pathways are common; the detection of the damaged DNA, incision at the abasic site by apurinic/apyrimidinic (AP)-endonuclease or by lyase activity of glycosylase and end processing. With the short-patch base excision repair, DNA polymerase β (pol β) is involved in the insertion of the incised single nucleotide, whereas in the long-patch base excision repair two to twelve nucleotides are incised by FEN1, DNA pol β, DNA polymerase δ and/ or DNA polymerase ε. The gap is repaired and ligated by DNA ligase 3, pol β and XRCC1 in the short-patch base excision repair and DNA ligase 1, pol β, pol δ/ε, PCNA, FEN1, XRCC1 and APRATAXIN (APTX) in the long patch base excision repair, respectively (Robertson *et al.*, 2009, Caldecott, 2008, Fortini *et al.*, 2003). PARP1 was shown to interact with base excision repair genes, ligases and polymerases in mammalian cells, OGG1, XRCC1, DNA pol β, DNA ligase 3, PCNA and APTX, and therefore was suggested to have a role in the initial steps of base excision repair and single stranded DNA repair (De Vos *et al.*, 2012, Dantzer *et al.*, 2000, Noren Hooten *et al.*, 2011, Frouin *et al.*, 2003, Harris *et al.*, 2009, Heale *et al.*, 2006).

Base excision repair genes, such as *UNG*, *APEX1*, *POLB* and *OGG1*, have been shown to be expressed in rhesus monkey oocytes (Zheng *et al.*, 2005) and in human oocytes and blastocysts (Menezo *et al.*, 2007, Jaroudi *et al.*, 2009). Studies suggest that base excision repair may play an important role during mouse spermatogenesis, in that high expression levels of base excision repair genes were detected in spermatogenic germ cell nuclear extracts and in the testis (Walter *et al.*, 1996, Mackey *et al.*, 1997).

Studies have shown that correct functioning of base excision repair is crucial in embryonic development since studies in knock-out mouse have shown that in the absence of base excision repair proteins, such as Fen1, Apex, DNA ligase 1 and DNA pol β, embryos are not viable (Park and Gerson, 2005). *FEN1*, *APEX*, *MPG*, *UNG* and *HAP1* were detected in germ cells of rat and human (Olsen *et al.*, 2001).

Somatic mutations in DNA pol β have been associated with human cancers. Biallelic mutations of *Mut Y homologue* (*MYH*) gene, which is involved in base excision repair to prevent 8-oxo-dG induced mutagenesis, are shown to be associated with increased susceptibility to colorectal cancer (Jones *et al.*, 2002, Lipton *et al.*, 2003, Sampson *et al.*, 2005, Makridakis *et al.*, 2009).

Figure 1-3 Schematic diagram of base excision repair pathway.

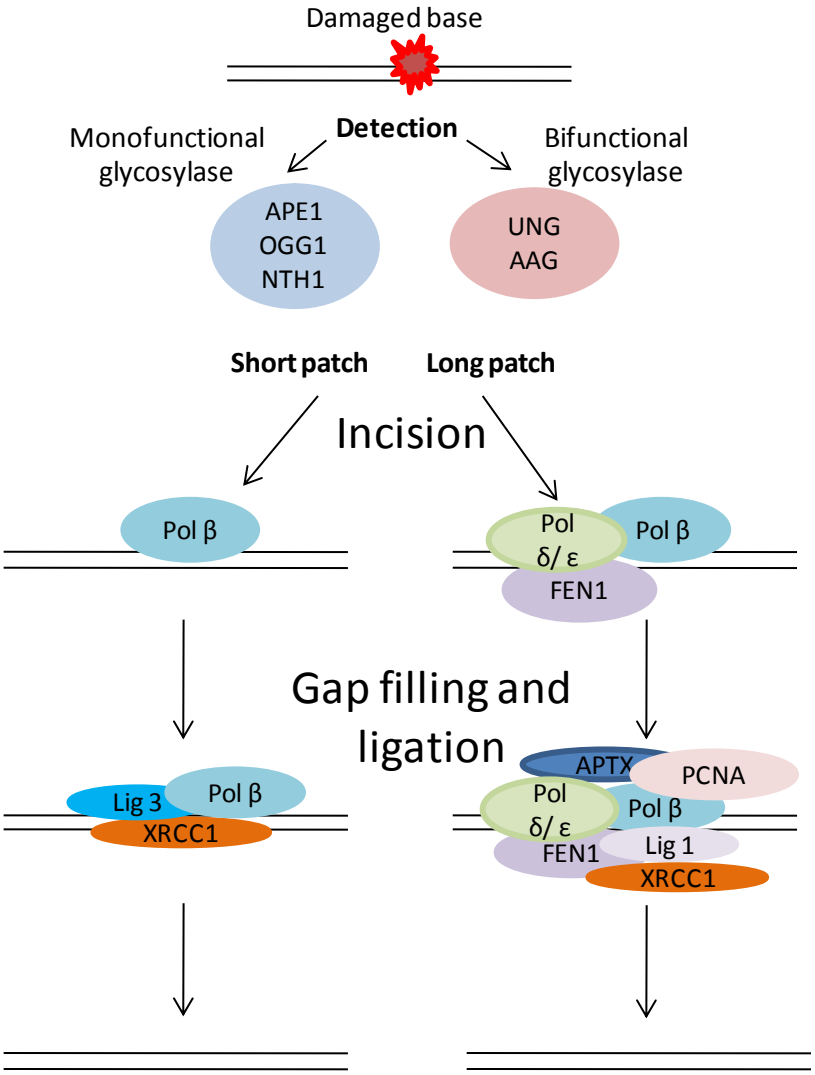

Detection, end processing, gap filling and ligation steps involve multiple genes, proteins and polymerases. These steps were summarised with the genes and proteins involved in the repair. Base excision repair involves two pathways; short patch, which repairs one nucleotide, and long patch, which repairs 2-12 nucleotides. These two pathways follow the same initial steps where a lyase removes the damaged base and end processing takes place with multiple proteins, polymerases, and ligases. The gap formed is processed with different proteins and ligation involves XRCC1 and LIG 3 in short patch and PCNA and LIG 1 in long-patch base excision repair.

1.3.1.3.3. Expression of nucleotide excision repair genes in gametes and preimplantation embryos

Nucleotide excision repair is a multi-protein repair system that is involved in repairing the majority of DNA damage caused by photoproducts from UV radiation, environmental carcinogens, endogenous free radicals and bulky

lesions in mouse and Xenopus laevis embryos (Lund *et al.*, 2009, Friedberg *et al.*, 2000). This repair pathway is suggested to be the most versatile repair system (Lund *et al.*, 2009). Nucleotide excision repair differs from base excision repair in that instead of searching for damage due to a particular base change, this mechanism checks any distortions in the double helix. Nucleotide excision repair is mainly active at the G1 (gap 1) stage of cell cycle (Branzei and Foiani, 2008).

This repair pathway is divided into two subgroups, global genomic repair (GGR) and transcription-coupled repair (TCR), and the difference between these two pathways is the proteins involved in the initial recognition step. In humans, global genomic repair, which removes DNA damage from non-transcribed DNA, involves initiation with UV-DDB (DDB1 and DDB2) and XPC-HR23B; whereas transcription-coupled repair, which repairs transcriptionally active DNA, involves initiation with RNA polymerase II (Christmann *et al.*, 2003, Shuck *et al.*, 2008, Li *et al.*, 2011). A detailed review on DNA damage response *via* transcription-coupled repair was published previously (Lagerwerf *et al.*, 2011). In humans multiple proteins, TFIIH (ERCC3, ERCC2), XPA, RPA, RNA polymerase II and XPG, bind to the damaged lesion and nucleotide excision repair multi-protein complex with ERCC1-XPF. ERCC3 (XPB) and ERCC2 (XPD) remove the lesion by DNA helicase activity (Barnes *et al.*, 1993, van Brabant *et al.*, 2000). DNA polymerases δ or ε and other replication proteins, PCNA, RPA and RFC, resynthesise the gap formed after the lesion is removed and DNA ligase 1 ligates the nick on the repaired DNA strand (Figure 1.4) (Riedl *et al.*, 2003).

The activity of nucleotide excision repair has been shown to be lower in murine sperm germ cells compared to somatic cells (Xu *et al.*, 2005) and low levels of nucleotide excision repair genes were found to be expressed in rhesus monkey oocytes (Zheng *et al.*, 2005). In contrast many nucleotide excision repair genes were shown to be highly expressed in human oocytes and blastocysts; *TFIIH CDK7*, *CCNH*, *MNAT1*, *RPA1*, *ERCC6* (*CSB*) and *LIG1*; (Jaroudi *et al.*, 2009, Menezo *et al.*, 2007). Expression of *ERCC6* (CSB), *GTF2H1*, *GTF2H2*,

GTF2H5, *RAD23B* and *MMS19L*, which are involved in transcription-coupled repair pathway, was also detected in human oocytes (Menezo *et al.*, 2007).

Deficiency in Ercc1, which functions in double strand break repair as well, leads to infertility in female and male mice and the correct functioning of this gene was shown to be crucial in gametogenesis (Hsia *et al.*, 2003). In the absence of Ercc1, the oocytes were shown to degenerate lacking primary follicles. Low levels of Ercc1 and Xpf were observed in mouse spermatogonia and high levels in spermatocytes and round spermatids (Shannon *et al.*, 1999). Mouse studies have shown that particular nucleotide excision repair gene mutations, such as *Xpd*, can be embryonic lethal or cause reduced life span (Friedberg and Meira, 2000). Homozygous germline mutations of nucleotide excision repair genes have been associated with DNA repair disorders, such as Xeroderma pigmentosum (*XP* genes mutations), Cockayne syndrome (*CSA* and *CSB* mutations) and Trichothiodystrophy (*XPB* or *XPD* mutations) (Lehmann, 2003).

Figure 1-4 Schematic diagram of nucleotide excision repair pathway; global genomic repair, transcription-coupled repair.

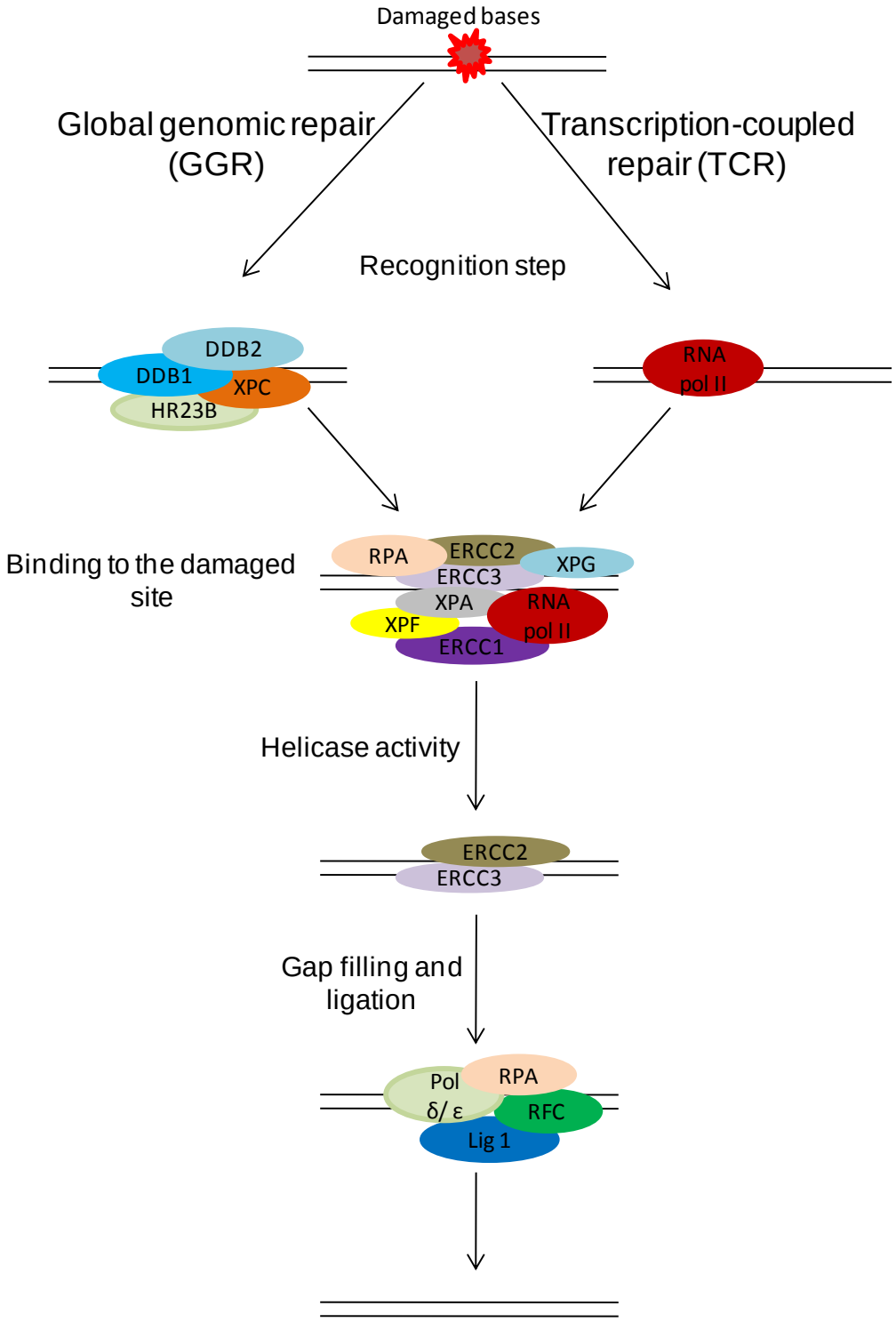

Nucleotide excision repair involves multiple proteins. The repair involves two pathways, global genomic repair and transcription coupled repair. Only the initial steps of these pathways are different. UV-DDB (DDB1 and DDB2) and XPC-HR23B are used to remove the damaged bases in global genomic repair, whereas TFIIH (ERCC3, ERCC2), XPA, RPA, RNA polymerase II and XPG are used in transcription-coupled repair. Damage recognition, DNA opening, incision, excision and resynthesis steps were summarised with the genes and proteins involved in the repair.

1.3.1.3.4. Expression of double strand break repair genes in gametes and preimplantation embryos

Double strand break repair is involved in repairing double strand breaks (DSBs) that are formed upon broken sugar backbones disturbing Watson-Crick pairings and breaking DNA double strands (Bassing and Alt, 2004). Unrepaired double strand breaks are involved in genotoxic damage and cell death *via* apoptosis (Rich *et al.*, 2000, Pfeiffer *et al.*, 2000). Furthermore, if DNA repair mechanisms do not function properly, unrepaired double strand breaks can lead to loss of chromosome segments and rearrangements, such as tumourgenic chromosome translocations in mammalian cells and yeast (Dikomey *et al.*, 1998, Pfeiffer *et al.*, 2000, Aten *et al.*, 2004).

It has been shown that in mammalian cells double strand breaks are repaired by non-homologous end joining (NHEJ) and homologous recombination (HR) repair (Figure 1.5) (Haber, 2000; Johnson and Jasin, 2000; Cromie *et al.*, 2001). A detailed review of the two double strand break repair pathways has been published (Kasparek and Humphrey, 2011). It has been suggested that these two pathways compete with each other. A possible suppression of the KU proteins by RAD18, RAD52 and PARP1 is suggested to direct the repair towards an homologous recombination repair pathway in mammalian cells (Saberi *et al.*, 2007, Van Dyck *et al.*, 2001, Bassing and Alt, 2004, Hochegger *et al.*, 2006).

Figure 1-5 Schematic diagram of double strand break repair pathway; non-homologous end joining and homologous recombination.

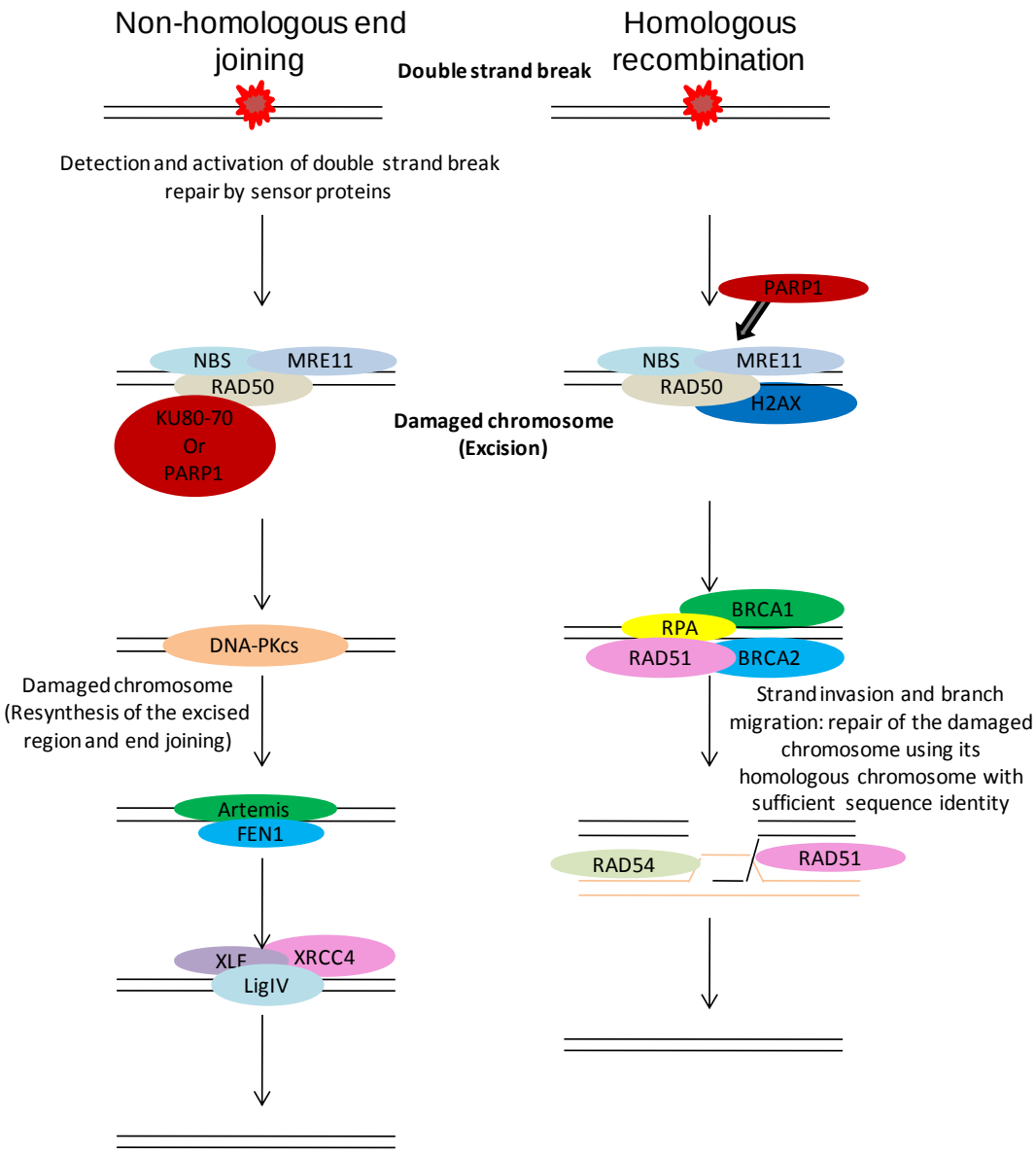

Damage recognition, DNA processing, gap filling and ligation steps were summarised with the genes and proteins involved in the repair. Non-homologous end joining repairs double strand breaks by joining the two ends of broken DNA strands, whereas homologous recombination repairs double strand breaks by using the homologous chromosome of the broken DNA strand where sufficient sequence identity can be established.

1.3.1.3.5. Homologous recombination repair

Homologous recombination repair is suggested to be an error-free repair pathway that is active in the late S (synthesis) and G2/M (gap2/mitosis) phase of the cell cycle. A detailed review of the homologous recombination pathway and its regulation was published by Krejci *et al.* (2012). Homologous

recombination repairs the damaged chromosome by using its homologous sequence as a template since it requires a template with sufficient sequence identity to the damaged molecule (Sonoda *et al.*, 2001). Histone variant H2AX is one of the first initial sensor proteins in DSB response that regulates DNA repair, replication, recombination and cell cycle (Wang *et al.*, 2012). Homologous recombination repair starts when MRN complex (MRE11-RAD50-NBS1) binds to exonuclease I (Exo I) and to the damaged part of the chromosome activating ATM. In mammalian cells single stranded DNA is released and subsequently RAD51 and the single-strand binding replication protein A (RPA) bind to RAD52 (Kagawa *et al.*, 2001, Park *et al.*, 1996). BRCA1 and BRCA2 facilitate DNA binding to RAD51 (Valerie and Povirk, 2003). When BRCA2 is associated with RAD51, the cyclin-dependent kinase (CDK) regulatory pathway through homologous recombination repair is activated (Hashimoto *et al.*, 2010, Lomonosov *et al.*, 2003, Schlacher *et al.*, 2011). Interaction of RAD51 with the DNA template initiates the repair using complementary strand by displacing one strand as a D-loop (Baumann and West, 1997). Homologous recombination repair *via* ATR (Ataxia telangiectasia and Rad3 related) can also be activated upon the interaction of FANCD2 or FANCI with BRCA1. Exonucleolytic digestion of the single stranded DNA is protected by RAD52 binding (Singleton *et al.*, 2002, Stasiak *et al.*, 2000, Christmann *et al.*, 2003). Repaired strands are elongated by polymerase and sealed by DNA ligase 1 and they are released following the resolution of the Holliday junctions (Bassing and Alt, 2004, Schlissel *et al.*, 1993).

Several homologous recombination repair genes were shown to be expressed in human oocytes and blastocysts, such as *FANCD2*, *BRCA1*, *BRCA2*, *RAD51* and *RAD52* (Jaroudi *et al.*, 2009, Menezo *et al.*, 2007, Wells *et al.*, 2005). Several other important genes, *NBS1*, *RAD50*, *ATM* and *53BP1*, involved in the activation and control of the homologous recombination repair pathway was shown to be expressed in human and bovine oocytes and blastocysts (Jaroudi *et al.*, 2009, Henrique Barreta *et al.*, 2012, Wells *et al.*, 2005). Of these genes *53BP1* and *RAD52* were shown to be up-regulated before bovine embryonic

genome activation which may indicate a role in the transition of maternal to embryonic genome (Henrique Barreta *et al.*, 2012).

Inhibition or deletion of *Parp1* in mouse was associated with increased exchange rates of spontaneous sister chromatids and homologous recombination (Oikawa *et al.*, 1980, Wang *et al.*, 1997). Deficiency of *PARP1* leads to aberrant recruiting of MRN complex with stalled or collapsed replication forks (Bryant *et al.*, 2009). Moreover, defective *ATM* activity was observed in the deficiency of *PARP1* suggesting a possible role of *PARP1* in homologous recombination repair pathway (Heitz *et al.*, 2010).

In HeLa cells inhibition of some of the *RAD51* paralogs (*RAD51B*, *RAD51C*, *RAD51D* and *XRCC3*) have been associated with cell cycle defects. The absence of *XRCC3* caused checkpoint abnormalities with incorrect centrosome defects, chromosome alignments, anaphase bridges and aneuploidy (Rodrigue *et al.*, 2012). Inhibition of *RAD51B* and *RAD51C* caused cell cycle arrest at the G2/M phase in HeLa cells (Rodrigue *et al.*, 2012).

Inaccurate functioning of homologous recombination repair, such as mutations in human homologous recombination genes, *RAD51*, *RAD51C/D*, *BRCA1/2* and *XRCC2/3*, has been correlated with high incidence of leukaemia, breast-ovarian cancers and premature aging (Valerie and Povirk, 2003, Krejci *et al.*, 2012).

1.3.1.3.6. Non-homologous end-joining repair

Non-homologous end joining repair is the main pathway in mammals which is error-prone (Haber, 2000, Johnson and Jasin, 2000, Cromie *et al.*, 2001, Jaroudi *et al.*, 2009). Non-homologous end joining is active throughout the cell cycle, especially at the G1 phase. Non-homologous end joining is suggested to have two pathways, the predominant pathway C-non-homologous end joining (classical non-homologous end joining) and *PARP1*-dependent B- non-homologous end joining (back up non-homologous end joining) (Wang *et al.*, 2012).

In cell lines non-homologous end joining involves binding of heterodimeric KU complex (KU70-KU80) to the damaged DNA to protect digestion of DNA ends by exonuclease activity (Jeggo *et al.*, 1999, Reeves *et al.*, 1989). In cell extracts, cell lines and humans DNA-dependent protein kinase (DNA-PK) holoenzyme is formed upon the interaction of the KU complex with the catalytic subunit of DNA-PK (DNA-PKcs) (Hartley *et al.*, 1995, Sipley *et al.*, 1995, Gottlieb and Jackson, 1993, Smith and Jackson, 1999). DNA-PKcs targets XRCC4 which forms a stable complex with DNA ligase 4 (LIG4) and link the duplex DNA molecules with complementary but non-ligatable ends (Leber *et al.*, 1998, Hammarsten *et al.*, 2000, Martensson and Hammarsten, 2002, Bassing and Alt, 2004). DNA-PKcs activates the protein Artemis where it forms a single strand specific endonuclease that is essential in the processing of overhanging 5' and 3' ends (Stracker *et al.*, 2009). Complementary DNA molecules are then ligated mainly by the MRN complex by removing excess DNA at the 3' end or by FEN1 *via* removing 5' end (Maser *et al.*, 1997, Nelms *et al.*, 1998).

Similar to homologous recombination repair pathway, PARP1 is suggested to take a part in non-homologous end joining repair pathway. When KU proteins and the classical non-homologous end joining pathway are inactive, PARP1-dependent back-up- non-homologous end joining is suggested to take over the repair process. When PARP1 dependent non-homologous end joining is active, PARP1 binds to the double strand breaks and directs the MRN complex to the double strand break in hamster cell lines. Resection of the double strand breaks is followed by XRCC1 and DNA ligase 3 activities to ligase the gap (Mansour *et al.*, 2010).

Several non-homologous end joining genes, such as *XRCC4*, *KU70* (*XRCC5*) and *KU80* (*XRCC6*), have been shown to be expressed in human oocytes and blastocysts (Zheng *et al.*, 2005, Ronen and Glickman, 2001, Jaroudi *et al.*, 2009). *DCLRE1C* (*ARTEMIS*) was only detected in human blastocysts and *LIG4* was neither present in human oocytes nor in human blastocysts (Jaroudi *et al.*, 2009).

Deficiency of ATM and DNA-PKcs was shown to be synthetic lethal in developing mouse embryos. DNA-PKcs were shown to play an important role in the initiation of the cell cycle checkpoint response and to sustain the chromosome stability at the S/G2 cell cycle phase (Stracker *et al.*, 2009). Defects in the non-homologous end joining repair pathway has been associated with human diseases, such as severe combined immunodeficiency (SCID) (Park and Gerson, 2005).

1.3.1.3.7. Expression of mismatch repair genes in gametes and preimplantation embryos

Mismatch repair plays an important role in mammalian gametogenesis (Baarends *et al.*, 2001). Mismatch repair protects the genetic code integrity by repairing DNA synthesis and replication errors (Aquilina *et al.*, 1999) and it is known to be effective in repairing base-base mismatches in addition to insertion and deletion of loops (Marquez *et al.*, 2003, Carethers *et al.*, 1996, Hawn *et al.*, 1995, Aquilina *et al.*, 1999). Mismatch repair is primarily active in the G2 cell cycle checkpoint (Marquez *et al.*, 2003, Carethers *et al.*, 1996, Hawn *et al.*, 1995, Baarends *et al.*, 2001).

Mismatch repair involves three main stages; recognition, excision and DNA synthesis (Modrich and Lahue, 1996, Kunkel and Erie, 2005) (Figure 1.6). The mechanism of the initial recognition step is not very well understood but there are multiple proposals. Studies in humans suggest that MSH proteins (MutSα: MSH2/MSH6 and MutSβ: MSH2/MSH3) bind to the DNA with a mismatch or a loop, respectively (Buermeyer *et al.*, 1999, Jiricny and Nystrom-Lahti, 2000, Harfe and Jinks-Robertson, 2000). In yeast and human cell extracts studies suggest that recognition takes place through the replication fork structure (Modrich, 1987, Kunkel and Erie, 2005, Umar *et al.*, 1996). The mechanism of excision is also not well established. The excision may be initiated by ATP hydrolysis-dependent translocation in *Escherichia Coli* (*E*. *Coli*) (Allen *et al.*, 1997) or by ATP binding-dependent diffusional sliding in humans (Gradia *et al.*, 1997). Exonucleases are suggested to digest one strand of DNA from 5’-3’ and some studies suggest that the digestion can also take place from 3’-5’ ends of

Okazaki fragments in mouse and humans (Genschel *et al.*, 2002, Wei *et al.*, 2003). Some studies suggest that in human cell extracts the excision from 5'-3' and 3'-5' is initiated by a pre-existing nick or a gap (Wang and Hays, 2007) and mismatch repair directs excision along shorter nick-mismatch path (Wang and Hays, 2003, Fang and Modrich, 1993).

Many mismatch repair genes have been shown to be expressed in rhesus monkey (Zheng *et al.*, 2005), mouse and human oocytes, such as *MLH1*, *MSH2*, *MSH3*, *MSH6* and *PMS2* (Richardson *et al.*, 2000, Jurisicova *et al.*, 1998, Ronen and Glickman, 2001) and also *PMS1* in human oocytes and blastocysts (Jaroudi *et al.*, 2009, Menezo *et al.*, 2007).

Aberrant expression of mismatch repair genes have been associated with abnormal spermatid phenotypes. The expression of *Msh2*, *Msh3* and *Pms2* were found to be reduced and lost in elongated murine spermatids after meiosis is completed (Richardson *et al.*, 2000). Knock-out studies of *Pms2* and *Mlh1* showed infertility in both male and female mice and the meiotic recombination is affected, respectively (Baker *et al.*, 1996, Baker *et al.*, 1995, Wang *et al.*, 1999). In additional to these genes, in mammals MSH4 was suggested to be involved in meiotic recombination (Santucci-Darmanin and Paquis-Flucklinger, 2003). Absence of *Pms2* in mouse oocytes were still able to complete meiotic chromosome pairing (Baarends *et al.*, 2001), however knocking-out *Mlh3* in mouse oocytes caused failure of meiosis I completion (Lipkin *et al.*, 2002). Similarly, when *Msh4* and *Msh5* are inactivated, meiosis in mouse is stopped both in males and females and homologous chromosome pairing is reduced greatly (Edelmann *et al.*, 1999, de Vries *et al.*, 1999, Kneitz *et al.*, 2000). A double-mutation of *Fancd2* and *Mlh1* in mouse model showed that these embryos have growth retardation leading to embryo death (van de Vrugt *et al.*, 2009). Mutations in *MLH1*, *MSH2* and *MSH6* cause hereditary non-polyposis colorectal cancers (HNPCC) in humans (de Vos *et al.*, 2005).

Mutations of mismatch repair proteins may cause microsatellite instability (MSI) that is observed in many human cancers. Microsatellite instability is short

tandem repetitive DNA sequences (Laghi *et al.*, 2008) that are highly unstable (Martorell *et al.*, 1997, White *et al.*, 1999). Different forms of microsatellites are present in the human genome with the most common being the mononucleotide repeats and less common dinucleotide, tetranucleotide and trinucleotide repeats (Eckert and Hile, 2009, Subramanian *et al.*, 2003). *Mlh3* and *Pms2* deficient mice were shown to have microsatellite instability, as a result of a defective response to DNA damage and increased risk of gastrointestinal tumours (Flores-Rozas and Kolodner, 1998, Lipkin *et al.*, 2000, Gurtu *et al.*, 2002).

Figure 1-6 Schematic diagram of mismatch repair.

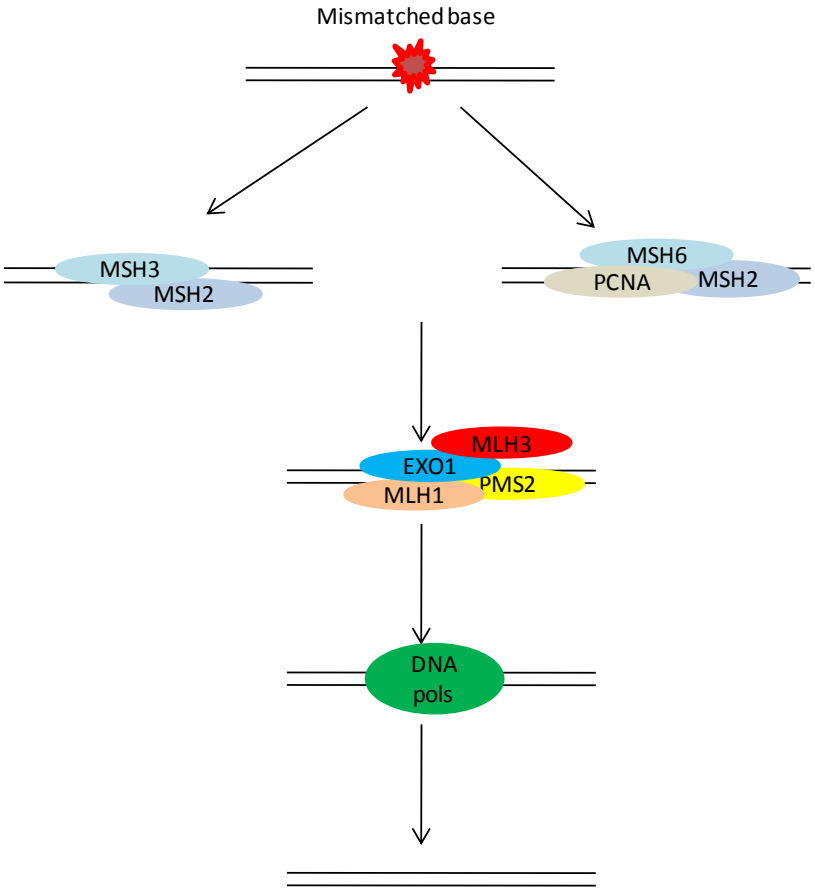

Damage is recognised by MutSα or MutSβ proteins in the presence of PCNA. DNA processing involves excision of the mismatched base or removing the inserted loop with a combination of proteins with MutLα, PMS2 and EXO1. Gap filling and ligation steps involve DNA polymerases.

1.3.1.3.8. Interstrand crosslink repair

Exposure to environmental mutagens and toxins cause DNA interstrand crosslinks (ICL) that are highly toxic lesions. These interstrand crosslinks inhibit DNA strand separation and stop transcription and replication. A detailed review of the formation and repair of interstrand crosslinks at different cell cycle stages was published by Dean and West (2011).

Interstrand crosslinks were shown to be repaired by a combination of repair pathways including nucleotide excision repair, homologous recombination repair, translesion synthesis (TLS) polymerases and Fanconi anemia pathway (Figure 1.7). Fanconi anemia is a rare autosomal recessive or X-linked genetic disease and one of the most known cellular characteristics of Fanconi anemia is the hypersensitivity to interstrand crosslinks (Sasaki, 1975).

In humans, the initial recognition of interstrand crosslink repair was shown to be through Fanconi anemia (FA) pathway for the replication-coupled repair of interstrand crosslinks or by RAD18, PCNA and DCLRE1A (Bouwman and Jonkers, 2012). Fanconi anemia complementation group M (FANCM) is one of the initial sensor proteins that recognise interstrand crosslink and recruits the Fanconi anemia core complex, Bloom's syndrome complex (BTR) and ATR-CHK1 signalling cascade. It was shown that in chicken cells Fanconi anemia pathway directs the repair towards homologous recombination by counteracting KU70 (Pace *et al.*, 2010). Nucleotide excision repair genes were suggested to be involved in the excision step, whereas during S (synthesis) phase of the cell cycle double strand breaks were suggested to be repaired by a combination of homologous recombination repair and translesion synthesis proteins (Figure 1.7). Several Fanconi anemia proteins, such as FANCJ (Suhasini *et al.*, 2013), MRE11, BRCA1 (Bogliolo and Surralles, 2010), BRCA2/FANCD1 and FANCD2, were suggested to protect stalled replication forks from degradation in homologous recombination repair pathway (Schlacher *et al.*, 2012).

Figure 1-7 Schematic diagram of interstrand crosslink repair pathway at different stages of cell cycle.

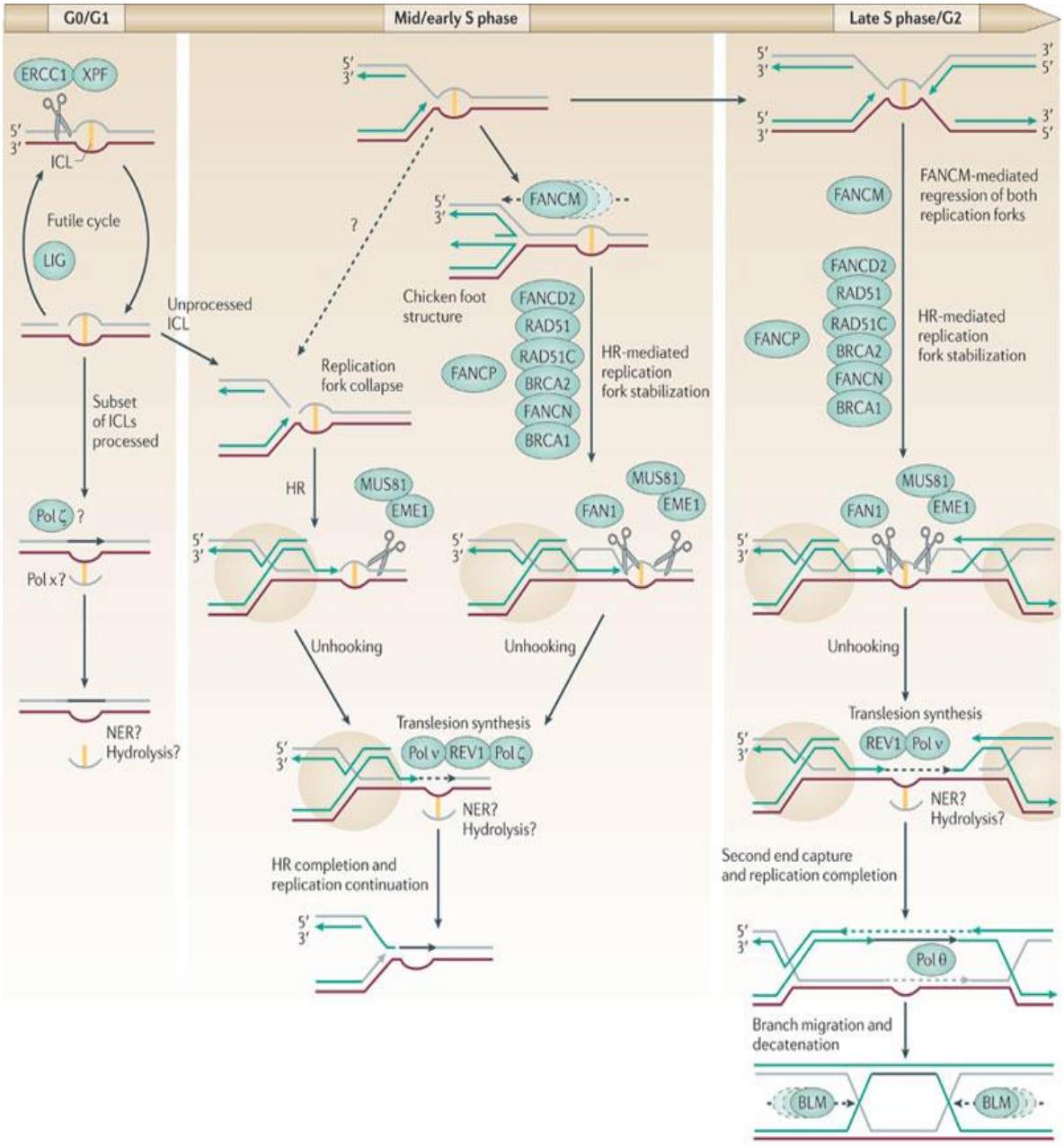

Interstrand crosslink involves repair by a combination of different repair genes and pathways including Fanconi anemia, homologous recombination and nucleotide excision repair. These different pathways are involved in interstrand crosslink repair at different stages of cell cycle (Deans and West, 2011). Copyright (2011), Rights Managed by Nature Publishing Group.

To sum up, DNA repair involves complex systems. Although correct expression of repair genes from different pathways may be crucial, if one is not expressed this may not impair the repair due to the existence of alternative pathways, such as PARP1 directed non-homologous end joining and base excision repair, and CDK or ATR directed homologous recombination repair. Therefore it is important to examine DNA repair pathways individually as well as together with the other pathways.

1.4. Control of gene expression

For a normal developing embryo, expression of both maternal and paternal genes is required. Several factors are involved in the regulation of parental genes in preimplantation embryos. In mammals, an intense epigenetic change occurs upon fertilisation to establish pluripotency (McClay and Clarke, 2003). In embryonic stem cells, the majority of the genes involved in differentiation are regulated at the chromatin level by histone modification and nucleosome rearrangements (Li *et al.*, 2012). These chromatin modifications involve many proteins in mouse including Polycomb-group (PcG) and Trithorax group (TrxG) proteins (Dean *et al.*, 2003). One of the most common forms of epigenetic modification at the DNA level is the methylation of cytosines at CpG islands (Li *et al.*, 2012). Both methylation and chromatin modifications play crucial roles in determining the transcriptional state of genes in mouse fibroblast cells, *Neurospora crassa* and *Arabidopsis thaliana* (Tamaru and Selker, 2001, Jackson *et al.*, 2002, Fuks *et al.*, 2003). More recently miRNAs, which are a category of small non coding RNAs, have been shown to play a role in gene regulation during mouse, bovine and human preimplantation embryo development (Yang *et al.*, 2009, Tang *et al.*, 2007, McCallie *et al.*, 2009, Mondou *et al.*, 2012).

1.4.1. Control of gene expression by methylation

Methylation of the CpG dinucleotides in the promoter regions of genes may cause gene silencing. The mechanism leading to changes in methylation is not well established, but it has been suggested that at the early stages of mouse preimplantation embryo development reprogramming takes place by passive and active demethylation (Dean *et al.*, 2003). Methylation is important at two stages; in preimplantation embryo development and primordial germ cell development.

1.4.1.1. Methylation status of the zygote and the preimplantation embryos

In mammals the zygote undergoes genome-wide demethylation (Oswald *et al.*, 2000, Mayer *et al.*, 2000, Beaujean *et al.*, 2004a) (Figure 1.8). Imprinted genes are the only exception to this genome-wide demethylation where the methylation is maintained (Olek and Walter, 1997, Howell *et al.*, 2001, Reik *et al.*, 2001).

Upon fertilisation, the nuclear envelope of the mouse sperm breaks and protamines are replaced with histones, the chromatin decondenses and pronucleus is formed (Wright, 1999). In the absence of DNA replication asymmetric methylation of sister chromatids within the male pronucleus of the mouse zygote takes place suggesting that active demethylation of the male pronucleus occurs (Rougier *et al.*, 1998, Dean *et al.*, 2001, Oswald *et al.*, 2000, Mayer *et al.*, 2000). Following sperm decondensation, selective demethylation of the male pronucleus of the zygote takes place in humans and with some variations in mouse (Beaujean *et al.*, 2004a, Santos and Dean, 2004, Santos *et al.*, 2002). This demethylation process is not well established however multiple mechanisms have been proposed. Active demethylation may take place where hydroxylation of 5-methylcytosine (5mC) may either be by ten-eleven translocation3 enzyme (TET3) (Gu *et al.*, 2011) or by glycosylation or alternatively some nucleotides may be removed by nucleotide excision repair locally (Dean *et al.*, 2003, Weiss *et al.*, 1996, Razin *et al.*, 1986).

The female pronucleus of the mouse zygote remains highly methylated (Beaujean *et al.*, 2004a, Santos and Dean, 2004, Santos *et al.*, 2002). In mouse, demethylation of the maternal genome starts with the first cleavage divisions (Rougier *et al.*, 1998, Monk *et al.*, 1987, Howlett and Reik, 1991). Unlike sperm, demethylation of the maternal genome is suggested to take place by passive demethylation and it is proposed to be replication dependent. In mouse, demethylation of the maternal genome could take place due to removal of DNA methyltransferase 1 (Dnmt1) from the nucleus (Howlett and Reik, 1991, Carlson *et al.*, 1992).

The loss of Dnmt1 and semi-conservative replication state establishes a status of hemi-methylated and unmethylated regions of the chromosome by the eight-cell stage of the mouse embryo (Dean *et al.*, 2003). It is possible that at this stage where methylation status of the parental genomes is different, the maternal and paternal genes are differentially expressed. Therefore one of the aims of this project was based on this theory to investigate differential gene expression in human embryos at cleavage, morula and blastocyst stages. Further analysis was based on investigation of possible effect of parental origin of a mutation on the development stage of embryos on day 5/6 post fertilisation that could be affected due to the differential gene expression and methylation status of the embryos.

By the morula stage, the mouse preimplantation embryos become undermethylated and the remethylation process starts shortly after implantation (Santos *et al.*, 2002, Mayer *et al.*, 2000, Davis *et al.*, 2000, Monk *et al.*, 1987).

Figure 1-8 Schematic diagram showing the methylation status of gametes and preimplantation embryos based on evidence on mouse studies.

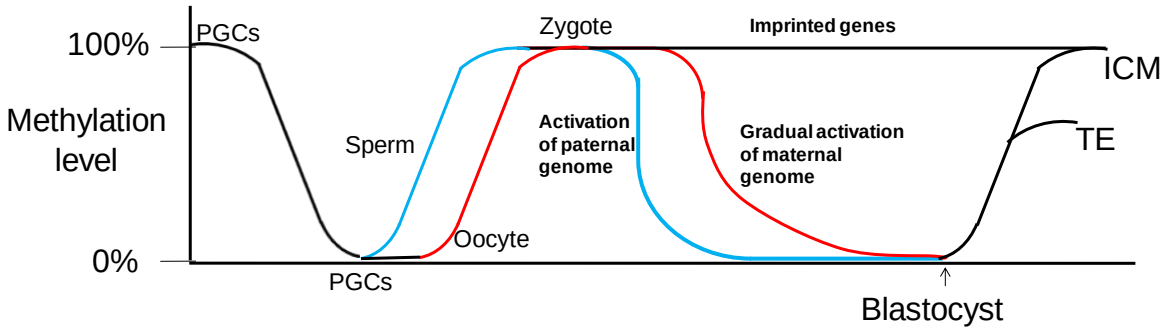

At the zygote stage, demethylation occurs differently in the paternal (blue) and maternal (red) genome in mouse, such that the paternal genome starts demethylation earlier than the maternal genome. During implantation, *de novo* methylation takes place leading to differential methylation of the ICM (inner cell mass) and TE (trophectoderm). DNA demethylation occurs as the primordial germ cells (PGCs) migrate to the gonads that are followed by immediate *de novo* methylation by the zygote stage (Dean *et al.*, 2005). Adopted from (Smallwood and Kelsey, 2012). Copyright (2012), Elsevier.

1.4.1.2. Methylation status of the gametes

Methylation status of mouse primordial germ cells reduces when they reach to the gonads (Figure 1.8). When demethylation is completed, primordial germ cells either enter mitosis in males, or arrest at meiosis in females. Studies suggest that in female mice, remethylation occurs after birth when the oocytes are in the process of development (Seki *et al.*, 2005).

1.4.2. Control of gene expression by miRNA regulation

MiRNAs, short non-coding RNAs of 17-25 nucleotides (nt) in length (Tang *et al.*, 2007), have been shown to be involved in many important biological processes that includes regulation of cell cycle, apoptosis, cell differentiation, imprinting, and development (Harfe *et al.*, 2005). MiRNAs were discovered two decades ago in *C. Elegans* (Lee *et al.*, 1993). Cloning and bioinformatics studies have enabled identification of miRNAs in many more organisms, such as flies, fish, frogs, mammals and plants (Lee and Ambros, 2001).

The majority of the miRNA sequences are conserved among mammals (Niwa and Slack, 2007). The nomenclature of miRNAs between different species is identified by the first three letters, where *homo sapiens* is defined as hsa (hsa-miR-145) and *mus musculus* as mmu (mmu-miR-145) (Griffiths-Jones *et al.*, 2006). The majority of miRNA sequences are conserved among different species, however some miRNA sequences vary only at a single nucleotide (Tesfaye *et al.*, 2009). These miRNAs are defined with suffixes, such as miR-181a and miR-181b. If the origin of miRNAs belongs to separate genomic loci, these miRNAs are assigned numerical suffices, such as miR-6-1 and miR-6-2 (Griffiths-Jones *et al.*, 2006, Ambros *et al.*, 2003).

1.4.2.1. MiRNA biogenesis

Correct miRNA biogenesis is shown to be crucial and any defects in the biogenesis may lead to abnormalities in the mouse embryos or may even cause embryo death at the early stages of preimplantation embryo development (Tang *et al.*, 2007, Bernstein *et al.*, 2003, Alvarez-Garcia and Miska, 2005).

Biogenesis of a small group of miRNAs was shown to be induced by ATM-dependent manner and these miRNAs were shown to be associated with KH-type splicing regulatory protein (KSRP), which is an AU-rich binding protein involved in Drosha and Dicer processing and in mRNA decay in cytoplasmic extracts and mouse embryonic fibroblasts (Liu and Lu, 2012, Zhang *et al.*, 2011, Trabucchi *et al.*, 2009).

Generally in eukaryotes the biogenesis of miRNAs follows two pathways; canonical and non-canonical (Figure 1.9). Only the initial steps of these two pathways are different. RNA polymerase II transcribes miRNAs into pri-miRNAs that have a stem-loop structure in the canonical pathway (Liu *et al.*, 2005). Intergenic miRNAs, which contain their own promoters and regulatory units, are transcribed into pri-miRNA by RNA polymerase II (Issabekova *et al.*, 2011). On the other hand, intronic miRNAs are co-transcribed with host genes from a common promoter (Issabekova *et al.*, 2011). Pri-miRNAs are then cleaved by a 30-160kDa protein, Drosha with one dsRNA-binding and two catalytic domains (Filipowicz *et al.*, 2008). Pasha/DiGeorge syndrome critical region gene 8 (DGCR8) is required at this step of cleavage. DGCR8 cuts both strands of the hairpin forming pre-miRNA at approximately 70nt in length (Berezikov *et al.*, 2007). Both of these genes play crucial roles in the maturation of miRNAs. Drosha cleavage is suggested to define the 5’ and 3’ ends of the mature miRNAs. If the cleavage of miRNAs by Drosha is disturbed, the seed sequence of miRNAs may be altered (Gregory *et al.*, 2004) (Table 1.1). Computational analyses and studies in human colon cancer cell lines showed that the interaction of p53 with Drosha and DGCR8 complex up-regulated miRNAs upon ionising radiation-induced DNA damage (Suzuki *et al.*, 2009, Boominathan, 2010). Defects in cell proliferation was observed in the absence of DGCR8, however these aberrations were eliminated in mouse embryonic stem cells once injected with miR-19, miR-20a, miR-20b, miR-294 and miR-295 (Wang *et al.*, 2007).

The non-canonical pathway does not involve the cleavage by Drosha and DGCR8. In mouse embryonic stem cells and Drosophila this pathway involves

cleavage either by other endoculeases or the short hairpin RNA is directly transcribed (Babiarz *et al.*, 2008, Okamura *et al.*, 2007, Ruby *et al.*, 2007).

Following this cleavage stage, both canonical and non-canonical pathways follow the same steps to complete the miRNA biogenesis. A nucleocytoplasmic transporter from karyopherin family exportin-5 (Exp5) has binding sites for pre-miRNAs in the presence of Ras-related nuclear protein (Ran) and Guanosine triphosphate (GTP). Pre-miRNAs are transported from the nucleus into the cytoplasm by Exp5 (Lund *et al.*, 2004, Yi *et al.*, 2003). Exp5 was shown to play an important role in miRNA processing in Drosophila and human. Knock-out studies of Exp5 showed a decreased level of miRNA as well as transfer RNA (tRNA) in human and Drosophila, respectively (Shibata *et al.*, 2006). Additionally, accumulation of pre-miRNA within the nucleus was observed in the absence of Exp5 (Yi *et al.*, 2003). Upon over-expression of Exp5, endogenous and exogenous miRNA levels were increased (Yi *et al.*, 2005). These findings indicate that Exp5 is important in stabilising the level of pre-miRNAs (Yi *et al.*, 2003).

Double stranded 21-22nt miRNAs are formed by Dicer processing. Dicer processing of miRNAs is suggested to be vital at the transition of G1/S cell cycle in stem cells of Drosophila since the absence of Dicer delayed this transition in the developing animals (Hatfield *et al.*, 2005).

The expression of Dicer mRNA was shown to be higher in mouse oocytes compared to other cells that may indicate a role of Dicer in female germline (Murchison *et al.*, 2007). Complete loss of Dicer in somatic cells of mouse reproductive tract caused reduced expression of miRNAs leading to infertility in female mice (Tang *et al.*, 2007). Additionally, in mouse and *C. Elegans* Dicer mutant oocytes were compromised with reduced and disorganised spindles with incorrect chromosome alignments (Tang *et al.*, 2007, Alvarez-Garcia and Miska, 2005).

Figure 1-9 Schematic diagram of miRNA biogenesis.

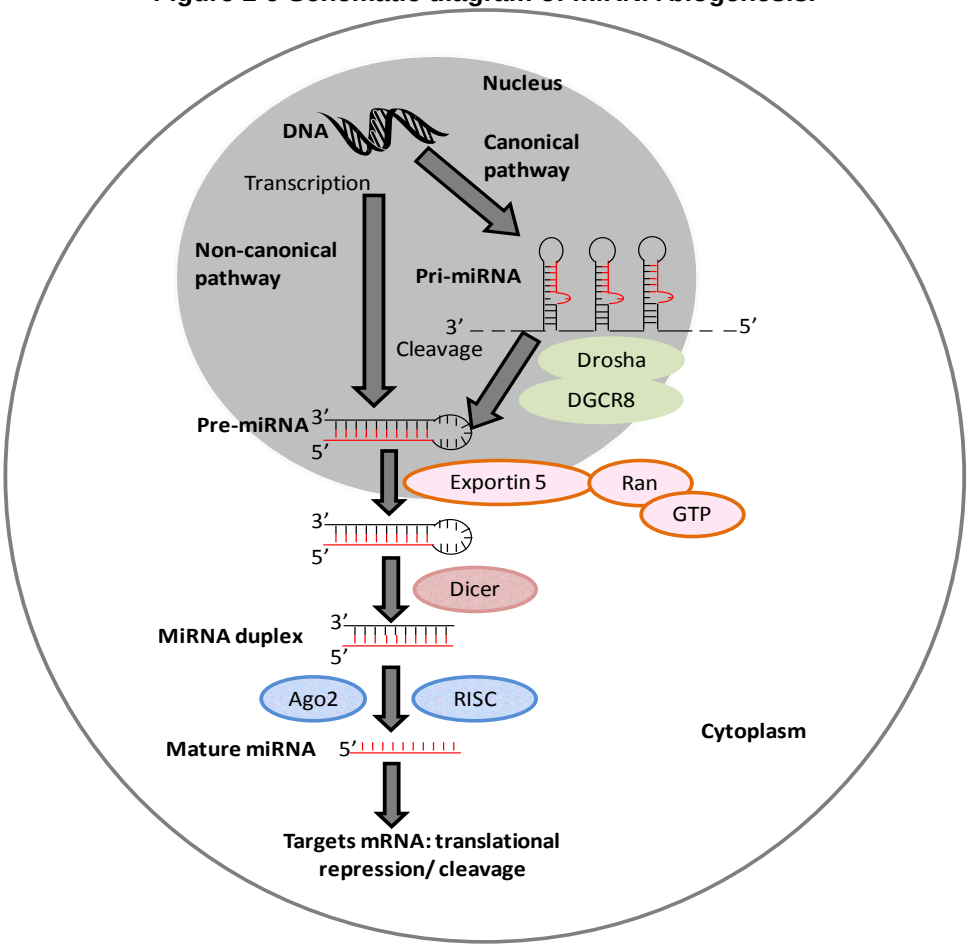

There are two main pathways for miRNA biogenesis. In the canonical pathway, pri-miRNA is formed after transcription. Pri-miRNAs are cleaved by Drosha/DGCR8 complex and they produce pre-miRNA. In the non-canonical pathway pre-miRNAs are formed without Drosha/DGCR8 complex cleavage. These pre-miRNAs are transported into the cytoplasm by Exp5 that are then processed by Dicer and Ago2/RISC complex forming mature miRNA. Adapted from (Suh and Blelloch, 2011). Copyright adapted with permission "Development"; *via* DOI:-http://dev.biologists.org/content/138/9/1653.long/.

As in the female germ cells, Dicer aberrations led to defects in male germline. Male mice suffered with reduced fertility in the absence of Dicer (homozygote Dicer) due to abnormal spermatogenesis (Maatouk *et al.*, 2008). Mutant testis with abnormal Sertoli tubes was observed in Dicer deficient mice (Maatouk *et al.*, 2008). Moreover, Dicer deficiency in male mice caused poor proliferation of spermatogonia. Abnormal spermatid and spermatocyte phenotypes with condensed nucleus were observed with lower number of germ cells (Maatouk *et al.*, 2008). Sperm motility was also affected in Dicer deficient mice (Maatouk *et*

al., 2008) and sperm loss was observed in the absence of Dicer (Hayashi *et al.*, 2008, Tang *et al.*, 2007, Yu *et al.*, 2007, Yan *et al.*, 2009).

MiRNA processing by Dicer was shown to be essential to prevent any developmental defects (Giraldez *et al.*, 2005, Zhao *et al.*, 2009). In Dicer mutant zebrafish, although the early differentiation of maternal to zygotic transition was normal, embryonic death was observed in the absence of Dicer in zebrafish (Wienholds *et al.*, 2005) and in mice around embryonic day 7.5 (Tang *et al.*, 2007, Bernstein *et al.*, 2003, Alvarez-Garcia and Miska, 2005). Abnormal somitogenesis and morphogenesis affecting gastrulation and developmental defects, such as in heart and limb, were observed in Dicer mutant vertebrates (Harfe, 2005, Alvarez-Garcia and Miska, 2005, Giraldez *et al.*, 2006, Mishima *et al.*, 2006, Zhao *et al.*, 2005). These aberrations of gastrulation and somatogenesis were partially repaired upon injection of miR-430, which functions to hasten the deadenylation and degradation of maternal mRNAs, in zebrafish and *C. Elegans* (Alvarez-Garcia and Miska, 2005, Giraldez *et al.*, 2006).

Prior to argonaute (Ago)-protein-containing complex and RISC/miRNP (RNA-induced silencing complex/mi-ribonucleoprotein) processing, one strand of the double stranded-miRNA is generally degraded; however both strands may be associated with Ago-RISC/miRNP complex. Degradation of one of these strands is random, however the strand known as the regulator and is involved in loading of the other strand onto Ago2, miR*, is the one that is usually degraded in mammals and if it remains active, it may cause silencing of wrong genes (Czech and Hannon, 2011). Ago2 deficiency was shown to reduce mature miRNA levels in knock-out mouse embryonic fibroblasts and hematopoietic cells (Diederichs and Haber, 2007, O'Carroll *et al.*, 2007, Hayashi *et al.*, 2008). Aberrant spindles and chromosome alignment were observed in Ago2 deficient mouse oocytes with reduced expression levels of miRNAs. Loss of Ago2 function was shown to be embryonic lethal around embryonic day 9.5 in mouse (Liu *et al.*, 2004).

To sum up, the importance of correct miRNA biogenesis has been shown in *C. Elegans*, embryonic stem cells, zebrafish and mouse oocytes and blastocysts. When miRNA biogenesis is disturbed due to the defects in miRNA processing genes, abnormal miRNA maturation and therefore defects in gametes and developing embryos were observed. These results indicate that miRNAs are functionally active in gametes and embryos. Although these studies are limited to mouse and zebrafish, miRNAs are suspected to be functionally active in human gametes and developing embryos.

Table 1-1 Summary table showing the functions of miRNA processing genes and defects caused by abnormal functioning of these genes.

Genes	Functions	Defects caused by abnormal functioning of genes
Drosha	• Vital for the formation of mature miRNA • MiRNA processing by cutting both strands of miRNA forming pre-miRNA product in the presence of DGCR8 (Wang *et al.*, 2007, Filipowicz *et al.*, 2008)	• 5' and 3' nucleotides of the mature miRNA are determined by Drosha cleavage and any defects in the Drosha cleavage may lead to changes in the seed sequence of miRNAs (Gregory *et al.*, 2004)
Exp5	• Stabilisation of pre-miRNAs (Yi *et al.*, 2005) • Transport of pre-miRNAs from the nucleus into the cytoplasm in the presence of Ran and GTP (Lund *et al.*, 2004, Wang *et al.*, 2007, Yi *et al.*, 2003)	• Knock-down of Exp5 was shown to reduce the miRNA expression (Shibata *et al.*, 2006)
Dicer	• Maturation of miRNA (Schwarz and Zamore, 2002, Filipowicz *et al.*, 2008, Bernstein *et al.*, 2003)	• Cell proliferation defects • Lack of Dicer in Drosophila germ line stem cells postponed the G1/S phase transition • Dicer deletion in hippocampal, mouse and zebrafish initiated problems in nervous system and led to inability of forming mature miRNAs that resulted in variations of brain morphogenesis and differentiation of neurons (Barbato *et al.*, 2008, Davis *et al.*, 2008) • Complete loss of Dicer1 caused reduced expression of miRNAs and infertile female mice (McCallie *et al.*, 2009, Tang *et al.*, 2007) • Homozygote Dicer1 germ-line mutant male mice caused decreased male fertility • Dicer deficiency led to embryo death in mouse around embryonic day 7.5 (Tang *et al.*, 2007, Bernstein *et al.*, 2003, Alvarez-Garcia and Miska, 2005) and in zebrafish (Wienholds *et al.*, 2005)
Ago2	• Component of miRISC (Schwarz and Zamore, 2002, Filipowicz *et al.*, 2008) • MiRNAs associated with Ago2/RISC complex target mRNAs	• In the absence of Ago2, oocytes were developed to the mature oocytes but reduced miRNA expression levels, abnormal spindles and chromosomes were not able to unite properly with (Liu *et al.*, 2004)

1.4.2.2. Regulation of mRNA expression by miRNAs

Mouse, bovine, metazoan and human studies showed that miRNAs are involved in transcriptional and post-transcriptional regulation of many mRNAs and a single miRNA may target multiple mRNAs (Moskwa *et al.*, 2010, Bagga *et al.*, 2005, Hayashi *et al.*, 2008, Tesfaye *et al.*, 2009, Bartel, 2004, Bartel and Chen, 2004, Miranda *et al.*, 2006). MiRNAs regulate mRNAs that encode up to 30% human protein-coding genes (Malumbres, 2012). Mouse embryonic stem cell studies showed that miRNAs recognises their target mRNAs by base complementation of the seed sequence that is the 7-mer sequence present at positions of two to eight nucleotides within the open reading frame and 3' untranslated region of the mRNA sequence (Babiarz and Blelloch, 2009).

The mRNA regulation by miRNAs involves complex mechanisms. It is well established that in *C. Elegans*, metazoans, mouse and humans miRNAs target mRNAs for translational inhibition, cleavage, degradation or destabilisation (Bagga *et al.*, 2005, Hayashi *et al.*, 2008, Tesfaye *et al.*, 2009, Bartel, 2004, Bartel and Chen, 2004, Miranda *et al.*, 2006). However, more recently it has been suggested that these non-coding RNAs also play a role in stabilising their targets (Salmena *et al.*, 2011, Seitz, 2009, Arvey *et al.*, 2010, Lee *et al.*, 2009, Poliseno *et al.*, 2010, Franco-Zorrilla *et al.*, 2007, Cazalla *et al.*, 2010). This direct relationship between miRNA and mRNAs is not well understood, however several possible mechanisms have been proposed. The first proposal suggests mRNA stabilisation through binding of miRNA to AU rich elements of proteins and activation of cell-dependent regulation of mRNAs (Wilusz *et al.*, 2001, Carroll *et al.*, 2012). Another study also proposed a cell cycle-dependent miRNA regulation by repression and activation of mRNAs (Vasudevan *et al.*, 2007). Pseudogenes were suggested to be endogenous decoys for miRNAs by competing with the legitimate genes and reducing the repression activity of miRNAs on their target genes (Cazalla *et al.*, 2010, Lee *et al.*, 2009, Poliseno *et al.*, 2010, Franco-Zorrilla *et al.*, 2007). Circular RNAs, which have covalently linked ends and are generated by seemingly RNA splicing errors, have been recently suggested to act as miRNA decoys in HEK (human embryonic kidney)

and HeLa cells (Wilusz and Sharp, 2013, Hansen *et al.*, 2011, Memczak *et al.*, 2013). These circular RNAs were shown to bind to miR-7 and reduce the binding efficiency of miR-7 to other RNAs. Similarly, mouse *Sry* was shown to generate a circular RNA that has multiple miRNA binding sites for miR-138 (Hansen *et al.*, 2013). From a similar point of view, when a single miRNA has multiple mRNA targets the down-regulatory role of the miRNA is reduced in HeLa cells (Arvey *et al.*, 2010). Based on these observations, competitive endogenous RNA (ceRNA) hypothesis was proposed where coding and non-coding RNAs can regulate mRNA/miRNA association by competing for the miRNA binding sites in humans (miRNA response elements, MRE) (Salmena *et al.*, 2011). Interactions among different miRNAs were suggested to have a positive regulatory role for their targets since one miRNA may down-regulate the other leading to an increased expression of its target gene in HeLa, HEK-293 and SH-SY5Y cell lines (Carroll *et al.*, 2012).

1.4.2.3. MiRNA expression in gametes and preimplantation embryos

Expression of miRNAs has been observed in mouse, bovine and human gametes (Appendix 7.1.1). MiRNAs are suggested to regulate more than one third of the maternal genes in mouse oocytes (Tang *et al.*, 2007). The study of immature and mature human oocytes have revealed different expression patterns of miRNAs; such as for hsa-miR-602, hsa-miR-193a-5p, hsa-miR-297, hsa-miR-625, hsa-miR-888, hsa-miR-212, hsa-miR-662, hsa-miR-299-5p, hsa-miR-339-5p, hsa-miR-20a, hsa-miR-486-5p, hsa-miR-141, hsa-miR-768-5p, hsa-miR-376a and hsa-miR-15a; that suggests a developmental stage dependent expression of miRNAs (Xu *et al.*, 2011).

Expression of miRNAs has been observed in sperm and about 20% of these miRNAs are present within the nuclear or perinuclear part of the sperm. This may imply that at fertilisation, these sperm-borne miRNAs are transferred to the zygote (Liu *et al.*, 2005). Initially it was proposed that these miRNAs were involved in the degradation of maternal transcripts. However, it was shown that these miRNAs do not play a significant role in mouse (Amanai *et al.*, 2006).

Many miRNAs have also been shown to be expressed in mouse, bovine and human preimplantation embryos (Appendix 7.1.1) (Rosenbluth *et al.*, 2012, McCallie *et al.*, 2009, Tang *et al.*, 2007, Tesfaye *et al.*, 2009, Yang *et al.*, 2008, Xu *et al.*, 2011). Similar expression profiles of miRNAs in mature mouse oocytes and in the early developing embryos were observed that may be due to the maternally inherited miRNAs in the early embryo (Tang *et al.*, 2007). Expression levels of these miRNAs vary during cleavage stage divisions, such that in murine embryos when the maternally inherited miRNAs are being degraded, a 60% decrease in the miRNA expression was observed. However, the overall expression of miRNAs was shown to be increased towards the blastocyst stage (Tang *et al.*, 2007, Yang *et al.*, 2008).

1.4.2.4. Regulation of DNA repair genes by microRNAs expressed in gametes and preimplantation embryos

Many miRNAs were shown to be induced after DNA damage and regulate DNA repair genes in *C. Elegans,* human cell lines and tissues (Aqeilan *et al.*, 2009, Krichevsky and Gabriely, 2009, Navarro *et al.*, 2008). This formed the basis of one of the aims in this project: "Potential correlation analysis between miRNA and their target repair transcripts in human oocytes and preimplantation embryos". Since several miRNAs were shown to be expressed in mouse, bovine and human oocytes and embryos and that some of these miRNAs were shown or suspected to regulate repair genes in cell lines or tissues, it is possible that these miRNAs also regulate repair genes in human gametes and preimplantation embryos.

The expression levels of miRNAs were shown to vary depending on the level of damage, such that some were shown to be down-regulated upon DNA damage; let-7 in *C. Elegans* and human glioma cells (Weidhaas *et al.*, 2007, Chaudhry *et al.*, 2010); and some were up-regulated; miR-15a, miR-16, miR-143, miR-155, miR-21 in human glioma cells (Chaudhry *et al.*, 2010) and miR-99 in human prostate cancer cell lines (Mueller *et al.*, 2012). This section focuses only on the miRNAs that have been shown to be expressed in mouse or bovine or human gametes and preimplantation embryos and that were shown or predicted to

have a role in regulating or being regulated by DNA damage, DNA repair or cell cycle checkpoint genes.

Cell cycle checkpoint genes and miRNAs expressed in preimplantation embryos

Cell cycle checkpoints play a crucial role in response to DNA damage. Studies in *C. Elegans* and human cell lines and tissues showed that many miRNAs are involved in regulating the cell cycle checkpoint genes as well as being regulated by these genes (Noto and Peek, 2012, Aqeilan *et al.*, 2009, Krichevsky and Gabriely, 2009, Jurado *et al.*, 2012, Massirer *et al.*, 2012).

Computational studies showed that DNA damage-induced transcription factors p53/p63/p73 regulate and are regulated by many miRNAs, such as miR-15/16a, miR-145, miR-26, miR-29, miR-146a, let-7 and miR-34 families, that are expressed during preimplantation embryo development (Tang et al., 2007, Yang et al., 2008, Boominathan, 2010). In human colon cancer cell lines miR-16-1, miR-143 and miR-145 were shown to be up-regulated by p53 and p68/p72 dependent pathway upon DNA damage (Suzuki *et al.*, 2009). The expression of p53 and its related family member p63 was shown to be inhibited by several miRNAs in hepatocellular carcinoma tissues, neuroblastoma and embryonic cells (Jiang *et al.*, 2008, Eggert and Schulte, 2010). These miRNAs, such as miR-125b, miRNA-380-5p, miR-34 and miR-200 families, are also shown to be expressed in preimplantation embryos (Tang *et al.*, 2007, Yang *et al.*, 2008). Additional miRNAs that are expressed in preimplantation embryos are also shown to be involved in the regulation of p53 transcription, such as miR-192, miR-194, miR-215, miR-17-92 clusters in SJSA (osteosarcoma cell line), HCT (human colon carcinoma) $DICER^{ex5}$ cell lines, multiple myeloma cells and tumour and normal tissues (Georges *et al.*, 2008, Braun *et al.*, 2008, Yan *et al.*, 2008, Pichiorri *et al.*, 2010) and miR-34 family in tumour-derived cell line A549 (He *et al.*, 2007). These miRNAs were also shown to regulate G1/S and G2/M checkpoint genes and ectopic expression of these miRNAs caused cell cycle arrest in adenocarcinoma, squamous cell carcinomas, normal epithelium and

dysplasia specimens (Jiang *et al.*, 2008, Feber *et al.*, 2008, Adare *et al.*, 2010, Cannell *et al.*, 2010, Braun *et al.*, 2008, Georges *et al.*, 2008). In addition to these miRNAs, miR-21 (Pauli *et al.*, 2011, Wang *et al.*, 2009), miR-17-92 in colon cancer cells (Gunaratne, 2009), miR-371 in mouse embryonic stem cells, miR-302 in human embryonic stem cells (Kim, 2008) and miR-34c in mouse embryonic fibroblasts and HeLa cells (Cannell *et al.*, 2010) were shown to be involved in G1/S cell cycle regulation upon DNA damage. Inhibition of miR-34c prevents the cell cycle arrest at the S phase caused by DNA damage (Cannell *et al.*, 2010). The efficiency of the S cell cycle checkpoint was shown to be influenced by the ectopic expression of miR-421, where *ATM* kinase is down-regulated and the sensitivity for the ionising radiation was shown to be increased. Once the interaction of miR-421 and *ATM* 3'UTR was hindered, this affect was reversed in neuroblastoma cell lines (Hu *et al.*, 2010). *ATM* and DNA-PKcs protein levels were also shown to be reduced by up-regulation of miR-421 and miR-101 in human osteosarcoma and colorectal cancer cell lines U2OS, MG63, RKO and HT-29 (Mishra *et al.*, 2009). Wip1 phosphates, a key inhibitor of *ATM*-p53 signalling pathway, were shown to be suppressed by miR-16. This miRNA was also shown to target Cyclin D1 and *BCL2* in cancer cells of prostate tumours in mouse (Bonci *et al.*, 2008). G2 checkpoint arrest due to DNA damage-induced death was shown to be prevented by over-expression of miR-143 in lung cancer cells 293T and A549 (Lin *et al.*, 2011).

Figure 1.10 shows the relationship of genes and proteins involved in the cell cycle and miRNAs expressed in mouse, bovine and/or human preimplantation embryos.

Figure 1-10 Main regulators of the cell cycle and their association with miRNAs.

a) MiRNAs involved in the regulation of cell cycle checkpoint genes at G0, S, G2 and M phases.

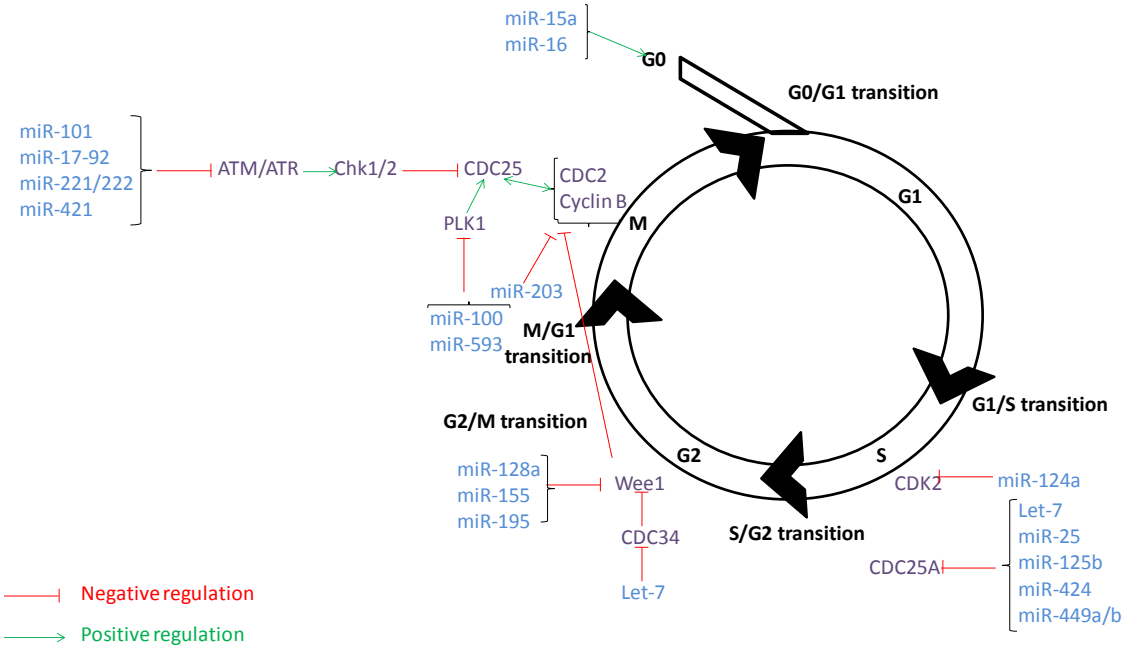

b) MiRNAs involved in the regulation of cell cycle checkpoint genes at the G1/S transition.

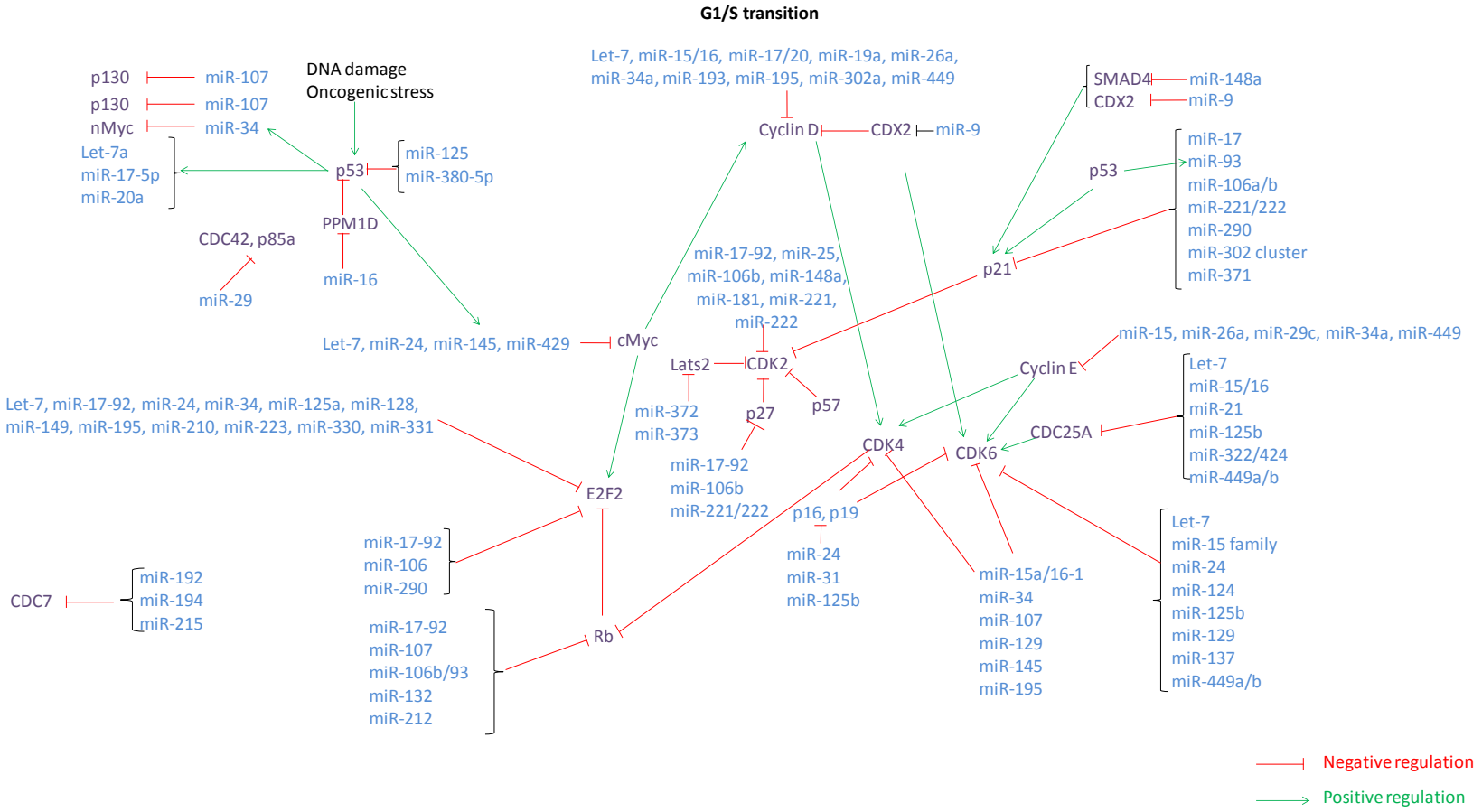

c) MiRNAs involved in the regulation of cell cycle checkpoint genes at G0/G1 and S/G2 transitions.

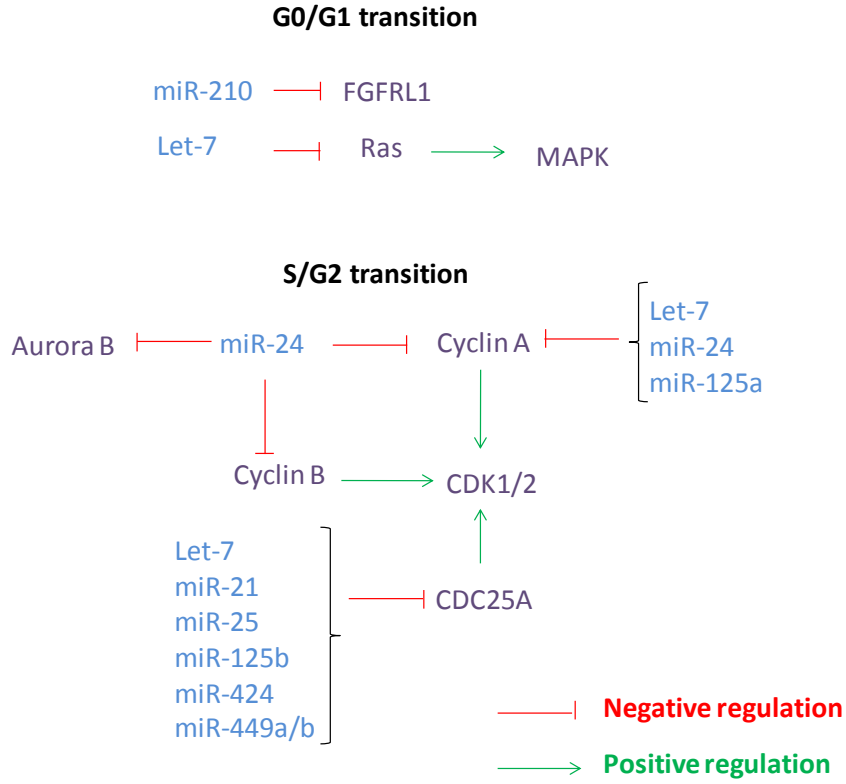

d) MiRNAs involved in the regulation of cell cycle checkpoint genes at G2/M and M/G1 transitions.

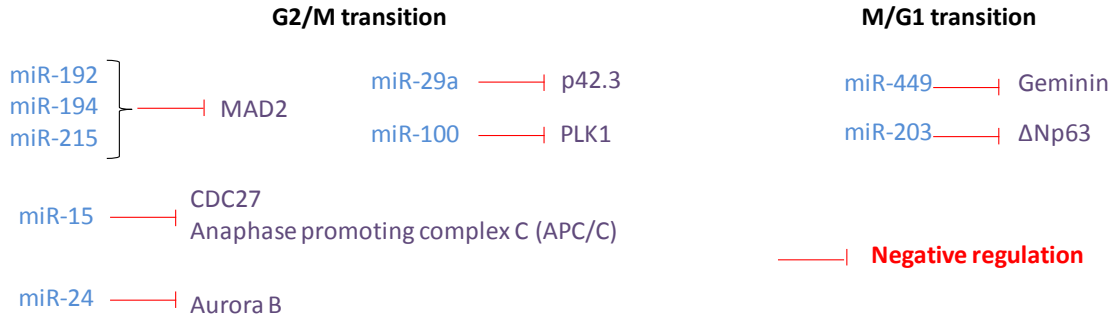

Main cycles of checkpoint; G1 (first gap phase), S (synthesis phase), G2 (second gap phase), M (mitosis) and G0; are shown. Cell cycle regulators and effectors (purple labelled), which regulate and/or are regulated by miRNAs (blue labelled) expressed in preimplantation embryo development, are grouped according to the cell cycle phase. Positive (green labelled) and negative (red labelled) relationship between miRNAs and mRNAs are shown according to the cell cycle: a) MiRNAs involved in the regulation of cell cycle checkpoint genes at G0, S, G2 and M phases. b) MiRNAs involved in the regulation of cell cycle checkpoint genes at the G1/S transition c) MiRNAs involved in the regulation of cell cycle checkpoint genes at G0/G1 and S/G2 transitions and d) MiRNAs involved in the regulation of cell cycle checkpoint genes at G2/M and M/G1 transitions (Hermeking, 2012, Biggar and Storey, 2010, Eggert and Schulte, 2010, Kim, 2008, Noto and Peek, 2012, Bueno and Malumbres, 2011, Song and Meltzer, 2012, Zhang *et al.*, 2010a, Ryazansky and Gvozdev, 2008, Liang and He, 2011, Hu and Gatti, 2010, Hu *et al.*, 2010, Yan *et al.*, 2010, Zhang *et al.*, 2010b).

Base excision repair genes and miRNAs expressed in preimplantation embryos

Several genes, proteins and polymerases are involved in base excision repair. Although expression of several genes was shown to be regulated by miRNAs, the possible association of the expression of miRNAs and base excision repair genes remains to be analysed. However bioinformatics studies identified several miRNAs with putative base excision repair gene targets. *PARP1* is mainly involved in double strand break repair in mammalian cells and this gene was shown to interact with many base excision repair genes (Dantzer *et al.*, 1999, Dantzer *et al.*, 2000). In the absence of *PARP1*base excision repair was shown to be impaired. The association of PARP1 with base excision repair genes and miRNAs are shown in figure 1.11. In addition to this gene, bioinformatics studies showed that miRNAs are also involved in the regulation of PCNA (Figure 1.11, Appendix 7.1.1, http://www.targetscan.org/, http://www.microrna.org/microrna/home.do and http://mirdb.org/miRDB/). Therefore, it is likely that some or all of these base excision repair genes identified by bioinformatics analyses are regulated by miRNAs in human oocytes and embryos.

Figure 1-11 Schematic diagram of base excision repair pathway with genes and miRNAs regulating these genes.

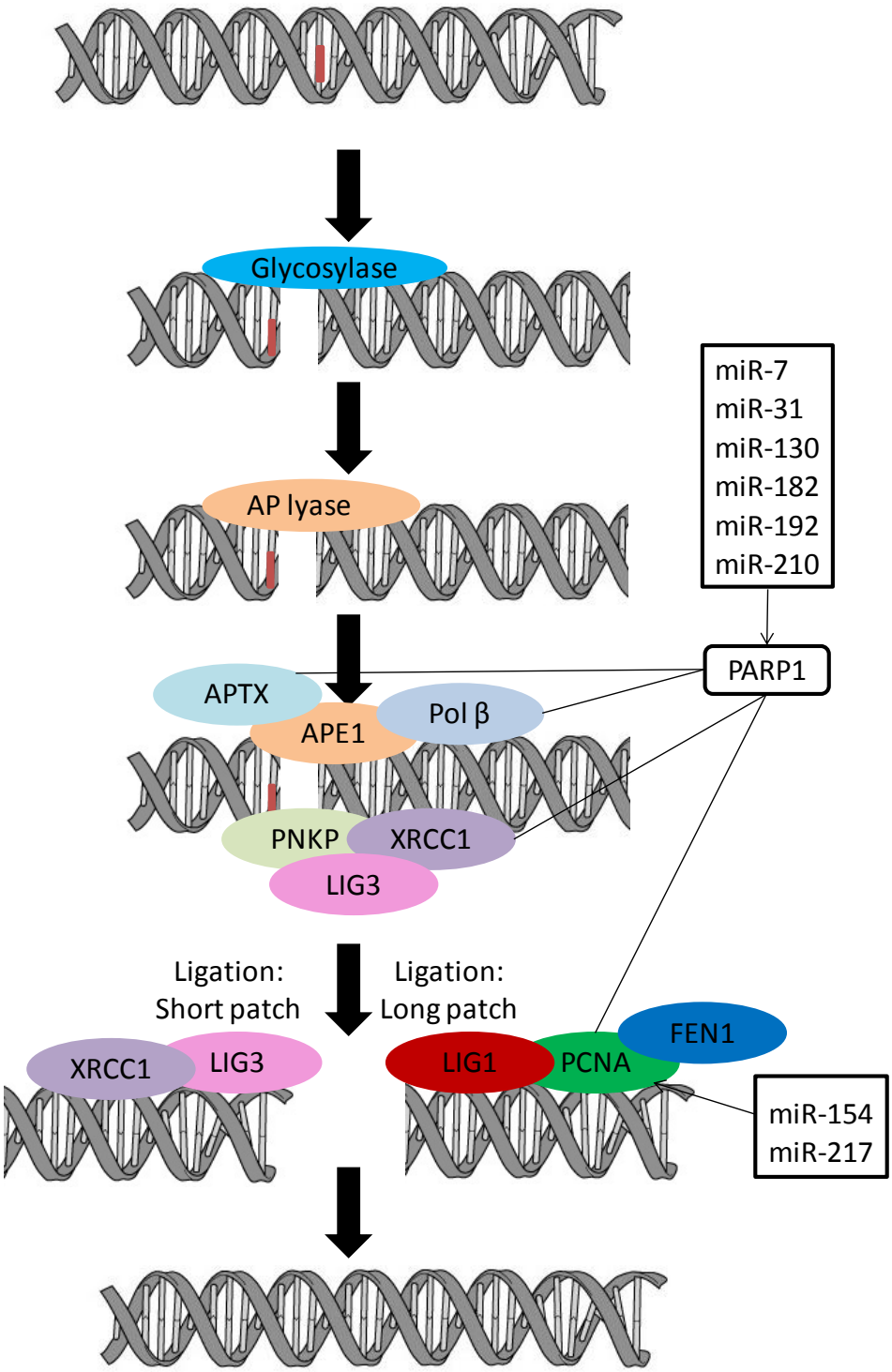

Genes involved in base excision repair and miRNAs that are predicted to regulate these genes are shown (http://www.microrna.org/microrna/home.do, http://www.targetscan.org/, http://mirdb.org/miRDB/). Several miRNAs were shown to target PARP1, which was shown to interact with several genes involved in base excision repair and genes functioning at later stages of base excision repair pathway. Bioinformatics studies also showed that PCNA is regulated by two miRNAs. Although a direct relationship among miRNAs and base excision repair genes, proteins and polymerases has not been established, there may be an indirect regulation of base excision repair components through miRNA regulated PARP1.

Nucleotide excision repair genes and miRNAs expressed in preimplantation embryos

Nucleotide excision repair is a multi-protein repair system. MiRNAs were shown or are suggested to regulate expression of several nucleotide excision repair genes, such as forced expression of miR-192, which is expressed in bovine oocytes, was shown to impair nucleotide excision repair. MiR-192 was shown to regulate *ERCC3* (*XPB*) and *ERCC4* (*XPF*), i.e. increased expression of this miRNA down-regulated *ERCC3* expression in hepatoma cell line HepG2.2.15 cells (Xie *et al.*, 2011). It is possible that miR-192 also down-regulates these genes in gametes and preimplantation embryos.

Bioinformatics analyses also suggested that several other nucleotide excision repair genes are regulated by miRNAs (Figure 1.12), such as hsa-miR-23, hsa-miR-101, hsa-miR-128, hsa-miR-181c and hsa-miR-212 are suggested to target *GTF2H2* (http://www.microrna.org/microrna/home.do,http://www.targetscan.org/ and http://mirdb.org/miRDB/). Although the association of these miRNAs and *GTF2H2* have not been analysed previously, it is possible that these miRNAs have a regulatory role on *GTF2H2* in gametes and embryos.

Figure 1-12 Schematic diagram of nucleotide excision repair pathway with genes and miRNAs regulating these genes.

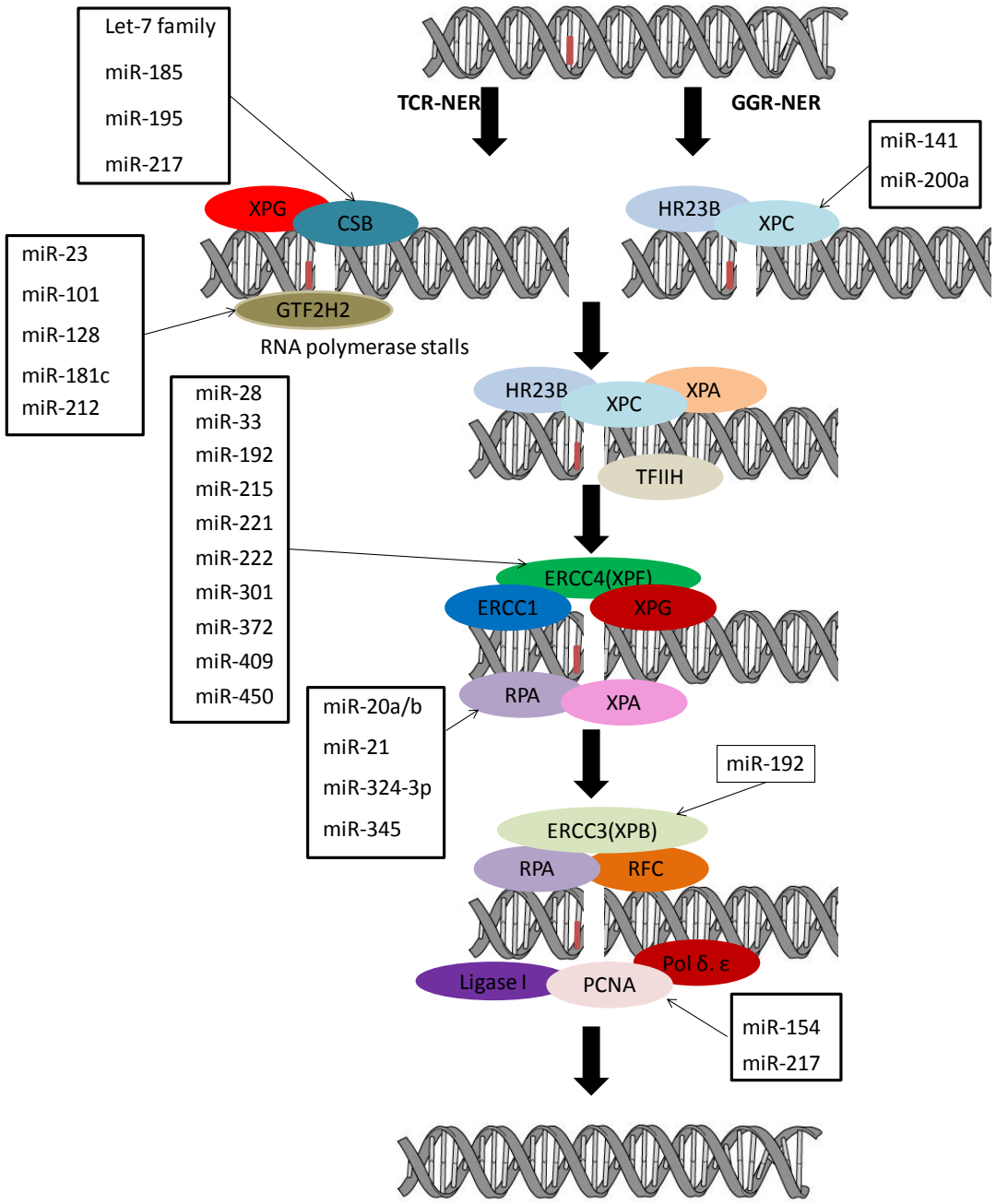

Genes involved in nucleotide excision repair and miRNAs that are predicted to regulate these genes are shown (http://www.microrna.org/microrna/home.do, http://www.targetscan.org/, http://mirdb.org/miRDB/). Several miRNAs were shown or suggested to target the initial sensor genes and genes functioning at later stages of nucleotide excision repair pathway.

Double strand break repair and miRNAs expressed in preimplantation embryos

Several double strand break repair genes, such as *H2AX*, *BRCA1*, *PARP1*, *RAD23B*, *RAD51*, *RAD52* and *MRE11*, were shown to be targeted by miRNAs that are expressed during preimplantation embryo development (Figure 1.13). In U2OS human osteosarcoma cell lines and humans, H2AX, a sensor protein in double strand break repair response, was shown to be targeted by miR-138 (Wang *et al.*, 2011), miR-24 (Adare *et al.*, 2010), miR-23b and miR-145 (Revel *et al.*, 2011). Ectopic expression of miR-138 in U2OS human osteosarcoma cell line was shown to lower γ-*H2AX* formation, hindered homologous recombination and increased sensitivity to DNA damaging agents (Wang *et al.*, 2011). Over-expression of miR-24 caused reduced *H2AX* expression and increased sensitivity to ionising radiation with reduced repair capacity (Adare *et al.*, 2010).

Expression of homologous recombination repair proteins were shown to be changed by forced expression of miR-210 and miR-373. The forced expression of these miRNAs was shown to reduce *RAD52* expression and over-expression of miR-373 reduced the expression of *RAD23B* and *RAD52* in HeLa cells (Crosby *et al.*, 2009). Unlike this negative regulation, *MRE11* was unaffected by the over-expression of these miRNAs (Crosby *et al.*, 2009).

MiR-99 was shown to reduce the repair efficiency by disturbing the localisation of *RAD51* and *BRCA1* to DNA damaged site in human prostate and breast cancer cell lines (Tanic *et al.*, 2011, Mueller *et al.*, 2012). *BRCA1* was shown to be down-regulated by over-expression of miR-146 and miR-182 in sporadic breast tumours (Moskwa *et al.*, 2010). Over-expression of miR-182 also caused an increased sensitivity to *PARP1* inhibition in cultured cells (Moskwa *et al.*, 2010, Tanic *et al.*, 2011). It is possible that presence of these miRNAs or abnormal expression, such as over-expression of these miRNAs, would have similar regulatory effects in human gametes and embryos.

Figure 1-13 Schematic diagram of the double strand break repair pathways with genes and miRNAs regulating these genes.

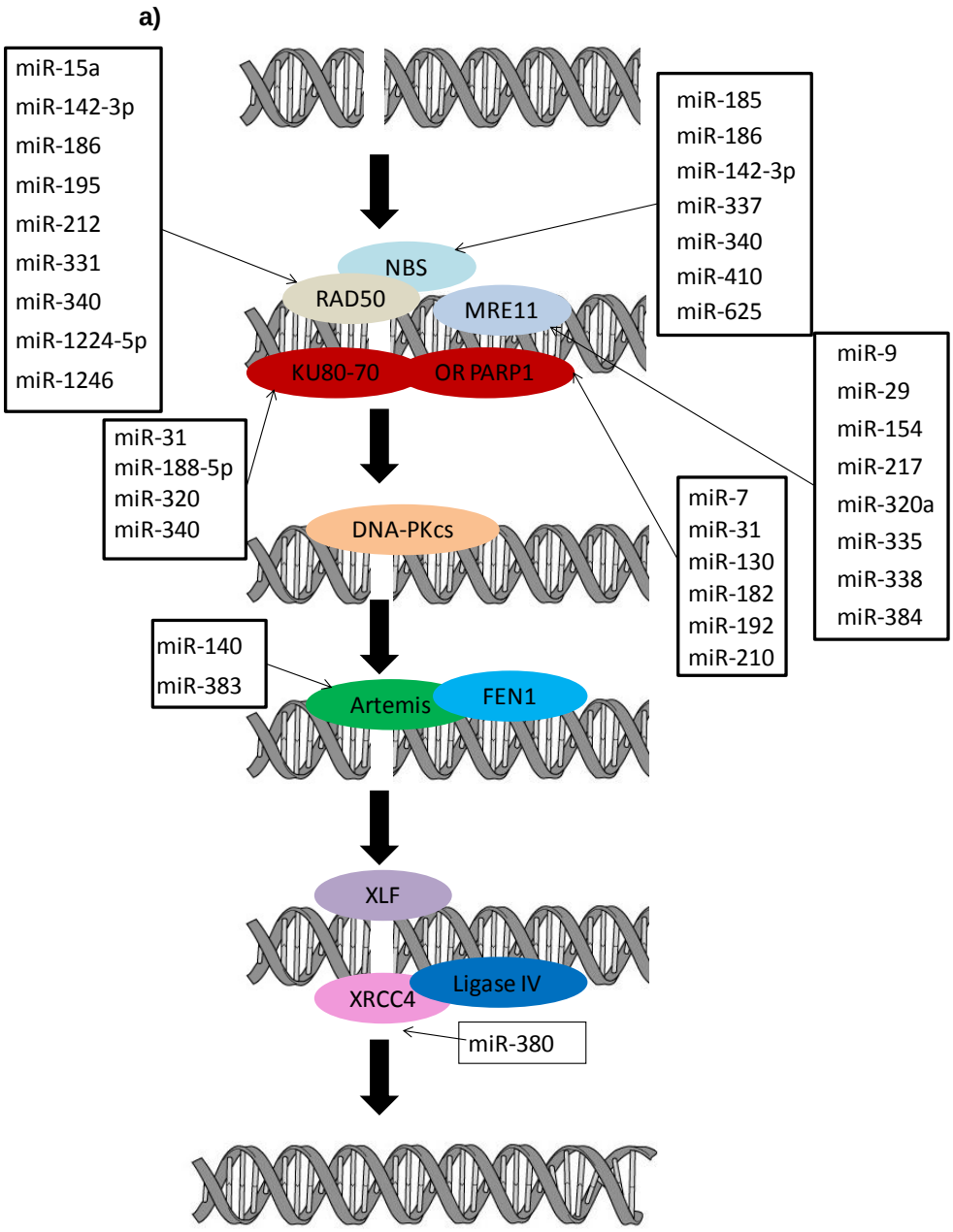

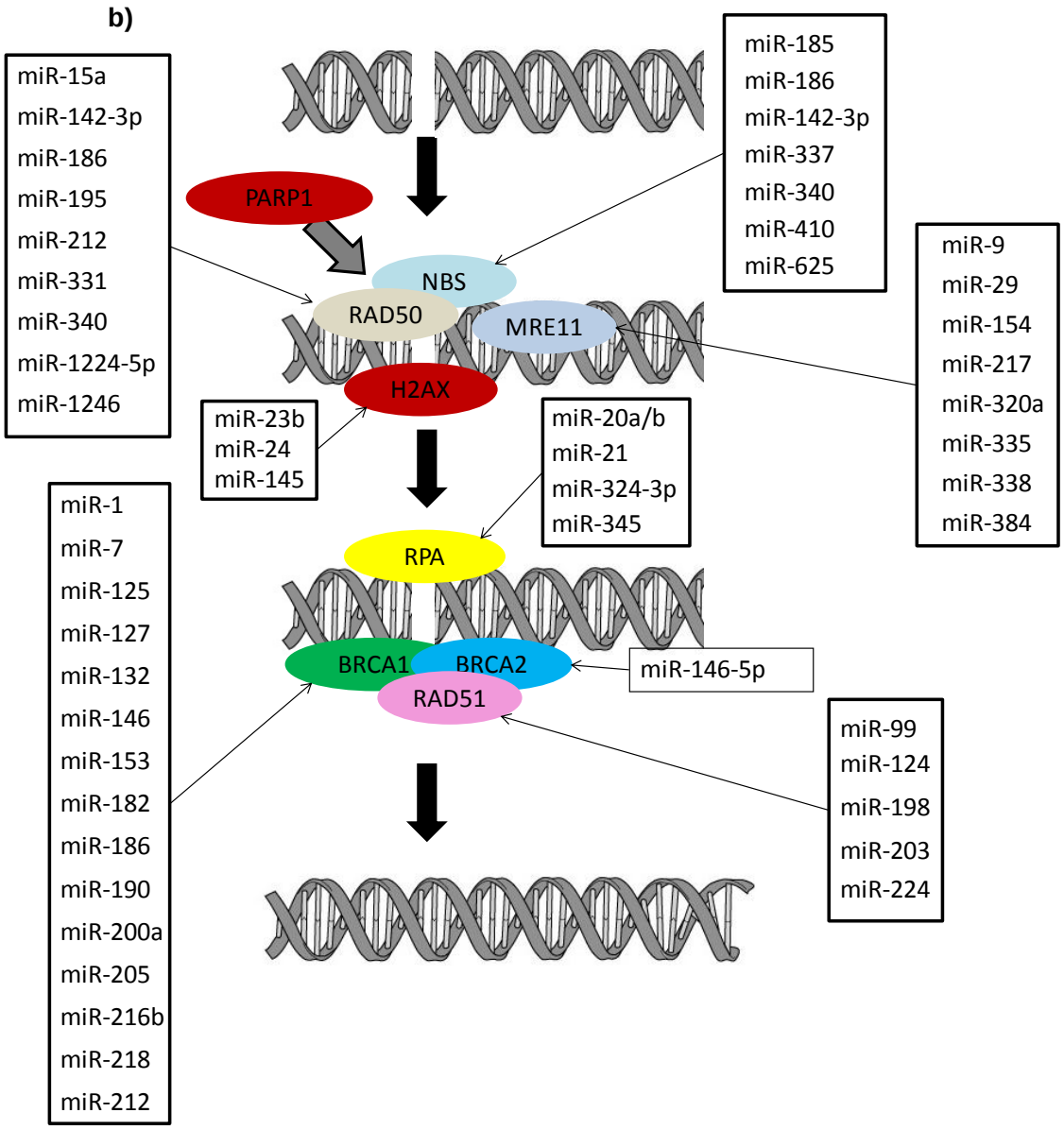

Genes involved in a) Non-homologous end joining and b) Homologous recombination pathways and miRNAs that are predicted to regulate these genes are shown (http://www.microrna.org/microrna/home.do,http://www.targetscan.org/,http://mirdb.org/miRDB/). Several miRNAs were shown to target the initial sensor genes of non-homologous end joining and homologous recombination repair pathways. Several more miRNAs were shown to regulate the expression of genes functioning at later stages of both non-homologous end joining and homologous recombination repair pathways.

Mismatch repair and miRNAs expressed in preimplantation embryos

Jaroudi *et al.* (2009) showed that mismatch repair genes were expressed in human oocytes and blastocysts. These genes were shown to be regulated by several miRNAs (Figure 1.14). MiR-155, expressed in mouse preimplantation embryos, was shown to down-regulate mismatch repair heterodimer proteins *MSH2-MSH6*, *MLH1* and *PMS2* in human hepatoma cell lines (Valeri *et al.*, 2010, McPhee *et al.*, 2012). Similarly, high expression of miR-21 was shown to down-regulate *MSH2* and *MSH6* in colorectal tumours (Valeri *et al.*, 2010).

MiRNA expression was also associated with microsatellite instability, such that differential expression of miRNAs, miR-31, miR-552, miR-592, miR-625, miR-196b and miR-181c, was observed in tumours with microsatellite instability and/or absence of protein expression *hMLH1* relative to the tumours with no microsatellite instability and normal protein expression of *hMLH1*. Thirty nine more miRNAs were differentially expressed between normal colon tissue and tumour specimens (Medina and Slack, 2008). Moreover, increased expression of miR-101, miR-192 and miR-212 was associated with microsatellite instability compared to miRNAs associated with microsatellite stable samples (Schepeler *et al.*, 2008). Increased expression of let-7a, miR-31 and miR-145 was shown to be linked with low levels of microsatellite instability compared to miRNAs associated with both stable and high levels of microsatellite instability indicating that the presence of these miRNAs lowers the risk of microsatellite instability (Earle *et al.*, 2010). Two miRNAs, miR-181c and miR-196b were shown to be down-regulated in tumours with microsatellite instability and/or in the absence of protein expression *hMLH1* (Sarver *et al.*, 2009, Medina and Slack, 2008). Since these miRNAs were shown to be expressed in mouse embryos (Tang *et al.*, 2007, Yang *et al.*, 2008), they may play a role in stabilising microsatellites or *hMLH1* in human embryos.

Figure 1-14 Schematic diagram of mismatch repair pathway with genes and miRNAs regulating these genes.

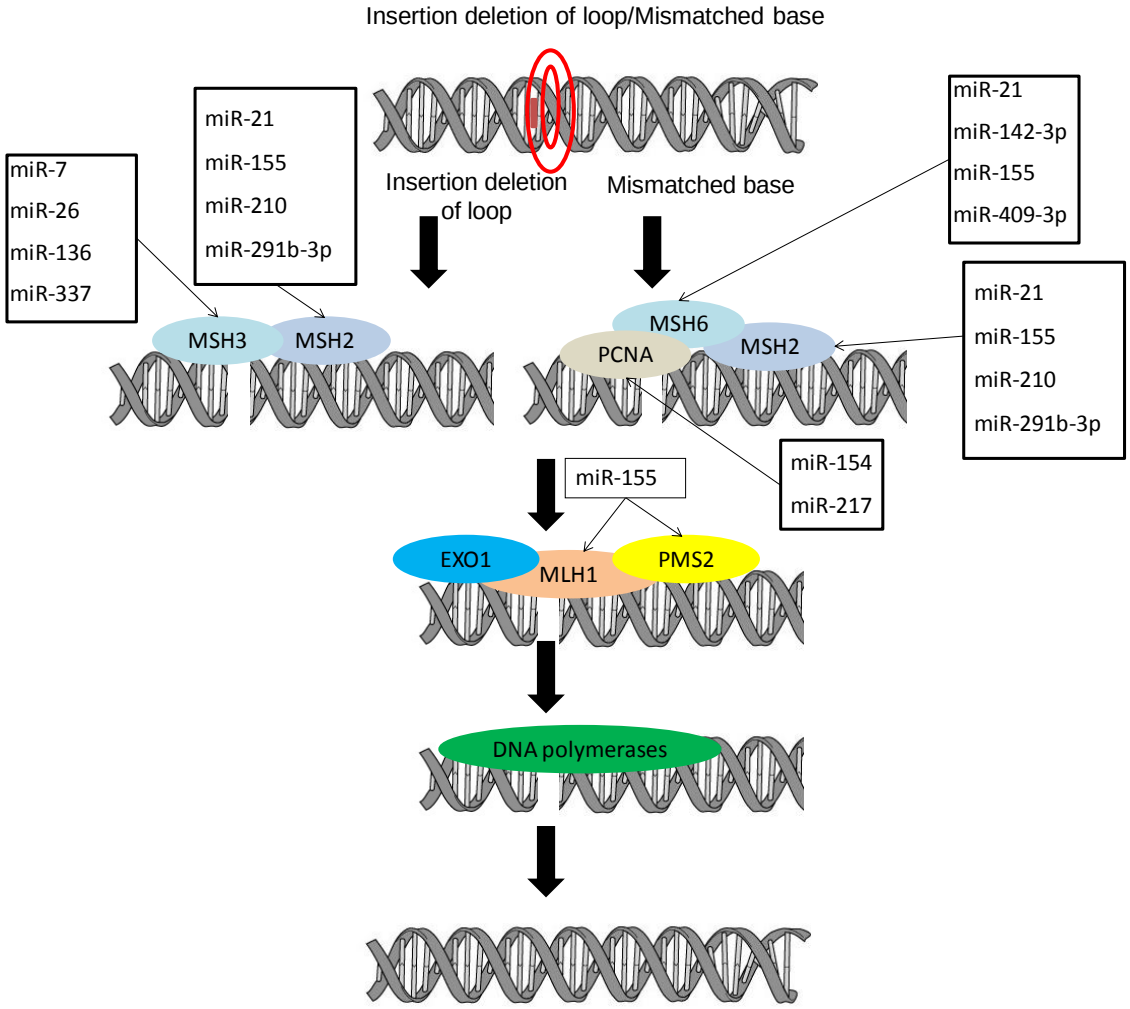

Genes involved in mismatch repair and miRNAs that are predicted to regulate these genes are shown (http://www.microrna.org/microrna/home.do, http://www.targetscan.org/, http://mirdb.org/miRDB/). Multiple miRNAs are suggested to regulate the expression of mismatch repair sensor genes (*MSH2*, *MSH3*, *MSH6*, *PCNA*) and genes functioning at later stages of mismatch repair (*MLH1* and *PMS2*).

1.5. Aims and hypothesis

1) The expression level of miRNAs and their target repair transcripts in human oocytes and preimplantation embryos

Expression of DNA repair genes in human oocytes and embryos was investigated by Jaroudi *et al.* (2009). Similarly, the expression of miRNAs in mouse and bovine oocytes and preimplantation embryos at different stages of development has been studied (Yang *et al.*, 2009, Tang *et al.*, 2007, Mondou *et al.*, 2012, Ro *et al.*, 2007, Xu *et al.*, 2011). To date only three studies have investigated the miRNA expression in human oocytes (Xu *et al.*, 2011) and blastocysts (McCallie *et al.*, 2009, Rosenbluth *et al.*, 2012). As described in section 1.4.2.4 several miRNAs were shown to be involved in the regulation of numerous DNA repair genes in human cell lines, (Aqeilan *et al.*, 2009, Krichevsky and Gabriely, 2009, Navarro *et al.*, 2008, Wang *et al.*, 2011, Tanic *et al.*, 2011, Mueller *et al.*, 2012, Valeri *et al.*, 2010, McPhee *et al.*, 2012). However, there have not been any studies focusing on the relationship between miRNAs and the expression of genes involved in DNA repair in gametes and preimplantation embryos.

It was hypothesised that miRNAs have regulatory roles on their target mRNAs. Since the majority of the previously published studies showed that miRNAs down-regulate their targets, it was hypothesised that in these cases an inverse correlation would be observed between miRNAs and their target mRNAs. However, it was also hypothesised that some miRNAs may have a direct relationship with their target mRNAs since recent studies have shown a stabilisation effect of miRNAs on their targets.

The first aim of this project was to investigate the possible correlations of miRNAs and their target mRNAs involved in different repair pathways.

In order to identify target miRNAs and mRNAs, a literature review was performed. The expression level of the selected miRNA and mRNA was investigated by quantitative real time PCR (using TaqMan assays). Since it was

difficult to obtain cleavage stage human embryos, this analysis was performed in individual human oocytes and individual human blastocysts. A student's T-test was applied to investigate if there was significant association in the expression of the mean mRNA and miRNA levels in oocyte relative to the blastocyst. Pearson correlation with Dunnett's post testing was used to identify significant association between the levels of miRNAs and their target mRNAs.

2) Differential gene expression in preimplantation embryos and potential relation with differential methylation

Investigation of epigenetic modifications and differential methylation of parental genomes in mouse preimplantation embryos are established (Dean *et al.*, 2003, Tamaru and Selker, 2001, Jackson *et al.*, 2002, Fuks *et al.*, 2003). Studies in mouse, bovine and human suggest that there is rapid demethylation of the paternal genome post fertilisation whereas demethylation of the maternal genome is gradual (Fulka *et al.*, 2004, Beaujean *et al.*, 2004b, Santos *et al.*, 2003). At this stage of development it is possible that parental genes are differentially expressed.

The hypothesis of this study was that up to blastocyst stage global differential demethylation of parental genomes may result in preferential parental gene expression. When a repair gene carries a mutation, preferential parental gene expression may affect preimplantation embryo development. Therefore, it was hypothesised that the development of preimplantation embryos may be impaired when the embryo carries a paternally inherited mutation compared to the embryo with maternally inherited mutation.

The second aim of this project was to investigate the differential parental expression of *ACTB*, *SNRPN*, *H19* and *BRCA1* in human preimplantation embryos obtained from patients undergoing preimplantation genetic diagnosis (PGD). A further analysis was conducted to investigate if the differential parental expression of *BRCA1* affects the developmental progression of the embryos depending on the parental inheritance.

In order to investigate differential parental gene expression in embryos, informative single nucleotide polymorphisms (SNPs) between couples were required. SNPs with high heterozygosity were identified using Ensembl genome browser within the coding region of preselected genes. The alleles at the SNP sites were identified by sequencing analysis for each couple. Embryos from couples with informative SNPs were used to investigate differential expression of parental transcripts. cDNA from these embryos were semi-quantitatively analysed by mini-sequencing (SNaPshot) analysis. Differential parental expression was examined by calculating the peak height ratios of the alleles for the SNPs analysed. Statistical analysis was performed by applying student's T-test to investigate if there was significant difference in the expression levels of parental transcripts (*ACTB*, *SNRPN*, *H19* and *BRCA1*) in embryos. Methylation status of the embryos was analysed by bisulfite conversion followed by methylation specific PCR to investigate if the differential gene expression profile was due to methylation.

The final part of this study investigated if there was any difference in the developmental stage of embryos with paternally inherited *BRCA1* and *BRCA2* mutations compared to the maternally inherited *BRCA1* and *BRCA2* mutations on day 5/6 post fertilisation. A chi-squared test was applied to investigate if this difference was significant.

3) Functional assay development for mismatch repair

Expression and proteomic analyses provide an indication of which DNA repair pathways are functionally active in preimplantation embryos. However these analyses still do not provide the actual capacity of a cell to perform DNA repair. There are no studies analysing mismatch repair efficiency in human preimplantation embryos and current techniques analysing mismatch repair efficiency require construction of plasmids that are time consuming and expensive. It is important to develop an assay sensitive enough to detect the mismatch repair efficiency in embryos.

It was hypothesised that oocytes and blastocysts have mismatch repair activities since previous studies showed that mismatch repair genes are expressed both in oocytes and blastocysts.

The last aim of this project was to develop a simple and sensitive functional assay to detect the efficiency of mismatch repair in oocytes and preimplantation embryos. Mismatch repair activity was optimised *in vitro* by exposing heteroduplex constructs to commercially available nuclear and whole cell extracts. Mismatch repair efficiency was detected by mini-sequencing (SNaPshot) analysis. The optimised functional assay was then applied to whole cell extracts obtained from pooled mouse and human oocytes and blastocysts, respectively.

2. Materials and Methods

2.1. General laboratory methods and standards

A general code of laboratory practice and workflow is described. The methodology to achieve all three aims is presented in two main sections; 1. sample collection, 2. sample processing and analysis. The sample collection section describes the sample types, selection of the samples used for each aim, how they were collected and processed immediately for the subsequent experimental work. The sample processing section explains all the methodology and analysis used to accomplish each aim, such as DNA/RNA extraction, DNA amplification, sequencing and microarrays and statistical analysis. The workflow outlining each methodology used for this study is presented in table 2.1.

All solutions were prepared with deionised water and they were autoclaved. The pH of all the buffers was measured at room temperature (RT). Unless otherwise stated all reagents were from VWR (International) and were of Analar Quality including ethanol 99.7-100% v/v and salts used for the preparation of buffers, such as sodium chloride (NaCl), orthoboric acid and Tris (hydroxymethyl) methylamine (TRIS). Molecular grade reagents were supplied by Sigma (UK) including ethylenediaminetetra-acetic acid anhydrous 99% (EDTA), adenosine 5'-triphosphate disodium salt hydrate (ATP), beta-mercaptoethanol (β-Me), bovine serum albumin (BSA), ethidium bromide, ethylene diamine tetraacetic acid, glutathione, phosphate buffered saline (PBS), polyvinyl alcohol (PVA), sodium acetate (3M solution), sodium dodecyl sulfate (SDS) and agarose type I. Of these reagents ATP and glutathione were stored at 4ºC, BSA at -20ºC and the rest at RT. Proteinase K was supplied by Roche (UK) and Exo I and shrimp alkaline phosphate (SAP) were obtained from New England Biolabs (UK). All these enzymes were stored at -20ºC.

For each experiment, dedicated areas were used. All preparations, such as single cell isolation, blastomere tubing, PCR, whole genome amplification (WGA) and cDNA synthesis preparations were carried out in a dedicated single cell room. In the single cell room the air was filtered and replaced 20 times per hour under positive pressure. All the equipment and consumables, such as boxes containing filter tips, tubes, gloves, pipettes and ice trays entering the

room for the first time, were wiped with ethanol. These boxes were then exposed to ultraviolet light (Template Tamer, Qbiogene, UK) for at least 10 minutes to remove DNA contaminants. A microflow advanced Bio-safety cabinet class II was used to set up all the PCRs, WGA and cDNA synthesis reactions and all the preparations for these reactions were carried out on ice trays. These reactions were set up using DNase- and RNase-free water (Promega, UK) in DNA-, DNase-, RNase- and pyrogen-free tubes (Molecular BioProducts, Inc, UK).

Extra caution was taken for all the expression experiments, such as RNA isolation, cDNA synthesis and real time PCR. RNA isolations were carried out in a designated area outside the single cell room. Pipettes, filtered pipette tips and tube racks designated for RNA isolation only were used through the expression studies. In order to reduce RNase contamination, all the equipment and the designated laboratory area were cleaned with 70% ethanol and RNase ZAP (Ambion Inc, UK), rinsed with distilled water and dried with clean tissue before each experiment. Gloves were frequently changed to reduce any risk of contamination.

All the centrifugation was carried out in a bench top microfuge (MSE Microcentaur, Sanyo, UK and Labofuge 400, Heraeus Instruments, UK). All the PCRs, WGA and cDNA synthesis reactions were carried out in either of two PCR thermocyclers; Mastercycler Gradient® thermal cycler (Eppendorf, UK) and GeneAmp PCR System 9700 (Applied Biosystem, UK). All the PCR products (PCR analyses including mini-sequencing following PCR) were handled in a separate laboratory using pipettes and pipette tips dedicated for post-PCR products. A PCR workstation (Template Tamer, Qbiogene, UK) was used to carry out all the post-PCR analysis and all the consumables, including pipettes and pipette tips, were exposed to UV for at least 10 minutes after each use to decontaminate them prior to next use.

All the samples were collected from patients undergoing *in vitro* fertilisation (IVF)/ intracytoplasmic sperm injection (ICSI)/ PGD at the Centre for

Reproductive and Genetic Health (CRGH) and the UCL Centre for PGD who had given an informed consent to donate samples for this project. This work was licensed by the Human Fertilisation and Embryology Authority (HFEA project reference: RO113) and ethical approval was granted by the National Research Ethics Service (NRES), Research Ethics Committee (REC reference number: 10/H0709/26).

2.2. Potential correlation analysis between miRNA and their target repair transcripts in human oocytes and preimplantation embryos

The workflow for correlation analysis of miRNAs and mRNAs in human oocytes and preimplantation embryos is summarised in figure 2.1.

Figure 2-1 Workflow of correlation analysis between miRNAs and mRNAs in human oocytes and blastocysts.

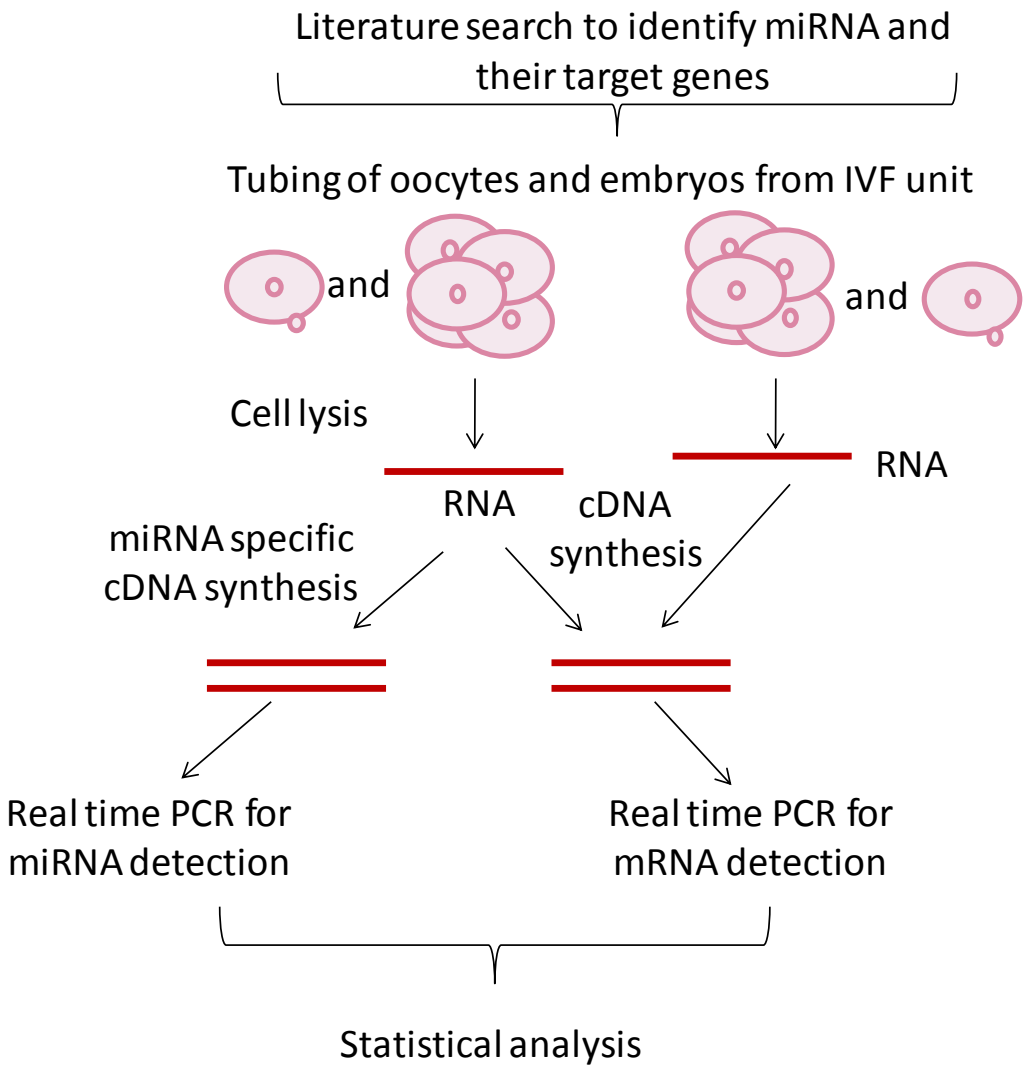

Literature search was performed to identify target miRNAs and mRNAs to be analysed in this study. After initial cell lysis, samples were reverse transcribed for specific miRNAs and analysed by quantitative real time PCR for miRNA expression. Similarly for mRNA expression, samples were reverse transcribed into cDNA and real time PCR was performed to quantitatively analyse the expression of mRNA targets.

2.2.1. Sample collection

A total of 31 immature oocytes and 33 surplus embryos from patients undergoing IVF were collected for this project. Oocytes and embryos were transported in culture dishes from the Centre for Reproductive and Genetic Health in a closed thermally insulated carrier (IsoTherm-System®, Eppendorf, UK). These samples were processed immediately, especially for the RNA expression studies to minimise degradation of RNA. Oocyte and embryo morphology grading was performed by the embryologists at the Centre for Reproductive and Genetic Health on the day of sample collection. Oocytes were grouped in meiosis I (MI) and meiosis II (MII) stages. The blastocysts were scored according to Cornell grading (Veeck *et al.*, 2004) (Table 2.1).

Table 2-1 Cornell grading scheme for the blastocysts.

Grade	Expansion	Grade	Inner Cell Mass (ICM)	Grade	Trophectoderm
1 	Early blastocyst	A 	Compact cells	A 	Good cells with a cohesive epithelium
2 	Blastocyst				
3 	Full blastocyst	B 	Large, loose cells	B 	Few large healthy cells
4 	Hatching blastocyst	C 	ICM is not distinguishable	C 	Poor very large/ unevenly distributed cells
5 	Fully hatched blastocyst				
6 	Hatching or hatched blastocyst with PGD	D 	ICM is degenerative	D 	Cells are degenerative

This figure shows blastocyst grading according to Cornell grading scheme depending on the stage of expansion, inner cell mass and trophectoderm. The first number scored the expansion, second character scored the quality of ICM and the last character scored the quality of the trophectoderm, respectively. Images were adopted from (Veeck *et al.*, 2004). Copyright (2004) Elsevier.

All the donated oocytes and embryos were collected and tubed in 0.3U/µl RNasin plus RNAse inhibitor (Promega, UK) using an inverted microscope (Olympus, Optech microscope services, UK). A hand pipette (Cook, UK) using a 0.3mm polycarbonate microcapillary (Biohit, Finland) was used for tubing all the oocytes and embryos and the samples were stored at -80ºC. This process

involved removing the zona pellucida prior to tubing any blastomeres. Oocytes and embryos were exposed briefly to acidified Tyrode's solution (MediCult Ltd, UK) to remove the zona pellucida. The cells freed from zona pellucida were washed three times in fresh drops of RNasin buffer. The washed cells from the individual embryos were transferred into a thin walled 0.2ml microfuge tubes. The nomenclature for the embryos collected were presented with the patient number followed by embryo number, such that the first digit represents the couple number and the second digit represents their embryo numbers; i.e. 1.1 represent couple one's first embryo, 1.2 represent couple one's second embryo.

2.2.2. Target selection

In order to identify the target mRNAs and miRNAs, a *Medline* literature search was performed using the keywords "DNA repair genes", "miRNA", "expression", "embryo", "oocyte", "sperm", "human" and "preimplantation development". An expression profile of DNA repair genes in human oocytes and blastocysts was previously investigated by Jaroudi *et al.* (2009). A group of DNA repair genes showing differential expression between oocytes and blastocysts was identified using these data. A further *Medline* search was carried out to identify miRNAs expressed in mouse, bovine and human oocytes. From this profile, miRNAs associated with DNA repair genes, especially with the previously identified differentially expressed repair genes, were investigated using the keywords "miRNA", "DNA repair", "nucleotide excision repair", "base excision repair", "mismatch repair", "double strand break repair" and "DNA damage". In addition to these published articles, databases were searched to investigate if miRNAs expressed in bovine, mouse and human gametes and embryos have any putative targets that are involved in DNA repair (http://www.targetscan.org/, http://www.microrna.org/microrna/home.do and http://mirdb.org/miRDB/).

These two profiles of differentially expressed mRNAs between human oocytes and blastocysts and miRNAs expressed in bovine, mouse and human and were also shown to be involved in different repair pathways, were used to select the targets. It was aimed to select one sensor gene or a gene functioning at the earlier stages of the particular repair pathway and one gene functioning at later

stage of the repair pathway to identify which repair pathway may be functionally active. The expression of one miRNA processing gene, *DICER*, was also selected to be examined in order to show that miRNA processing genes are present at these stages. MiRNAs, which were shown to be expressed in mouse and bovine gametes and preimplantation embryos and target multiple selected mRNAs, were selected for this analysis. TaqMan assays were used to target both miRNAs and mRNAs in human oocytes and blastocysts. Following cell lysis, cDNA synthesis was performed to investigate mRNA expression. Customised TaqMan primer assays specific for each mRNA and miRNA were used. Neither of the primer assays (mRNA and miRNA) required further optimisation prior to analysis.

For each target, expression analyses were performed in repeat samples to eliminate the sample variation. Each mRNA or miRNA had a total of six repeats (six individual oocytes and six individual blastocysts) and between two to three replicates. Replicates involved analysis of the miRNA expression in the same oocyte and blastocyst sample in duplicate to have an internal check of the fidelity of the experiment. The samples were grouped together according to the oocyte and blastocyst morphologies for each target to avoid inter-individual variation. Only meiosis I (MI) and meiosis II (MII) oocytes were used for the analysis. Similar developmental stage blastocysts were grouped together to investigate the expression of each target. Due to the scarcity of human oocytes and blastocysts, the maternal age could not be used as criteria to group the samples. Overall, each embryo was tested for between four to nine mRNAs and/or miRNAs.

2.2.3. Sample processing and analysis

The expression of nine mRNA and one miRNA processing gene was analysed using the TaqMan® gene expression cells-to-Ct™ (cycle threshold) kit (Ambion, Life Technologies, UK) in nine single human oocytes and ten single human blastocysts. The expression of 20 miRNAs that target these mRNAs in 22 human oocytes and 23 blastocysts were analysed using the TaqMan® microRNA cells-to-Ct™ kit (Ambion, Life Technologies, UK). Both analyses involved three main steps; lysis, reverse transcription and real time PCR. Lysis of oocytes and blastocysts was performed by addition of 25µl lysis solution with 0.25µl DNase I to each sample and incubation at RT for 8 minutes. The lysis was stopped by addition of the 2.5µl stop solution and incubation at RT for 2 minutes.

2.2.3.1. Reverse transcription for mRNA and miRNA expression

A master mix consisting of 25µl of 2xRT buffer, 2.5µl of 20xRT enzyme mix and 12.5µl of nuclease-free water was added to 10µl of the lysate for the analysis of mRNA expression. Reverse transcription was carried out in a thermal cycler at 37ºC for 1 hour and the reaction was inactivated at 95ºC for 5 minutes.

Reverse transcription was carried out for each miRNA specifically. Three µl of miRNA specific RT primer was added to a master mix of 1.5µl of 10xRT buffer, 0.15µl of dNTP mix, 0.19µl of RNase inhibitor, 1µl of MultiScribe™ RT and 4.16µl of nuclease-free water. Five µl of lysate was added for each reaction. The annealing was carried out in a thermal cycler at 16ºC for 30 minutes followed by reverse transcription at 42ºC for 30 minutes. The reverse transcription was stopped at 85ºC for 5 minutes.

Reverse transcription was carried for each reaction in the absence of embryo lysate as a negative control.

2.2.3.2. Real time PCR for mRNA and miRNA

Real time PCR for each sample in duplicates was carried out to analyse the relative expression of mRNAs and miRNAs between oocytes and blastocysts using the Light cycler Nano (Roche, UK). A negative control for each real time PCR was analysed in the absence of cDNA.

For mRNA analysis, a master mix of 5µl of 2xTaqMan® gene expression mix, 0.5µl of 20xTaqMan® gene expression assay and 2.5µl of nuclease-free water was added to 2µl of reverse transcription product. The real time PCR conditions involved an enzyme activation step at 95ºC for 10 minutes followed by denaturation at 95ºC for 15 seconds and annealing and extension at 60ºC for 1 minute for 50 cycles.

For miRNA analysis, a master mix of 5µl of 2xTaqMan® mix, 0.5µl of TaqMan® microRNA assay and 2.5µl of nuclease-free water was added to 2µl of reverse transcription product. Real time PCR was carried out by an initial enzyme activation step at 95ºC for 10 minutes and denaturation at 95ºC for 15 seconds and annealing and elongation at 60ºC for 1 minute for 50 cycles.

Cq values were assigned automatically by the Light cycler Nano software (Roche, UK) and they represent the number of cycles required for the fluorescent signal entering the exponential phase. Lower Cq values indicate greater expression in the sample.

For comparative Cq analysis, ΔCq values for mRNA and miRNA were investigated by normalisation to the reference gene *ACTB* for mRNA and RNU48 for miRNA, respectively:

ΔCq = Cq_ target oocyte/blastocyst - Cq_*ACTB* oocyte/blastocyst

ΔCq=Cq_ target oocyte/blastocyst - Cq_RNU48 oocyte/blastocyst

Fold change was analysed by the relative quantification method, 2^-ΔΔCq:

ΔΔCq = (Cq_target-Cq_*ACTB*)blastocyst - (Cq_ target-Cq_*ACTB*)oocyte

ΔΔCq=(Cq_target-Cq_RNU48)blastocyst-(Cq_ target-Cq_RNU48)oocyte

2.2.3.3. Statistical analysis

GraphPad prism v6 software was used for the statistical analyses. The expression level of each mRNA expression was examined by one-way ANOVA with Dunnett's multiple comparison post test. Similarly, each miRNA expression was examined by one-way ANOVA with Dunnett's multiple comparison post test.

Each mRNA and miRNA expression in oocytes relative to blastocysts was examined by applying an unpaired two-tailed student's T-test with the Welch correction. Pearson correlation test was used to correlate expression of each miRNA with its target mRNA. An inverse correlation was defined as r=-1 and a direct correlation as r=+1 following Pearson correlation test. The closer the r value was to +1 or -1, the stronger was the correlation. Similarly, a perfect correlation was defined as Pearson's r^2 coefficient equal to 1. For all the statistical analysis, $p<0.05$ indicated a statistical significance.

2.3. Differential gene expression in preimplantation embryos and potential relation with differential methylation

The workflow for differential gene expression in preimplantation embryo analysis is summarised in figure 2.2.

Figure 2-2 Workflow of correlation analysis between miRNAs and mRNAs in human oocytes and blastocysts.

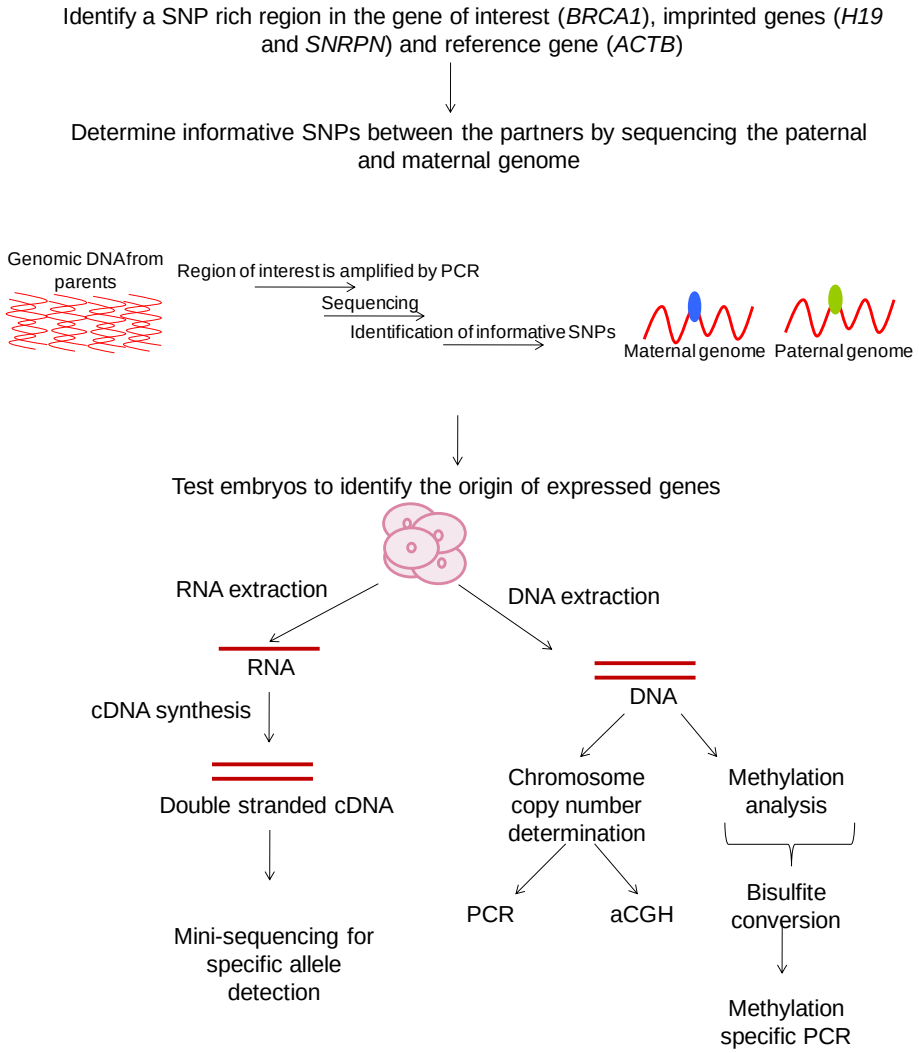

Informative SNPs between the male and female partners were identified by sequencing. RNA from the couple's embryos was extracted and cDNA was synthesised. Differential parental gene expression was analysed in the embryos by mini-sequencing. DNA from the embryos was also extracted to test the aneuploidy status of the embryos and to analyse the methylation status by bisulfite conversion followed by methylation specific PCR.

2.3.1. Sample collection

This project involved blood samples from the patients undergoing PGD. Bloods were collected in sodium ethylenediaminotetra acetic acid (EDTA) tubes for DNA extraction or Lithium heparin tubes for lymphocyte separation. If the DNA extraction (2.3.2.1) was not carried out on the same day as it was collected, the sample was stored at -80ºC until the day of the extraction. Lymphocyte separation (2.3.2.2) and single cell isolations were carried out on the same day that the samples were received. In the first part of this study, differential expression analysis, embryos diagnosed as affected following PGD for a range of monogenic disorders or were unsuitable for transfer were collected on days 5/6 post fertilisation and tubed in RNAsin solution as described in section 2.2.1. A total of 95 embryos at cleavage and blastocyst stages were collected for this study. The cleavage stage embryos were graded according to Bolton *et al.* (1989) and the number of cells and the presence of fragments were recorded. Grade 1 represent the ideal symmetrical and even-sized blastomeres with no fragmentation, 1- is symmetrical and even blastomeres with less than 10% fragmentation, grade 2+ is uneven blastomeres with less than 20% fragmentation, grade 2 is compromised development with uneven blastomeres with 25-50% fragmentation and grade 3 is the compromised development with uneven blastomeres with more than 50% fragmentation. The blastocysts were graded as described in section 2.1.1. In the second part of the study, the developmental progression of 16 embryos with maternally inherited *BRCA* mutations were compared to 15 embryos with paternally inherited *BRCA* mutations.

2.3.1.1. Sample selection

To investigate the parental origin of genes expressed in preimplantation embryos, SNP rich regions were amplified and sequenced using the DNA obtained from couples undergoing PGD. Complete updated DNA sequences of *ACTB*, *GAPDH*, *SNRPN, IGF2*, *H19*, *UBE3A* and *BRCA1* including the locations of SNPs with heterozygosity information were obtained using Ensembl genome browser, http://www.ensembl.org/index.html. Primers were designed to

amplify SNP rich areas within the coding regions of these genes as described in 2.3.2.3. All the primer sequences and the amplified regions for these genes are shown in Appendix 7.2.1.1 (a). Sequencing panels obtained from GeneScan analysis^{TM} on ABI Prism^{TM} 3100 of each partner were compared to the gene sequences of *ACTB* (ENSG00000075624, Ensembl release 60), *GAPDH* (ENSG00000111640, Ensembl release 60), *SNRPN* (ENSG00000128739, Ensembl release 60), *UBE3A* (ENSG00000114062, Ensembl release 60), *IGF2* (ENSG00000167244, Ensembl release 60), *H19* (ENSG00000130600, Ensembl release 60) and *BRCA1* (ENSG00000012048, Ensembl release 60) on the Ensembl genome browser (Appendix 7.2.1.1.b).

A couple was defined as fully-informative for an SNP if each partner was homozygous or heterozygous for different alleles. Similarly, they were considered to be semi-informative for an SNP when one partner was homozygous and one heterozygous sharing one allele. The embryos from these couples where the origin of parental transcripts could be distinguished were selected for this study.

2.3.2. Sample processing and analysis

2.3.2.1. DNA extraction from whole blood samples

DNA extraction from whole blood was carried out using Qiagen QIAamp maxi kit edition 3 (Qiagen, UK) according to the manufacturer's protocol. Briefly, 500µl protease was mixed with 5ml of blood. Six ml of buffer AL was added to the mixture and the sample was incubated at 70°C for 10 minutes in a waterbath. Five ml of 100% ethanol was added to the sample and mixed. The sample was transferred onto the QIAamp Maxi column and centrifuged at 3000rpm for 3 minutes in a microfuge. Five ml of Buffer AW1 was added to the column and the sample was centrifuged at 4000rpm for 1 minute in a microfuge. Five ml of buffer AW2 was added to the column and it was centrifuged at 4000rpm for 15 minutes in a microfuge. The column was incubated for 10 minutes at 70°C in an incubator to evaporate residual ethanol. DNA was collected by applying 600µl buffer AE directly onto the membrane of the column.

The sample was incubated at RT for 5 minutes and DNA was eluted by centrifugation at 5000rpm for 2 minutes in a microfuge. This step was repeated one more time to achieve higher DNA concentration.

2.3.2.2. Lymphocyte separation using the ficoll-paque plus method

Five ml of blood was diluted 1:1 with 0.9% sodium chloride (NaCl). Six ml of ficoll-paque was added to a 15ml centrifuge tube and 8ml of diluted blood was layered. The samples were centrifuged at 1300rpm for 30 minutes at RT in a bench top centrifuge (the brake of the centrifuge was removed). The lymphocyte layer was removed and placed in a new tube. The layer was washed with 0.9% NaCl by centrifugation at 1300rpm for 15 minutes in a centrifuge. Supernatant was discarded and the pellet was washed two more times. The pellet was resuspended in a fresh 2ml 0.9% NaCl. The cell suspension was stored at 4°C until single cell isolation for no longer than two days.

Cell clumps consisting of 50, 100 and 150 cells were isolated similar to embryo tubing as described in section 2.1.1 excluding the exposure of the cells to acidified Tyrode's solution step. These clumps of cells were used to optimise RNA extraction prior to processing the embryos.

2.3.2.3. Primer design

For sequencing analysis primers were designed using the Primer3 tool in a product size range of 120- 600bp (http://primer3.sourceforge.net/) within the exonic region of *ACTB*, *GAPDH*, *SNRPN, IGF2*, *H19*, *UBE3A* and *BRCA1*. The best primer pairs had lengths of 18-30bp, a maximum guanine-cytosine (GC) base of 50%, similar melting temperature (Tm) values between the forward and the reverse primers and did not have any SNPs within the primer sequence. The selected primers were then analysed on Basic Local Alignment Search Tool (BLAST) program in order to confirm that the primer did not bind non-specifically anywhere else in the genome.

All the primers were ordered in lyophilised form (Eurogentec, UK) and resuspended in Tris-EDTA buffer (Promega, USA). Each primer was aliquoted in 20µl volumes at 50µM upon arrival to prevent multiple freeze-thawing. These aliquots were kept at -20ºC whereas the original stocks were stored at -80ºC.

Primers amplifying short tandem repeat sequences were found using www.genloc.com. These primers were labelled with a fluorochrome at the 5'-end for fluorescent PCR analysis and were designed for aneuploidy screening (Appendix 7.2.1.1.d).

2.3.2.4. Polymerase chain reaction (PCR)

PCR was performed prior to sequencing analysis. DNA obtained from five couples were amplified by PCR for one exonic region within *GAPDH*, three within *ACTB*, five within *UBE3A*, six within *SNRPN*, two within *IGF2*, two within *H19* and eleven within *BRCA1*, respectively (Appendix 7.2.1.1.a and b). PCR was carried out using 1x Qiagen Taq PCR master mix consisting of final concentrations of 2.5 units Taq DNA Polymerase, 1.5mM $MgCl_2$ and 200µM dNTPs (Qiagen, UK). PCR amplification was performed in a final volume of 24µL containing 12.5µL QiaTaq buffer and final concentrations of 0.2-0.3µM forward and reverse primers (Eurogentec, UK) (Appendix 7.2.1.1.a and b) in nuclease-free water. One µL of genomic DNA extracted from blood from couples who donated embryos to this project was added to each reaction mixture making the final volume of 25µL. For each PCR one negative control sample was used in the absence of DNA. Thermal cycling conditions involved denaturation, annealing and extension steps (Table 2.2).

Table 2-2 PCR cycling conditions.

Number of cycles	Temperature (°C)	Time of incubation
1	94	3 minutes
10-30	96	15 seconds
	54-60	45 seconds- 1 minute
	72	1 minute
30-50	94	15 seconds
	54-60	45 seconds
	72	1 minute
1	72	10 minutes
1	4	Hold

PCR conditions were carried out as suggested by the manufacturer (Qiagen, UK) with slight modifications. Briefly, one cycle of initial denaturation step at 94ºC was carried, followed by a total of 40-80 cycles of denaturation at 96ºC, annealing at 54-60ºC and extension at 72ºC. A final annealing was performed at 72ºC.

Successful amplification was examined by observing the intensity of the band with appropriate product size on ethidium bromide stained (2%/1xTBE, tris-borate-EDTA) agarose gel electrophoresis as described in section 2.3.2.5. Failed amplifications and no DNA control samples were detected by the lack of a band.

2.3.2.5. Agarose gel electrophoresis

Non-fluorescent PCR products were analysed by agarose gel electrophoresis. DNA molecules were separated by size using 1-2% agarose gel (agarose powder type 1, Sigma, USA) in 50µL of 1xTris/Borate/EDTA (TBE) buffer. Ten times concentrated TBE buffer was prepared from 108g Tris(hydroxyl)methylamine, 55g orthoboric acid and 40ml of 0.5M EDTA (Sigma, USA) in 900ml deionised water at pH 8. Agarose and TBE mixture was heated in a microwave at medium-high for 2 minutes. One and a half µL of 10mg/ml ethidium bromide was added to the melted agarose (Sigma, USA) to make DNA bands visible on the agarose gels. The warm melted agarose was poured into a gel mould and allowed to set. To have a molecular weight comparison, 1.5µL of GeneRuler™ 100bp-1kb plus DNA ladder (Fermentas, UK) was used. Five µL of product was mixed with 6xloading dye (10mM Tris-HCl at pH 7.6, 0.03% bromophenol blue, 0.03% xylene cyanol FF, 60% glycerol and 60mM EDTA) and the mixture was pipetted into the wells of the gel. The samples were run on the gel in 1xTBE buffer at 150V for 15-20 minutes. The

analysis of DNA bands on agarose gel was carried out with an ultraviolet lamp transilluminator at 360nm (Alpha Innotech Corporation, MultiImage Light Cabinet, Flowgen Staffordshire). The gel was photographed with a camera and the image was analysed on the computer.

2.3.2.6. Sequencing

Successfully amplified samples were sequenced following an initial purification of the samples.

Purification of amplified samples

The amplified products were purified using Microcon Centrifugal Filter Device version PR02725 Rev.B, 07/09 (Millipore, UK) following manufacturer's protocol. Briefly, the amplified products were transferred into a Microcon Centrifugal Filter Device. The sample was centrifuged at 14000rcf for 5 minutes in a microfuge. Four hundred µl DNase- and RNase-free water was added to the sample and they were centrifuged at 14000rcf for 5 minutes in a microfuge. The purified product was then collected by centrifugation at 1000rcf for 2 minutes in a microfuge.

Cycle sequencing reaction

Cycle sequencing was carried out using the BigDye® Terminator v1.1 Cycle Sequencing kit (ABI, UK). The amount of amplified product used for sequencing was estimated from the intensity of the PCR product on agarose gel. If a good amplification (a band with a strong signal on agarose) was observed, 2µl of product was used. If the amplification was moderate (poorer signal on agarose), 4µl of the product and if the amplification was poor (faint signal on agarose), 8µl of the product was used for cycle sequencing. Two to eight µl of amplified sample was mixed with 1µl cycle sequencing primer (2.5µM final concentration), 2µl Big Dye Terminator v1.1 cycle sequencing mix, 3µl BigDye terminator v1.1 5xsequencing buffer and 6-12µl DNase- and RNase-free water. The reaction mixture was mixed and incubated at 96ºC for 10 seconds, 50ºC for 5 seconds and 60ºC for 4 minutes in a thermal cycler. This cycle was repeated 25 times.

Purifying the extension product

The amplified products were purified using DyeEx 2.0 clean up kit (Qiagen, UK) following manufacturer's protocol. Briefly, resin columns were vortexed and centrifuged for 3 minutes at 760g in a microfuge. The sample was applied on the resin and the purified product was collected by 3 minute centrifugation in a microfuge. The purified products were pipetted into 96-well PCR prism plates for sequencing analysis.

Analysis of sequencing products

The sequencing analysis was carried out by the automated laser DNA analyser (ABI Prism™ 3100, UK) using POP-4™ polymer with the dye/primer set of DT3100POP4(BDv3)v1.mob. The data was analysed by GeneScan analysis software (Applied Biosystems, UK). The informativity of the SNPs was investigated by comparing these sequences to the sequence from Ensembl genome browser (Appendix 7.2.1.1.b). If any semi/fully- informative SNPs were identified, RNA from the couple's embryos were extracted as described in section 2.3.2.7 and cDNA was obtained for differential expression analysis (2.3.2.9).

2.3.2.7. DNA and RNA extraction from embryos

Initial practices for RNA extraction were carried out on isolated clumps of lymphocytes (~150, 100 and 50 cells) using the AllPrep DNA/RNA Micro kit version 07/2007 (Qiagen, UK) and Absolutely RNA® Nanoprep kit (Agilent, USA) according to the manufacturer's instructions. DNA and RNA extraction from embryos for differential expression study was carried out using the AllPrep DNA/RNA Micro kit version 07/2007 (Qiagen, UK) with brief modifications to the manufacturer's instructions. Briefly, cells were disrupted by addition of 75µl Buffer RLT containing 0.1% beta-mercaptoethanol (β-Me). Due to the small number of cells, 200ng carrier RNA (Sigma, USA) was added to the Buffer RLT (5µl of 4ng/µl). DNA was retrieved on the AllPrep DNA spin column after centrifugation for 30 seconds at 13000rpm in a microfuge. Five hundred µl of

70% ethanol was added to the flow-through and transferred to the RNeasy MinElute spin column. The sample was centrifuged for 15 seconds at 13000rpm in a microfuge. The column was washed with 500µl of Buffer RPE followed by 500µl 80% ethanol, respectively. RNA was collected in 14µl elution buffer by centrifuging for 1 minute at 13000rpm in a microfuge.

DNA was extracted by washing the AllPrep DNA spin column with 500µl AW1 and AW2, respectively. DNA was eluted by adding 30µl preheated buffer EB (70ºC) to the spin column and centrifuging for 1 minute.

2.3.2.8. Assessment of nucleic acids by Nanodrop and Bioanalyzer

The concentration of DNA was investigated using the Nanodrop technology (Nanodrop, UK) according to manufacturer's protocol. The concentrations of nucleic acids were measured in sample volumes of 1µL at 260nm. The machine was calibrated with DNase- and RNase-free water. Measurements of DNA concentration were presented in ng/µL.

The Agilent 2100 Bioanalyzer (Agilent, CA, USA) was used to assess the quality of RNA and any DNA contamination. Eukaryote Total RNA Pico Series II chip (Agilent, UK) was used following manufacturer's protocol for quantification. This analysis revealed the concentration of RNA, rRNA ratio (28S/18S; ratios greater than 2 indicated lower RNA degradation) and the RNA Integrity Number (RIN) measured RNA quality by assignment of a number from 1 to 10 by the Agilent Bioanalyzer software where 10 indicated the most intact sample (Schroeder *et al.*, 2006).

GraphPad prism v6 software was used for the statistical analyses. RIN values and RNA and DNA concentrations examined by the Bioanalyzer and NanoDrop were analysed by one way ANOVA with Dunnett's post test to examine if there is a trend for RIN values and RNA and DNA concentrations among embryos at cleavage, morula and blastocyst stages due to the embryo quality and the number of cells present, respectively. Further analysis was performed by unpaired two-tailed student's T-test analysing these values.

2.3.2.9. Reverse transcription of RNA obtained from embryos

RNA obtained from embryos were reverse transcribed using the SuperScript™ III first-strand synthesis system for RT-PCR (Invitrogen, UK) following manufacturer's protocol. Briefly, a master mix of 1µl of 50ng/µl random hexamers and 1µl of 10mM dNTP mix was added to 6µl of extracted RNA and incubated at 65ºC for 5 minutes in a thermal cycler. Two µl of 10xRT buffer, 4µl of 25mM $MgCl_2$, 2µl of 0.1M DTT, 1µl of 40U/µl RNaseOut™ and 1µl of 200U/µl SuperScript™ RT were added to the mixture and the cDNA synthesis was carried out by incubation at 25ºC for 10 minutes and 50ºC for 50 minutes in a thermal cycler. This reaction was terminated at 85ºC for 5 minutes. Any mRNA template remaining in the reaction was digested by RNase H at 37ºC for 20 minutes.

cDNA obtained from the embryos was then amplified by PCR (2.3.2.4) and mini-sequencing (2.3.2.10) was carried out to establish a semi-quantitative analysis of differential parental gene expression. A detailed description on how the differential expression was evaluated in cDNA samples from embryos is summarised in section 2.3.2.10.

2.3.2.10. Mini-sequencing (SNaPshot™)

After an initial round of PCR with outer primers, 15µl of PCR product (40 cycles) was treated with 1U SAP (New England BioLabs, UK) and 1U Exo I (New England Biolabs, UK). The reaction mixture was incubated at 37ºC for 1 hour, followed by an enzyme deactivation step at 75ºC for 15 minutes.

SNaPshot™ (Applied Biosystems, UK) analysis involved detection of fluorescence of a single complementary base adjacent to the 3'end of the primer annealing site. Primers were designed to interrogate the base of interest (Appendix 7.2.1.1.c). The reaction was carried out following the manufacturer's instructions with slight changes. Briefly, 2µl SNaPshot™ multiplex ready reaction mix, containing AmpliTaq® DNA polymerase, fluorescently labelled ddNTPs and reaction buffer, 3µl of SAP/Exo I treated PCR product were mixed

with 1µl mini-sequencing primer (final concentration of 0.1µM) and deionised water to make the final reaction volume of 10µl. For each mini-sequencing analysis, genomic DNA from the couple was examined to show the robustness of this technique. The reaction mixture was denatured at 96ºC for 10 seconds, followed by annealing at 50ºC for 5 seconds and elongation at 60ºC for 30 seconds for 25 cycles in a thermal cycler. Each ddNTP was labelled with different fluorescent dyes yielding different product sizes by the SNaPshot™ reaction. ddGTP was labelled with dR110 (blue), ddATP with dR6G (green), ddCTP with dTAMRA™ (black) and ddTTP with dROX™ (red), respectively.

SNaPshot™ products were analysed by ABI Prism™ 310/3100, UK. A mixture of 0.5µl SNaPshot product, 9µl formamide and 0.3µl Liz 120 size standard (PE Applied Biosystems, UK) were aliquoted into lidless tubes (PE Applied Biosystems, UK). All tubes were secured with septa lids (PE Applied Biosystems, UK) and they were denatured for 5 minutes at 95ºC in a thermal cycler. The denatured SNaPshot products were subjected to capillary electrophoresis with the matrix of POP-4™ G5 module 5, 5 seconds of injection at 15 KV and run temperature at 60ºC for 15 minutes (Applied Biosystems, UK). SNaPshot products were analysed by GeneScan analysis software (Applied Biosystems, UK).

Differential expression of parental genes was analysed at previously selected SNP sites. For each SNP analysed paternal to maternal allele peak height ratios was calculated. Differential expression was defined as an allele peak height ratio greater than 1:2. Therefore if the paternal to maternal peak height ratio was equal or more than 2, this was defined as differential expression favouring the paternal transcript. Similarly if the maternal to paternal peak height ratio was 2 or more, this was defined as differential expression favouring the maternal transcript. If the ratio was between 1 and 2, this was defined as similar parental expression level. Mono-allelic or preferential allelic gene expression was only considered in embryos where both parental alleles could be identified at the SNP in the cDNA from the embryo and the only expressed allele present in the cDNA could be attributed to a single parent. In the cases

where a shared allele was the only allele, the sample was excluded from the differential gene expression analysis for that locus (inconclusive result).

Statistical analysis was performed using GraphPad prism v6 software. Significance of differential paternal and maternal expression of the four genes was examined in the embryos using the peak heights of the SNaPshot products.

2.3.2.11. SNaPshot assay sensitivity for semi-quantitative analysis

2.3.2.11.1. Real time PCR validation

cDNA samples obtained from the embryos were amplified by real time PCR to confirm that the parental transcripts can still be quantified accurately and that the product has not reached to plateau prior to mini-sequencing analysis. The same SNP regions analysed in the embryo by SNaPshot assay were quantitatively amplified using high resolution melting (HRM) kit (HRM, Roche, UK) using LightCycler® 480 High Resolution Melting kit (Roche, UK) following manufacturer's protocol. Briefly, 10µl of the Melting Master mix, 0.1µl of the forward and reverse primer (0.25µM), 2µl (2.5mM) $MgCl_2$ in nuclease free water were added to 1µl of cDNA sample in a final reaction volume of 20µl. The cycling conditions for HRM are shown in table 2.3.

The Cq values (the cycle number calculated at the start of the exponential phase of linear amplification) were analysed.

Table 2-3 High resolution melting cycling conditions.

Number of cycles	Temperature (°C)	Ramp (°C/s)	Time of incubation (seconds)	Acquire
1	95	4	600	
45	95	5	10	
	58	4	25	
	72	4	15	Yes

2.3.2.11.2. Chromosome copy number determination by PCR

Copy number of chromosomes 7, 11, 15 and 17 was examined by haplotyping using fluorescently labelled polymorphic short tandem repeat (STR) markers to confirm that the quantification detected by SNaPshot assay was not due to a loss or gain of a chromosome. PCR was carried out as described in section 2.3.2.4 using DNA obtained from embryos and polymorphic markers shown in appendix 7.2.2.1.d. Polymorphic markers used for the analysis of chromosome 7 were linked to *CF* gene, chromosome 11 markers were linked to *HBB*, chromosome 15 to *FBN1* and chromosome 17 to *BRCA1*, respectively.

Fluorescent PCR products were separated and the fragment analysis was performed with an automated laser DNA analyser (ABI Prism™ 310/3100, Applied Biosystems, UK). A mixture of 1μL fluorescent PCR product, 12μL formamide (Applied Biosystems, UK) and 0.3μL ROX size standard (Applied Biosystems, UK) were aliquoted into lidless tubes (Applied Biosystems, UK) and the mixture was denatured at 95ºC for 5 minutes. The denatured PCR products were subjected to capillary electrophoresis with the matrix of Performance Optimised Polymer 4 (POP-4™ G5 module 5, 5 seconds of injection at 15 KV and run temperature at 60ºC for 24 minutes) (Applied Biosystems, UK).

The copy number of the chromosomes was only scored if the embryo was heterozygote and the origin of the parental alleles at that locus can be distinguished. Loss of a chromosome was verified if only one unshared allele was detected. Similarly, gain of a chromosome was detected when three alleles were detected at the locus analysed. Gain of a chromosome due to an isodisomy of the same chromosome could not be detected by this analysis. If only the shared allele was detected, this result was concluded as inconclusive. Allele drop out (ADO) was defined as amplification failure of one of the alleles in a heterozygote cell for that particular region.

2.3.2.11.3. Aneuploidy screening by aCGH

In order to investigate the aneuploidy status of all the chromosomes in the embryos including isodisomies of the same chromosome, aCGH was performed. Whole genome amplification, labelling, hybridisation and microarray kits were performed according to manufacturer's protocol (BlueGnome, UK) (Figure 2.3).

Figure 2-3 Schematic diagram of embryo analysis for chromosomal imbalances using aCGH.

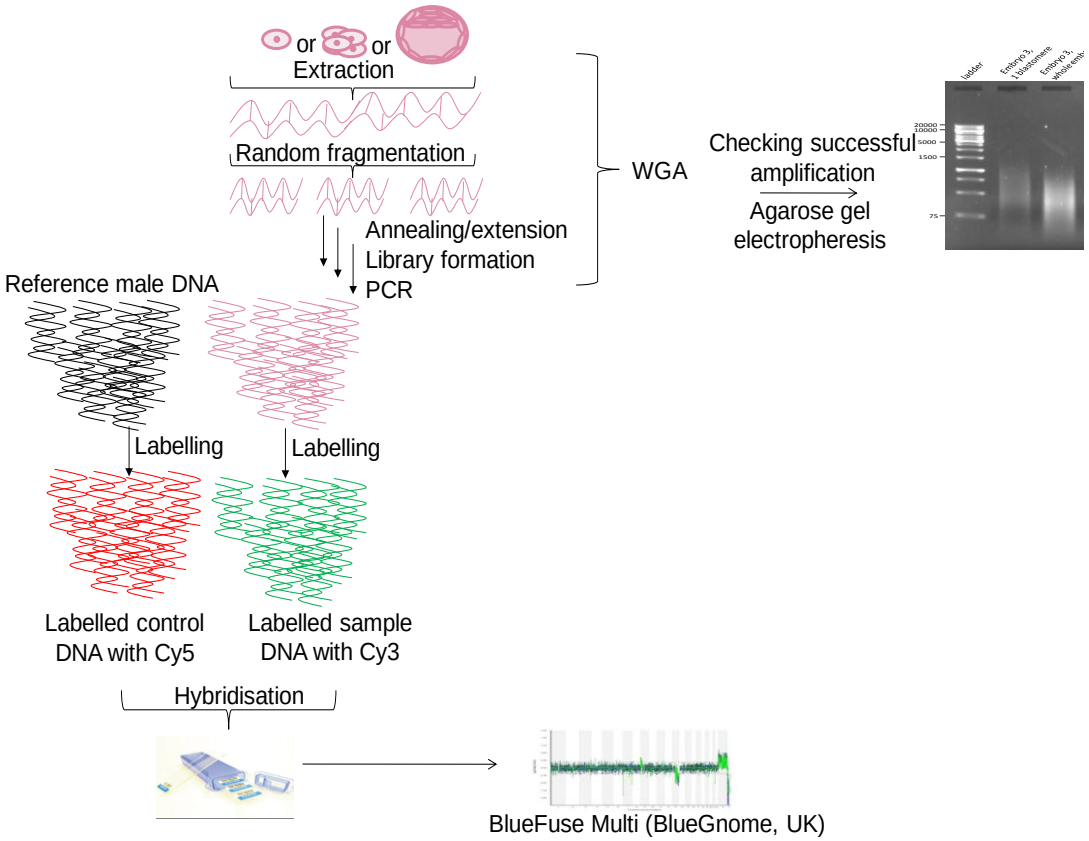

Embryos was analysed for aneuploidy screening by aCGH. The initial step was whole genome amplification by extraction of DNA from cells and formation of library by random fragmentation. The successful WGA was checked by agarose gel electrophoresis. The amplified sample and the reference DNA were labelled with different dyes, respectively and hybridised on arrays. This was then analysed by BlueFuse Multi program.

Whole genome amplification

DNA obtained from embryos was whole genome amplified using SurePlex DNA amplification system v3 (BlueGnome, UK). Whole genome amplification was carried out as described by the manufacturer. The first step was extraction of

DNA from the cells. Three µl extraction buffer was added to each sample. A mixture of 4.8µl extraction enzyme dilution buffer and 0.2µl cell extraction enzyme was added to the sample. DNA was extracted by incubating the reaction mixture at 75ºC for 10 minutes and 95ºC for 4 minutes in a thermal cycler.

A DNA library was created based on random fragmentation using universal primers. A mixture of 4.8µl SurePlex pre-amp buffer and 0.2µl SurePlex pre-amp enzyme was added to the extracted sample. The thermal cycling condition for the pre-amplification is shown in table 2.4.

Table 2-4 Thermal cycling conditions for pre-amplification step of WGA.

Number of cycles	Temperature (ºC)	Time of incubation
1	95	2 minutes
12	95	15 seconds
	15	50 seconds
	25	40 seconds
	35	30 seconds
	65	40 seconds
	75	40 seconds
1	4	Hold

The final step of amplification was carried out by adding 25µl SurePlex amplification buffer, 0.8µl SurePlex amplification enzyme and 34.2µl nuclease-free water to the samples. The amplification cycling condition is shown in table 2.5.

The successful amplification was analysed by observing the intensity of smear and the size range produced on 1%/1xTBE agarose gel as described in 2.3.2.5. Failed amplifications were identified when the smear was absent.

Table 2-5 Thermal cycling conditions for amplification step of whole genome amplification.

Number of cycles	Temperature (ºC)	Time of incubation
1	95	2 minutes
14	95	15 seconds
	65	1 minute
	75	1 minute
1	4	Hold

Successfully amplified embryonic and reference male genomic DNA (BlueGnome, UK) samples were labelled using BlueGnome (UK) fluorescent labelling system, pack 1 v1.1 according to manufacturer's protocol (Figure 2.2). Labelled test and reference samples were hybridised on 24Sure and 24Sure+ bacterial artificial clone (BAC) microarrays, consisting of 3226 BAC clones spaced 1Mb apart for 24Sure and higher resolution of 0.5Mb BACs across genome and 0.25Mb in peri/sub-telomeric regions of human genome for 24Sure+, respectively.

Labelling of the test and reference samples

All labelling steps were carried out on ice and in a darkened room with samples covered during incubation steps. Briefly, 5µL reaction buffer, 5µL primer solution and 5µL dCTP-labelling mixes were added to both test and reference sample tubes, respectively. One µL Cy3 and one µL Cy5 fluorophore were added to test and reference tubes, respectively. Eight µL of amplified libraries of DNA from embryos and reference DNA were added to the sample tubes, respectively. The test and reference tubes were denatured in a pre-warmed thermal cycler for 5 minutes at 94ºC. One µL of Klenow enzyme was added to each tube and the samples were labelled by incubation at 37ºC in a pre-warmed thermal cycler for 16 hours.

Combination and ethanol precipitation

The labelled test (Cy3 fluorophore labelled) and reference samples (Cy5 fluorophore labelled) were mixed. Twenty five µL of 0.1mg/ml COT-1 Human DNA (BlueGnome, UK) was used to suppress the hybridisation of highly repetitive sequences and 7.5µL of 3M sodium acetate (Sigma, USA) were added to each tube for co-precipitation. Absolute ethanol (VWR, UK) was added to each tube and the samples were mixed. The reaction mixture was precipitated at -80ºC for 10 minutes. Labelled samples were pelletted by centrifugation at 13000rpm in a microfuge for 10 minutes. After the supernatant was discarded, the mixture was washed with 500µL of 70% ethanol and air-dried for 2 minutes.

Hybridisation

The pellets were re-suspended in 21µL of pre-warmed 15% dextran sulphate (DS) buffer at 75ºC to ensure that the pellet was completely dissolved. The samples were denatured at 75ºC for 10 minutes in a heating block (VWR, USA). During this time interval, hybridisation chamber was prepared. A slide box with correct dimensions, that enable slides to be laid horizontally across the width of the box, was used. A tissue was saturated with 2xsaline sodium citrate (SSC)/50% formamide (20xSSC: 175.3g of 3M NaCl and 88.2g of 0.3M tris-sodium citrate at pH 7.2). The cover-slips were placed on an array template provided by BlueGnome (UK). Eighteen µL of labelled sample was placed in the centre of each cover-slip and they were transferred to the slide by lowering the slide with the barcode-down. The slides were placed in the hybridisation chamber box where the wet tissue was not in contact with the slides. The box was wrapped with Parafilm (Bemis, USA) and incubated in hybridisation chamber for 3 hours at 47ºC water bath.

Washes

The cover slips were removed manually by agitating in a coplin jar with 2xSSC/0.05% Tween20 (100ml 20xSSC, 899.5ml dH_2O, 0.5ml Tween20) and the slides were washed to remove any un-hybridised DNA as shown in table 2.6. The slides were dried by centrifugation at 11000rpm for 3 minutes in a centrifuge and they were stored in the original blue box until scanning for analysis.

Table 2-6 Washing conditions following aCGH hybridisation.

Wash	Volume	Temperature	Time of incubation	Agitation	Buffer
1	500ml	RT	10 minutes	Stirrer	1xPBS/0.05% Tween 20
2	500ml	RT	10 minutes	Stirrer	1xPBS/0.05% Tween 20
3	500ml	RT	10 minutes	Stirrer	1xPBS/0.05% Tween 20
4	100ml	42°C	30 minutes	Rocker	2xSSC/50% formamide
5	500ml	RT	10 minutes	Stirrer	1xPBS/0.05% Tween 20
6	500ml	RT	5 minutes	Stirrer	1xPBS
7	500ml	RT	5 minutes	Stirrer	1xPBS

Scanning and analysis of aCGH slides

aCGH slides were scanned with slide scanner (ScanArray Express, Perkin Elmer, USA) and analysed using BlueFuse Multi analysis software v.2.6 (BlueGnome, UK). The data was evaluated in two stages. The first stage was carried out during array scanning procedure by checking the intensity and evenness of the fluorescence derived from WGA product and photomultiplier (PMT) values of the individual clones on the array. The second part of the evaluation was carried out after the BlueFuse Multi analysis of the array. This evaluation included checking the number of clones included in the analysis (>60%) and the relation of the autosomes observed within the threshold of ±3xSD (standard deviation). The cut-off for a gain of a segment/whole chromosome was considered when the log2 ratio was more than +0.3 following the BlueFuse Multi analysis v.2.6 (BlueGnome, UK). When the log2 ratio was less than -0.3, this was considered to be loss of that particular segment/whole chromosome.

2.3.2.11.4. Methylation studies

Bisulfite conversion followed by methylation specific PCR was used to investigate the methylation status of *ACTB*, *H19* and *BRCA1* in embryos. EpiTect Bisulfite conversion kit v09/2009 (Qiagen, UK) was used for DNA treatment according to the manufacturer's protocol. Briefly, 85µl bisulfite mix was added to a total volume of 40µl of DNA and water mixture (maximum value of DNA being 40µl). Fifteen µl DNA protect buffer was added to the DNA-bisulfite mixture to prevent fragmentation caused by bisulfite treatment at high temperatures and low pH. The bisulfite conversion was carried out by denaturation and incubation steps in a thermal cycler (Table 2.7).

Table 2-7 Thermal cycling conditions for bisulfite conversion.

Number of cycles	Temperature (°C)	Time of incubation
1	95	5 minutes
1	60	25 minutes
1	95	5 minutes
1	60	85 minutes
1	95	5 minutes
1	60	175 minutes
1	20	Hold

Five hundred and sixty µl of buffer BL with 10µg/ml carrier RNA was added to each sample. This mixture was transferred into the EpiTect spin columns and they were centrifuged at 14000rpm for 1 minute in a top bench centrifuge. The flow-through was discarded and the columns were washed with 500µl buffer BW by centrifuging at 14000rpm for 1 minute. The columns were incubated at RT for 15 minutes with desulfonation buffer and the columns were centrifuged for 1 minute at 14000rpm. The columns were then washed twice with 500µl buffer BW. The columns were incubated for 5 minutes at 56ºC in a water bath to remove any residual liquid. Converted DNA was eluted in 40µl of EB buffer.

Primer design for methylation-specific PCR

Promoter regions of three genes, *ACTB*, *H19* and *BRCA1*, were amplified by nested PCR using outer primer sequences directed to the bisulfite converted sequence and excluding CpG dinucleotides. Two sets of inner primers directed to CpG dinucleotides were designed. One primer was designed to amplify converted and fully methylated sequences producing a product only if the sequences were fully methylated. If the sequence was not methylated, no product was obtained. The second primer was directed to the converted and fully unmethylated sequences. Therefore a product was only obtained when the sequence was unmethylated and if the sequence was methylated, no product was obtained.

Outer primer pairs with no CpG dinucleotides were designed for amplification of bisulfite converted DNA of *ACTB*, *H19* and *BRCA1*. As a result of bisulfite conversion, unmethylated CpG were altered to TpG. Methylated CpG were protected from bisulfite conversion and therefore the sequence remained unchanged. Two sets of inner primer pairs were designed to amplify the converted DNA; one that would bind to the sequence of a fully methylated DNA template and another one that was complementary to a fully unmethylated and therefore to the bisulfite converted template. The primer sets for *ACTB* were designed using the sequence E01094, AF125183 for *H19* and U37574 for *BRCA1* (Esteller *et al.*, 2000), respectively. Primer sequences and the expected

product sizes for these genes are shown in (Appendix 7.2.1.1.e). PCR products were analysed by observing a band and size range produced on 1%/1xTBE agarose gel as described in 2.3.2.5. The absence of a band indicates a failed amplification determining the methylated and unmethylated status.

2.3.2.12. Analysis of developmental progression in embryos carrying *BRCA* mutations

Developmental progression of all the embryos with *BRCA* mutations was examined on day 5/6 post fertilisation. Statistical analysis was performed to investigate if there is significant difference in the developmental progression of embryos with paternally inherited *BRCA* mutations compared to the maternally inherited *BRCA* mutations by Chi-square test using GraphPad prism software v6. The number of embryos with maternally inherited *BRCA* mutations arrested at the cleavage stage was compared to the number of embryos with paternally inherited mutations. Similarly, the significant difference was analysed between the number of embryos arrested at morula stage and embryos that reached to the blastocyst stages depending on the parental inheritance.

2.4. Functional assay development for mismatch repair

2.4.1. Sample collection

A total of 15 immature oocytes and 12 blastocysts were obtained from mouse MF1 strain. Five and ten MF1 oocytes were pooled together, respectively. Four and eight MF1 blastocysts were pooled together, respectively. Good quality 11 surplus human blastocysts were obtained and pooled together from *in vitro* fertilisation (IVF) patients for this project. Embryos were tubed as described in section 2.2.1 with slight changes. The oocytes and blastocysts freed from zona pellucida were washed with 0.1% PBS/PVA and they were pooled together.

2.4.2. Sample processing and analysis

2.4.2.1. Formation of homo/heteroduplex constructs

Homo/heteroduplex molecules were constructed using commercially available oligonucleotides. The oligonucleotides (two complementary strands) with different alleles around rs1981929 SNP site were designed on the *MSH2* gene on chromosome 2 (2p22-p21) by Dr Jaroudi using Ensembl genome browser (http://www.ensembl.org/index.html). Two forward sequences with the same sequence and one complementary (reverse) strand; A, G and T; were used to form homo/heteroduplex constructs, respectively (Table 2.8). The location of the oligonucleotides within the *MSH2* gene is shown in Appendix 7.2.1.2. The original stocks for oligonucleotides at 50/100µM were kept at -20ºC and 5µM working aliquots were prepared to avoid multiple freeze-thawing.

Table 2-8 Oligonucleotide sequences used to make homo/heteroduplexes.

a)

Strand	Oligonucleotide sequence	Fragment size
Forward Strand A —— A ——	5'-TAAAATAAATTGAGTACGAAACAATTTGAATTAAAACACCTGA GTAAATAGTAACTTTGGAGACCTACTGTACTATTTGTACCTTTTG GATCAAATGATGCTTGTTTATCTCAGTCAAAATTTTATGATTTGTA TTCTGTAAAATGAGATCTTTTTATTTGTTTGTTTTACTACTTTCTT-3'	180 bases
Forward Strand G —— G ——	5'-TAAAATAAATTGAGTACGAAACAATTTGAATTAAAACACCTGA GTAAATAGTAACTTTGGAGACCTGCTGTACTATTTGTACCTTTTG GATCAAATGATGCTTGTTTATCTCAGTCAAAATTTTATGATTTGTA TTCTGTAAAATGAGATCTTTTTATTTGTTTGTTTTACTACTTTCTT-3'	180 bases
Reverse Strand T —— T ——	5'- AAGAAAGTAGTAAAACAAACAAATAAAAAGATCTCATTTTACAG AATACAAATCATAAAATTTTGACTGAGATAAACAAGCATCATTTGA TCCAAAAGGTACAAATAGTACAGTAGGTCTCCAAAGTTACTATTTA CTCAGGTGTTTTAATTCAAATTGTTTCGTACTCAATTTATTTTA-3'	180 bases
Reverse Strand Ta ——Ta——	5'-AAGAAAGTAGTAAAACAAACAAATAAAAAGATCTCATTTTACAG AATACAAATCA-3'	55 bases
Reverse Strand Tb ——Tb——	5'-TAAAATTTTGACTGAGATAAACAAGCATCATTTGATCCAAAAGG TACAAATAGTACAGTAGGTCTCCAAAGTTACTATTTACTCAGGTGT TTTAATTCAAATTGTTTCGTACTCAATTTATTTTA-3'	125 bases

b)

Primer	Primer sequence	Locus	Product size
ForA/G (F)	5'-TAAATAGTAACTTTGGAGACCT-3'	2p22-p21	23 bases
RevT/C (R)	5'-GGTACAAATAGTACAG-3'	2p22-p21	17 bases

a) The oligonucleotide sequences around the SNP site rs1981929 showing A and G sequences and the complementary sequence of T and the nicked T; Ta and Tb. The alleles at the SNP site rs1981929 are highlighted in yellow. b) Primer sequences for mini-sequencing analysis. For A/G primer was complementary to T and Tb sequences, and Rev T/C primer was complementary to A and G sequences, respectively.

The mismatched substrates were constructed using the G and T sequences (G-T, Eurogentec, UK) at equal molarity by denaturing at 95ºC for 5 minutes and incubating at 37ºC for 16 hours (Table 2.8). Similarly, a homoduplex (A and T sequences) was constructed by incubation of two complementary strands. Nicked homo/heteroduplex constructs were formed (A/G sequence with Ta and Tb sequences, A-Tn and G-Tn, Table 2.8.a) to test whether the repair was nick-directed (Figure 2.4).

The successful formation of the constructs was confirmed by SNaPshot™ analysis as described in 2.3.2.10 with slight changes. Two primers were designed to detect the allele at the SNP site rs1981929 with different product

sizes (Table 2.8b). The “For A/G” primer binds to the T sequence and “Rev T/C” primer binds to the A and G sequences showing the complementary allele at the SNP site rs1981929, respectively. Two different SNaPshot reaction conditions were applied for each sample. The first condition involved 25 cycles of denaturation at 96ºC for 10 seconds, annealing at 30ºC for 5 seconds and elongation at 37ºC for 30 seconds. The second condition involved the same steps excluding the denaturation step (only annealing at 30ºC for 5 seconds and elongation at 37ºC for 30 seconds for 25 cycles) to test whether there was excess sequences present in the reaction mixture. In the denatured samples, the same fluorescence of each amplified allele as the single sequences should be detected; whereas in the non-denatured constructs, unless excess single sequences were present in the reaction mixture, no fluorescence should be detected (Figure 2.4).

Figure 2-4 Schematic diagram of experimental procedures for assessment of mismatch repair functional assay.

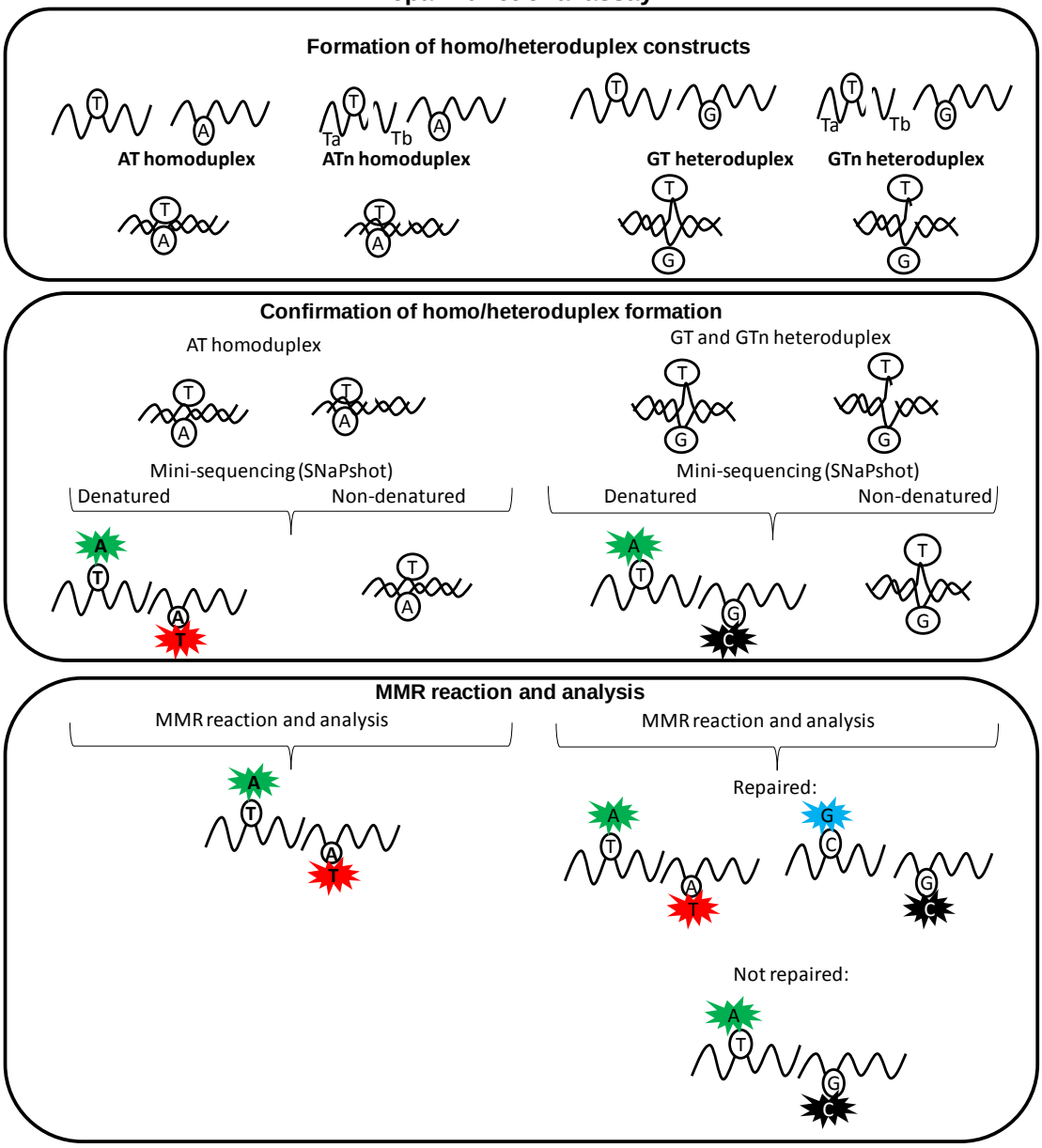

The homoduplex constructs were formed with the two complementary A and T sequences. Mismatched heteroduplex constructs were formed with two complementary sequences; G and T except at the SNP site rs1981929. Nicked heteroduplex constructs were formed using the G sequence and Ta and Tb sequences that are complementary to the G sequence. Successful formation of homo/heteroduplex constructs was confirmed by SNaPshot™ assay using two different cycling conditions by detecting the allele at the SNP site rs1981929. Each allele fluorescences with a different colour; A in green, T in red, C in black and G in blue. Denatured SNaPshot reaction showed all the alleles at the SNP site within that reaction, whereas in the non-denatured samples the alleles that are present in the mixture belonged to the excess sequences following the formation of homo/heteroduplex constructs. Mismatch repair reaction was carried out in the presence and absence of mismatch repair proteins. The mismatch repair efficiency was evaluated by SNaPshot™ assay by detecting the allele at the SNP site rs1981929.

2.4.2.2. Mismatch repair using commercially available nuclear cell extracts

DNA repair efficiency was assessed by exposure of homo/heteroduplex constructs to commercially available nuclear extracts (HeLa, mismatch repair efficient and LoVo, mismatch repair deficient human colorectal cancer cell lines). The reaction conditions were adopted from Wang and Hays (2002b). Briefly, 5-2.5µl homo/heteroduplex DNA constructs (3.33-1.67µg/µl final) were mixed with 13.35-1.33µg nuclear extract in the presence of 3µl of 5x mismatch repair buffer (Table 2.9). Each experiment was also carried out in the absence of nuclear extract or mismatch repair buffer as negative controls. Mismatch repair reaction mixture was incubated at 37ºC for 1-23 hours in a thermal cycler. The reaction was stopped by addition of 30µl stop solution (Table 2.9) and incubation in a thermal cycler at 37ºC for 30 minutes followed by an enzyme deactivation step at 75ºC for 15 minutes.

DNA constructs were purified immediately using DNA clean and concentrator™ (Zymo research corporation, USA) following manufacturer's protocol. Briefly, 90µl of binding buffer was added to each sample and transferred to the column. The reaction mixture was centrifuged at 13000rpm for 30 seconds in a microfuge. The columns were washed twice with 200µl wash buffer and centrifuged at 13000rpm for 30 seconds in a microfuge. The purified product was eluted in 30µl nuclease free water and the products were stored at 4ºC. The purified repaired/non-repaired DNA constructs were analysed by SNaPshot assay as described in 2.3.2.10. The alleles at the SNP site was evaluated for repair, i.e. on a G-T heteroduplex, allele G could be repaired to allele A, or allele T to allele C or partial repair of both sequences could be observed. The peak sizes were compared to obtain an estimate of the repair efficiency for each allele.

2.4.2.3. Mismatch repair using commercially available whole cell extracts

The reaction conditions were optimised to assess mismatch repair in whole cell extract. Similar to the nuclear cell extract assay, DNA constructs at final concentrations of 0.83-0.33µg/µl were incubated with 5-2.5 µg/µl whole cell extract in the presence of 3µl of 5x mismatch repair (MMR) buffer (Table 2.9). The products were purified and analysed as described for the nuclear extracts (2.4.2.2).

Table 2-9 Summary of mismatch repair buffer and stop solution reagents and the preparation of these solutions.

MMR Reaction Mix	
Reagents used in the MMR reaction (final concentrations)	**Preparation of each reagent**
MMR buffer	**Step1: Preparation of 10ml of MMR buffer:**
20mM Tris-HCl (ph 7.6), 1.5mM ATP, 1mM Glutathione, 0.1mM of each of the 4 dNTPs, 5mM $MgCl_2$ and 110mM KCl	7.5 ml nuclease free water + 2ml 1M Tris-HCl at pH 7.6 (VWR International, UK) + 0.5ml 1M stock $MgCl_2$ (Sigma-Aldrich, USA) + 0.82g KCl (Sigma-Aldrich, USA)
	Step 2: Preparation of 10x MMR buffer with ATP and Glutathione
	1ml of 10xsolution1 + 0.008g ATP (Sigma-Aldrich, USA) + 0.003g Glutathione (Sigma-Aldrich, USA)
	Step3: Preparation of 0.1ml of 5 x MMR buffer:
	45µl of 10 x solution1 (from 1ml to which ATP & Glutathione were just added) + 5µl dNTPs (Promega Corp., USA) + 1.25µl BSA (20mg/ml stock concentration, Sigma-Aldrich, USA) + 40µl nuclease free water
Stop Solution	For 30µl of stop solution (for one reaction):15µl of 50mM EDTA (Sigma-Aldrich, USA) + 11.94µl nuclease free water + 2.01µl 10% SDS + 1.05µl Proteinase K (Roche Diagnostics, USA)
25mM EDTA, 0.67% SDS, 9001µg/ml Proteinase K	

Mismatch repair buffer was prepared fresh for each experiment. 10x mismatch repair buffer was prepared first that was then diluted to 5x mismatch repair buffer as the working solution. Stop solution was also prepared fresh for each experiment.

2.4.2.4. Mismatch repair using extracted protein from mouse blastocysts

Total protein was extracted from ten and fifteen pooled MF1 strain mouse blastocysts using AllPrep RNA/protein kit using manufacturer's protocol.

2.4.2.5. Mismatch repair using whole cell extracts from mouse oocytes and mouse and human blastocysts

Whole cell extraction from pooled oocytes and blastocysts was carried out using the whole cell extraction kit (Millipore,UK) following manufacturer's protocol with slight changes. Briefly, each pooled oocyte and blastocyst (mouse MF1 strain and human, respectively) samples were mixed with 20-30µl of extraction buffer mixture and incubated on ice for 15 minutes. This mixture was then centrifuged to obtain the whole cell extract at full speed in a bench top centrifuge. The concentration of proteins within the whole cell extract was measured using the NanoDrop technology (NanoDrop, UK) as described in 2.3.2.8.

Mismatch repair reaction was carried out as described in 2.4.2.2 by exposing a final concentration of 1.67 of heteroduplex to 67% (volume of protein/volume of mismatch repair mixture) oocyte or embryo extract to mismatch repair (MMR) buffer. Semi-quantitative analysis was performed by SNaPshot™ assay as described in 2.3.2.10.

3. Results and Discussion:

The expression level of miRNAs and their target repair transcripts in human oocytes and preimplantation embryos

3.1 Results

Aims summary:

Gene expression is regulated by complex mechanisms. Previous studies showed that miRNAs are involved in the regulation of mRNA expression, such that knocking-down a miRNA led to increased expression of its target mRNA. Similarly, over-expression of a certain miRNA caused reduced expression of its target mRNA. To date, there has not been any study analysing the possible correlation of the expression level of miRNAs with their target repair mRNAs in gametes or preimplantation embryos. The first aim of this project was to investigate if there was any correlation between the expression of miRNAs and their target repair genes in human oocytes and blastocysts. If the expression of a target gene is regulated by a miRNA then the level of expression of the target gene might be expected to be correlated with the level of expression of the corresponding miRNA across samples. A literature search was performed to identify miRNAs and their targets that were shown to play roles in DNA repair (Figure 3.1). The expression of these miRNAs and mRNAs were analysed by real time PCR using TaqMan assays. The possible correlation between the level of each miRNA and its target mRNA in human oocyte and blastocyst samples available was analysed by Pearson correlation test.

3.1.1 Identification of target mRNAs and miRNAs

Differentially expressed DNA repair genes in human oocytes and blastocysts were identified previously (Jaroudi *et al.*, 2009). A literature search to identify miRNAs expressed in human oocytes and blastocysts was performed. This search was narrowed down on the miRNAs that were shown or predicted to regulate these differentially expressed DNA repair genes. From these mRNA and miRNA profiles, repair genes such as miRNAs targeting an important cell cycle checkpoint gene, sensor genes from each pathway and genes involved in different repair pathways, were selected to be analysed in this study (Table 3.1). MiRNAs were selected to target more than one gene that is involved in different repair pathways to be able to have a general idea of the possible regulatory roles of miRNAs in DNA repair pathways.

Figure 3-1 Schematic diagram of the complex association of miRNAs in DNA repair pathways.

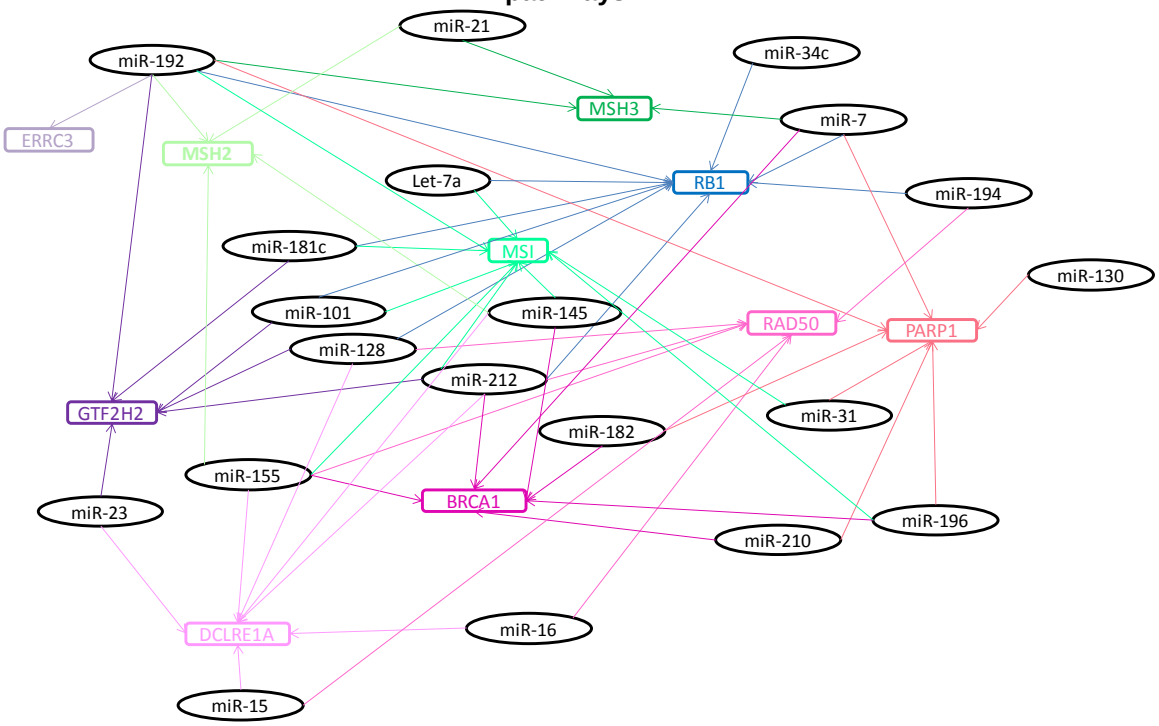

MiRNAs that were shown or predicted to target genes involved in repair were shown in a target map. MiRNAs that were associated with microsatellite instability (indicative of defective mismatch repair) were also shown in this diagram. MiRNAs were colour coded according to their target mRNAs. Double strand break repair genes (*DCLRE1A*, *PARP1*, *BRCA1* and *RAD50*) are shown in pink, mismatch repair genes (*MSH2* and *MSH3*) and microsatellite instability in green, nucleotide excision repair genes (*ERCC3* and *GTF2H2*) in purple and checkpoint genes (*RB1* and) in blue shades, respectively.

Table 3-1 List of miRNAs and their association with DNA repair.

Cell Cycle Checkpoint	Nucleotide Excision Repair		Base Excision Repair	Double Strand Break Repair				Mismatch Repair		
RB1	***GTF2H2***	***ERCC3***	***PARP1***	***DCLRE1A***	***PARP1***	***BRCA1***	***RAD50***	***MSH2***	***MSH3***	***MSI***
Let-7	miR-23b	miR-192	miR-7	miR-15a	miR-7	miR-7	miR-15a	miR-21	miR-7	Let-7a
miR-7	miR-101		miR-31	miR-16	miR-31	miR-145	miR-16	miR-145	miR-21	miR-31
miR-34c	miR-128		miR-130	miR-23b	miR-130	miR-155	miR-128	miR-155	miR-192	miR-101
miR-101	miR-181c		miR-182	miR-128	miR-182	miR-182	miR-155	miR-192		miR-145
miR-128	miR-192		miR-192	miR-145	miR-192	miR-196	miR-194			miR-155
miR-181c	miR-212		miR-196	miR-155	miR-196	miR-210	miR-212			miR-181c
miR-192			miR-210	miR-212	miR-210	miR-212				miR-192
miR-194										miR-196b
miR-212										miR-212

Genes involved in cell cycle checkpoint, nucleotide excision, base excision, double strand break and mismatch repair pathways and the miRNAs targeting these genes are listed. These associations were either published previously as discussed in section 1.4.2.2 or bioinformatics studies showed that these miRNAs target the mRNAs (http://www.targetscan.org/, http://www.microrna.org/microrna/home.do, http://mirdb.org/miRDB/).

3.1.2 mRNA and miRNA expression

Both mRNA and miRNA expression were analysed in human oocytes and blastocysts. mRNA expression was successfully analysed in nine oocytes from 6 women (average age of 32.6±6 years) and ten blastocysts from 8 couples (average age of the women 36.5±7 years) (Table 3.2). Similarly, expression of twenty miRNAs was examined in a total of 22 oocytes from 13 women (average age of 35.3±7) and 23 blastocysts from eight couples (average age of women 36.3±5) (Table 3.2). For each mRNA analysis, *ACTB* was quantified as an internal control in each oocyte and blastocyst samples and for each miRNA analysis, RNU48 was quantified in each oocyte and blastocyst sample.

Table 3-2 Patient and sample details used in the analysis of a) mRNA and b) miRNA expression.

a) Patient and sample information used in the analysis of mRNA expression

Patient ID	Sample number (Developmental stage of the oocytes and blastocysts)	Number of samples used for mRNA expression
4	4.6 (MI)	1
5	5.3 (MI)	1
10	10.2 (MI), 10.3 (MI), 10.4 (MI), 10.5 (MI)	4
22	22.1 (MII)	1
23	23.1 (MI)	1
24	24.1 (MII)	1
15	15.5 (3BA)	1
17	17.2 (3BC)	1
18	18.1 (5AA), 18.2 (5AA), 18.4 (5AA)	3
19	19.5 (1-2CC)	1
25	25.1 (4AB)	1
26	26.1 (1BB)	1
27	27.1 (1AA)	1
28	28.1 (5AA)	1

b) Patient and sample information used in the analysis of miRNA expression

Patient ID	Sample number (Developmental stage of the oocytes and blastocysts)	Number of samples used for miRNA expression
1	1.1 (MI)	1
2	2.1 (MII)	1
3	3.1 (MI)	1
4	4.1 (MII), 4.2 (MII), 4.3 (MII), 4.4 (-MI), 4.5 (MII)	5
5	5.1 (MI), 5.2 (MII)	2
6	6.1 (MI), 6.2 (MII), 6.3 (MII)	3
7	7.1 (MI), 7.2 (MI)	2
8	8.1 (MI)	1
9	9.1 (MII), 9.2 (MII)	2
10	10.1 (MI)	1
11	11.1 (MI)	1
12	12.1 (MI)	1
13	13.1 (MI)	1
14	14.1 (2BB), 14.2 (2CB), 14.3 (2BB), 14.4 (3BB)	4
15	15.1 (2BB), 15.2 (1BB), 15.3 (3BB), 15.4 (2BB)	4
16	16.1 (2BB),16.2 (2BB)	2
17	17.1 (3BC)	1
18	18.1 (5AA), 18.2 (5AA), 18.3 (5AA), 18.4 (5AA), 18.5 (5AA), 18.6 (5AA)	6
19	19.1 (3BB), 19.2 (2AB), 19.3 (2BB), 19.4 (2BB)	4
20	20.1 (3BB)	1
21	21.1 (3BB)	1

Patient ID, sample ID, developmental stage of the sample and number of samples used from this patient investigating a) mRNA and b) miRNA expression are listed. MI represents meiosis I and MII represents meiosis II. The blastocyst grading scheme is described in section 2.2.1.

The expression of each mRNA and miRNA was analysed in a minimum of six individual samples with replicates of two (Table 3.3). Mainly samples were grouped according to the developmental stage to test the expression of one target, i.e. meiosis I (MI) and meiosis II (MII) stage oocytes and similar developmental stage blastocysts were grouped together. A negligible inter-sample variation for the repeats was observed as discussed in sections 3.1.3 and 3.1.4.

Table 3-3 Information for the repeat and replicate oocyte and blastocyst samples used in the analysis of mRNA and miRNA expression.

a) Information of oocyte and blastocyst samples used in the analysis of mRNA expression.

mRNA tested	Samples tested (replicates) in oocytes						Samples tested (replicates) in blastocysts						
RB1	4.6(2)	5.3(2)	10.2(2)	10.3(2)	10.4(2)	10.5(2)	15.5(2)	17.2(2)	18.1(2)	18.4(2)	19.5(2)	25.1(2)	-
GTF2H2	4.6(2)	5.3(2)	10.5(2)	22.1(2)	23.1(2)	24.1(2)	17.2(2)	19.4(2)	25.1(2)	26.1(2)	27.1(2)	28.1(2)	-
ERCC3	4.6(2)	5.3(2)	10.2(2)	10.3(2)	10.4(2)	10.5(2)	17.2(2)	18.1(2)	18.2(2)	18.4(2)	19.5(2)	25.1(2)	-
PARP1	4.6(2)	5.3(2)	10.2(2)	10.3(2)	10.4(2)	10.5(2)	17.2(2)	18.1(2)	18.2(2)	18.4(2)	19.5(2)	25.1(2)	-
DCLRE1A	4.6(2)	5.3(2)	10.2(2)	10.3(2)	10.4(2)	10.5(2)	17.2(2)	18.1(2)	18.2(2)	18.4(2)	19.5(2)	25.1(2)	-
BRCA1	4.6(2)	5.3(2)	10.2(2)	10.3(2)	10.4(2)	10.5(2)	17.2(2)	15.5(2)	18.1(2)	18.4(2)	19.5(2)	25.1(2)	-
RAD50	4.6(2)	5.3(2)	10.2(2)	10.3(2)	10.4(2)	10.5(2)	17.2(2)	18.1(2)	18.2(2)	18.4(2)	19.5(2)	25.1(2)	-
MSH2	4.6(2)	5.3(2)	10.2(2)	10.3(2)	10.4(2)	10.5(2)	15.5(2)	17.2(2)	18.1(2)	18.4(2)	19.5(2)	25.1(2)	-
MSH3	4.6(2)	5.3(2)	10.2(2)	10.3(2)	10.4(2)	10.5(2)	15.5(2)	17.2(2)	18.1(2)	18.2(2)	18.4(2)	19.5(2)	25.1(2)
DICER1	10.2(2)	10.3(2)	10.4(2)	22.1(2)	23.1(2)	24.1(2)	18.1(2)	18.4(2)	25.1(2)	26.1(2)	27.1(2)	28.1(2)	-

b) Information of oocyte and blastocyst samples used in the analysis of miRNA expression.

miRNA tested	Samples tested (replicates) in oocytes							Samples tested (replicates) in blastocysts						
hsa-let-7a	1.1(3)	2.1(3)	3.1(3)	4.1(2)	4.2(2)	4.3(2)	5.1(2)	14.1(3)	14.2(2)	14.3(2)	15.1(3)	15.2(2)	16.1 (2)	-
hsa-miR-7-2	4.1(2)	4.2(2)	4.4(2)	5.1(2)	6.1(2)	7.1(2)	-	14.1(2)	15.2(2)	16.1 (2)	16.2 (2)	17.1 (2)	18.1 (2)	-
hsa-miR-15a	1.1(3)	2.1(3)	8.1(3)	4.1(2)	4.2(2)	4.4(2)	5.1(2)	15.1(2)	15.3(2)	16.1 (2)	18.2(2)	19.1(2)	20.1(2)	-
hsa-miR-16	4.5(2)	5.2(2)	6.2(2)	6.3(2)	7.1(2)	9.1(2)	-	14.1(2)	14.2(2)	15.2(3)	19.2(2)	19.3 (2)	19.4(3)	-
hsa-miR-21	2.1(3)	3.1(3)	4.1(2)	4.2(2)	4.3(2)	5.1(2)	10.1(3)	14.2(2)	14.4(2)	15.1(3)	15.4(2)	16.1 (2)	17.1 (2)	-
hsa-miR-23b	2.1(3)	4.1(2)	4.2(2)	11.1(2)	12.1(2)	10.1(2)	10.1(2)	14.4(2)	15.2(3)	15.3(3)	16.1 (2)	17.1 (2)	21.1 (2)	-
hsa-miR-31	4.4(2)	4.5(2)	5.3(2)	6.1(2)	7.1(2)	9.2(3)	13.1(3)	18.1(2)	18.2(2)	18.3(2)	18.4(2)	18.5(2)	18.6(2)	-
hsa-miR-34c	2.1(2)	4.3(2)	4.4(2)	10.1(2)	11.1(2)	12.1(2)	-	14.4(2)	15.2(3)	15.4(2)	17.1 (2)	18.2(2)	21.1 (2)	-
hsa-miR-101	4.4(2)	4.5(2)	5.2(2)	7.1(2)	7.2(2)	13.1(2)	-	18.1(3)	18.2(2)	18.3(2)	18.4(2)	18.5(2)	18.6(2)	-
hsa-miR-128	1.1(3)	2.1(3)	3.1(3)	4.3(2)	4.5(3)	9.2(2)	-	14.1(3)	14.2(2)	14.3(2)	14.4(2)	15.1(3)	17.1 (2)	-
hsa-miR-130	4.1(2)	4.2(2)	4.4(2)	5.1(2)	6.1(2)	7.1(2)	-	14.1(2)	15.2(3)	16.1(2)	16.2(2)	17.1(2)	18.1(2)	-
hsa-miR-145	2.1(3)	3.1(3)	7.2(2)	4.1(2)	4.2(2)	4.3(2)	5.1(2)	14.1(2)	14.2(2)	14.4(2)	15.1(3)	15.1(3)	16.2(2)	17.1(2)
hsa-miR-155	1.1(3)	3.1(3)	4.3(2)	4.5(2)	5.1(2)	5.1(2)	8.1(3)	14.2(2)	15.3(3)	16.1 (2)	16.2 (2)	18.1 (2)	19.1(2)	-
hsa-miR-181c	4.5(2)	5.1(2)	6.1(2)	6.2(2)	6.3(2)	9.2(2)	-	14.1(2)	14.2(2)	16.2 (2)	19.1(2)	19.3(3)	19.4(3)	-
hsa-miR-182	2.1(3)	4.3(2)	4.4(2)	10.1(2)	11.1(2)	12.1(2)	-	14.4(2)	15.3(3)	16.2 (2)	17.1(2)	18.2(2)	20.1(2)	21(2)
hsa-miR-192	4.5(2)	5.2(2)	6.1(2)	6.2(2)	6.3(2)	7.1(2)	9.1(2)	14.2(2)	16.1 (2)	16.2 (2)	19.2(2)	19.3(2)	19.4(2)	-
hsa-miR-194	5.2(2)	6.1(2)	6.2(2)	6.3(2)	7.1(2)	9.1(2)	-	14.1(2)	14.2(2)	16.2 (2)	19.2(2)	19.3(3)	19.4(3)	-
hsa-miR-196	4.1(2)	4.2(2)	4.3(2)	5.2(2)	9.2(2)	13.1(2)	-	18.1(2)	18.2(2)	18.3(2)	18.4(2)	18.5(2)	18.6(2)	-
hsa-miR-210	4.4(2)	4.5(2)	5.2(2)	6.1(2)	7.2(2)	13.1(2)	-	18.1(2)	18.2(2)	18.3(2)	18.4(2)	18.5(2)	18.6(2)	-
hsa-miR-212	4.1(2)	4.2(2)	4.4(2)	5.1(2)	6.1(2)	7.1(2)	-	14.1(2)	15.1 (2)	16.1(2)	16.2(2)	17.1 (2)	18.2(2)	-

The sample IDs representing the samples (as shown in table 3.2) used to investigate the expression level of each a) mRNA and b) miRNA are listed. The expression of each mRNA and miRNA was analysed in six different samples in duplicates or triplicates shown in parenthesis.

3.1.3 mRNA expression in human oocytes and blastocysts

This study showed that all the genes involved in cell cycle checkpoint and DNA repair, *PARP1*, *BRCA1*, *RAD50*, *MSH2*, *MSH3*, *GTF2H2*, *ERCC3*, *DCLRE1A*, *RB1*, and the miRNA processing gene *DICER*, were expressed in both oocytes and blastocysts. The expression levels ΔCq, fold change and log2 ratio, of all the mRNAs analysed in this study relative to the control gene *ACTB* are shown in table 3.4. Negative controls of real time PCR with no cDNA samples were clear for all the experiments. Sample-sample variation was observed among

individual samples, such that slight variation in the level of expression was observed for the same mRNA in different oocyte and blastocyst samples. Standard deviation of this variation is shown in table 3.4.

Table 3-4 ΔCq values and fold changes for mRNA expression in blastocysts compared with oocytes.

a) List of mRNAs, individual ΔCq and average ΔCq values from 6 repeats in oocytes and blastocysts.

mRNA	Oocyte		Blastocyst	
	Normalised ΔCq values of duplicate PCRs from 6 individual repeats	**Average normalised ΔCq values of duplicate PCRs from 6 individual repeats (SD)**	**Normalised ΔCq values of duplicate PCRs from 6 individual repeats**	**Average normalised ΔCq values of duplicate PCRs from 6 individual repeats (SD)**
RB1	5.20, 5.22, 6.01, 3.67, 4.55, 6.03	5.12 (0.90)	7.98, 12.01, 8.69, 9.59, 11.13, 9.26	9.78 (1.51)
GTF2H2	1.31, 0.49, 1.48, -2.08, -2.12, 2.09	0.69 (1.69)	5.86, 7.76, 7.55, 3.40, 4.59, 5.10	5.71 (1.70)
ERCC3	2.86, 0.15, 0.27, -0.35, -0.46, 0.59	0.51 (1.21)	6.76, 4.78, 5.93, 5.34, 8.19, 6.79	6.30 (1.21)
PARP1	2.81, 2.49, 1.98, 1.14, 2.94, 3.09	2.41 (0.73)	8.18, 7.11, 6.68, 7.27, 9.11, 8.19	7.75 (0.89)
DCLRE1A	1.08, -0.48, -0.22, -0.91, -0.12, -0.41	0.13 (0.91)	9.74, 8.97, 9.11, 7.94, 10.88, 9.71	9.39 (0.97)
BRCA1	2.58, 1.61, 1.65, 1.19, 2.43, 2.79	2.04 (0.64)	7.59, 9.01, 7.78, 10.23, 9.48, 9.62	8.95 (1.05)
RAD50	3.45, 1.21, 0.87, 0.54, 0.90, 2.77	1.62 (1.19)	9.02, 7.68, 9.01, 7.78, 9.82, 9.35	8.77 (0.86)
MSH2	0.93, 0.21, 0.23, 0.49, 0,10, 1.44	0.56 (0.52)	5.78, 6.49, 5.61, 7.41, 7.34, 6.95	6.59 (0.77)
MSH3	2.86, 0.71, 0.83, 0.24, 0.73, 2.52	1.32 (1.09)	7.79, 8.97, 8.52, 10.15, 10.25, 9.99	9.34 (1.00)
DICER	1.80, 1.06, 2.00, -1.12, -0.78, -1.12	0.31 (1.47)	7.57, 8.29, 9.20, 4.95, 4.82, 5.33	6.33 (1.71)

b) List of mRNAs, fold difference in blastocyst compared with oocyte and log2 of fold difference.

mRNA	Fold difference (2ˆΔΔCq) in blastocyst compared with oocyte	Log2 of fold difference
RB1	25.37	4.67
GTF2H2	29.91	4.90
ERCC3	55.32	5.79
PARP1	40.68	5.34
DCLRE1A	615.84	9.27
BRCA1	120.12	6.91
RAD50	142.49	7.15
MSH2	65.47	6.03
MSH3	251.46	7.97
DICER	65.05	6.02

a) mRNAs and ΔCq values in oocytes and blastocysts are listed. Average normalised ΔCq values generated from six repeats with duplicate of each sample is shown. Standard deviation (SD) for each data point of ΔCq is shown in parenthesis. The greater Cq values reflect lower expression. b) mRNAs, fold difference and log2 of fold change in blastocyst compared with oocyte are listed. Fold change was calculated by relative quantification method (2^ΔΔCq). The log2 scale transformation of the fold change facilitates interpretation of the difference in expression between the two samples.

One-way ANOVA with Dunnett's multiple comparison post test was used to analyse the expression of all the normalised target mRNAs in the oocytes and blastocysts in comparison with *GTF2H2*, which is expressed the highest in blastocysts and one of the highest in oocytes (Cq values in Table 3.4 and Figure 3.2). In oocytes, high levels of expression were observed for *GTF2H2, MSH2*, *MSH3*, *ERCC3*, *DCLRE1A* and *DICER*, whereas in blastocysts, high expression levels were observed for *GTF2H2, MSH2*, *ERCC3* and *DICER*.

Figure 3-2 Expression of all the normalised repair genes in comparison with *GTF2H2*.

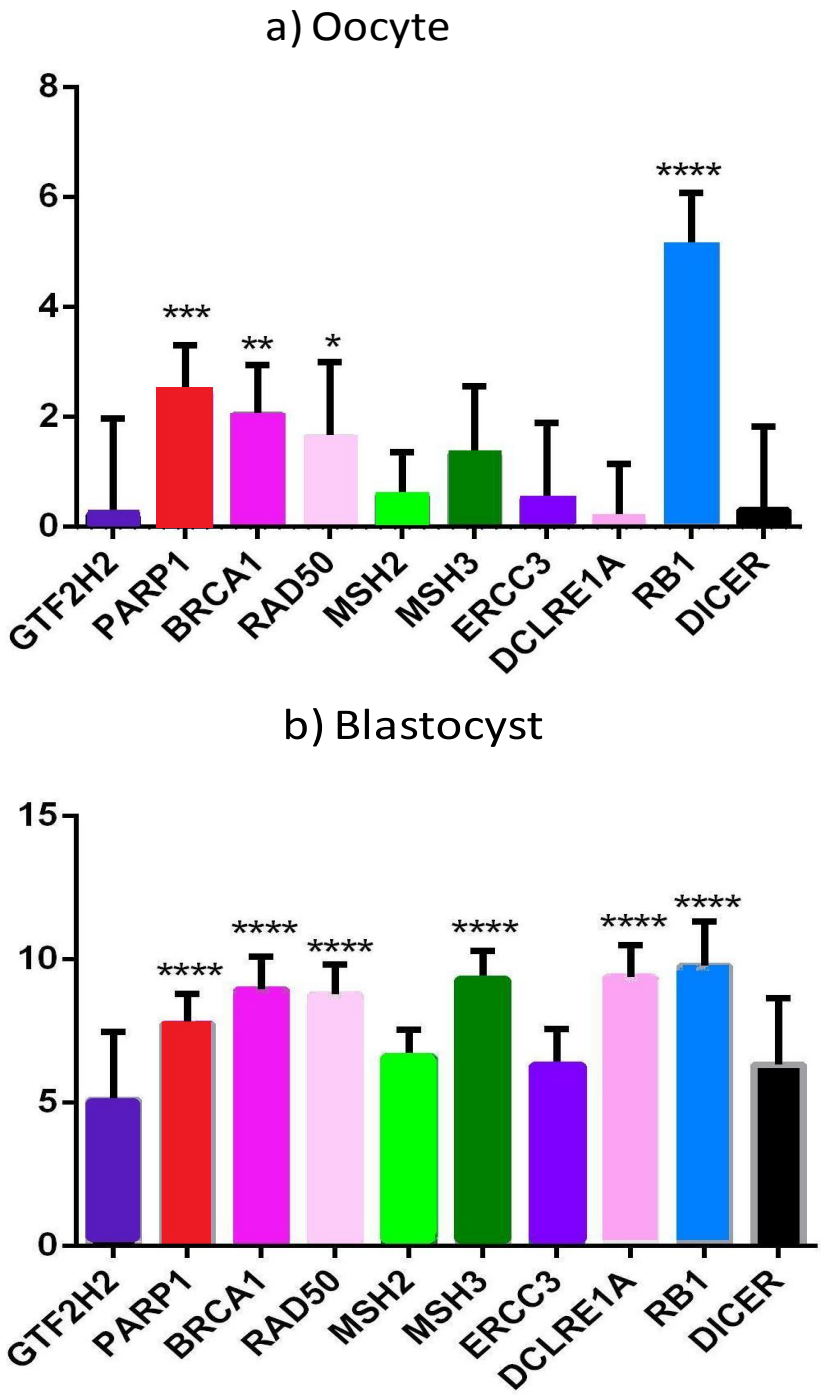

Quantification of target mRNAs compared to *GTF2H2*, which was shown to be expressed at the highest level in a) oocytes and b) blastocysts. ANOVA followed by Dunnett's post test was applied to all the mRNA normalised to *ACTB*; where ****p<0.0001 indicates the most statistical significance, ***0.0001<p<0.001, **0.001<p<0.01, *0.01<p<0.05 less statistical significance and p≥ 0.05 indicates no statistical significance. The x-axis represents all the miRNAs analysed in this study and the y-axis represents the ΔCq values. *GTF2H2* is shown in purple, *PARP1* in red, *BRCA1* in pink, *RAD50* in light pink, *MSH2* in light green, *MSH3* in dark green, *ERCC3* in purple, *DCLRE1A* in mid pink, *RB1* in aqua, and *DICER1* in black shades, respectively.

Expression of each mRNA in oocytes compared with blastocysts was analysed by an unpaired two-tailed student's T-test with the Welch correction. Expression levels of all these genes were significantly higher in oocytes compared with blastocysts (Figure 3.3, $p < 0.05$).

Figure 3-3 mRNA expression levels quantified by real time PCR after normalisation with the endogenous control, *ACTB*.

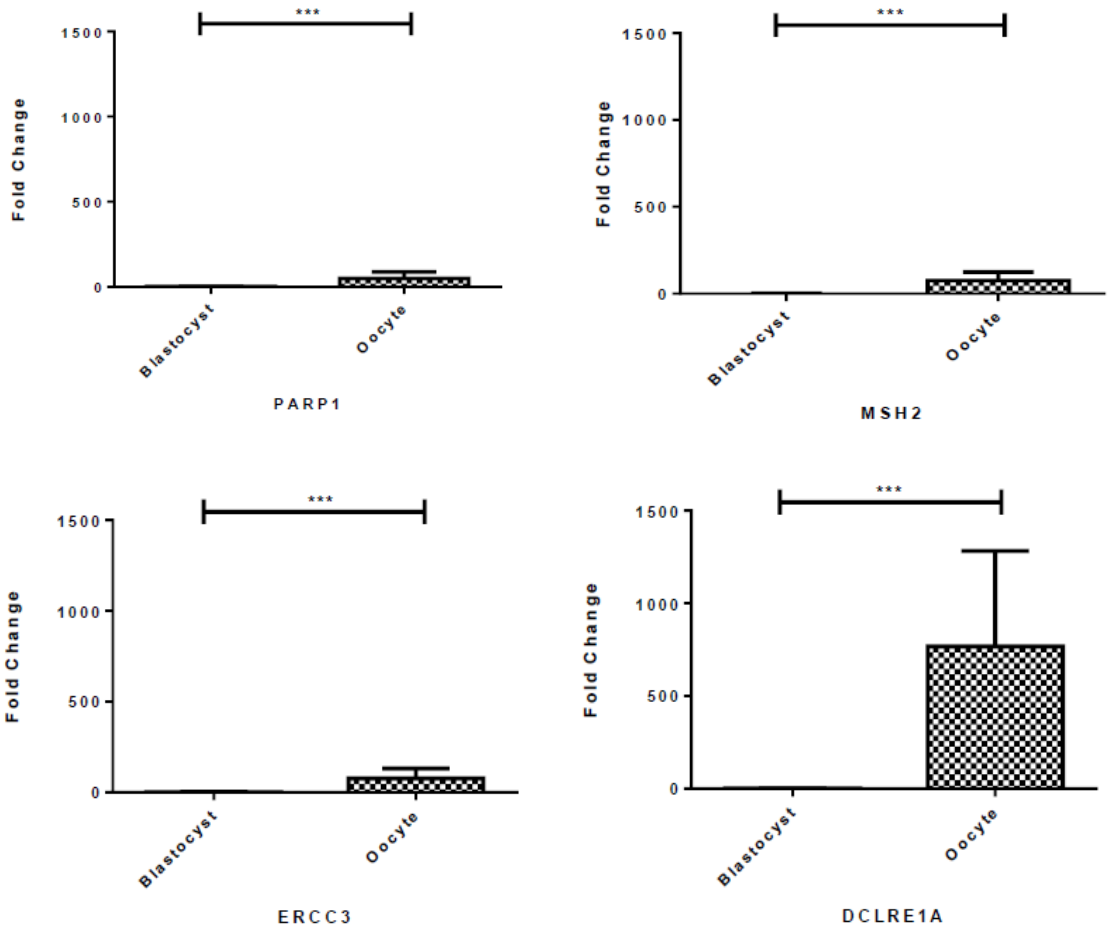

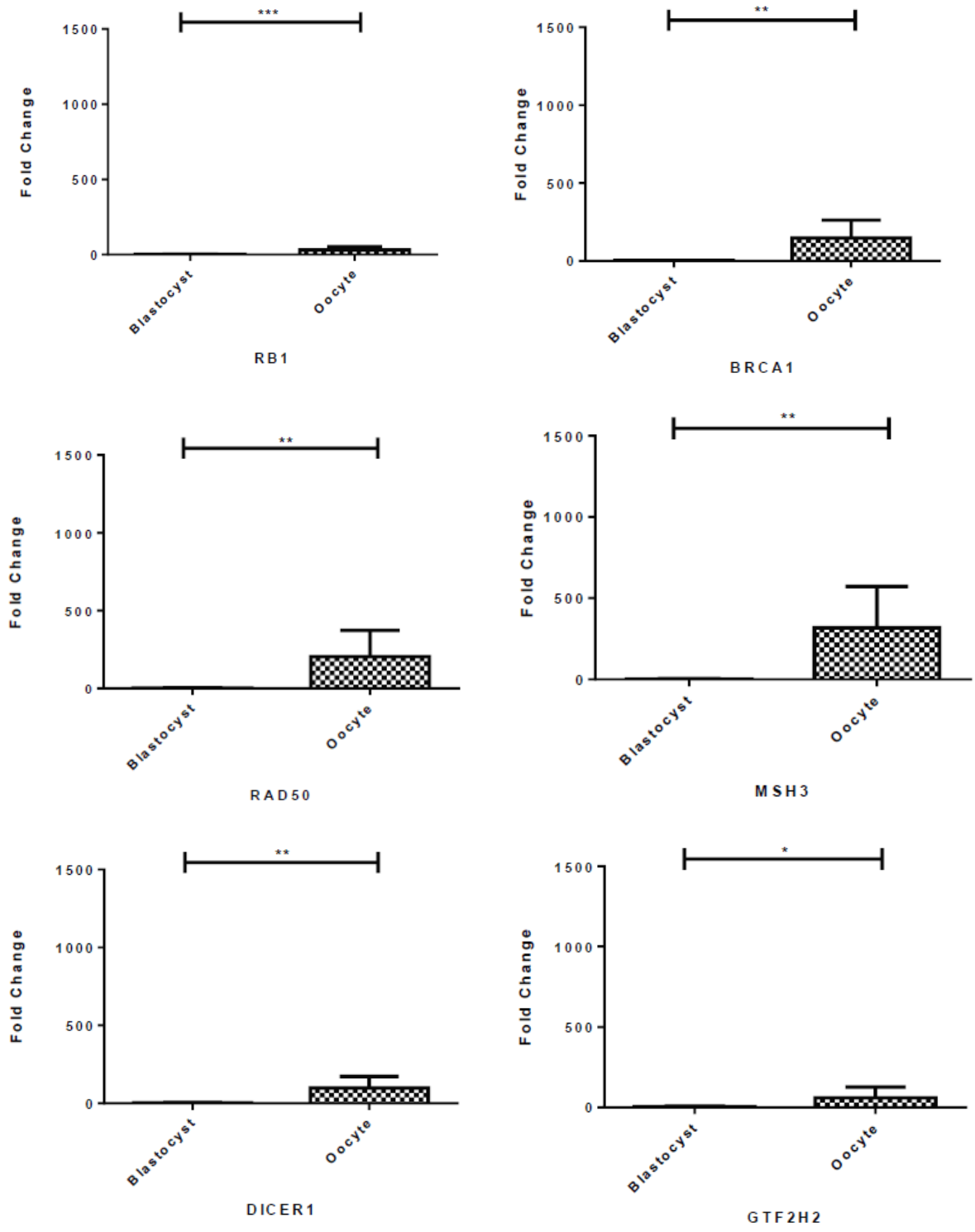

Each gene was analysed in six individual oocytes and six individual blastocysts revealing significantly higher expression levels in the oocytes compared to the blastocysts with ***p<0.001 for *PARP1*, *MSH2*, *ERCC3*, *DCLRE1A* and *RB1*, **p<0.012 for *BRCA1*, *RAD50*, *MSH3* and *DICER* and *0.01<p<0.05 for *GTF2H2*. The x-axis represents blastocyst and oocyte samples and the y-axis represents the fold change.

3.1.4 MiRNA expression in human oocytes and blastocysts

Expression of 20 miRNAs was quantified in oocytes and blastocysts. Of the 20 miRNAs analysed, eleven (hsa-let-7a, hsa-miR-16, hsa-miR-21, hsa-miR-31, hsa-miR-101, hsa-miR-145, hsa-miR-182, hsa-miR-192, hsa-miR-194, hsa-miR-210 and hsa-miR-212) were detected in oocytes. Eighteen miRNAs (hsa-let-7a, hsa-miR-7-2, hsa-miR-15a, hsa-miR-16, hsa-miR-21, hsa-miR-23b, hsa-miR-31, hsa-miR-34c, hsa-miR-101, hsa-miR-128, hsa-miR-130, hsa-miR-145, hsa-miR-155, hsa-miR-182, hsa-miR-192, hsa-miR-194, hsa-miR-210 and hsa-miR-212) were detected in blastocysts, of which seven miRNAs; hsa-miR-7-2, hsa-miR-15a, hsa-miR-23, hsa-miR-34, hsa-miR-128, hsa-miR-130 and hsa-miR-155 were only present in blastocysts. Two miRNAs; hsa-miR-181c and hsa-miR-196; were neither expressed in oocytes nor in blastocysts. All the ΔCq values, fold difference and log2 ratios of these miRNAs in oocytes and blastocysts are listed in table 3.5.

Table 3-5 Average normalised ΔCq values and fold changes for miRNA expression in blastocysts compared with oocytes.

a) List of miRNAs, individual Cq and average Cq values from 6 repeats in oocytes and blastocysts.

miRNA	Oocyte		Blastocyst	
	Normalised ΔCq values of duplicate PCRs from 6 individual repeats	Average normalised ΔCq from 6 individual repeats (SD)	Normalised ΔCq values of duplicate PCRs from 6 individual repeats	Average normalised ΔCq from 6 individual repeats (SD)
let-7a	6.9, 6.4, 5.1, 5.9, 5.3, 6.9	6.11 (0.81)	8.78, 9.22, 13.88, 14.12, 11.67, 10.98	11.44 (2.00)
miR-7-2	Not detected		10.90, 12.22, 16.38, 16.39, 11.76, 14.25, 18.06	13.93 (2.81)
miR-15a	Not detected		8.32, 8.05, 9.24, 7.27, 8.90, 8.30	8.34 (0.69)
miR-16	-1.5, -2.5, -3.1, -0.95, -1.85, -1.20	-1.87 (0.91)	0.48, 1.62, 0.71, 1.09, 0.34, 0.51	0.79 (0.48)
miR-21	5.7, 6.8, 6.1, 5.6, 5.3, 5.4	5.8 (0.61)	5.82, 5.93, 7.13, 3.97, 5.04, 6.04	5.69 (1.06)
miR-23b	Not detected		8.41, 8.38, 9.79, 8.11, 10.94, 9.44	9.17 (1.08)
miR-31	1.7, 1.6, 3.4, 2.5, 3.0, 3.1, 2.4	2.55 (0.72)	6.30, 6.47, 5.61, 6.46, 6.53, 6.21	6.24 (0.33)
miR-34c	Not detected		7.35, 8.40, 8.55, 8.72, 7.55, 7.98	8.03 (0.56)
miR-101	5.5, 6.7, 8.5, 8.5, 10.0, 9.3	8.26 (1.91)	11.20, 10.31, 12.47, 10.17, 10.46,10.3	10.03 (0.92)
miR-128	Not detected		7.96, 6.67, 8.67, 8.48, 8.89, 7.80	8.09 (0.91)
miR-130	Not detected		8.09, 6.75, 6.84, 7.32, 7.78, 7.36	7.36 (0.52)
miR-145	7.95, 10.32, 9,38, 6.11, 6.91, 7.17	7.94 (1.59)	10.81, 11.57, 12.42, 12.16, 12.83, 11.90	11.91 (0.64)
miR-155	Not detected		11.40, 9.12, 12.40, 11.43, 11.23, 11.02	10.97 (1.07)
miR-181	Not detected		Not detected	
miR-182	6.33, 6.81, 6.20, 6.00, 7.82, 5.85	6.49 (0.72)	5.11, 6.27, 6.15, 5.63, 5.78, 7.75	6.11 (0.90)
miR-192	2.42, 4.08, 2.32, 2.71, 4.91, 4.25	3.45 (1.1)	1.87, 6.73, 4.81, 7.34, 2.33, 2.51	4.27 (2.38)
miR-194	6.07, 5.51, 4.42, 6.05, 4.83, 5.7	5.90 (0.67)	3.42, 5.34, 4.18, 7.38, 4.87, 4.51 (1.35)	4.95
miR-196	Not detected		Not detected	
miR-210	4.14, 7.65, 5.16, 7.36, 4.64, 6.51	5.91 (1.44)	7.60, 7.17, 7.16, 9.01, 7.83, 7.69	7.75 (0.67)
miR-212	5.36, 8,71, 6.59, 6.38, 4.96, 5.27	6.29 (1.38)	8.92, 9.93, 8.20, 7.56, 9.83, 10.05	9.08 (1.03)

b) List of miRNAs, fold difference in blastocyst compared with oocyte and log2 of fold change difference.

miRNA	Fold difference (2^-ΔΔCq) in blastocyst compared with oocyte	Log2 of fold difference
let-7a	14.39	3.85
miR-7-2	N/A	N/A
miR-15a	N/A	N/A
miR-16	6.63	2.73
miR-21	0.59	-0.74
miR-23b	N/A	N/A
miR-31	12.84	3.68
miR-34c	N/A	N/A
miR-101	6.26	2.65
miR-128	N/A	N/A
miR-130	N/A	N/A
miR-145	17.17	4.10
miR-155	N/A	N/A
miR-181	N/A	N/A
miR-182	0.74	-0.43
miR-192	1.52	0.60
miR-194	0.52	-0.94
miR-196	N/A	N/A
miR-210	2.37	1.24
miR-212	7.47	2.90

a) miRNAs and ΔCq values in oocytes and blastocysts are listed. Average normalised ΔCq values generated from six repeats with two replicates of each sample is shown. Standard deviation (SD) for each data point of ΔCq is shown in parenthesis. The greater Cq values reflect lower expression. b) MiRNAs, fold change difference and log2 of fold change in blastocyst compared with oocyte are listed. Fold change was calculated by relative quantification method (2^-ΔΔCq). The log2 scale transformation of the fold change facilitates interpretation of the difference in expression between the two samples. The negative log2 values indicated increased expression of the gene in the blastocyst compared with the oocyte. N/A stands for not applicable.

The expression of each normalised miRNA was examined in comparison with hsa-miR-16, expressed highest in the oocytes and blastocysts, by one-way ANOVA with Dunnett's multiple comparison post test. All the miRNAs tested were expressed at significantly lower levels compared to hsa-miR-16 (Cq values in Table 3.5 and Figure 3.4).

Figure 3-4 Expression of all the miRNAs in comparison with hsa-miR-16.

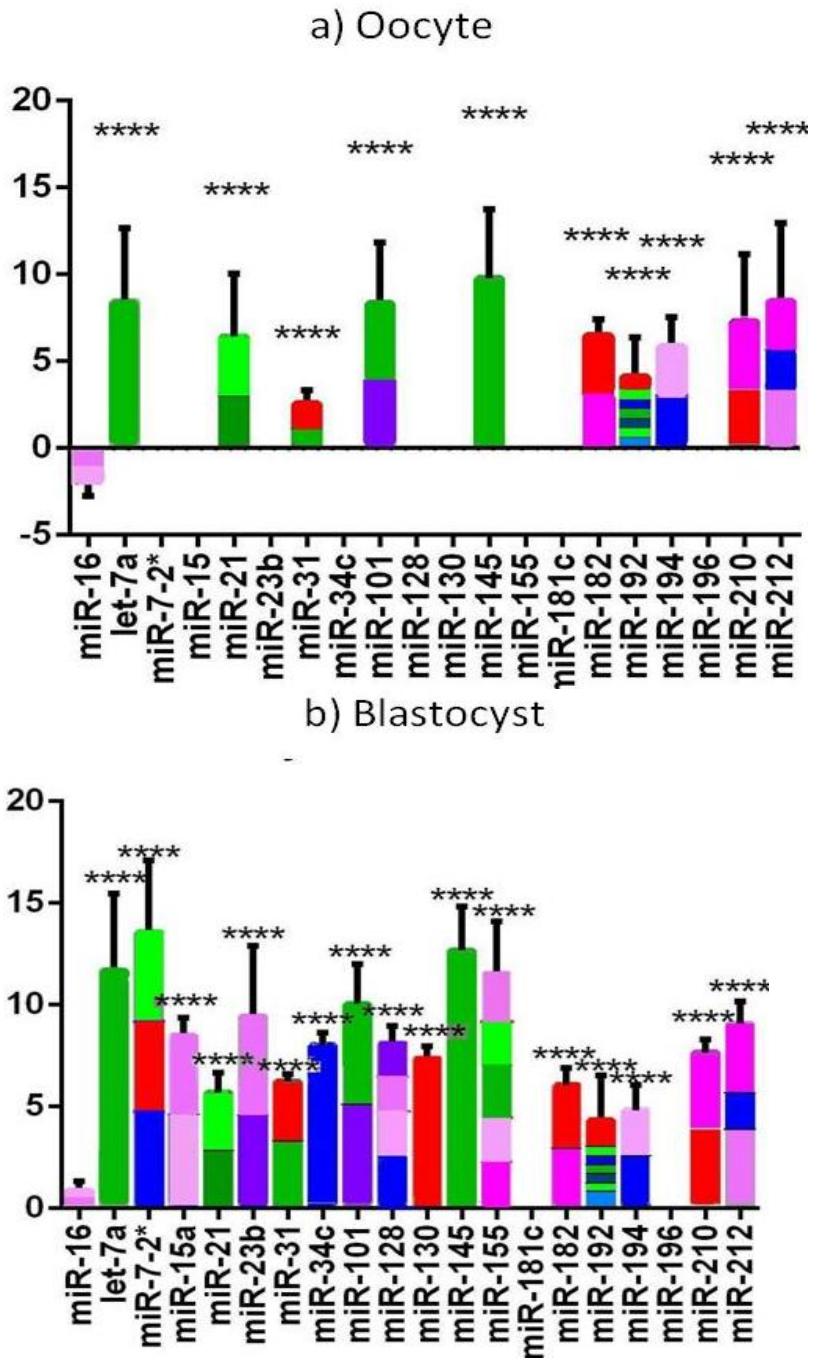

Quantification of target miRNAs compared to hsa-miR-16 a) in oocytes and b) in blastocysts. ANOVA followed by Dunnett's post test was applied to all miRNAs compared to hsa-miR-16. The x-axis represents all the miRNAs analysed in this study and the y-axis represents the ΔCq values. In oocytes the expression of hsa-miR-16 was at a higher expression level compared to the endogenous control RNU48 represented by a negative profile for this miRNA. MiRNAs were colour-coded according to their target genes as in figure 3.1, i.e. miRNAs targeting *PARP1* is shown in red, *BRCA1* in pink, *RAD50* in mid pink, *DCLRE1A* in light pink, *MSH2* in light green, *MSH3* in dark green, *ERCC3* in purple, *GTF2H2* in lilac and *RB1* in aqua shades, respectively. **** represents that the difference in level of expression of the miRNA from that of hsa-miR-16 is statistically significant ($p<0.001$).

Similar to the statistical analysis performed for mRNA expression analyses, unpaired two-tailed student's T-test with the Welch correction was applied on eleven miRNAs expressed both in oocytes and blastocysts. For the rest of the nine miRNAs, statistical analysis could not be carried out since these miRNAs were not expressed in oocytes or in blastocysts. Expression levels of six miRNAs (for hsa-let-7a, hsa-miR-16, hsa-miR-31, hsa-miR-145, hsa-miR-210 and hsa-miR-212) in oocytes were significantly higher than in the blastocysts ($p < 0.01$, Figure 3.5). Although hsa-miR-101 and hsa-miR-192 were expressed at higher levels in the oocyte, this increase was not significant. Similarly even though hsa-miR-21, hsa-miR-182 and hsa-miR-194 were expressed more in the blastocyst, this increased expression was also not significant (Figure 3.5)

Figure 3-5 MiRNA expression levels quantified by real time PCR after normalisation with the endogenous control, RNU48.

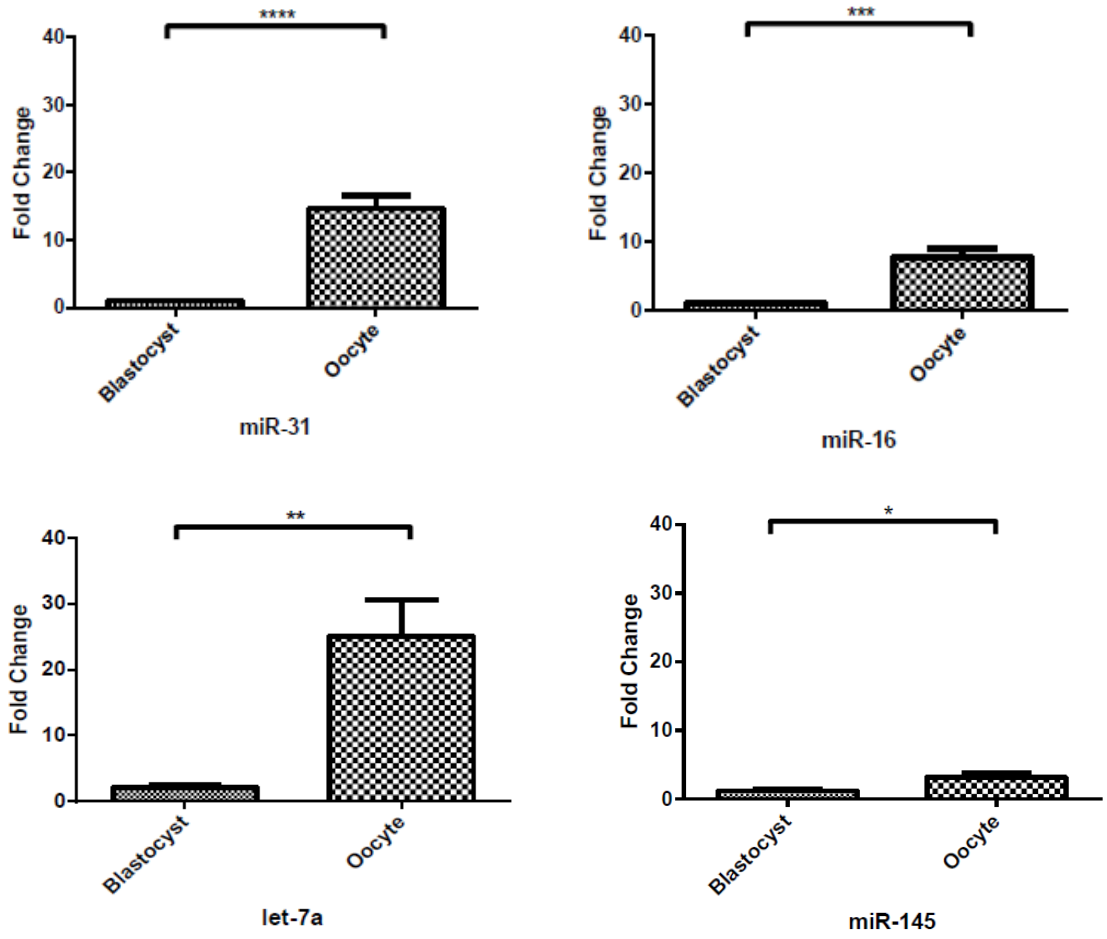

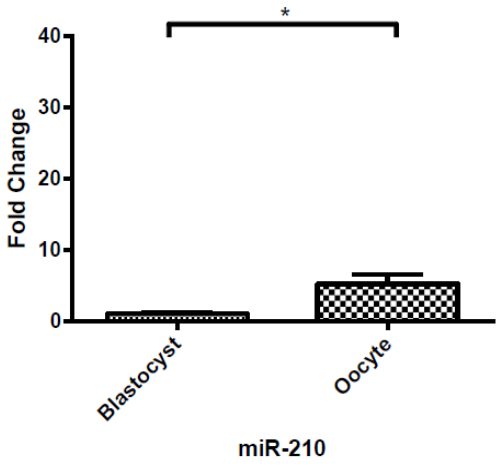

miR-210

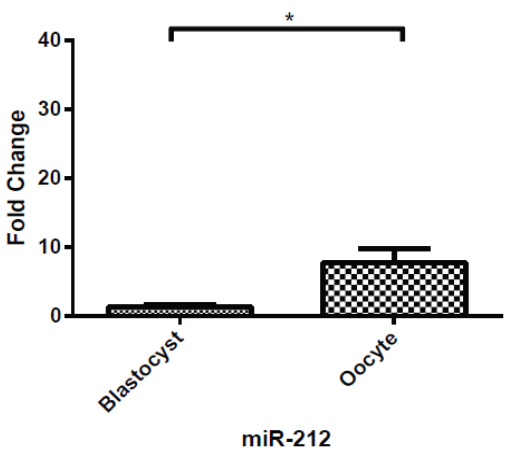

miR-212

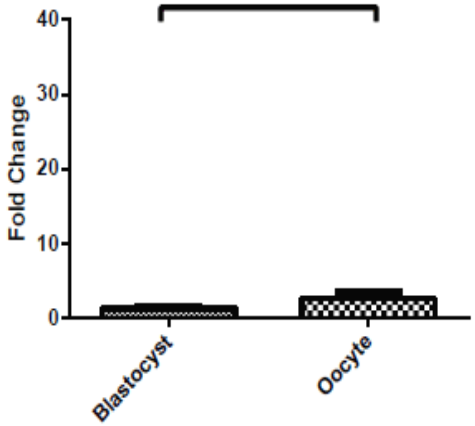

miR-21

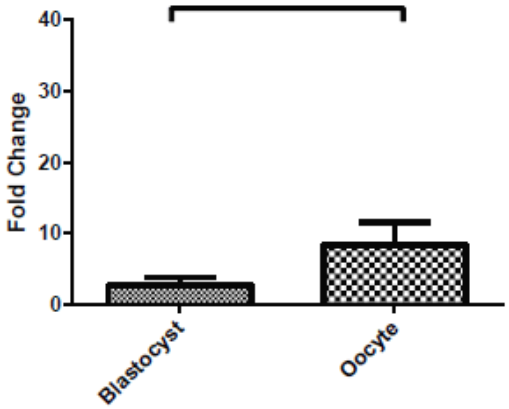

miR-101

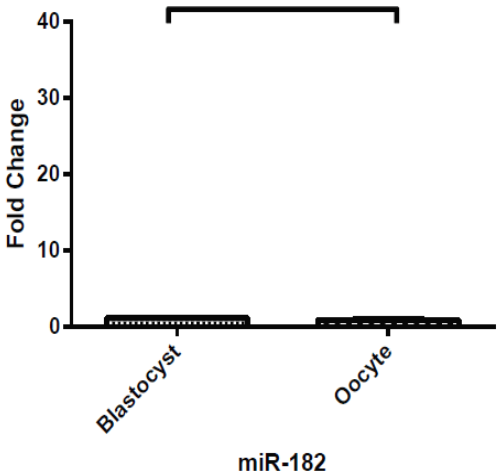

miR-182

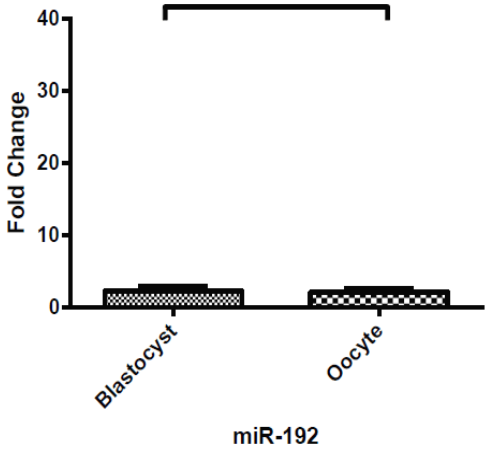

miR-192

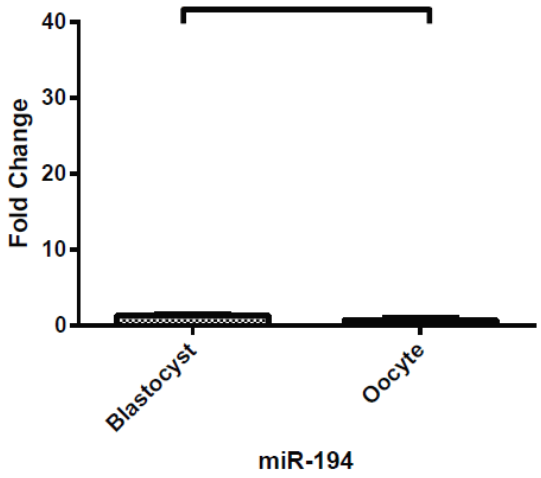

Each gene was analysed in six individual oocytes and six individual blastocysts revealing significantly higher expression levels in the oocytes compared to the blastocysts in hsa-miR-31 (****p<0.005), hsa-miR-16 (***p<0.05), hsa-let-7a (**p<0.001), hsa-miR-145 (*0.01<p<0.05), hsa-miR-210 (*0.01<p<0.05) and hsa-miR-212 (*0.01<p<0.05). The remaining five miRNAs (hsa-miR-21, hsa-miR-101, hsa-miR-182, hsa-miR-192 and hsa-miR-194) showed no significant difference in the levels of expression. The x-axis represents blastocyst and oocyte samples and the y-axis represents the fold change.

3.1.5 Correlation between the expression of miRNAs and their target mRNAs

Overall these results showed that the expression level of most of the miRNAs analysed and their target repair mRNAs are higher in oocytes than in blastocysts after normalisation with endogenous control transcripts (summarised in Table 3.6). In addition the question of whether those individual samples with higher miRNA levels might tend to have lower levels of the target mRNAs or perhaps a consistent correlation in the other direction was asked. Either of these findings might be suggestive that the target mRNA was being regulated primarily by its miRNA and perhaps provide insight into the mechanism. In order to investigate this, the expression levels of each miRNA (normalised using RNU48) and target mRNA (normalised using *ACTB*) were plotted against each other and a Pearson correlation test was applied. It was immediately apparent that there were both negative and positive correlations in the different comparisons and only a few showed statistical significance. In fact after correction for multiple testing none was statistically significant (threshold of

0.002 in oocytes and 0.001 in blastocyst). This data was summarised in Table 3.6.

3.1.6 Summary of miRNA and mRNA expression analysis

Technical aspects

- Real time PCR for a total of 31 oocytes and 33 blastocysts was successfully performed for mRNA and miRNA expression analyses.
- The expression of 20 miRNAs and 10 mRNAs was successfully analysed in six individual oocyte and blastocyst samples, respectively.

Biological aspects

- A summary table shows a list of mRNAs and miRNAs detected in human oocytes and blastocysts (Table 3.6). MiRNAs expressed at significantly higher levels in oocytes compared blastocysts are listed.

Table 3-6 Summary table of mRNAs and miRNAs expressed in oocytes and blastocysts and the significant expression of mRNAs and miRNAs with correlation analysis.

mRNAs expressed in oocytes	mRNAs expressed in blastocysts	MiRNAs expressed in oocytes	MiRNAs expressed in blastocysts	Significantly higher expression in oocytes relative to blastocysts of	
				mRNAs	miRNAs
RB1	*RB1*	let-7a	let-7a	*RB1*	let-7a
GTF2H2	*GTF2H2*	miR-16	miR-7-2	*GTF2H2*	miR-16
ERCC3	*ERCC3*	miR-21	miR-15a	*ERCC3*	miR-31
PARP1	*PARP1*	miR-31	miR-16	*PARP1*	miR-145
DCLRE1A	*DCLRE1A*	miR-101	miR-21	*DCLRE1A*	miR-210
BRCA1	*BRCA1*	miR-145	miR-23b	*BRCA1*	miR-212
RAD50	*RAD50*	miR-182	miR-31	*RAD50*	
MSH2	*MSH2*	miR-192	miR-34c	*MSH2*	
MSH3	*MSH3*	miR-194	miR-101	*MSH3*	
DICER	*DICER*	miR-210	miR-128	*DICER*	
		miR-212	miR-130		
			miR-145		
			miR-155		
			miR-182		
			miR-192		
			miR-194		
			miR-210		
			miR-212		

Each mRNA and miRNA expressed in human oocytes and blastocysts are listed (first four columns). mRNAs and miRNAs showing significant higher expression levels in oocytes compared with blastocysts are listed. In the last two columns results of correlation analysis are shown. Significant direct and inverse correlation results were only observed in blastocysts and miRNAs. List of miRNAs and their target mRNAs with significant correlations are listed.

3.2 Discussion

The level of gene expression is affected by many factors including miRNA regulation. Several studies have investigated the regulation of DNA repair gene transcripts by miRNAs in cell lines and in tissues. In this project, the possible correlation between the expression level of DNA repair gene transcripts and miRNAs in human oocytes and blastocysts was investigated.

3.2.1 Expression of mRNAs

The expression of one miRNA processing gene (*DICER*), one cell cycle checkpoint gene (*RB1*), four double strand break repair genes (*PARP1*, *BRCA1*, *RAD50*, *DCLRE1A*), two mismatch repair genes (*MSH2*, *MSH3*) and two nucleotide excision repair genes (*GTF2H2*, *ERCC3*) were analysed successfully by quantitative real time PCR (using TaqMan assays). The overall expression levels of these mRNAs were significantly higher in human oocytes compared to blastocysts. The high level of expression of all the repair genes in oocytes suggests that the early developing embryo is packed with transcripts to detect and initiate repair pathways if subjected to DNA damage. Although there are functional studies showing mismatch repair and double strand break repair in Xenopus oocytes and in extracts (Maryon and Carroll, 1989, Oda *et al.*, 1996, Petranovic *et al.*, 2000, Varlet *et al.*, 1996, Labhart, 1999, Jeong-Yu and Carroll, 1992), recent studies in mouse oocytes showed that damage is detected at MII oocytes, but the repair is impaired (Marangos and Carroll, 2012). Therefore, although the expression of repair genes were detected in oocytes and blastocysts, the functional activity of DNA repair pathways may vary due to the regulatory factors of repair genes and proteins, such as miRNA regulation at protein level. In oocytes where high expression levels of repair mRNAs were detected, it is possible that miRNAs destabilise translation causing impairment of repair pathways.

3.2.2 Expression of miRNAs

The expression of twenty miRNAs targeting the nine genes involved in different DNA repair pathways was analysed. The expression levels of 73% (6/11) of

these miRNAs (hsa-let7a, hsa-miR-16, hsa-miR-31, hsa-miR-145, hsa-miR-210 and hsa-miR-212) were significantly higher in the oocytes compared with the blastocysts. This high expression of miRNAs in the oocytes may be required to degrade maternal mRNAs or stabilise some of their target genes during embryonic genome activation (Giraldez *et al.*, 2006).

3.2.3 Possible correlation of miRNA expression with mRNA expression

The correlation analysis was performed for each miRNA and its target mRNA in order to investigate if the expression level of mRNA tends to vary depending on the expression level of miRNAs. Overall only a few miRNAs and mRNAs showed significant correlation (summarised in table 3.6) with both negative and positive correlations and no consistent pattern was observed. Furthermore following correction for multiple testing, no statistical significance was observed. The lack of any meaningful correlation in the expression levels of the miRNAs and their targets was perhaps not surprising. The small quantities of the samples prevented us from conducting the most meaningful comparisons, which would have been to look at the developmental trends. One of the possibilities to overcome this limitation would have been to pool samples of the same developmental stage and to investigate the expression of all the miRNAs and their targets using the same set of pooled samples and eliminate large sources of variation.

3.2.4 Conclusion and future work

The overall expression level of the repair genes was shown to be higher in oocytes compared to blastocysts as also shown by Jaroudi *et al.* (2009). Similarly, many of the miRNAs (6/11) looked at in this study were expressed significantly more in the oocytes compared to the blastocysts.

Regulation of mRNAs involves complex mechanisms, amongst which are included the action of miRNAs. Adding to this complexity is that each miRNAs may have multiple mRNA targets, and also that each mRNA may be regulated

by more than one miRNA. The failure to detect any clear relationship in the patterns of expression is therefore not all that surprising.

One of the main limitations of this study was the practical inability of following the expression of miRNA and mRNA through different developmental stages. Due to the scarcity of human samples and the expense of the expression analysis, only a limited number of miRNA and mRNA targets were analysed, furthermore in different oocyte and blastocyst samples. With hindsight the experimental design might have been improved. Another limitation was the small number of target genes including the house keeping gene analysed. Although genome wide expression analyses have been performed in human oocytes and preimplantation embryos; no gene has been identified as a robust housekeeping gene (or genes). Therefore more than one candidate housekeeping gene should have been included in the experimental design of this study. However this was not possible in this project due to the limited number of samples available and cost of the analyses.

Further studies will aim to focus on expression of more miRNA and target mRNAs, preferably within the same oocyte and blastocyst samples. Once the expression profiles of miRNAs and DNA repair gene transcripts has been established, it may be possible to shed light as to whether there is any correlation between miRNA and their target mRNAs. Finally functional studies would be necessary to validate information on the regulatory roles of miRNAs on their target mRNAs.

4. Results and Discussion

Differential allelic expression in preimplantation embryos and potential relation with differential methylation

4.1 Results

Aims summary

Differential expression of parental genes is suspected to be present in embryos due to the differential methylation of parental genomes observed in the early developing mouse embryos (Dean *et al.*, 2003, Tamaru and Selker, 2001, Jackson *et al.*, 2002, Fuks *et al.*, 2003). Parental expression of imprinting genes has been analysed in human embryos. However, there are no studies analysing differential parental expression of repair genes in preimplantation embryos. It is possible that differential gene expression is present in the early stages of human preimplantation embryos due to the differential methylation of parental genomes.

The second aim of this project was to investigate if there was differential parental expression of *ACTB*, *SNRPN*, *H19* and *BRCA1* in human embryos due to the differential demethylation of the parental genomes. A further analysis was performed to investigate if the presence of maternally or paternally inherited *BRCA* mutations affects the development of the preimplantation embryos depending on the parental inheritance. Semi-quantitative mini-sequencing analysis was performed on the cDNA of embryos to target informative SNPs identified by sequencing the parental genomic DNA. The methylation status of a subset of embryos were confirmed by bisulfite conversion followed by methylation specific PCR.

4.1.1 Sample selection

Initial screening by sequencing identified informative SNPs within *ACTB*, *SNRPN*, *H19* and *BRCA1* for five couples (Figure 4.1, Appendix 7.3.1.1). Ten more couples were further tested by mini-sequencing targeting these selected SNPs. Overall, 15 couples were shown to be semi- or fully-informative for a total of five SNPs within four genes (Table 4.1). Twenty seven exonic regions within three more genes (*GAPDH*, *UBE3A*, *IGF2*) were sequenced, however none of the couples were informative for the SNPs analysed.

Figure 4-1 Sequencing panels obtained from genetic analyser ABI Prism™ 3100.

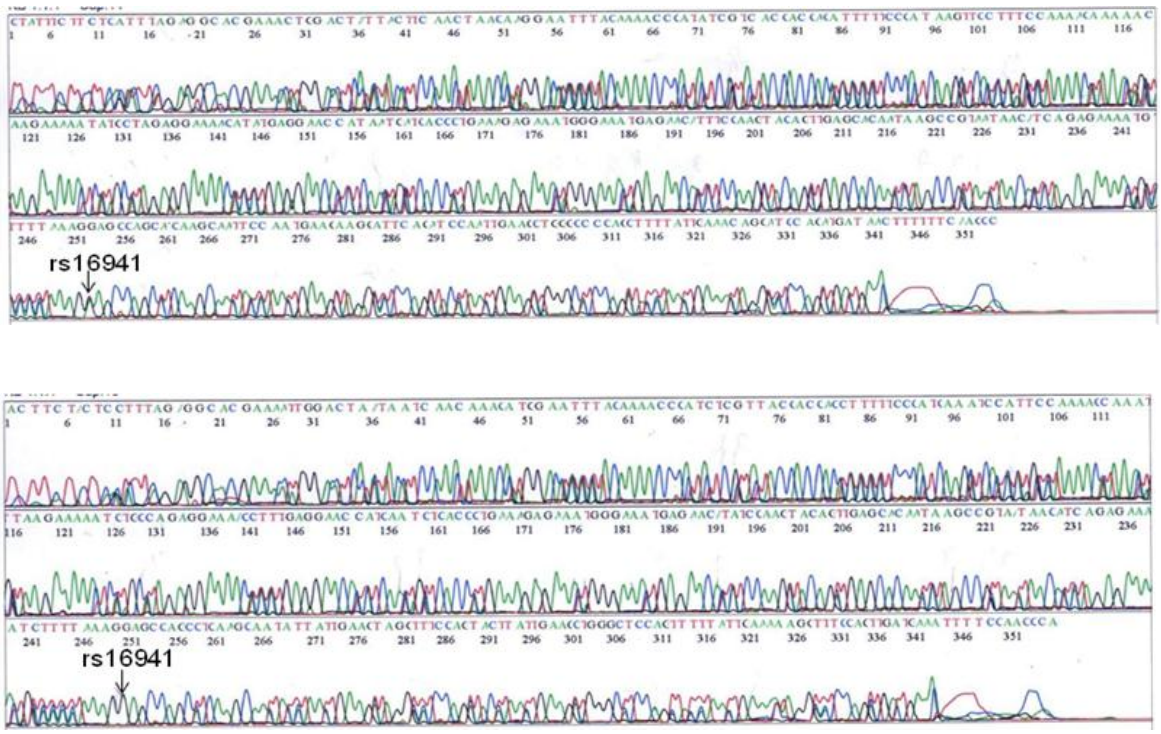

Top panel shows the female partner of couple 29 who is heterozygote (G/A) and the bottom panel represents the male partner of couple 29 who is homozygote (G/G) for the SNP rs16941 within *BRCA1*.

Table 4-1 Collective results of sequencing and mini-sequencing analyses showing the alleles at each SNP site analysed for fifteen couples.

Couple ID	*ACTB* SNP site rs852423		*SNRPN* SNP site rs75184959		*H19* SNP site rs11542721		*BRCA1* SNP site rs16941		*BRCA1* SNP site rs1060915	
	Female	Male	Female	Male	Female	Male	Female	Male	Female	Male
29	G/A	G/G	T/T	C/C	C/T	T/T	G/A	G/G	C/T	C/C
30	G/A	G/A	C/T	C/C	C/T	C/C	G/A	G/G	C/T	C/C
31	G/A	G/A	T/T	C/T	C/T	C/C	A/A	A/A	C/T	T/T
32	A/A	G/A	C/T	C/T	C/T	C/C	G/A	A/A	C/T	T/T
33	G/A	G/A	T/T	C/T	C/T	C/C	A/A	G/A	C/C	C/T
34	A/A	A/A	T/T	T/T	T/T	C/T	G/A	G/G	C/T	T/T
35	G/A	G/G	C/T	C/T	C/T	C/T	G/G	A/A	C/C	T/T
36	G/A	A/A	T/T	T/T	C/T	C/T	G/A	G/A	C/T	C/T
37	A/C	A/C	C/T	T/T	T/T	T/T	A/A	A/A	T/T	T/T
38	A/A	A/A	C/C	C/T	T/T	T/T	A/A	G/A	C/T	T/T
39	A/A	A/A	T/T	T/T	C/T	T/T	A/A	G/A	T/T	C/T
40	A/A	A/A	C/T	C/T	C/T	T/T	G/A	G/G	C/T	T/T
41	A/A	A/A	T/T	C/C	T/T	T/T	G/A	G/A	C/T	C/T
42	A/A	A/A	C/C	C/T	T/T	T/T	A/A	A/A	T/T	T/T
43	G/A	A/A	C/T	C/T	C/C	T/T	G/A	G/A	C/T	C/T

Couple ID, and the alleles present at the SNP site for *ACTB*, *SNRPN*, *H19* and *BRCA1* analysed are shown in this table. For *ACTB*, a total of four couples (29, 32, 35 and 36) couples were shown to be semi-informative for the SNP rs852423, couples 29 and 41 were fully informative for *SNRPN* SNP 75184919, couples 30, 31, 33, 37, 38 and 42 were semi-informative for *SNRPN* SNP 75184919, couples 29, 30, 33, 34, 39 and 40 were semi-informative for *H19* SNP rs115442721 and 42 was semi-informative for *H19* SNP rs115442721 and a total of ten couples were shown to be fully/semi-informative for *BRCA1* SNPs rs16941 and rs1060915.

4.1.2 Quality and concentration of RNA and DNA extracted from human preimplantation embryos

Optimisation of total RNA extraction for the investigation of differential gene expression was carried out on isolated clumps of lymphocytes from an anonymous donor consisting of 150, 100 and 50 cells. Initially two different kits, AllPrep DNA/RNA Micro Kit, Qiagen (A), UK and Absolutely RNA® Nanoprep kit, Agilent (B), were tested for total RNA extraction. The successful RNA extraction from lymphocyte clumps was assessed by Nanodrop quantification (Table 4.2). The ratio of the absorbance at 260nm and 280nm was expected and found to be more than 2ng/µl indicating pure and good quality RNA sample. Total RNA and DNA from surplus embryos were obtained using AllPrep DNA/RNA Micro Kit.

Table 4-2 Summary of initial RNA extraction optimisation experiments.

Sample number	Number of lymphocytes from each clump	Kit used for extraction	260/280 ratio	Concentration (ng/µl)
1	50	A	0.01	2.4
2	50	A	6.94	1.1
3	50	A	1.95	1.7
4	100	A	0.02	6.7
5	100	A	1.66	3.6
6	100	A	2.37	5.6
7	100	A	1.43	3.7
8	100	B	2.05	6.4
9	100	B	1.64	9.9

RNA extraction using clumps of cells, kits used, NanoDrop readings including 260/280 ratio and concentrations of the extracted RNA. It was observed that as the RNA extraction involved more cells, the concentration of RNA was increased.

Total RNA and DNA were extracted from 95 embryos derived from 15 couples to investigate the parental differential expression of *ACTB*, *SNRPN*, *H19* and *BRCA1* (Table 4.3). The Agilent 2100 Bioanalyzer was used to quantify RNA (Figure 4.2, Appendix 7.3.1.2). RIN values for both cleavage and morula stage embryos (***p= 0.0009) were considerably lower compared to blastocyst samples (**** p< 0.0001). However, there was no significant difference in the RNA concentration of cleavage, morula and blastocyst stage embryos (Appendix 7.3.1.2, p=0.1). DNA contamination of these RNA samples was tested by amplifying an intronic and exonic region of *DMPK* gene and no contamination was detected in any of the cDNA samples obtained from these embryos. The overall DNA concentration in embryos at cleavage, morula and blastocyst was at similar levels (Appendix 7.3.1.2).

Figure 4-2 Assessment of RNA samples from human embryos using the Agilent 2100 Bioanalyzer Pico chip electrophoresis.

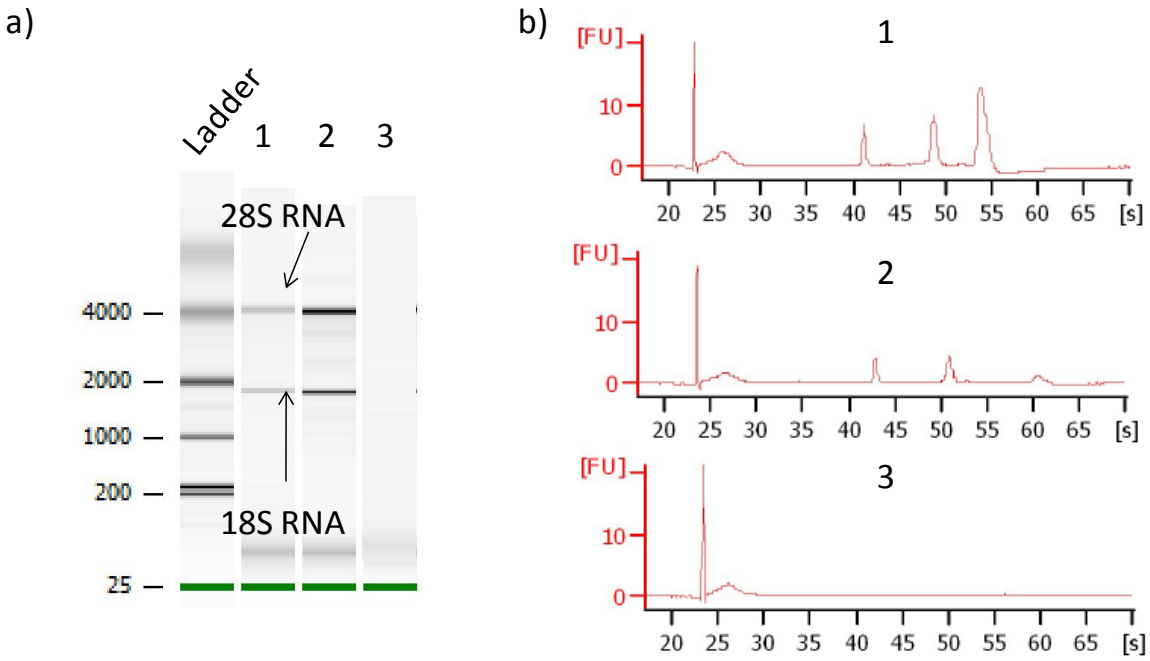

a) Electropherograms of embryos 1, 2 and 3 showing the 18S and 28S rRNA. The electropherogram for the sample 3 indicates a poor quality of RNA. b) Peaks in the individual electropherograms of embryos 1, 2 and 3 on Pico chip.

Table 4-3 Patient and embryo information for the analysis of differential gene expression.

Patient	Disorder	Embryo ID	PGD outcome
29	*BRCA1*	1	Affected
30	*BRCA1*	2	Affected
		3	Affected
		4	Affected
31	*BRCA1*	5	No PGD
		6	No PGD
32	*BRCA2*	7	Affected
		8	Affected
		9	Affected
		10	Affected
		11	Affected
		12	Affected
		13	Affected
		14	No *BRCA2* mutation
		15	Affected
		16	Affected
		17	No *BRCA2* mutation
		18	Affected
33	*MLH1*	19	Affected
		20	Inconclusive
		21	Inconclusive
		22	Inconclusive
		23	Inconclusive
		24	No *MLH1* mutation
		25	Inconclusive
		26	Affected
		27	Affected
		28	Affected
34	*APC*	29	No PGD
		30	No *APC* mutation
		31	Affected
		32	No *APC* mutation
		33	Affected
		34	Affected
		35	No *APC* mutation
		36	Affected
		37	Affected
		38	No result
		39	No PGD
		40	No *APC* mutation
		41	Affected
		42	Affected
		43	No result
		44	Affected
		45	No result
		46	No PGD
35	*NF1*	47	Affected
		48	Maternal only
		49	No *NF1* mutation
		50	No *NF1* mutation
		51	Affected
		52	No *NF1* mutation
		53	Affected
36	*RB1*	54	Affected
		55	Affected
		56	Affected
		57	Maternal only for chromosome 13
		58	Affected
		59	Affected
		60	No *RB1* mutation
		61	Affected
37	*Men2b*	62	Affected
		63	Affected
		64	Inconclusive
38	*PRKAR1A*	65	Affected
		66	Affected
		67	Affected
		68	Affected
		69	Inconclusive
		70	No PRKAR1
		71	Affected
		72	Inconclusive
39	*DMPK*	73	No result
		74	No result
		75	Affected
		76	Affected
		77	Inconclusive
		78	Affected
		79	Affected
		80	Affected
		81	Paternal only for chromosome 19
		82	Inconclusive
		83	Paternal only for chromosome 19
40	*DMPK*	84	Affected
		85	Inconclusive
		86	Inconclusive
41	*DMPK*	87	No result
		88	Affected
		89	Affected
		90	Affected
42	*DMPK*	91	No *DMPK* mutation
		92	Affected
		93	Affected
43	*DMPK*	94	No result
		95	Affected

Couple and embryo IDs, disorder, affected partner and developmental stages of the embryos are listed. PGD results were also shown for each embryo for the particular single gene disorder for which it was diagnosed.

4.1.3 Differential expression of parental genes in preimplantation embryos

A results summary including the list of genes analysed (*ACTB*, *SNRPN*, *H19* and *BRCA1*), number of embryos showing differential expression favouring paternal and maternal transcripts and the number of embryos excluded from the analysis are shown in table 4.4. Statistical analysis was performed by applying a student's T-test to all the embryos examining preferential paternal expression relative to preferential maternal expression (Figure 4.3). The difference between the parental allelic peak height ratios of *SNRPN* and *BRCA1* transcripts was statistically significant (Figure 4.3).

Expression of the house keeping gene, *ACTB*, was observed to be similar between maternal and paternal transcripts in all the embryos that were successfully analysed (Table 4.4 and Figures 4.3, 4.4, 4.5). There was no significant difference in the expression levels of maternal and paternal *ACTB* transcripts (Figure 4.4).

Figure 4-3 Overall differential expression analysis of paternal and maternal transcripts for four genes in human embryos.

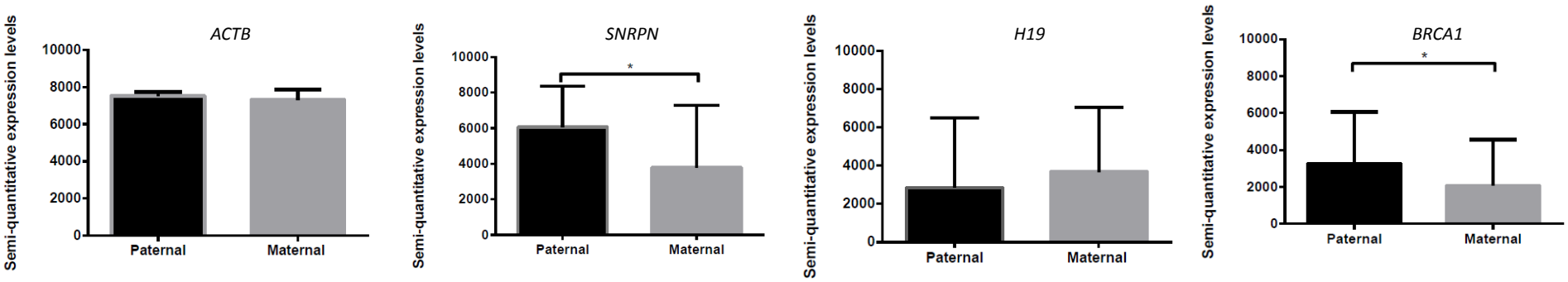

The differential expression of *ACTB*, *SNRPN*, *H19* and *BRCA1* was analysed in all the embryos at cleavage, morula or blastocyst stages. In heterozygotes, there was no significant difference in the level of the parental transcripts of *ACTB* (p=0.2). Paternal *SNRPN* transcripts were expressed at significantly higher levels than the maternal transcripts (*p= 0.01). Although higher levels of maternal *H19* transcripts were detected in embryos, this difference was not statistically significant (p=0.4) in the embryos analysed. However, paternal *BRCA1* (*p= 0.03) was significantly higher relative to the maternal transcripts (*p= 0.03) in the embryos.

Figure 4-4 Differential parental expression analysis of *ACTB* transcripts on cDNA from embryos examined at SNP rs852423 by mini-sequencing (SNaPshot™).

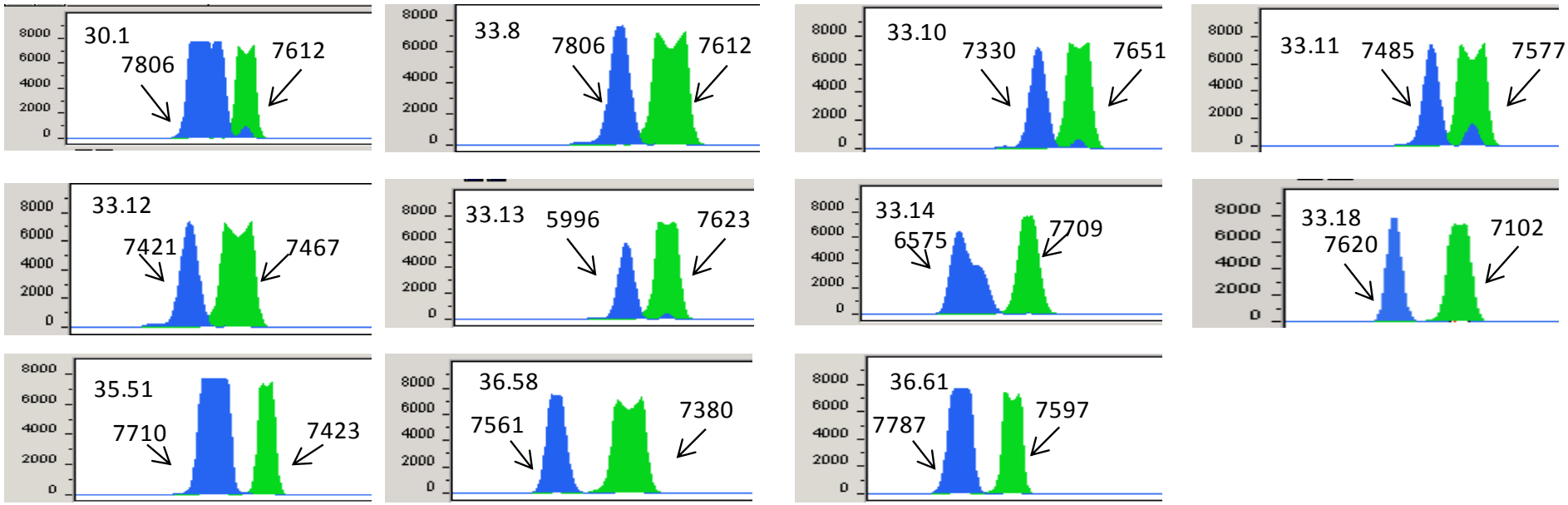

The couple ID and embryo numbers are shown at top of each panel separately. The peak height, which represents the amount of cDNA product from each allele, is also labelled. Blue peak represents allele G and green allele A, respectively. Each embryo is showing that the parental *ACTB* transcripts are expressed at similar levels, where the ratio of maternal to paternal *ACTB* transcript was approximately 1:1. The x-axis shows the alleles detected at the SNP and the y-axis shows the peak heights. The embryos analysed in this study were mainly shown to express both parental alleles for the imprinted genes, however the paternal *SNRPN* and the maternal *H19* transcripts were preferentially expressed in the majority of the embryos analysed as expected.

Overall, more than half of the embryos (*p=0.01; 56.5%, 13/23, Figure 4.3) preferentially expressed the paternal copy of *SNRPN* and 39% (9/23) had strictly monoallelic expression for the paternal transcript (Table 4.4 and Figures 4.5, 4.6). As the embryos developed to the blastocyst stage, the monoallelic expression and the differential expression favouring the paternal transcript increased such that differential expression of paternal *SNRPN* transcript was 61% (8/13) up to the morula stages whereas it was 70% (7/10) at the blastocyst stage. Similarly, the maternal transcript of *H19* was preferentially expressed in 60% (9/15) of the embryos and 78% (7/9) were strictly monoallelic for the maternal transcript. Differential expression of the *H19* transcript followed a similar trend as *SNRPN*, where 43% (3/7) had more maternal *H19* transcript compared to the paternal transcript at morula stage. This differential expression rose to 75% (3/4) at blastocyst stage. Sixty percent (3/5) of the embryos at the cleavage stage showed differential expression favouring the maternal *H19* transcript. There was no statistical significance of differential parental expression of *H19* when stage of embryo development was considered together (p=0.4; Figure 4.3). One embryo (embryo 83) was shown to have only the maternal copy of *H19* by haplotype analysis (Table 4.4 and Figures 4.5, 4.7) which accounted for the detection of the maternal *H19* transcript only in the SNaPshot assay.

Figure 4-5 Bar chart of differential gene expression analyses in embryos at cleavage, morula and blastocyst stages.

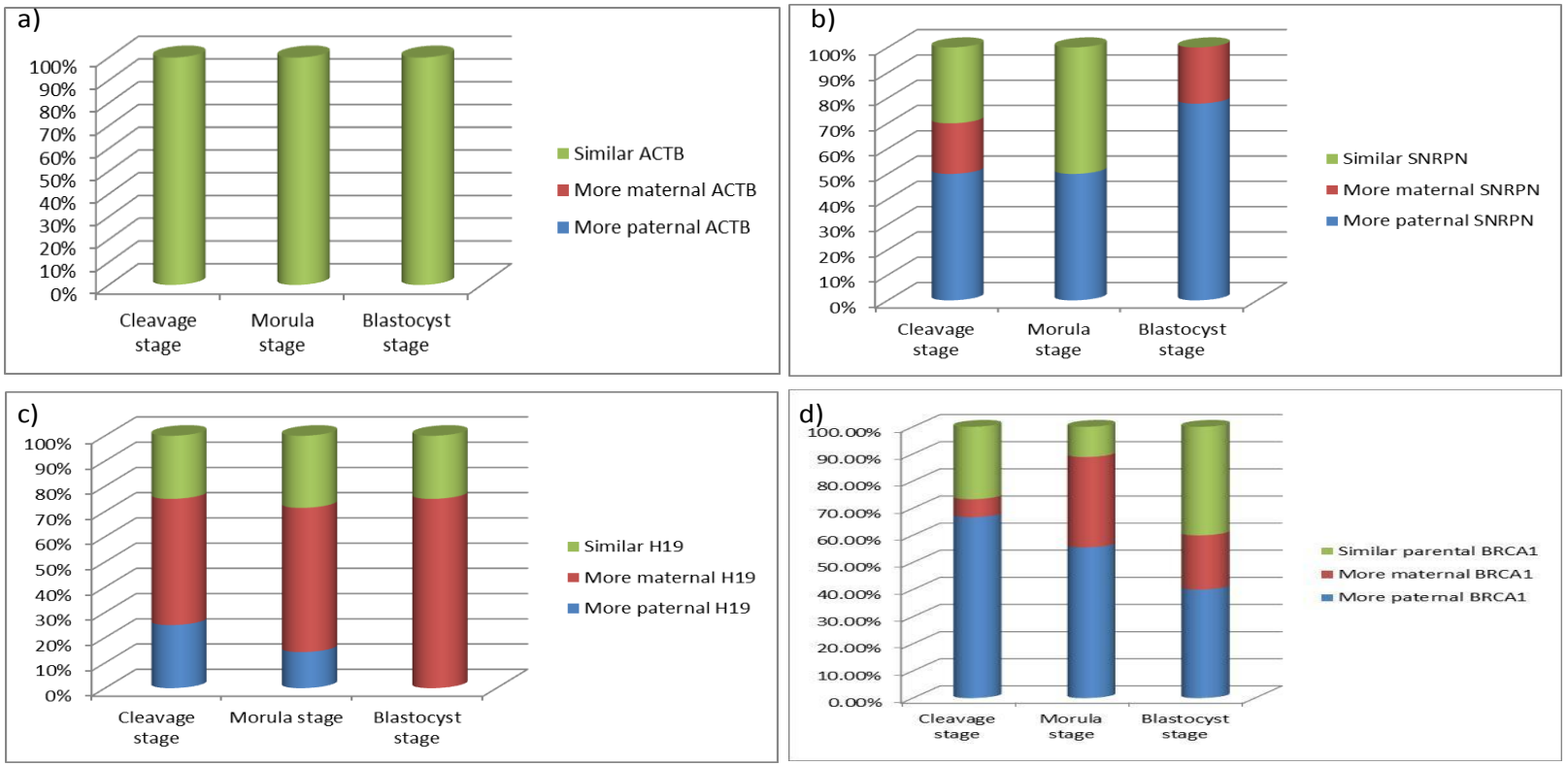

a) Differential expression of *ACTB* showing similar expression levels at cleavage, morula and blastocyst stage embryos. b) Overall differential expression of *SNRPN*. It was shown that at cleavage and morula stages, almost half of the embryos preferentially expressed the paternal *SNRPN* transcript. As the embryos developed to the blastocyst stage, paternal *SNRPN* predominated the embryo. c) Overall differential expression of parental *H19* transcripts. It was observed that in cleavage, morula and blastocyst stages, maternal *H19* transcripts predominated the embryo. As the embryos developed to the blastocyst stage, the preferential expression of *H19* transcript was considerably increased. d) Differential expression of *BRCA1* in embryos. Differential expression of paternal *BRCA1* transcript was more persistent at cleavage stage embryos compared to the morula and blastocyst stage embryos.

Figure 4-6 Differential parental expression analysis of *SNRPN* transcripts on cDNA from embryos examined at SNP rs75184959 by mini-sequencing (SNaPshot™).

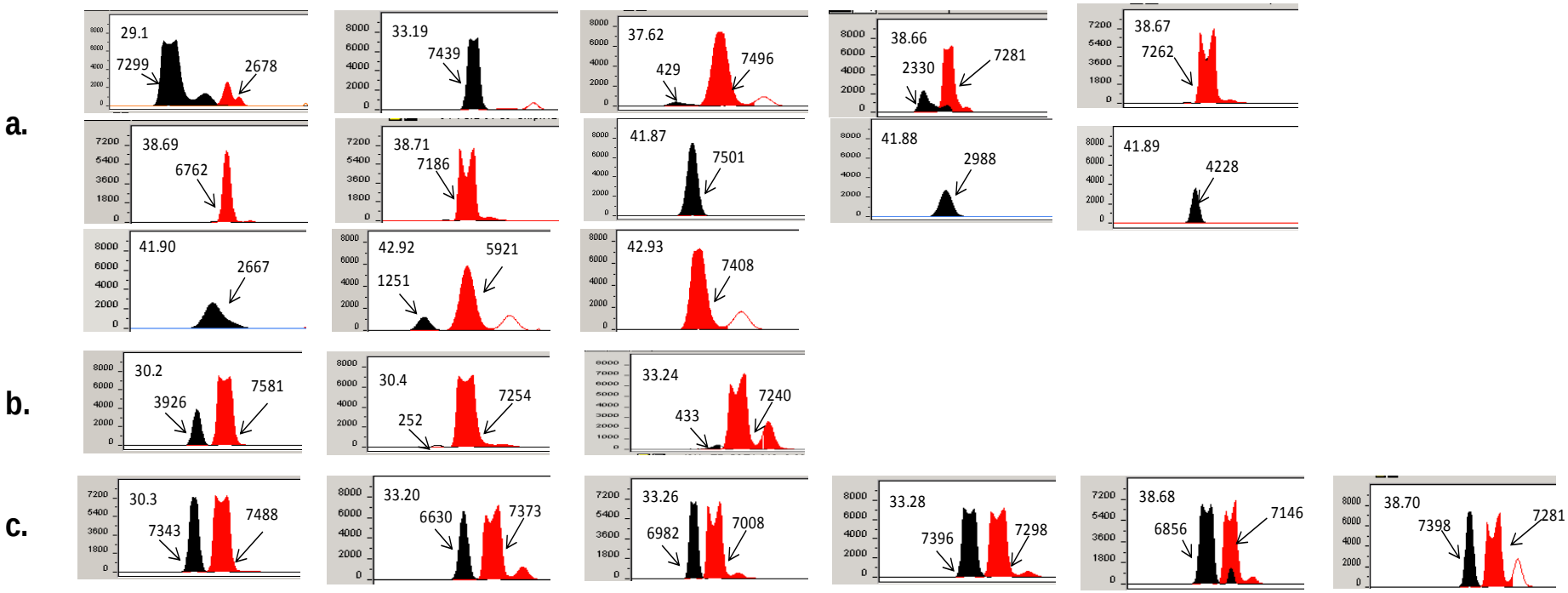

The couple ID and embryo numbers are shown at top of each panel separately. When the expression levels were low, an additional enlarged image within the same panel was placed. The peak height for each allele is also labelled. Black peak represents allele C and red allele T, respectively. The x-axis shows the alleles detected at the SNP and the y-axis shows the peak heights. a) Embryos showing differential expression for the paternal transcript of *SNRPN* (including monoallelic expression of the paternal *SNRPN*). When both parental *SNRPN* transcripts were detected, the ratio of paternal to maternal *SNRPN* transcripts was shown to be more than or equal to 2:1. b) Embryos showing differential expression for the maternal transcript of *SNRPN,* where the ratio of maternal to paternal *SNRPN* transcripts was shown to be more than or equal to 2:1. c) Embryos showing similar parental *SNRPN* expression, where the ratio of maternal to paternal *SNRPN* transcripts was approximately 1:1.

Figure 4-7 Differential parental expression analysis of *H19* transcripts on cDNA from embryos examined at SNP rs11542721 by mini-sequencing (SNaPshot™).

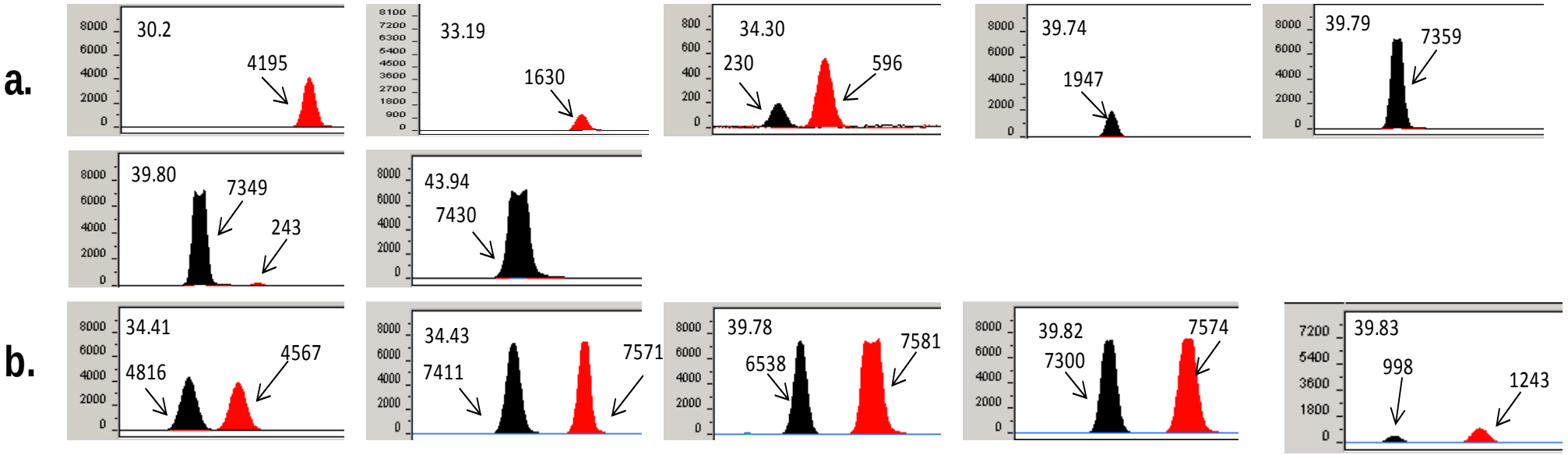

The couple ID and embryo numbers are shown at top of each panel separately. The peak height for each allele is also labelled. Black peak represents allele C and red allele T, respectively. The x-axis shows the alleles detected at the SNP and the y-axis shows the peak heights. a) Embryos showing differential expression for the maternal *H19* transcript (including monoallelic expression of the maternal *H19*). When both parental *H19* transcripts were detected, the ratio of maternal to paternal *H19* transcripts was shown to be 2:1 or higher. b) Embryos showing similar expression levels of parental *H19* transcripts, where the ratio of maternal to paternal *H19* transcript was approximately 1:1.

Two different SNPs were analysed to investigate differential expression of *BRCA1*, one located in exon 11 and one located in exon 12. However, in 16 embryos the pattern of the differential expression of parental *BRCA1* transcripts was not concordant at these two SNPs, such that an embryo with a preferential expression for the paternal *BRCA1* transcript at one locus was observed to have a preferential maternal expression in the other locus analysed. Therefore, these embryos were excluded from the analysis. An additional two embryos were excluded from the analysis for *BRCA1* since they were shown to have a gain of chromosome 17 (embryos 69 and 72) reflected by the differential expression favouring the paternal *BRCA1* transcript by SNaPshot analysis.

Overall, there was a significant differential parental expression for *BRCA1* in different stages of preimplantation embryos (*p=0.03, Table 4.4). The differential expression of the paternal *BRCA1* transcript was higher at cleavage stage embryos compared to the other stages (Figure 4.5). Sixty six percent (10/15) of the embryos arrested at the cleavage stage expressed the paternal *BRCA1* transcript more compared to the maternal (Figure 4.8 and 4.9). This was reduced to 55% (10/18) of embryos at the morula and to 50% (7/14) at the blastocyst stage.

Figure 4-8 Differential expression analysis of parental *BRCA1* transcripts with preferential paternal expression on cDNA from embryos by mini-sequencing (SNaPshot™).

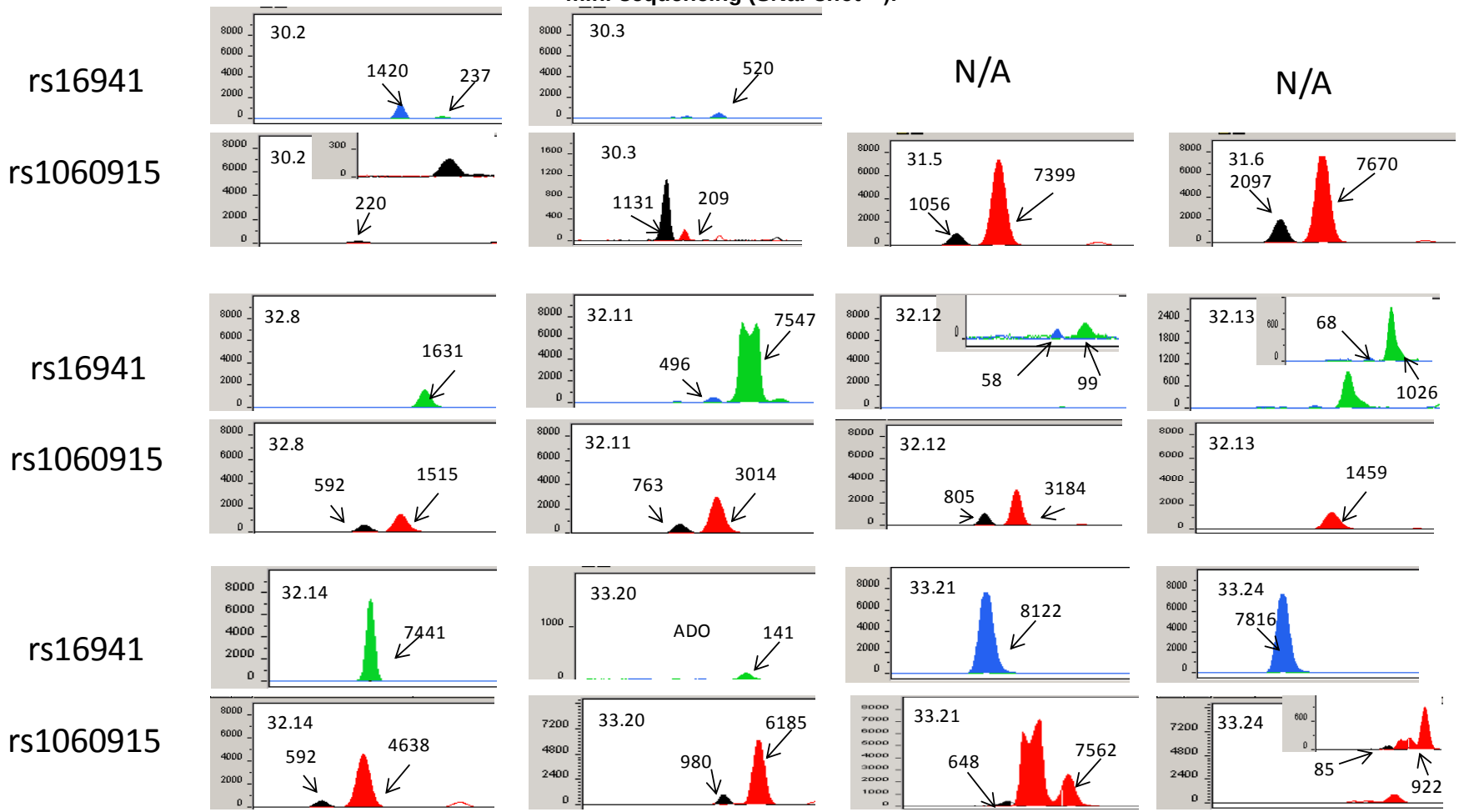

Results for differential allelic expression and embryo development

rs16941

rs1060915

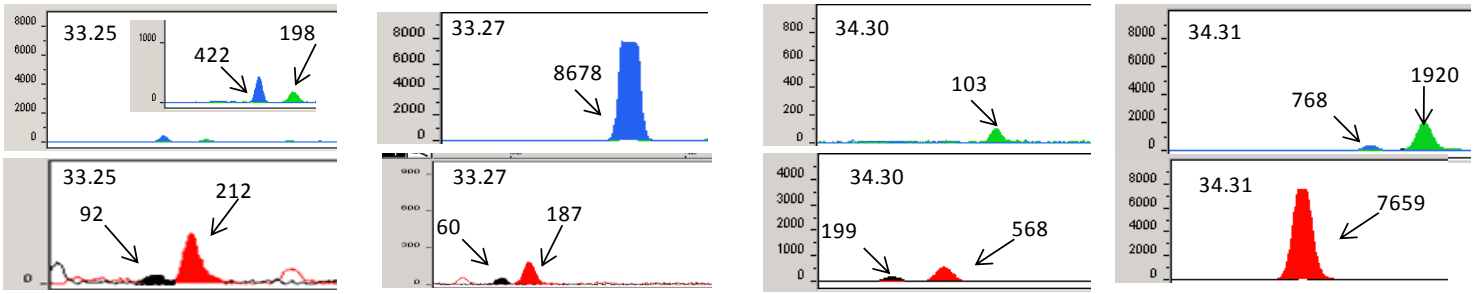

rs16941

rs1060915

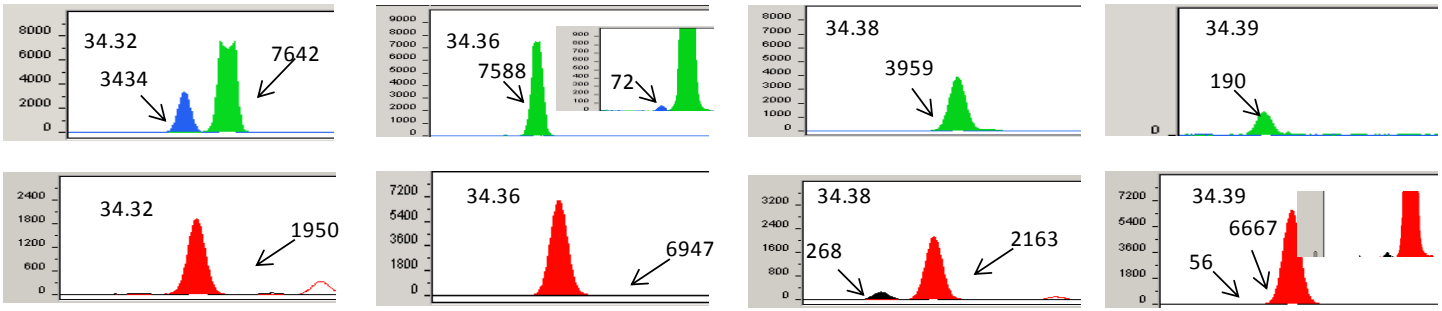

rs16941

rs1060915

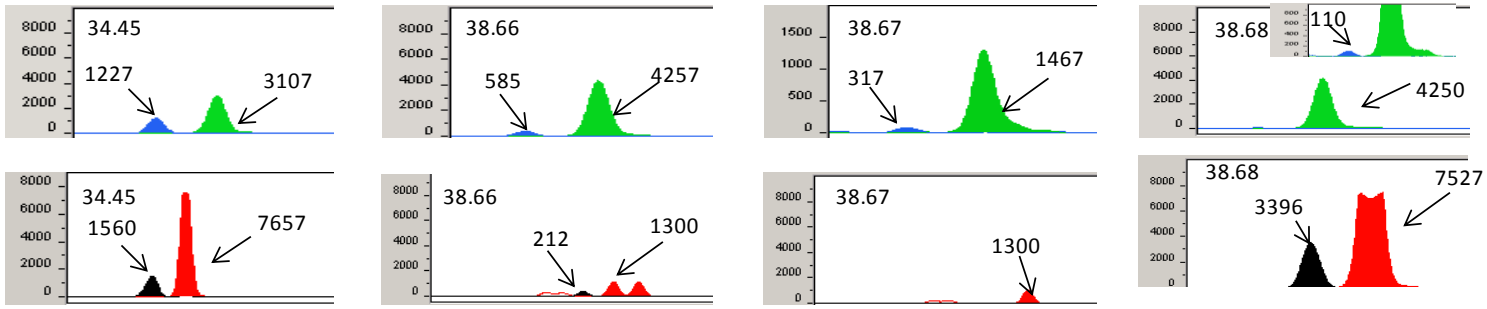

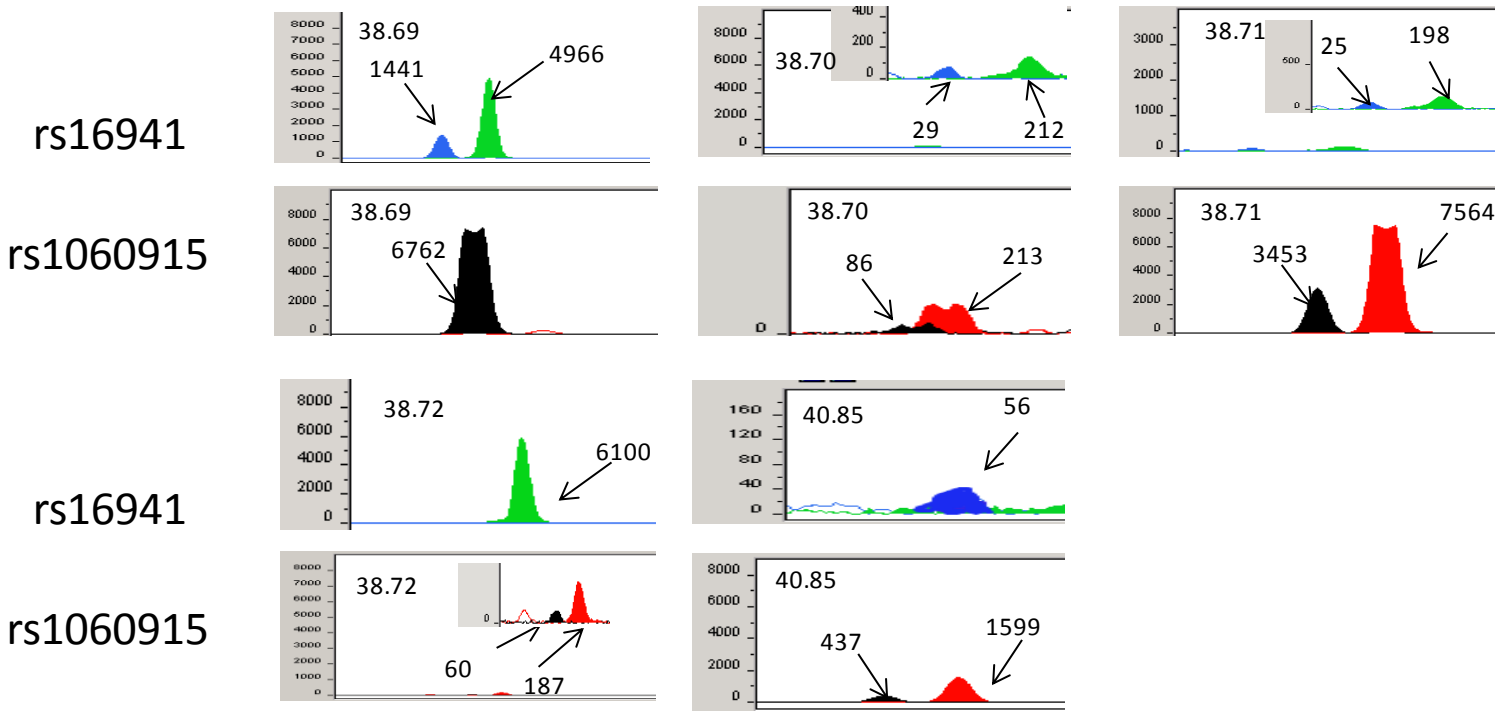

The couple ID and embryo numbers are shown at top of each panel separately. When the expression levels were low, an additional enlarged image within the same panel was placed. The peak height for each allele is also labelled. Blue peak represents allele G, green is allele A, black is allele C and red is allele T, respectively. The x-axis shows the alleles detected at the SNP and the y-axis shows the peak heights. The paternal *BRCA1* transcript was shown to be preferentially expressed, where the ratio of paternal to maternal *BRCA1* transcripts was shown to more than or equal to 2:1.

Figure 4-9 Differential expression analysis of parental *BRCA1* transcripts on cDNA from embryos examined by mini-sequencing (SNaPshot™).

a.

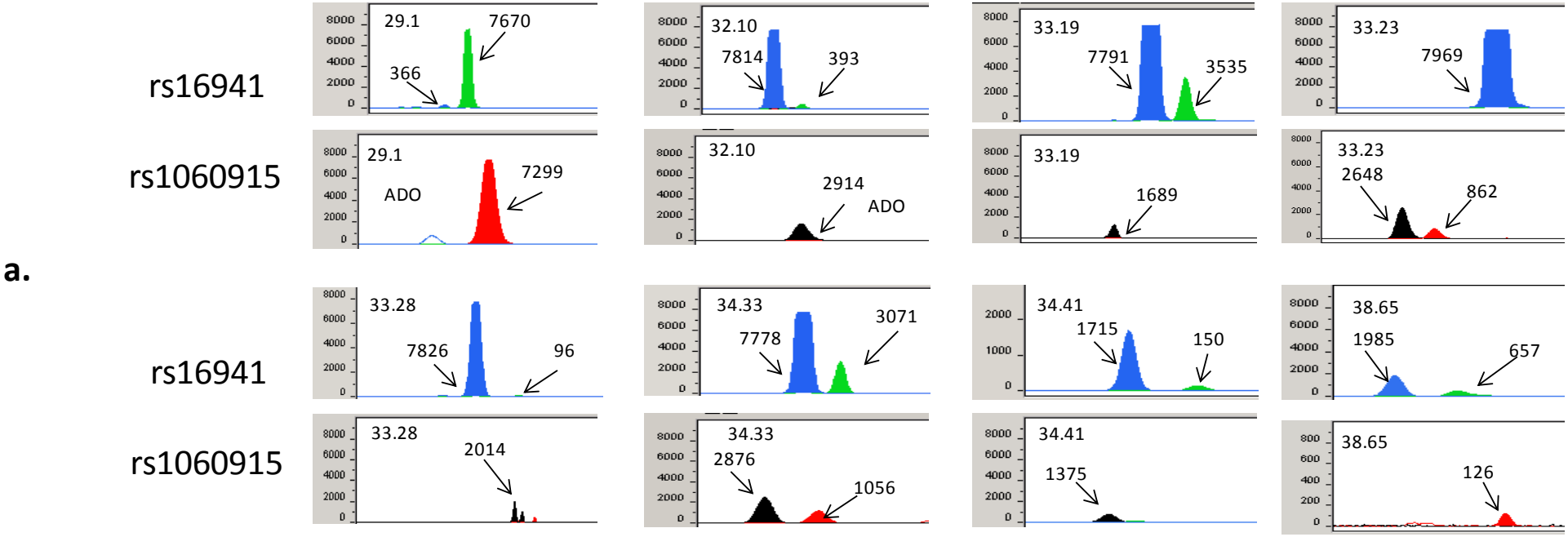

b.

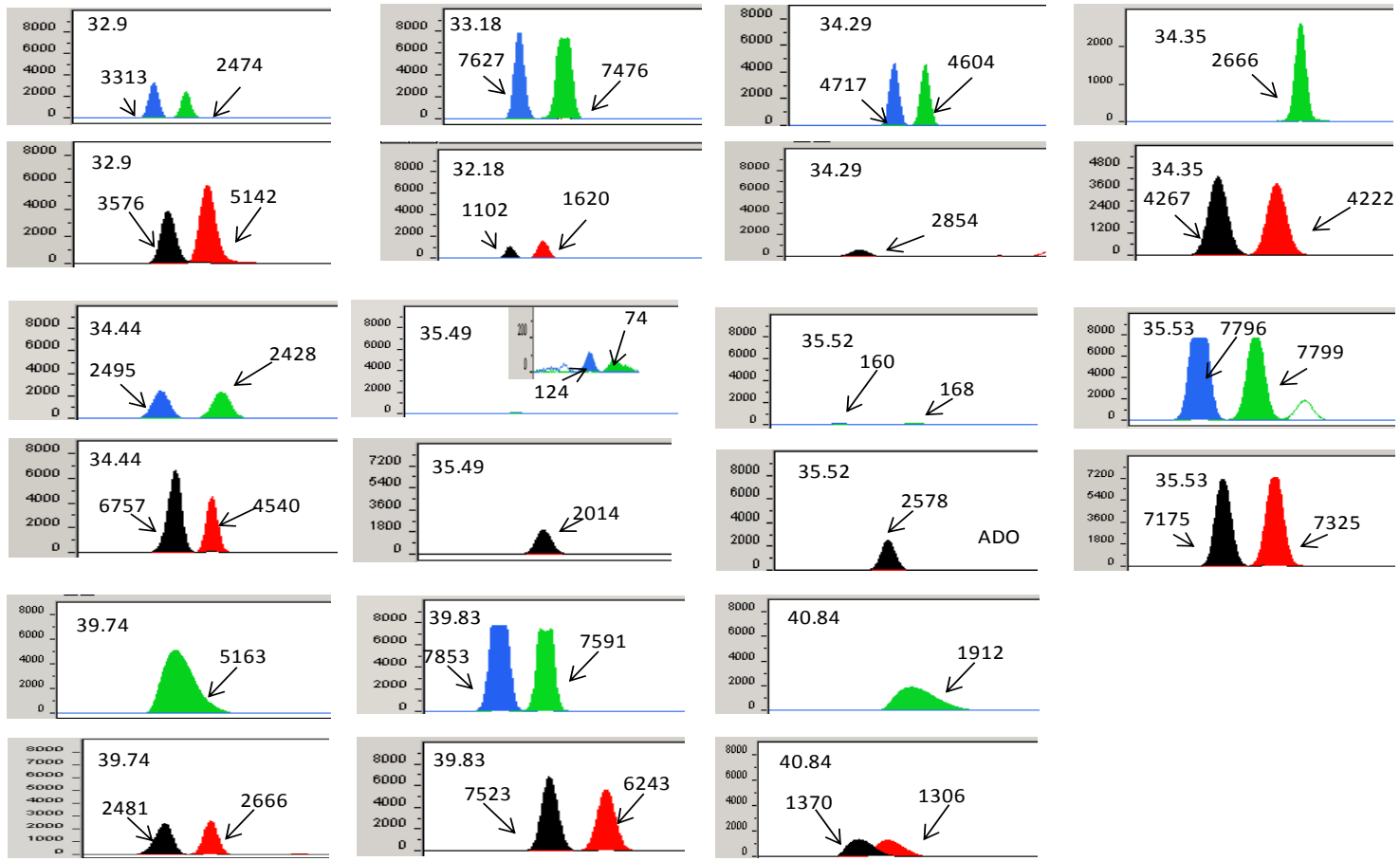

The couple ID and embryo numbers are shown at top of each panel separately. The peak height for each allele is also labelled. Blue peak represents allele G, green is allele A, black is allele C and red is allele T, respectively. The x-axis shows the alleles detected at the SNP and the y-axis shows the peak heights. a) Embryos showing differential expression favouring the maternal *BRCA1* transcript. The ratio of maternal to paternal *BRCA1* transcripts was shown to be more than or equal to 2:1. b) Embryos showing similar expression for *BRCA1* transcript. The ratio of maternal to paternal *BRCA1* transcripts was approximately 1:1.

Table 4-4 Summary of results for differential gene expression analysis in cDNA from embryos.

Genes analysed	Number of embryos included for the study	% of informative haplotypes (number of embryos)	% of embryos showing differential expression favouring: (number of embryos)			% of embryos with aneuploidy in chromosomes of genes analysed (number of embryos)	% of embryos with inconclusive result due to uninformativity of the SNP analysed (number of embryos)	% of embryos with ADO (number of embryos)	% embryos with amplification failure (number of embryos)
			Paternal	Maternal	Similar				
ACTB	30	36.7 (11)	0	0	100 (11)	0	73.7 (14)	0	17 (5)
SNRPN	34	67 (23)	56.5 (13)*	17 (4)	26 (6)	0	32 (11)	0	0
H19	48	33 (15)	20 (2)	60 (9)*	13 (4)	6.25 (1)	17 (8)	0	50 (24)
BRCA1	75	64 (49)	58 (29)	19 (9)	22 (11)	4 (2)	14 (11)	10 (5)	0

The genes analysed for differential expression, percentage of informative haplotypes where each parental allele was distinguished, percentage of embryos with differential gene expression favouring the paternal and maternal transcripts and embryos that were excluded from the analysis due to the aneuploidy status, uninformative state of SNP or amplification failure, were listed. *BRCA1* was analysed at two SNPs and the results shown here were collective from both SNPs. In ten embryos differential expression of *BRCA1* at two SNP sites did not agree and these were not included in the analysis. *Only the paternal expression of *SNRPN* was observed in 9/13 embryos and only the maternal expression of *H19* was observed in 7/9 embryos.

4.1.4 Assay sensitivity

Mini-sequencing analysis, SNaPshot assay, used for the quantification of differential parental expression, was validated by real time PCR. Additional validation involved aneuploidy screening for chromosomes 7, 11, 15 and 17 by haplotyping and aCGH to verify that the observed differential expression between the parental transcripts was not due to any gain or loss of the chromosome in the embryo. The final validation involved analysis of the methylation status of *ACTB*, *H19* and *BRCA1* in the embryos that were shown to have a differential gene expression.

4.1.4.1 Real time PCR quantification

cDNA from all the embryos showing differential parental expression for any of the genes analysed (*ACTB*, *SNRPN*, *H19* and *BRCA1*) were quantified by real time PCR. The Cq values represent the start of the exponential phase and ranged from 32 to 44 with the mean of 36 for *ACTB*, 34 for *SNRPN*, 41 for *H19* and 35 for *BRCA1*, respectively (Figure 4.10, Appendix 7.3.1.3). Therefore real time PCR analysis confirmed that after the initial PCR (40 cycles) prior to mini-sequencing analysis, the samples were still at the exponential phase and examination of correct differential analysis had been performed.

Figure 4-10 Quantitative analysis of *ACTB* in duplicate sample.

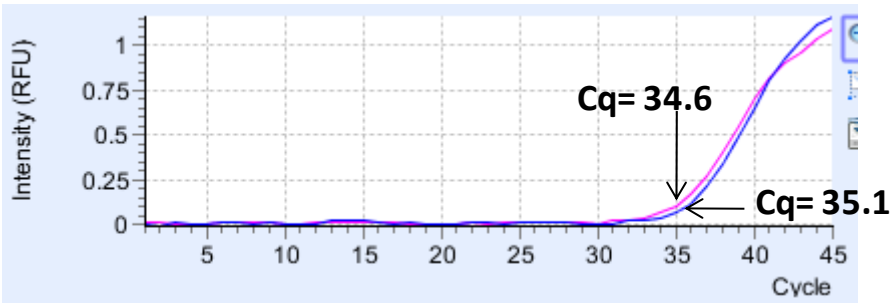

Cq value of the same sample in duplicate is shown. The two Cq values of the duplicate samples are relatively close,

4.1.4.2 Aneuploidy screening

Informative short tandem repeat polymorphic markers were identified between partners for chromosomes 7, 11, 15 and 17 (Appendix 7.3.1.4). The number of embryos analysed and the details of heterozygosity of the embryos for all the chromosomes analysed are listed in table 4.5. The copy number of chromosome 11 could not be verified in the embryos obtained from three couples since there were no informative polymorphic markers. Similarly copy number of chromosome 15 could not be verified in embryos obtained from three couples and copy number of chromosome 17 in embryos obtained from one couple, respectively. Three out of twenty one embryos that could not be analysed for the copy number of chromosome 11 by PCR were analysed by aCGH and the normal copy number of this chromosome was confirmed. Similarly, for 5/20 embryos where the copy number of chromosome 15 could not be verified by PCR were shown to be euploid for chromosome 15 by aCGH.

A total of 26 embryos were analysed by aCGH. Twelve embryos were shown to be euploid and the rest of the embryos showed various aneuploidies where two embryos (embryo number 69 and 72) were shown to have a gain of chromosome 17 (Figure 4.11). These embryos were excluded from the differential expression analysis. Aneuploidy rate in embryos with *BRCA* mutations were at similar level with the aneuploidy rate in embryos with no known *BRCA* mutations.

Table 4-5 Summary of results for haplotype analysis for the chromosomes of 7, 11, 15 and 17 in cDNA from embryos.

Chromosomes analysed	Number of embryos included for the study	% of informative haplotypes (number of embryos)	% of heterozygous embryos (number of embryo)	% of homozygous embryos with ADO (number of embryo)	% of embryos with inconclusive result due to uninformative polymorphic locus (number of embryo)	% of embryos with amplification failure (number of embryo)
7	30	86.7 (26)	86.7 (26)	0	0	13 (4)
11	34	53 (18)	94 (17)	3 (1)	21 (7)	26 (9)
15	48	25 (12)	91 (11)	9 (1)	71 (34)	4 (2)
17	75	68 (51)	94 (48)	6 (3)	4 (3)	19 (21)

Table summarises information for aneuploidy screening for four chromosomes (7, 11, 15 and 17) by haplotype analysis. Percentage of informative haplotypes, where each parental allele was distinguished, percentage heterozygote and homozygote embryos and embryos excluded from haplotyping analysis are summarised.

Figure 4-11 Array CGH profiles for two embryos.

Panel a:

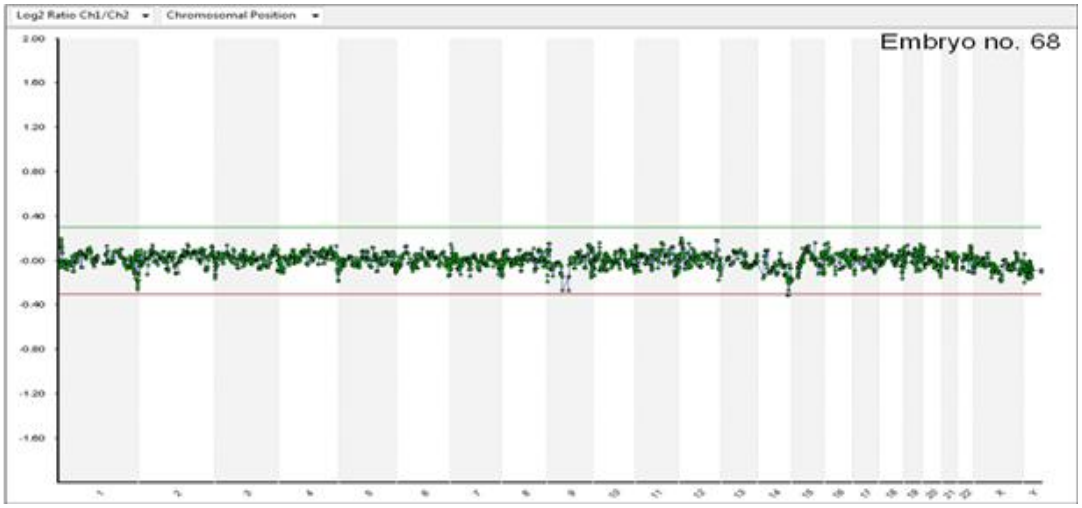

Panel b:

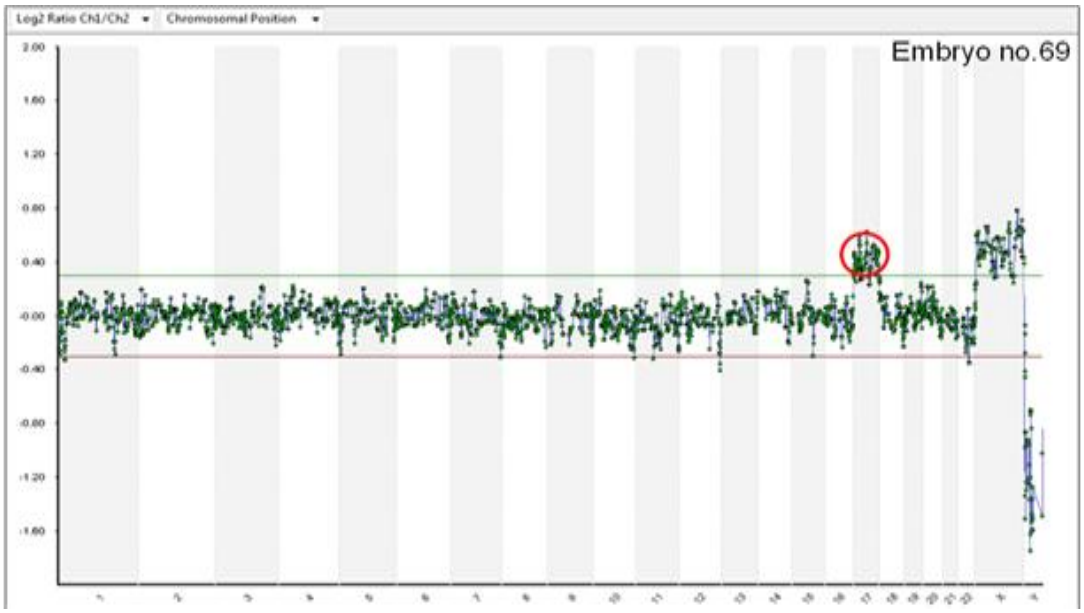

Aneuploidy screening was analysed by aCGH. Panel a shows a euploid embryo, number 68, and panel b represents embryo 69 with a gain of chromosome 17.

4.1.4.3 Differential methylation analysis

Methylation analysis was performed to confirm the differential gene expression in a subset of embryos by methylation specific PCR following bisulfite conversion. Due to insufficient starting material, the amount of DNA obtained from a single embryo, and bisulfite treatment being deleterious for DNA, sequencing analysis on the converted DNA could not be performed. Promoter regions of three genes, *ACTB*, *H19* and *BRCA1*, were amplified by nested PCR as described in section 2.3.2.11.4. When monoallelic expression of one parental transcript was observed by SNaPshot analysis, a hemi-methylated profile should be observed since only one parental transcript is present. When both parental transcripts were expressed at similar levels by SNaPshot analysis, an unmethylated profile should be observed representing both parental transcripts at similar levels.

Methylation analysis of *ACTB* in five embryos (embryo numbers 8, 11, 12, 13 and 14) showed that these embryos were homogenously unmethylated. Therefore methylation profile of *ACTB* confirmed the expression profile observed by SNaPshot analysis showing similar expression levels of parental transcripts.

The methylation status of *H19* was analysed in eight embryos. Methylation analysis of embryos 2 and 74 showed that these embryos were hemi-methylated. Methylation status of these two embryos confirmed the SNaPshot analysis that only showed the maternal transcript of *H19*. For embryo 82, an unmethylated profile was observed. This was reflected by the equal parental *H19* transcripts observed by SNaPshot analysis. Therefore, methylation analyses of these three embryos (embryos 2, 74 and 82) confirmed the expression profiles of *H19* transcripts determined by SNaPshot analysis. However, in five embryos (embryo numbers 19, 30, 39, 79 and 80), differential expression and methylation analyses were not concordant. Four embryos (embryos 19, 30, 79 and 80) were shown to have an unmethylated profile where

three were observed to be monoallelic for the maternal *H19* transcript and one was differentially expressed by SNaPshot analysis. One embryo (embryo 39) was shown to be fully methylated, whereas SNaPshot analysis showed that this embryo expressed only the paternal copy of *H19*.

The methylation status of *BRCA1* was analysed in 31 embryos. Fifty eight percent of the embryos (embryo numbers 1, 2, 9, 13, 14, 15, 19, 20, 26, 30, 36, 38, 65, 70, 74, 76, 80 and 82) were successfully analysed and *BRCA1* was shown to be hemi-methylated in all the embryos confirming the differential expression of parental transcript observed by SNaPshot analysis (Figure 4.12).

Figure 4-12 Agarose gel electrophoresis of embryos showing partial methylation for a) *H19* and b) *BRCA1*.

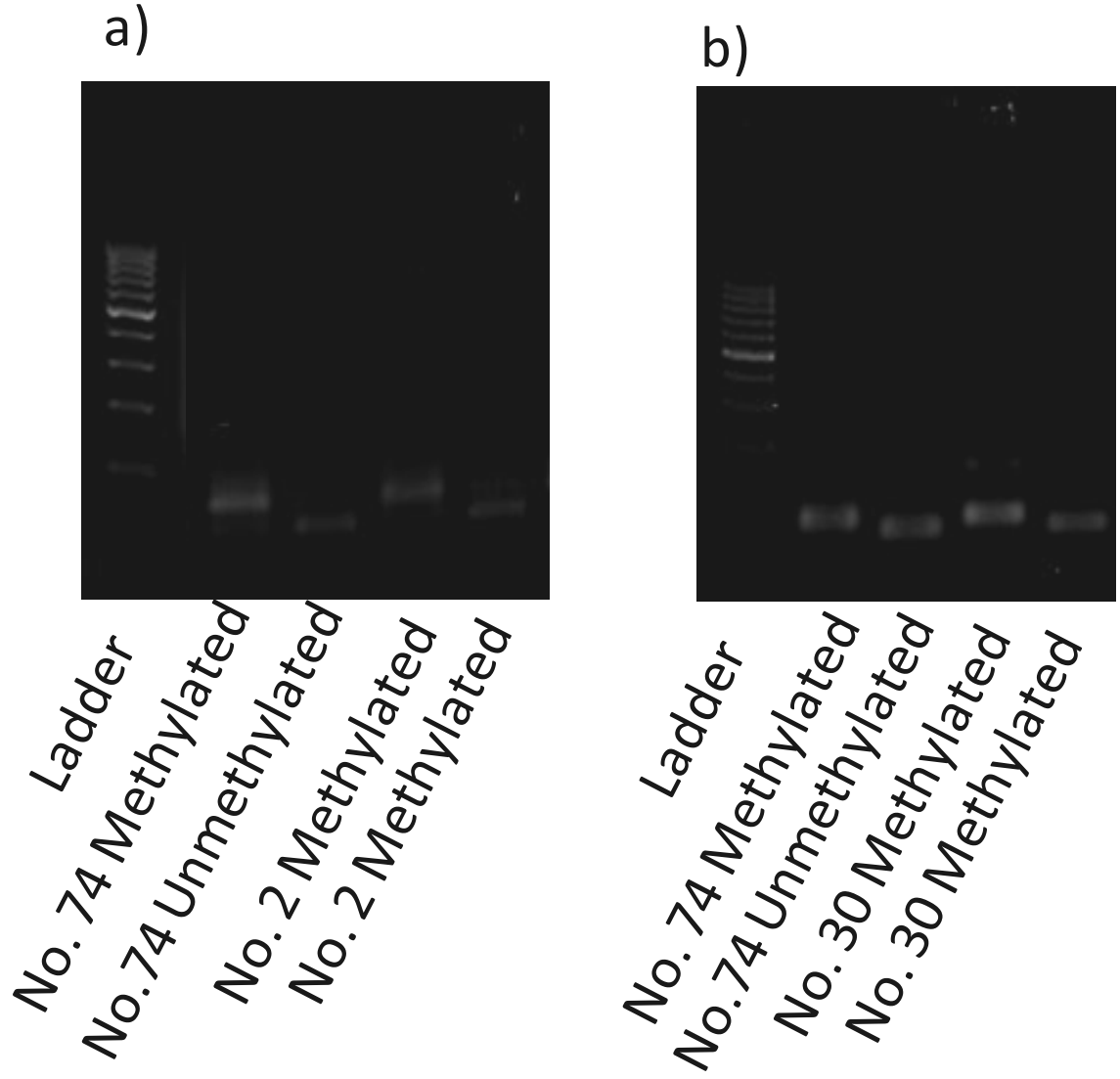

Lanes 1 for images a) and b) represent 100 base pair ladder and the rest of the lanes represent the methylation PCR product results of DNA obtained from embryos following bisulfite conversion. Embryo numbers are labelled for each lane and the PCR directed towards the methylated DNA is represented as “methylated” and the unmethylated DNA as “unmethylated”.

Developmental stage of embryos with *BRCA* mutations

The developmental progression of 16 embryos with paternally inherited *BRCA* mutations and 15 with maternally inherited *BRCA* mutations were analysed on day 5/6 post fertilisation (Table 4.6). It was shown that half of the embryos (8/16) with paternally inherited *BRCA* mutations were arrested at the cleavage stage on day 5/6 post fertilisation. Of these embryos, only 12.5% (2/16) reached to the blastocyst stage. Embryos with maternally inherited *BRCA1* mutations developed at a significantly greater rate compared to the embryos with paternally inherited *BRCA* mutations (Figure 4.13). Fifty three percent of the embryos with maternally inherited *BRCA1* mutations reached to blastocyst stage on day 5/6 post fertilisation.

Table 4-6 Patient and embryo details used for the analysis of developmental progression.

Patient	Disorder	Affected partner	Embryo ID	Morphology on day 5/6
29	*BRCA1*	Male	1	Premorlula
			96	3 cells
30	*BRCA1*	Male	2	Morula
			3	Vaculated with distinct cells
			4	6 cells
			97	Hatching blastocyst
			98	6 cells
			99	4 cells
32	*BRCA2*	Male	7	15 cells
			8	10 cells
			10	Morula ~20 cells
			11	15 cells
			12	Morula ~20 cells
			13	Pre-morula ~20 cells
			15	Morula
			18	Blastocyst
44	*BRCA1*	Female	100	Blastocyst
			101	Blastocyst
			102	Blastocyst
			103	5-7 cells
			104	5-7 cells
			105	Morula
			106	Blastocyst
			107	Fragmented morula
			108	Blastocyst
45	*BRCA1*	Female	109	Hatched blastocyst
			110	8 cells, degenerate
			111	Hatched Blastocyst
46	*BRCA1*	Female	112	Fragmented morula
			113	Blastocyst
			114	4 cells

Couple and embryo IDs, disorder, the affected partner and developmental stages of the embryos on day 5/6 post fertilisation are listed. All the embryos were shown to carry the mutation following PGD for *BRCA1* or *BRCA2*. The developmental progression of the embryos with paternally inherited *BRCA* mutations were compared to the embryos with maternally inherited *BRCA* mutations on day 5/6 post fertilisation.

Figure 4-13 Developmental stage of embryos carrying paternally inherited *BRCA* mutations compared to maternally inherited *BRCA* mutations.

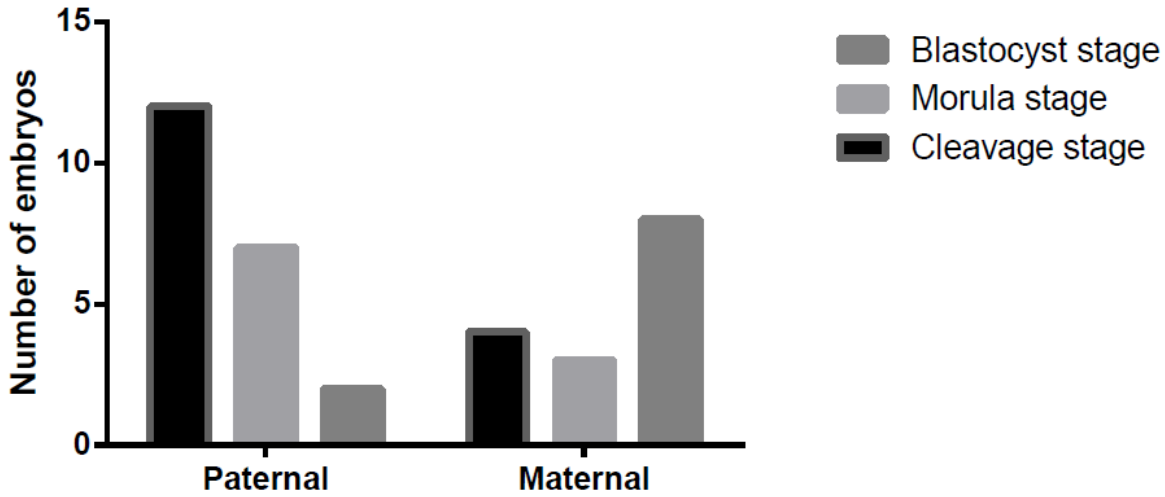

Developmental stage of embryos with *BRCA* mutations were analysed by Chi squared test. Significantly fewer embryos developed to the later stages of preimplantation development (morula and blastocyst stages) on day 5/6 post fertilisation compared to the embryos carrying maternally inherited mutations (*p=0.01). It was observed that more embryos with paternally inherited *BRCA* mutations were arrested at the cleavage stage, whereas more embryos with maternally inherited *BRCA* mutations reached to the blastocyst stage.

4.1.5 Summary of differential parental gene expression analysis

Technical aspects

- Extraction of RNA and DNA and synthesis of cDNA from a total of 95 embryos obtained from couples undergoing PGD was successfully performed.

- Sequencing analysis identified five couples who were informative for an SNP within *ACTB*, eight couples for *H19*, eight couples for *SNRPN* and ten couples for *BRCA1*, respectively.

- Semi-quantitative analysis of differential parental gene expression was performed successfully by targeting the informative SNPs in the embryos.

- The sensitivity of the SNaPshot assay was validated by performing real time PCR on the cDNA samples which confirmed that after the initial PCR, cDNA obtained from the embryos were still at an exponential amplification phase. To further validate the assay, aneuploidy status of the chromosomes 7, 11, 15 and 17 were investigated and three aneuploid embryos for these chromosomes were excluded from the analysis.

Biological aspects

- Table 4.7 summarises the differential expression patterns observed for *ACTB*, *SNRPN*, *H19* and *BRCA1* in human embryos. Methylation status of a subset of these embryos was also summarised for *ACTB*, *H19* and *BRCA1*. The developmental stage of embryos carrying maternally inherited and paternally inherited *BRCA* mutations was also summarised.

Table 4-7 Summary table for gene expression and developmental progression analyses.

Differential parental expression levels of (%)					Methylation analysis (%)				Developmental stage in *BRCA*		
Parental origin	*ACTB*	*SNRPN*	*H19*	*BRCA1*	Methylation status	*ACTB*	*H19*	*BRCA1*	Stage	Maternal origin	Paternal origin
Similar	100	26	26	11	Unmethylated	100	62.5	-	Cleavage	27	50
Maternal	-	17	60	19	Methylated	-	12.5	-	Morula	20	37.5
Paternal	-	57	13	58	Hemi-methylated	-	25	100	Blastocyst	53	12.5

Similar levels of parental transcripts for the house keeping gene, *ACTB*, were observed in the preimplantation embryos. Both parental transcripts of the imprinted genes, *SNRPN* and *H19*, were observed in a number of embryos. Overall, there was a significant difference in the differential parental expression favouring the paternal transcript of *SNRPN* in embryos at cleavage, morula and blastocyst stages. However, the difference in differential parental expression of *H19* was not significant. At the early stages of preimplantation embryo development, it was shown that there is a differential expression of *BRCA1*. This preferential expression was reduced as the embryos reached to blastocyst stage. Methylation analysis by bisulfite conversion followed by methylation specific PCR confirmed the expression pattern obtained by SNaPshot analysis for *ACTB* in 5/5 embryos, *H19* in 3/8 embryos and *BRCA1* in 18/18 embryos. Significantly more embryos with maternally inherited *BRCA* mutations developed to the later stages of preimplantation development (up to the blastocyst stage) compared to the embryos carrying paternally inherited *BRCA* mutations.

4.2 Discussion

Differential methylation of parental genomes was observed in mouse preimplantation embryos (Dean *et al.*, 2003, Tamaru and Selker, 2001, Jackson *et al.*, 2002, Fuks *et al.*, 2003). Studies investigated mono-allelic expression of imprinted genes in mice (Ferguson-Smith *et al.*, 1993, Szabo and Mann, 1995, Smith *et al.*, 2012) with a limited number of studies in human embryos (Monk and Salpekar, 2001, Huntriss *et al.*, 1998, Adjaye *et al.*, 1999). However, differential expression of other genes, such as repair genes, in embryos has not been analysed widely.

In the second part of this project differential expression of one housekeeping gene (*ACTB*), two imprinted genes (*SNRPN* and *H19*) and one double strand break repair gene (*BRCA1*) was investigated in preimplantation embryos. A further analysis focused on the embryos with *BRCA* mutations to investigate if the embryo development is affected by the sex of the partner passing on the mutation.

4.2.1 Differential expression

Analysis of differential parental gene expression in embryos required a polymorphism where paternal and maternal alleles could be distinguished. To identify informative polymorphisms between each partner the exonic regions of genes of interest from patients undergoing PGD were screened by sequencing. One of the main difficulties in this study was finding a heterozygote polymorphism that allowed parental allelic discrimination. Once the informative SNPs were identified for the couples, semi-quantitative analysis targeting these SNPs in the embryos was carried out by mini-sequencing (SNaPshot) assay.

A total of 95 embryos were analysed to investigate the differential parental expression in four genes. Transcripts of *ACTB*, *SNRPN*, *H19* and *BRCA1* were detected at all stages of preimplantation development. Thirteen embryos with *BRCA* mutations and 82 with no mutations or other mutations; *MLH1*, *NF1*, *RB1*, *Men2b*, *APC*, *PRKAR1A* and *DMPK*; were analysed to investigate the differential parental expression of the four genes. The parental transcripts of the

house-keeping gene *ACTB* were shown to be at similar levels in 11/11 at different stages of preimplantation embryo development.

4.2.1.1 Imprinting analysis

Differential gene expression of two imprinted genes *SNRPN* (maternally imprinted) and *H19* (paternally imprinted) was analysed in this study. Imprinted genes are expressed in a parent of origin manner, where only the paternal transcripts of the maternally imprinted genes or the maternal transcripts of the paternally imprinted genes were expected to be expressed in the embryos.

Differential expression of the *SNRPN* favouring the expression of paternal copy was detected in the majority of the embryos (*p=0.01; 56.5%, 13/23) analysed. Expression of the maternal copy of *SNRPN* was observed in 71% (14/23) of the embryos consisting of 4-10 cell, morula and blastocyst stage embryos. The origin of this expression may be due to an incomplete degradation of the maternal transcript from the oocyte. Previous studies also showed that *SNPRN* expression is detected in human oocytes and embryos. However, mono-allelic expression of the paternal allele was observed by the 4-cell stage (Monk and Salpekar, 2001, Huntriss *et al.*, 1998).

Contradictory results for the expression of *H19* in the human oocytes and preimplantation embryos have been reported. Some studies have shown expression of both parental alleles in slow growing embryos or morphologically poor embryos (Ibala-Romdhane *et al.*, 2011). Although one study showed expression of *H19* in one out of five blastocysts, *H19* transcripts were not detected in cleavage stage embryos (Monk and Salpekar, 2001). This explains the low detection levels of *H19* transcripts in the embryos analysed in this study. In the embryos where *H19* was detected, 60% (9/15) showed an increased maternal *H19* transcript with 78% (7/9) being strictly monoallelic (p=0.4). Similar to the *SNRPN*, some embryos showed both parental transcripts of *H19*. The embryos showing paternal alleles could be due to the partial resetting of the imprints in the sperm (Ibala-Romdhane *et al.*, 2011).

Studies have suggested that developmentally delayed embryos show an unexpected expression and methylation profile (Ibala-Romdhane *et al.*, 2011). In this study, embryos with similar parental expression of *H19* (embryos 43 and 82) and *SNRPN* (embryos 3, 17, 26, 27, 28, 43, 87, 88 and 89) developed at a slower rate where seven embryos were between 5-10 cell stage and two at morula stage on day 5/6 post fertilisation. Additionally, none of the embryos that reached to the blastocyst stage showed similar parental expression for these two imprinted genes. This observation was supported, such that the slow developing embryos were shown to have a balanced pattern of methylated and unmethylated strands of H19DMR (Khoueiry *et al.*, 2012).

The time of monoallelic expression of the imprinted genes was reported to vary during preimplantation embryo development (Huntriss *et al.*, 1998). Expression of both parental transcripts of the imprinted genes could be due to the late onset of the monoallelic expression of these genes. This could be embryo specific such that the monoallelic expression may vary between embryos or in human preimplantation embryos this may be at a later stage which was observed in some of the imprinted genes in humans, such as *IGF2*, *SNPRN* and *MEST* (Huntriss *et al.*, 1998, Lighten *et al.*, 1997).

4.2.1.2 *BRCA1* expression

Identifying SNPs where couples were informative (heterozygote or homozygote for different alleles) were proved to be difficult. Mainly one partner was heterozygote and the other partner was homozygote sharing one allele. Therefore some embryos were excluded from the analysis since only the shared allele was detected following mini-sequencing (SNaPshot) analysis. In order to investigate parental differential expression of *BRCA1* in these embryos, two different SNPs located on exon 11 and exon 12 were shown to be informative and included in the analysis. However, ten embryos were excluded from the analysis since differential expression of parental *BRCA1* did not agree between these two SNPs analysed within exons 11 and 12 of *BRCA1*, respectively. In 3/10 embryos with differential parental *BRCA1* profile within the

two exons the female partner was heterozygote. The difference observed in the parental expression at two exons could be due to maternal mRNA that is still in the process of degradation. This difference could also be caused by alternative splicing of *BRCA1*, which was shown to have multiple isoforms skipping exon 5, exons 2-10, exons 9-11, exon 11 only (Δ11), exons 14-17 and exons 14-18 (Tammaro *et al.*, 2012, Orban and Olah, 2003, Lixia *et al.*, 2007, Wilson *et al.*, 1997). If one of these spliced isoforms of *BRCA1* involving/excluding exon 11 were present in the embryos, this may cause the failure of amplification in exon 11, such as in embryo number 27, and led to altered differential expression profiles between exon 11 and 12. Additionally, studies showed that alternate spliced forms of mRNAs may introduce new miRNA binding sites for their target mRNAs leading to unusual regulation and therefore expression of mRNAs (Salmena *et al.*, 2011). Expression of only the spliced form of exon 11, Δ11, was shown to be embryonic lethal in mouse embryos (Ludwig *et al.*, 1997) and over-expression of this mRNA led to apoptosis due to failure of mitosis (Bachelier *et al.*, 2002). Additionally embryos with full length *BRCA1* transcripts were shown to repress several genes that were not observed in the embryos with the Δ11 isoform (Tammaro *et al.*, 2012).

SNaPshot assay sensitivity

Previous studies validated the use of allele peak heights at an SNP site to investigate the allelic imbalance for *BRCA1* and *BRCA2* (Caux-Moncoutier *et al.*, 2009). Additional validation was carried out in this project. Real time PCR confirmed that the samples were evaluated at a quantitative state and therefore the differential expression observed was not due to an amplification bias. The chromosome copy number of the genes analysed was detected to ensure that the detected differential expression was not due to an aneuploidy in embryo. The aneuploidy rate of 26 embryos was analysed by aCGH and the rate of aneuploidy incidence was investigated in embryos with *BRCA* mutations. It has been reported that embryos with mutations in double strand break repair genes may lead to an increased aneuploidy rate (Fragouli and Wells, 2012). However,

in this study no correlation was observed for the aneuploidy rate in embryos with *BRCA* mutations. A subset of embryos were analysed for the methylation status of *BRCA1* and all these embryos were hemi-methylated. Therefore, differential expression of parental genome may be due to the methylation mechanism of *BRCA1*. Sixty two percent (5/8) of the embryos analysed for the methylation status of *H19* were not concordant with the differential expression analysis by SNaPshot assay. This conflict may be caused by other factors affecting both the expression and methylation status of the imprinted genes, such as miRNA regulation and acetylation (Huang *et al.*, 2011).

4.2.2 Development stage of embryos with *BRCA* mutations

Embryos with paternally inherited mutations were shown to develop significantly slower compared to embryos with maternally inherited mutations. This may be due to the methylation status of the embryos at the early stages of preimplantation embryo development. Since the paternal genome undergoes a rapid demethylation starting at the early stages of preimplantation embryos, embryos with paternally inherited *BRCA* mutations and defective homologous recombination repair pathway may be prevented from developing to the later stages of preimplantation development. However, embryos with maternally inherited *BRCA* mutations may compensate with the mutation due to the presence of the paternal genome with no mutation present in the early developing embryo that can initiate the homologous recombination repair.

4.2.3 Conclusion and future perspectives

This preliminary study showed that *SNRPN*, *H19* and *BRCA1* were differentially expressed in preimplantation embryos. Further studies will involve analysis of other genes including repair genes and control genes to confirm the differential expression.

It was observed that if an embryo carried paternally inherited *BRCA* mutation, this affected the developmental progression of the embryo to a greater extent than a maternally inherited *BRCA* mutation. This suggests that when the

paternal transcript present in the embryo carries a mutation, the embryo is more vulnerable to stress due to rapid demethylation of the paternal genome and the gradual demethylation of the maternal genome. Therefore they are more likely to undergo abnormal development. Further extrapolation of this data suggests that the risk of transmitting a *BRCA* mutation may be modulated by the parental origin of the mutation. Further studies with increased sample size will be carried out. It would also be interesting to analyse the developmental progression of other embryos with mutations in other double strand break repair genes and other repair genes.

5. Results and Discussion

Functional assay development for mismatch repair

5.1 Results

Aims summary

Expression and proteomic studies were performed in human oocytes and blastocysts. However presence of a transcript or protein does not show that these transcripts and proteins are functionally active. Therefore, functional studies play a significant role in determining which pathways are capable of performing DNA repair in oocytes and embryos. The aim of the last part of this study was to develop a sensitive functional assay to measure the mismatch repair efficiency in oocytes and blastocysts. Heteroduplex constructs were formed using long oligonucleotides (5.1.1) and the repair of this heteroduplex to homoduplex was assessed semi-quantitatively by SNaPshot assay. The repair efficiency was estimated by calculating the peak height ratio of the repaired sequence of the homoduplex to the unrepaired sequence of the heteroduplex.

5.1.1 Formation of nicked and non-nicked homo/heteroduplexes

Two forward oligonucleotides with the same sequence but different alleles at the SNP site rs1981929 (allele G for one sequence of 180 bases and allele A for the other sequence of 180 bases) and a complementary sequence of 180 bases with the allele T corresponding to the *MSH2* SNP site rs1981929 were designed. Homo/heteroduplexes were constructed using these complementary sequences.

A nicked homo/heteroduplex molecule was also constructed to investigate if mismatch repair is nick-directed. A nicked heteroduplex was constructed using the G sequence of 180 bases and two complementary sequences; Ta of 55 bases and Tb of 125 bases (Table 2.10).

Prior to mismatch repair reaction, successful formation of the homo/heteroduplexes was confirmed by detecting the alleles at the SNP site by mini-sequencing (SNaPshot™) using two different conditions to ensure that the correct sequences was used to form the construct and to ensure that one

sequence was not present in excess compared to the other (Section 2.3.2.1). In the denatured samples the alleles at the SNP site rs1981929 of the homo/heteroduplex constructs were observed, such that alleles C and A were detected for the G-T heteroduplex and A and T alleles for the A-T homoduplex, respectively. However, when the samples were not denatured, alleles at the SNP site rs1981929 were only detected if there was excess sequence present in the mixture. This analysis showed small peaks for sequence G (corresponding to C allele in SNaPshot assay) in the heteroduplex construct mixture and sequence A and T in the homoduplex mixture indicating some excess sequences in the mixture (Figure 5.1). However since the excess sequences were present in minute amounts, they were negligible. This ensured that when the repair efficiency was assessed, if any sequences from the heteroduplex construct were detected, these were due to the unrepaired heteroduplex constructs and not because of an excess of sequence from the heteroduplex construct.

Figure 5-1 Analysis of correct formation of homo/heteroduplex constructs using two different mini-sequencing (SNaPshot) conditions.

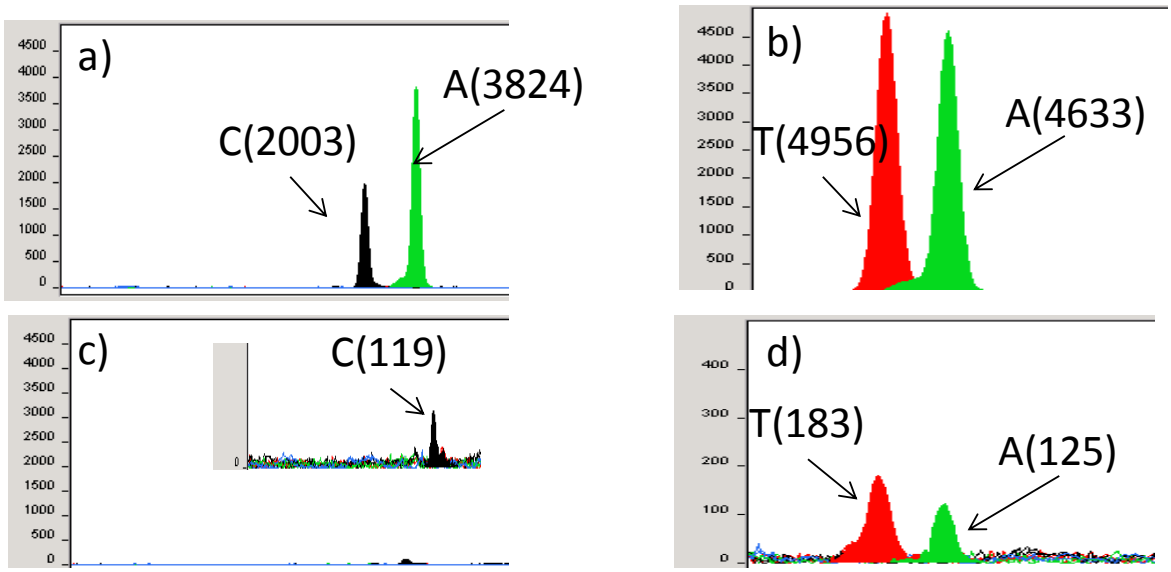

Confirmation of a) heteroduplex and b) homoduplex formation by SNaPshot assay by three cycles of denaturation, annealing and extension steps. This condition ensured that the correct sequences were used for the formation of hetero/homoduplex constructs. Confirmation of c) heteroduplex and d) homoduplex formation by optimised SNaPshot cycling conditions excluding the initial denaturation step followed by three cycles annealing and extension steps at low temperatures. These confirmed that there were no excess sequences in the reaction mixture was only a small amount of unused sequence left following the hetero/homoduplex construct formation. Since the C sequence was present at low levels, an additional enlarged image was included (panel c). For both heteroduplex and homoduplex constructs, mini-sequencing (SNaPshot) analysis showed that a small amount of excess sequence is left in the reaction. The peak height of sequence C which represents the approximate amount of the excess strand was only 119 (panel c), 183 for sequence T and 125 for sequence A (panel d), respectively.

5.1.2 Functional assay development for mismatch repair

5.1.2.1 Use of commercially available nuclear extracts

The repair efficiency was assessed by exposing the nicked and non-nicked homo/heteroduplexes to the nuclear extracts (HeLa S3 and LoVo carrying an *MSH2* mutation, Active Motif, Ca) as described in section 2.4.2.1. Since HeLa nuclear extract is known to repair mismatches, with the correct reaction conditions, such as concentration of constructs and extracts and correct incubation time, repair of heteroduplex to homoduplex should be observed. Different concentrations of nicked homo/heteroduplexes (3.33-0.33µM final in the mismatch repair reaction) were exposed to 14-1.33µg nuclear extracts (final

in the mismatch repair reaction) for 1 to 23 hours. These conditions and the results are shown in figure 5.2, 5.3 and table 5.1.

Repair of both nicked G-Tn and non-nicked G-T heteroduplex to G-C homoduplex was detected in one hour using 13.35µg of nuclear extract. As the concentration of the nuclear extract was lowered, the repair efficiency was reduced. As expected as the time of incubation increased, the repair efficiency was also increased, such that when the time of incubation was increased to 3, 6 (Figure 5.3), 15 and finally to 23 hours, the repair efficiency was improved even using as small as 1.33µg nuclear extracts. Higher concentrations of nuclear extract and/or higher incubation time were required for the mismatch repair deficient LoVo extract (100% repair efficiency with1.43µg HeLa nuclear extract for 23 hours) to repair the heteroduplex with similar efficiencies as the HeLa nuclear extract (100% repair efficiency with1.33µg HeLa nuclear extract for 15 hours).

Figure 5-2 Mini-sequencing (SNaPshot) analysis panels examining the mismatch repair efficiency of G-Tn after nuclear extract exposure for 1, 3 and 6 hours.

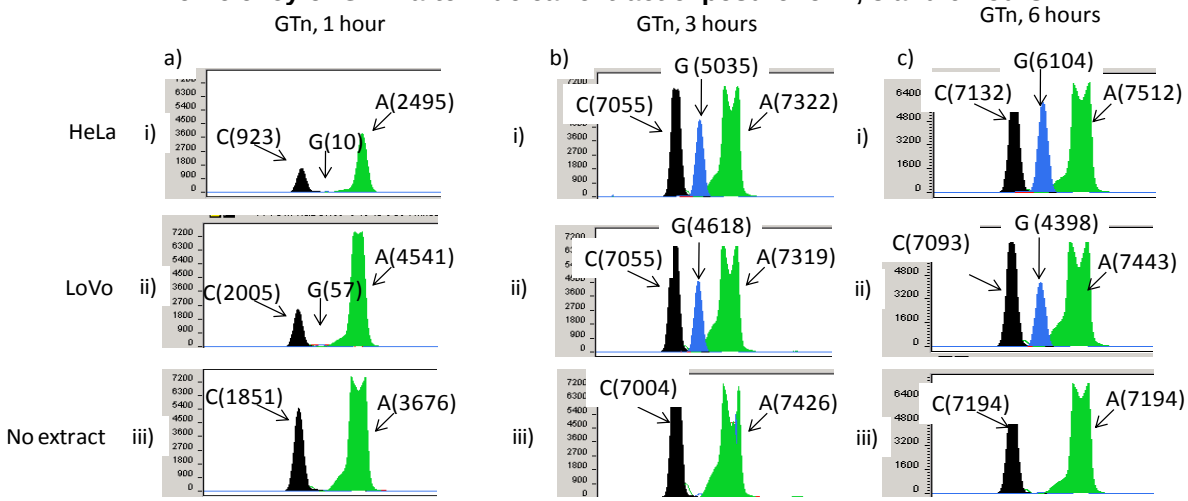

Black, blue and green peaks represent the C, G and A alleles, respectively. The peak heights (corresponding to the fluorescence intensity) are shown in parenthesis. (a)-(c) i. SNaPshot™ analysis of G-Tn exposure to HeLa nuclear extract for 1, 3 and 6 hours, respectively. (a)-(c) ii. SNaPshot™ analysis of G-Tn exposure to LoVo (mismatch repair deficient) nuclear extract for 1, 3 and 6 hours, respectively. (a)-(c) iii. SNaPshot™ analysis of G-Tn incubated in the absence of any nuclear extracts for 1, 3 and 6, respectively. As the time of incubation increased, the mismatch repair efficiency was also increased observed by the higher peak heights. Repair in the presence of HeLa nuclear extract was increased compared to the mismatch repair in the presence of LoVo nuclear extract.

Table 5-1 Summary of all the mismatch repair reactions by HeLa and LoVo nuclear extracts.

a) Summary table of repair efficiency of heteroduplex construct to homoduplex after HeLa nuclear extract exposure

Heteroduplex construct	Concentration of constructs (µM)	Concentration of HeLa (µg)	Time of incubation (hours)	Repair efficiency (Repaired/ unrepaired)
GTn	3.33	13.35	1	5%
GTn	1.67	13.35	1	1%
GTn	1.67	10.05	1	3%
GTn	1.67	6.75	1	17%
GTn	1.67	3.3	1	19%
GTn	1.67	1.95	1	1%
GT	1.67	1.33	1	0%
GTn	1.67	1.33	1	0%
GTn	1.67	1.33	3	70%
GTn	1.67	1.33	6	80%
GTn	1.67	1.33	15	100%
GTn	0.83	1.33	23	0%
GT	0.83	1.33	23	22%
GTn	0.67	1.33	23	4%
GT	0.67	1.33	23	50%
GTn	0.33	1.33	23	5%
GT	0.33	1.33	23	13%

b) Summary table of repair efficiency of heteroduplex construct to homoduplex after LoVo nuclear extract exposure

Heteroduplex construct	Concentration of constructs (µM)	Concentration of LoVo (µg)	Time of incubation (hours)	Repair efficiency (Repaired/ unrepaired)
GTn	3.33	14.4	1	6%
GTn	1.67	14.4	1	0%
GTn	1.67	10.8	1	4%
GTn	1.67	7.2	1	42%
GTn	1.67	3.6	1	29%
GTn	1.67	2.1	1	9%
GT	1.67	1.43	1	0%
GTn	1.67	1.43	1	1%
GTn	1.67	1.43	3	64%
GTn	1.67	1.43	6	71%
GTn	1.67	1.43	15	99%
GTn	0.83	1.43	23	100%
GT	0.83	1.43	23	27%
GTn	0.67	1.33	23	4%
GT	0.67	1.33	23	10%
GTn	0.33	1.33	23	4%
GT	0.33	1.33	23	13%

a) Summary table of repair efficiency of heteroduplex construct to homoduplex after HeLa nuclear extract exposure. b) Summary table of repair efficiency of heteroduplex construct to homoduplex after LoVo (mismatch repair deficient) nuclear extract exposure. In order to find the optimal concentrations of heteroduplex constructs and nuclear extracts with correct incubation times, series of optimisation experiments were performed. These tables summarise the final concentrations of nicked and non-nicked heteroduplex constructs, (a) HeLa and (b) LoVo nuclear cell extract concentrations and time of exposure for the mismatch reaction. The efficiency of mismatch analysed by SNaPshot™ reaction was shown as a percentage of the ratio of repaired/unrepaired sequence of the heteroduplex. GT represents the non-nicked heteroduplex complex and GTn represents the nicked heteroduplex constructs.

Figure 5-3 Scatter plot summarising different concentration of heteroduplex (G-T) and nuclear extracts HeLa and LoVo and time of incubation against percentage of repair ratios.

a) Scatter plot of HeLa nuclear extract concentration and repair efficiency of heteroduplex construct

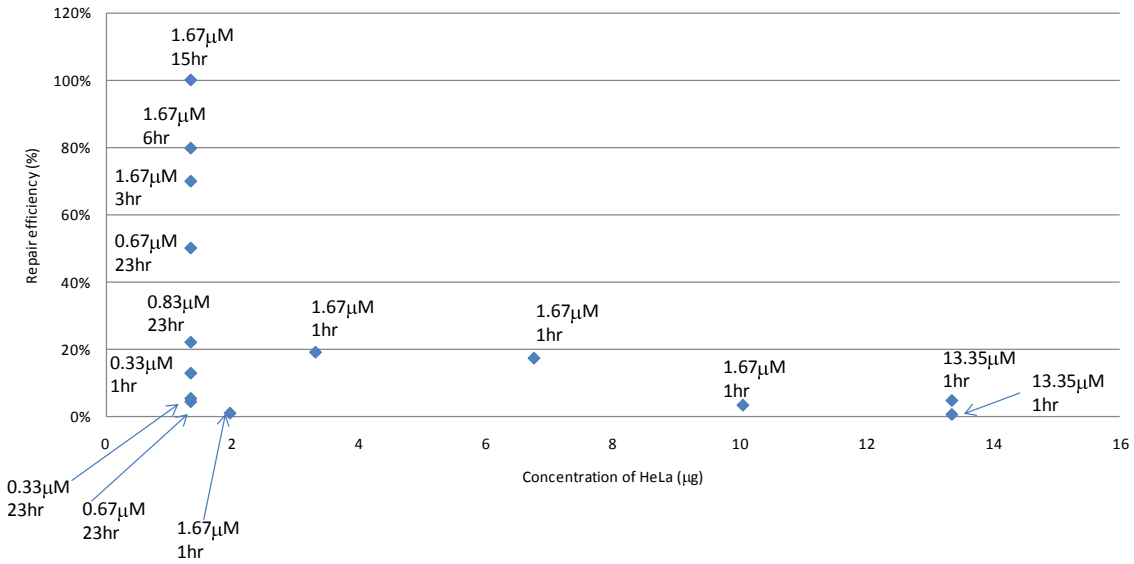

b) Scatter plot of LoVo nuclear extract concentration and repair efficiency of heteroduplex construct

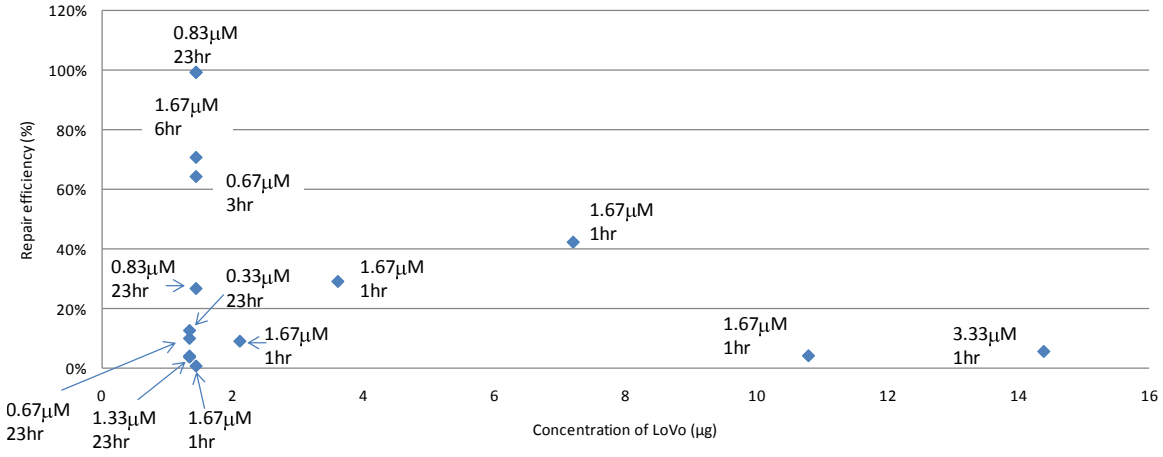

Optimisation results for mismatch repair assay using a) HeLa and b) LoVo nuclear cell extracts are shown in a scatter plot. The x-axis represents the concentration of extracts and the y-axis represents the percentage of repair ratio (percentage of repaired sequence/unrepaired sequence). Concentration of heteroduplex constructs and time of incubation for each data point are labelled. As the concentration of construct was decreased, the repair efficiency was also decreased. However, the repair efficiency was increased as the time of incubation was also increased. It was observed that although for some conditions, the repair efficiency of the mismatch repair deficient LoVo nuclear extract was similar with the HeLa nuclear extract, generally the repair efficiency was higher for HeLa nuclear extracts.

To ensure that exposing heteroduplex constructs to nuclear extracts in mismatch repair reagents for long hours does not cause any degradation of both the heteroduplex sequences and the nuclear extracts, a control sample, homoduplex, was constructed. The same reaction conditions were also applied to this homoduplex, such that the nicked (A-Tn) and non-nicked (A-T) homoduplex constructs were exposed to the nuclear extracts of the same concentration and incubation time. Figure 5.4 illustrates the SNaPshot™ analysis after the exposure of A-Tn homoduplex to nuclear extracts for 3 and 15 hours showing A and T alleles (corresponding to T and A sequences, respectively). No degradation of the sequences observed.

Figure 5-4 Mini-sequencing (SNaPshot) analysis panels examining the mismatch repair efficiency of A-Tn after nuclear extract exposure for 3 and 15 hours.

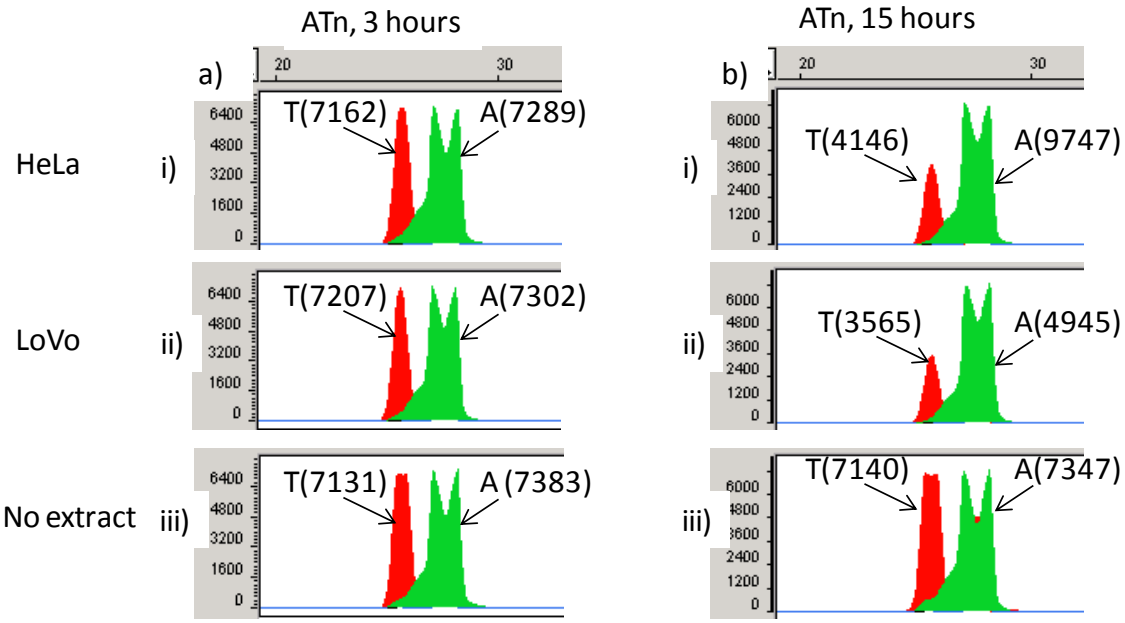

Red and green peaks represent the T and A alleles, respectively. The peak heights (corresponding to the fluorescence intensity) are shown in parenthesis. (a) and (b) i. SNaPshot™ analysis of A-Tn after 3 and 15 hours of HeLa nuclear extract exposure showing the T and A alleles, respectively. (a) and (b) ii. SNaPshot™ analysis of A-Tn after 3 and 15 hours of LoVo nuclear extract exposure showing the T and A alleles, respectively. (a) and (b) iii. SNaPshot™ analysis of A-Tn after incubation for 3 and 15 hours in the absence of nuclear extracts showing the T and A alleles, respectively.

5.1.2.2 Use of commercially available whole cell extracts

The aim of this project was to assess mismatch repair efficiency in oocytes and blastocysts. Since obtaining nuclear extracts from these samples are difficult,

the mismatch repair reaction was optimised using commercially available whole cell extracts. The nicked and non-nicked homo/heteroduplexes were exposed to HeLa whole cell extract (Table 5.2, Figures 5.5 and 5.6). Different concentrations of G-Tn and G-T heteroduplexes (0.83-0.33µM) were exposed to 5-2.5µg HeLa whole cell extract for 23 hours, respectively. As shown in figure 5.6, as the concentration of G-T was decreased, the repair efficiency was also decreased. The optimisation conditions are listed in table 5.2.

Figure 5-5 Mini-sequencing (SNaPshot) analysis panels examining the mismatch repair efficiency of G-T heteroduplex at different concentrations of commercially available whole cell extract.

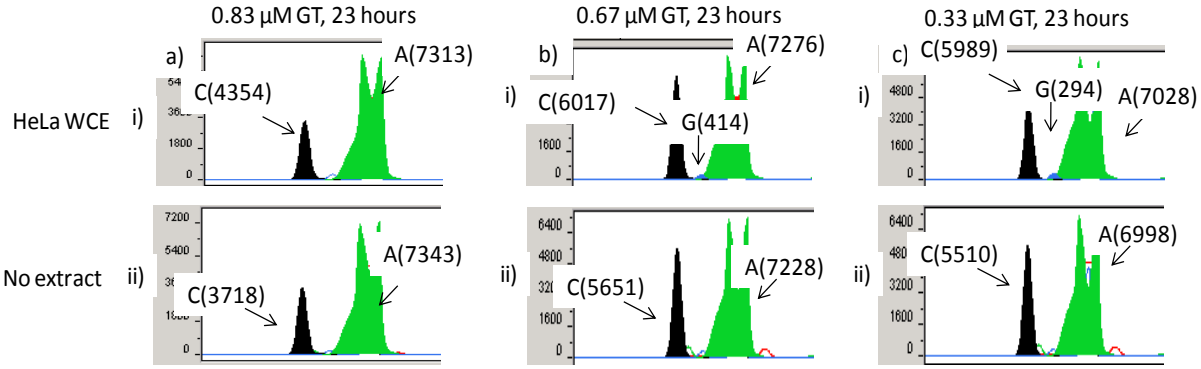

The peak heights (corresponding to the fluorescence intensity) are shown in parenthesis. Black, blue and green peaks represent the C, G and A alleles, respectively. (a)-(c) i. SNaPshot™ analysis of 0.83µM, 0.67µM and 0.33µM G-T after 23 hours of HeLa whole cell extract exposure, respectively. T sequences are shown to be repaired to C sequence (complementary G peak, black). (a)-(c) ii. SNaPshot™ analysis of 0.83µM, 0.67µM and 0.33µM G-T that was incubated for 23 hours in the absence of any whole nuclear extracts showing unrepaired heteroduplex sequences, respectively. Mismatch repair was observed at 0.67µM and 0.33µM of G-T heteroduplex to G-C homoduplex. The repair efficiency was lower when the heteroduplex concentration was reduced from 0.67µM to 0.33µM. There was no repair in the absence of whole cell extract.

Table 5-2 Summary table of repair efficiency of heteroduplex construct to homoduplex after HeLa whole cell extract exposure.

Heteroduplex construct	Concentration of constructs (µM)	Concentration of HeLa whole cell extract (µg)	Time of incubation (hours)	Repair efficiency (Repaired/ unrepaired)
GTn	0.83	5	23	34%
GTn	0.67	5	23	5%
GT	0.67	5	23	6%
GTn	0.33	5	23	3%
GT	0.33	5	23	4%
GTn	0.33	2.5	23	0%
GT	0.33	2.5	23	0%

This table summarises the final concentrations of the nicked and non-nicked heteroduplexes, final concentrations of whole cell extracts and time of exposure for the mismatch repair reaction. The efficiency of mismatch repair analysed by SNaPshot™ reaction was shown as a percentage of the ratio of repaired/unrepaired sequence of the heteroduplex. GT represents the non-nicked heteroduplex complex and GTn represents the nicked heteroduplex constructs.

Figure 5-6 Scatter plot summarising different concentration of heteroduplex (G-T) and HeLa whole extract against percentage of repair ratios.

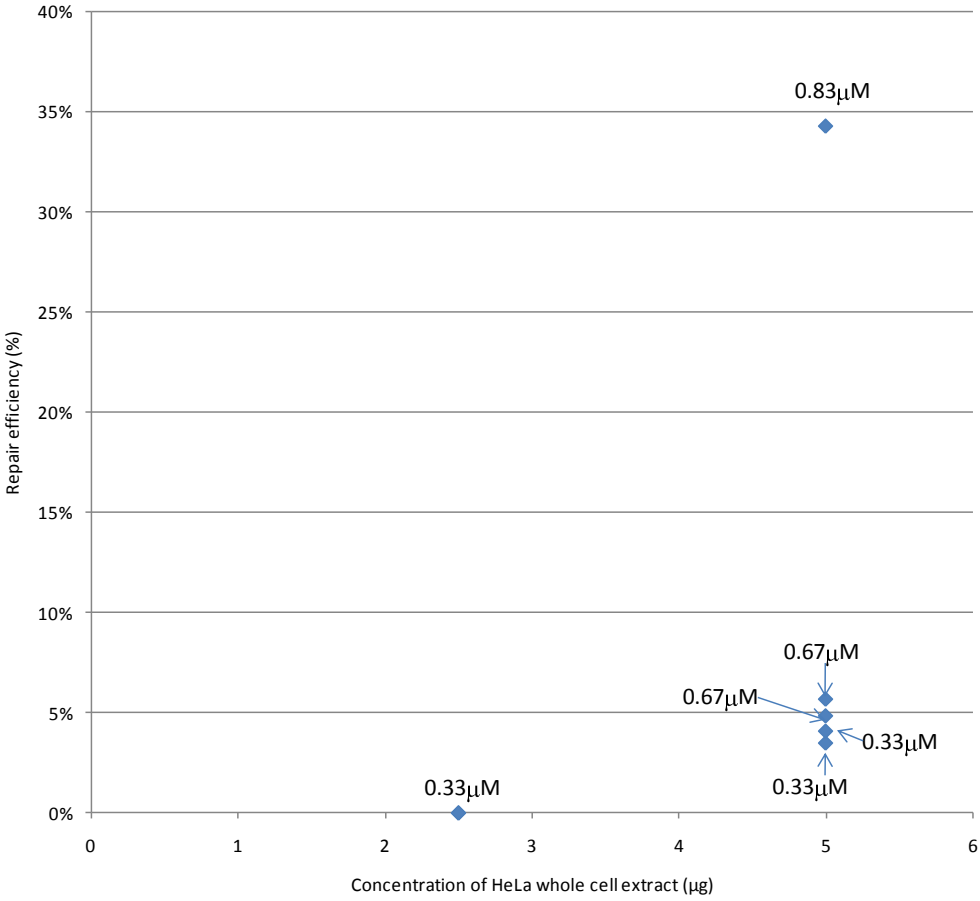

Optimisation results for mismatch repair assay using HeLa whole cell extracts are shown in a scatter plot. The x-axis represents the concentration of HeLa whole cell extract and the y-axis represents the percentage of repair ratio (percentage of repaired sequence/unrepaired sequence). The mismatch repair reaction was performed for 23 hours for different concentration conditions. Concentration of heteroduplex constructs for each data point is labelled. It was observed that as the concentration of the whole cell extract was reduced, the repair efficiency was also reduced. When the concentration of HeLa whole cell extract was lowered to 2.5µg, no repair was observed.

5.1.3 Mismatch repair in oocytes and blastocysts

The final part of this study focused on assessing mismatch repair efficiency in oocytes and blastocysts. For all the reactions, mismatch repair was assessed in two controls, one positive with HeLa extract and one negative with no extract. In the presence of HeLa whole cell extract, mismatch repair of the G-T heteroduplex to G-C was observed in all the reactions; whereas no repair was detected in the absence of whole cell extract. In some samples, mismatch repair was assessed in an additional negative control where mismatch repair

buffer involving dNTPs, ATP and glutathione was excluded from the analysis. Similarly no repair was observed in the absence of dNTPs, ATP and glutathione.

5.1.3.1 Use of protein extracts from mouse blastocysts

Protein was extracted from ten and fifteen pooled mouse embryos, respectively. Mismatch repair reaction was applied as optimised for the whole cell extracts with 0.33µM heteroduplex G-Tn and 73% (11µl of protein extract in 15µl mismatch repair mixture) protein in the presence of mismatch repair buffer. However, no repair was observed from two mismatch repair reactions using the protein extracts from 10 and 15 pooled mouse embryos, respectively.

5.1.3.2 Use of whole cell extracts from oocytes and blastocysts

Mismatch repair efficiency was assessed in pooled mouse oocytes and blastocysts and pooled human blastocysts using the optimised reaction conditions. Both mouse and human blastocysts were at similar developmental stage. However, differences in the repair efficiency of mouse and human blastocysts may be observed. This could be due to higher amount of proteins present in the mouse embryos. It may also be possible that higher repair efficiency may be observed if the extraction was performed at the earlier stages of embryo development due to the presence of maternal protein in the embryo.

Whole cell extraction was carried out from pooled 5 and 10 mouse oocytes, and 4 and 8 pooled mouse blastocysts, respectively. G-T heteroduplex molecules (0.33µM) were exposed to the whole cell extract obtained from these pooled oocytes and blastocysts for 23 hours at 37ºC. Mismatch repair was not observed in any of the oocyte samples. Mismatch repair of G-T heteroduplex to G-C homoduplex was observed in whole cell extract obtained from pooled mouse blastocysts of four and eight, respectively. The peak height observed for the repaired C sequence was at much lower level compared to the unrepaired heteroduplex sequences indicating that although mismatch repair took place, not all the G-T heteroduplex was repaired. However, the peak height of repaired allele C in eight pooled oocytes was doubled compared to the peak height of C

allele observed in four pooled blastocysts indicating an increased efficiency for the repair.

Whole cell extract was obtained from eleven pooled human embryos. G-Tn heteroduplex molecule (final concentration of 0.33µM) was exposed to the whole cell extract for 23 hours at 37ºC. Mismatch repair of G-Tn heteroduplex to G-C homoduplex was detected. However mismatch repair in human blastocysts was at a lower efficiency compared to the mouse blastocysts (Table 5.3 and Figure 5.7).

Figure 5-7 Mini-sequencing (SNaPshot) analysis panels examining the mismatch repair efficiency of G-T heteroduplex in whole cell extract from pooled 11 human embryos.

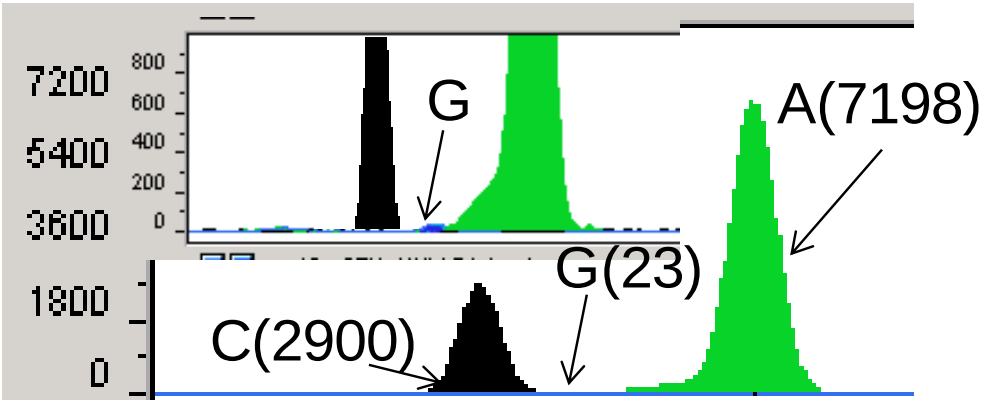

G-T heteroduplex was shown to be repaired to G-C. However, the repair efficiency was low since the C and A alleles corresponding to G-T sequences of the heteroduplex were still present in the reaction mixture. Since the repair was low, the G allele peak height was also low; therefore an additional enlarged image within the same panel was placed. Black, blue and green peaks represent the C, G and A alleles, respectively. The alleles and the peak heights in parenthesis (corresponding to the fluorescence intensity) are shown.

Table 5-3 Summary of the mismatch repair reactions by whole cell extracts obtained from pooled mouse oocytes, blastocysts and human blastocysts.

Heteroduplex construct	Concentration of constructs (µg/µl)	Number of oocytes/blastocysts pooled (mg/ml)		Time of incubation (hours)	Repair efficiency (Repaired/ unrepaired)
		Oocytes	Blastocysts		
GTn (Mouse)	0.33	5 (5840)	-	23	0%
GTn (Mouse)	0.33	10 (8700)	-	23	0%
GTn (Mouse)	0.33	-	8 (2770)	23	19%
GTn (Mouse)	0.33	-	4 (1115)	23	6%
GTn (Human)	0.33	-	11(8392)	23	0.3%

This table summarises the concentrations of the nicked heteroduplex constructs, number of oocytes and the initial concentrations of the whole cell extract obtained from mouse and human oocyte/blastocyst samples and time of exposure for the mismatch repair reaction. The efficiency of mismatch repair analysed by SNaPshot™ reaction was shown as a percentage of the ratio of repaired/unrepaired sequence of the heteroduplex. It was shown that there was no repair in pool of 5 and 10 mouse oocytes. Repair of G-T heteroduplex to G-C homoduplex was observed in whole cell extracts obtained from pool of 8 and 4 mouse blastocysts. Mismatch repair of G-T heteroduplex to G-C homoduplex was also observed in 11 pooled human blastocyst whole cell extract. However the repair efficiency in the human blastocysts was considerably lower compared to the mouse blastocysts.

5.1.4 Summary of functional assay for mismatch repair

Technical aspects

- Homo/heteroduplex molecules were successfully constructed using commercially available long oligonucleotides.
- Reaction to assess the efficiency of mismatch repair was initially optimised using commercially available mismatch repair efficient (HeLa) and mismatch repair deficient (LoVo) nuclear extracts.
- Mismatch repair reaction was then optimised on commercially available HeLa whole extracts.
- The optimal conditions for mismatch repair reactions were incubation of 1.67µM of heteroduplex construct with 1.33µg HeLa nuclear extract for 15 hours (100% repair efficiency). Slightly higher concentration of

mismatch repair deficient LoVo nuclear extract (1.43μg) with increased incubation time (23 hours) was required for 100% repair efficiency.

- The highest repair efficiency (34%) was obtained when 0.83μM heteroduplex construct was incubated with 5μg HeLa whole cell extract for 23 hours.

Biological aspects

- Mismatch repair was successfully assessed in mouse oocytes, blastocysts and human blastocysts. There was no mismatch repair detected in mouse oocytes.

- Mismatch repair efficiency in mouse blastocysts was shown to be more efficient in repairing G-T and G-Tn heteroduplex constructs compared to human blastocysts. These preliminary results suggest that mismatch repair may be functionally more active in mouse blastocysts compared to human blastocysts.

5.2 Discussion

DNA repair efficiency in gametes and preimplantation embryos is not well established. Therefore, gene expression and proteomic analyses play a crucial role to deduce which DNA repair pathways may be active in human oocytes and embryos. However, these analyses alone are not sufficient to assess repair efficiency since many genes and proteins are involved in a fully functioning repair pathway. Functional studies provide a better understanding of the repair capacity of DNA repair pathways. The aim of the last part of this project was to develop a sensitive functional assay to assess the activity of mismatch repair proteins initially in cell free content and then in preimplantation embryos.

The initial step of this project was to form the nicked/non-nicked heteroduplex constructs using oligonucleotides. Repair efficiency of G-T heteroduplex was analysed in this study since it has been shown that this mismatch is repaired efficiently by mismatch repair efficient cells, such as HeLa S3 extracts (Hays *et al.*, 2005, Holmes *et al.*, 1990, Thomas *et al.*, 1991). Additionally C to T point mutations were shown to be predominant in bacteria due to the deamination of cytosines in the non-transcribed DNA strand which was also shown to be the case in human genome by evolutionary analyses (Beletskii and Bhagwat, 1996, Mugal *et al.*, 2009, Franco-Zorrilla *et al.*, 2007, Riggs and Jones, 1983, Brown and Jiricny, 1988, Heywood and Burke, 1990a, Heywood and Burke, 1990b).

Two nuclear extracts were selected for this project, one mismatch repair protein efficient (HeLa S3) and another mismatch repair protein deficient involving a deletion within the *MSH2* gene (LoVo) (Umar *et al.*, 1994). These extracts are stable when they are stored at -80˚C up to six months (manufacturer's protocol). The nicked heteroduplexes at different concentrations (3.3-0.33µM) were incubated for 1, 3, 6, 15 and 23 hours in the presence of these two nuclear extracts at different concentrations (14-1.33µg) and in the absence of any nuclear extract or mismatch repair buffer as negative controls. Since this technique was being optimised to be applied in preimplantation embryos, the amount of nuclear extract was fundamental to the success of the assay. The

total amount of protein in mammalian oocytes and preimplantation embryos has been shown to be between 162ng to 50µg in preimplantation embryos (Grealy *et al.*, 1996, Thompson *et al.*, 1998). The final concentration of both nicked/non-nicked heteroduplexes and the final amount of the nuclear extract was reduced to 0.33µM and 1.33µg compared to previous assays that required 100ng substrate and 100µg nuclear extract for the mismatch repair reaction, respectively (Wang and Hays, 2002). Results of this study showed repair of both nicked G-Tn and non-nicked G-T heteroduplexes to G-C homoduplexes in the presence of HeLa and less efficiently in LoVo nuclear extracts. Studies showed that the G-T mismatches were preferentially repaired to G-C homoduplex (Wiebauer and Jiricny, 1989, Bill *et al.*, 1998). Although the repair efficiency was lower for 1 hour exposure compared to 3, 6 and 15 hour exposures, the repair was still detected.

In theory, any nuclear extract that is mismatch repair deficient should not repair the mismatches. However, studies have reported mismatch repair in the presence of LoVo nuclear extracts in *Saccharomyces cerevisiae* showing that *MSH3* can function as an alternate for *MSH2* (Marsischky *et al.*, 1996, Strand *et al.*, 1995) in endometrial cancer cell lines (Umar *et al.*, 1994), human colon carcinoma cell lines (Lei *et al.*, 2004) and in mouse embryo fibroblasts (Edelmann *et al.*, 1996). Another explanation of this mismatch repair activity is that other DNA repair mechanisms, such as base excision repair or nucleotide excision repair, may take part in the repair when mismatch repair is not active (O'Regan *et al.*, 1996, Huang *et al.*, 1994). Studies also identified a thymine DNA glycosylase that is specific for repairing the G-T mismatches to G-C in bacteria (Sohail *et al.*, 1990) and in mammalian cells (Wiebauer and Jiricny, 1989, Wiebauer and Jiricny, 1990, Bill *et al.*, 1998) that could be responsible for the repair in mismatch repair deficient cells. Any of these possibilities may take part in the repair of G-T heteroduplex to G-C homoduplex in LoVo nuclear extracts. Studies have shown that when the mismatched DNA was incubated with mismatch repair deficient cells for short periods, such as fifteen minutes, the mismatch repair efficiency was not as good as the repair by mismatch repair

efficient cells that may indicate the need of longer time for repair in the absence of mismatch repair system (Lei *et al.*, 2004).

Studies suggest that there is differential repair efficiency and biased repair. Several factors can affect the repair direction and the efficiency, such as the sequence of the strand, different mismatches, methylation status and DNA nicks (Brown and Jiricny, 1988, Hare and Taylor, 1985b, Hare and Taylor, 1985a, Grilley *et al.*, 1990, Bishop and Kolodner, 1986, Thomas *et al.*, 1991, Fang and Modrich, 1993). Different repair efficiencies depending on the mismatches were observed in circular plasmids in monkey and human cells (Brown and Jiricny, 1988), such that the repair of C-C and G-G mismatches were better compared to the repair efficiency of C-T and A-G mismatches. In contrast, a more recent study suggested that the repair efficiency of A-G and C-T mismatches was higher (Miller *et al.*, 1997). Conflicting studies suggest that the single-base mismatches did not have a significant effect on the repair efficiency (Bill *et al.*, 1998).

Another factor that was suggested to have an effect on the DNA repair efficiency was the presence of other nearby mismatches that may induce co-repair and it was proposed that this would increase the repair efficiency (Bill *et al.*, 1998, Carraway and Marinus, 1993, Weng and Nickoloff, 1998). The results of this study showed that both the nicked and non-nicked heteroduplexes were repaired at a similar repair efficiency indicating that the repair was not nick-directed. Studies suggested that nicks may improve the repair efficiency and the repair is initiated from the nick (Thomas *et al.*, 1991, Holmes *et al.*, 1990, Fang and Modrich, 1993, Umar *et al.*, 1994, Miller *et al.*, 1997, Taghian *et al.*, 1998). Conflicting studies in monkey COS-7 (CV-1 in Origin and carrying the SV40 genetic material) cells suggested that nicks did not have an effect in directing the strand repair (Heywood and Burke, 1990a, Heywood and Burke, 1990b). Additional studies supported this by showing equal mismatch repair efficiency with nicked and intact plasmid DNA in *in vivo* studies (Lei *et al.*, 2004). The similarity of the mismatch repair activity between nicked and intact plasmid DNA could be due to fast ligation of the nick followed by the repair of the mismatch.

Studies supported this hypothesis such that mismatch repair was more efficient in the presence of DNA ligase 3 with nicked plasmid DNA (Tomkinson *et al.*, 1993).

In addition to assessing DNA repair of nicked/non-nicked mismatches, a control sample, nicked/non-nicked homoduplexes (A-Tn and A-T), was analysed under the same conditions. Same concentrations of homoduplex, nuclear extract and time of incubation were applied to these samples. As expected, for all the analysis the only alleles that were detected were A and T following the SNaPshot™ analysis. This proved that addition of mismatch repair reagents did not yield any bias in the reaction and the longer incubation times for the mismatch repair reaction did not lead to degradation of the strands.

The second part of this study involved optimising this assay to detect mismatch repair activity using whole cell extracts. Similar to the nuclear extracts, whole cell extracts should be stable for six months (manufacturer's protocol). Different concentrations of G-Tn and G-T heteroduplexes were exposed to HeLa whole cell extract for up to 23 hours. The results have shown that as the concentration of the nicked/non-nicked heteroduplex was lowered, the efficiency of the repair was also lowered. When nicked/non-nicked heteroduplex was exposed to lower concentrations (2.5µg) of HeLa whole cell extract, there was no repair.

The final part of this study involved assessment of mismatch repair in oocytes and blastocysts. Mismatch repair was assessed using protein extracts obtained from pooled mouse blastocysts. However no repair was observed suggesting that other polymerases were required for the mismatch repair to take place. Therefore, whole cell extracts were obtained from pooled mouse oocytes and blastocysts and human blastocysts. Both these extracts were suspected to be stable for six months. However to avoid any degradation, the whole cell extracts from oocytes and blastocysts were used immediately. No mismatch repair activity was detected in pooled mouse oocytes suggesting that although repair transcripts are present in the oocytes (Latham *et al.*, 1992, Shi *et al.*, 1994), they may not be active. Repair of the heteroduplex was detected both in pooled

mouse and human blastocysts. However, the repair efficiency of the blastocysts was considerably lower compared to the mismatch repair observed in commercially available nuclear and whole cell extracts. This was expected since amount of protein present in mammalian oocytes and blastocysts is very small (0.1µg in oocytes and 0.16-50µg in preimplantation embryos) (Grealy *et al.*, 1996).

Conclusion and Future work

A simple and sensitive assay was developed to detect mismatch repair efficiency in oocytes and blastocysts. This method has advantages over the previously developed assays since small amounts of proteins can be used with this assay that enables mismatch repair assessment in embryos. This construct can easily be modified to detect different/multiple mismatches with different lengths in addition to modifying the construct into assessing insertion deletion loops with different sizes. Preliminary studies in repairing insertion deletion loops using PCR generated samples were carried out in the presence of nuclear extracts (Personal communications with Dr Jaroudi). By optimising this technique to a single cell level, mismatch repair activity can be investigated in embryos derived from patients with known repair mutations.

Concluding remarks and future work

DNA repair is likely to play a crucial role in preimplantation embryo development. However both gametes and blastocysts have complex DNA repair mechanisms and the activity of DNA repair genes and proteins is not well established. Genes involved in DNA repair have been shown to be expressed at the early stages of mammalian development. The regulation of gene expression is highly complex. Amongst those factors involved in this regulation are miRNAs and DNA methylation.

The first aim of this study was to analyse differences in expression of microRNAs and their target mRNAs involved in repair. This preliminary study showed that the levels of expression of most of the repair gene mRNAs are higher in oocytes than blastocysts and many of the miRNAs followed the same trend. A correlation test between the levels of expression of the miRNAs and their target mRNAs in the oocyte samples and in the blastocyst samples aimed to investigate a possible regulatory role of the selected miRNAs on candidate mRNAs coded by genes involved in DNA repair pathways. However, there was no clear cut pattern of differences in relative expression and a definite conclusion for the correlation analysis could not be drawn. This was likely due to the limited size and number of available samples. However, this project provided some data to guide future experiments in the selection of target genes and miRNAs. The ideal experiment design would be to analyse the expression of more miRNAs involved in DNA repair genes in the same oocyte and blastocyst samples, which could ultimately provide a better understanding of the regulatory roles of miRNAs on gene expression.

This study further focused on the expression of *BRCA1* in human preimplantation embryos and the developmental progression of embryos with *BRCA* mutations. It was shown that methylation affects the expression of genes during preimplantation embryo development. Parental *BRCA1* transcripts were differentially expressed in embryos that may be caused by the differential demethylation of the parental genomes. Because of this differential demethylation, it was observed that inheriting a mutation from one parent had a

greater impact compared to inheriting the mutation from the other parent. This study showed that embryos with paternally inherited *BRCA* mutations developed slower compared to the maternally inherited *BRCA* mutations. The main limitation of this study was the small number of embryos with *BRCA1* and *BRCA2* mutations that were collected. Collection of more of these samples in the future will enable a more definite conclusion on the developmental progression of the embryos depending on the parental transmission of *BRCA* mutations to be drawn. Similarly, analysis of more embryos for other genes, including additional house keeping genes, will shed light to differential expression due differential parental demethylation status of the embryos. This study showed key findings in gene expression of *BRCA1* and imprinted genes *SNRPN* and *H19*. A basis for future experiments was established and the current knowledge of variations in the gene expression due to the regulation of genome wide parental methylation in preimplantation embryos will be expanded. A more detailed analysis of genes involved in DNA repair will provide crucial information on the predicted embryo development progression when a couple is undergoing PGD for any mutations in repair genes. It may be possible to generalise a conclusion such that inheritance of paternal *BRCA* mutations impairs the embryo development and therefore is less likely to be transmitted to the next generation. Expression analyses and immunostaining studies play a vital role to demonstrate which DNA repair genes and proteins are present in the oocytes and embryos; however they cannot be fully associated with the activity of DNA repair mechanisms. The only way to assess the activity of the proteins involved in the complex repair pathways is by functional assays. Therefore the last part of this study focused on developing an easy and sensitive functional assay to assess mismatch repair activity in oocytes and blastocysts. This functional assay provides a total outcome for DNA repair activity including several factors, such as gene expression, protein functioning and any environmental factors. The mismatch repair functional assay developed in this study is unique for the amount of protein it requires to detect mismatch repair and it also provides an easy interpretation by mini-sequencing analysis. However, this assay still requires further optimisation to achieve sensitive

detection of mismatch repair in single human oocytes and blastocysts. Therefore, this study formed the basis of future studies to optimise a sensitive functional assay used in human preimplantation embryos and understand the repair capacity of these embryos.

In summary, expression of DNA repair genes is important to detect DNA damage and initiate the appropriate repair. Functional assessment of repair pathways provide better understanding of which ones are active in the early stages of preimplantation embryo development and predict which embryos have a better chance in preimplantation development and implantation.

6. References

ADARE, A., AFANASIEV, S., AIDALA, C., AJITANAND, N. N., AKIBA, Y., AL-BATAINEH, H., ALEXANDER, J., AOKI, K., ARAMAKI, Y., ATOMSSA, E. T., AVERBECK, R., AWES, T. C., AZMOUN, B., BABINTSEV, V., BAI, M., BAKSAY, G., BAKSAY, L., BARISH, K. N., BASSALLECK, B., BASYE, A. T., BATHE, S., BAUBLIS, V., BAUMANN, C., BAZILEVSKY, A., BELIKOV, S., BELMONT, R., BENNETT, R., BERDNIKOV, A., BERDNIKOV, Y., BICKLEY, A. A., BOK, J. S., BOYLE, K., BROOKS, M. L., BUESCHING, H., BUMAZHNOV, V., BUNCE, G., BUTSYK, S., CAMACHO, C. M., CAMPBELL, S., CHEN, C. H., CHI, C. Y., CHIU, M., CHOI, I. J., CHOUDHURY, R. K., CHRISTIANSEN, P., CHUJO, T., CHUNG, P., CHVALA, O., CIANCIOLO, V., CITRON, Z., COLE, B. A., CONNORS, M., CONSTANTIN, P., CSANAD, M., CSORGO, T., DAHMS, T., DAIRAKU, S., DANCHEV, I., DAS, K., DATTA, A., DAVID, G., DENISOV, A., DESHPANDE, A., DESMOND, E. J., DIETZSCH, O., DION, A., DONADELLI, M., DRAPIER, O., DREES, A., DREES, K. A., DURHAM, J. M., DURUM, A., DUTTA, D., EDWARDS, S., EFREMENKO, Y. V., ELLINGHAUS, F., ENGELMORE, T., ENOKIZONO, A., EN'YO, H., ESUMI, S., FADEM, B., FIELDS, D. E., FINGER, M., JR., FINGER, M., FLEURET, F., FOKIN, S. L., FRAENKEL, Z., FRANTZ, J. E., FRANZ, A., FRAWLEY, A. D., FUJIWARA, K., FUKAO, Y., FUSAYASU, T., GARISHVILI, I., GLENN, A., GONG, H., GONIN, M., GOTO, Y., GRANIER DE CASSAGNAC, R., GRAU, N., et al. (2010) Elliptic and hexadecapole flow of charged hadrons in Au+Au collisions at sq.rt(s(NN))=200 GeV. *Phys Rev Lett,* 105**,** 062301.

ADIGA, S. K., TOYOSHIMA, M., SHIMURA, T., TAKEDA, J., UEMATSU, N. & NIWA, O. (2007) Delayed and stage specific phosphorylation of H2AX during preimplantation development of gamma-irradiated mouse embryos. *Reproduction,* 133**,** 415-22.

ADJAYE, J., BOLTON, V. & MONK, M. (1999) Developmental expression of specific genes detected in high-quality cDNA libraries from single human preimplantation embryos. *Gene,* 237**,** 373-83.

ALLEN, D. J., MAKHOV, A., GRILLEY, M., TAYLOR, J., THRESHER, R., MODRICH, P. & GRIFFITH, J. D. (1997) MutS mediates heteroduplex loop formation by a translocation mechanism. *EMBO J,* 16**,** 4467-76.

ALVAREZ-GARCIA, I. & MISKA, E. A. (2005) MicroRNA functions in animal development and human disease. *Development,* 132**,** 4653-62.

AMANAI, M., BRAHMAJOSYULA, M. & PERRY, A. C. (2006) A restricted role for sperm-borne microRNAs in mammalian fertilization. *Biol Reprod,* 75**,** 877-84.

AMBROS, V., BARTEL, B., BARTEL, D. P., BURGE, C. B., CARRINGTON, J. C., CHEN, X., DREYFUSS, G., EDDY, S. R., GRIFFITHS-JONES, S. A. M., MARSHALL, M., MATZKE, M., RUVKUN, G. & TUSCHL, T. (2003) A uniform system for microRNA annotation. *RNA,* 9**,** 277-279.

AQEILAN, R. I., CALIN, G. A. & CROCE, C. M. (2009) miR-15a and miR-16-1 in cancer: discovery, function and future perspectives. *Cell Death Differ,* 17**,** 215-220.

AQUILINA, G., CRESCENZI, M. & BIGNAMI, M. (1999) Mismatch repair, G(2)/M cell cycle arrest and lethality after DNA damage. *Carcinogenesis,* 20**,** 2317-26.

ARVEY, A., LARSSON, E., SANDER, C., LESLIE, C. S. & MARKS, D. S. (2010) Target mRNA abundance dilutes microRNA and siRNA activity. *Mol Syst Biol,* 6**,** 363.

ATEN, J. A., STAP, J., KRAWCZYK, P. M., VAN OVEN, C. H., HOEBE, R. A., ESSERS, J. & KANAAR, R. (2004) Dynamics of DNA double-strand breaks revealed by clustering of damaged chromosome domains. *Science,* 303**,** 92-5.

BAARENDS, W. M., VAN DER LAAN, R. & GROOTEGOED, J. A. (2001) DNA repair mechanisms and gametogenesis. *Reproduction,* 121**,** 31-9.

BABIARZ, J. E. & BLELLOCH, R. (2009) Small RNAs- their biogenesis, regulation and function in embryonic stem cells. *StemBook,* 10.3824.

BABIARZ, J. E., RUBY, J. G., WANG, Y., BARTEL, D. P. & BLELLOCH, R. (2008) Mouse ES cells express endogenous shRNAs, siRNAs, and other microprocessorindependent, Dicer-dependent small RNAs. *Genes Dev,* 22**,** 2773-2785.

BACHELIER, R., VINCENT, A., MATHEVET, P., MAGDINIER, F., LENOIR, G. M. & FRAPPART, L. (2002) Retroviral transduction of splice variant Brca1-Delta11 or mutant Brca1-W1777Stop causes mouse epithelial mammary atypical duct hyperplasia. *Virchows Arch,* 440**,** 261-6.

BACHVAROVA, R. F. (1992) A maternal tail of poly(A): the long and the short of it. *Cell,* 69**,** 895-7.

BAGGA, S., BRACHT, J., HUNTER, S., MASSIRER, K., HOLTZ, J., EACHUS, R. & PASQUINELLI, A. E. (2005) Regulation by let-7 and lin-4 miRNAs results in target mRNA degradation. *Cell,* 122**,** 553-63.

BAKER, S. M., BRONNER, C. E., ZHANG, L., PLUG, A. W., ROBATZEK, M., WARREN, G., ELLIOTT, E. A., YU, J., ASHLEY, T., ARNHEIM, N., FLAVELL, R. A. & LISKAY, R. M. (1995) Male mice defective in the DNA mismatch repair gene PMS2 exhibit abnormal chromosome synapsis in meiosis. *Cell,* 82**,** 309-19.

BAKER, S. M., PLUG, A. W., PROLLA, T. A., BRONNER, C. E., HARRIS, A. C., YAO, X., CHRISTIE, D. M., MONELL, C., ARNHEIM, N., BRADLEY, A., ASHLEY, T. & LISKAY, R. M. (1996) Involvement of mouse Mlh1 in DNA mismatch repair and meiotic crossing over. *Nat Genet,* 13**,** 336-42.

BARNES, D. E., LINDAHL, T. & SEDGWICK, B. (1993) DNA repair. *Curr Opin Cell Biol,* 5**,** 424-33.

BARTEL, D. P. (2004) MicroRNAs: genomics, biogenesis, mechanism, and function. *Cell,* 116**,** 281-97.

BARTEL, D. P. & CHEN, C. Z. (2004) Micromanagers of gene expression: the potentially widespread influence of metazoan microRNAs. *Nat Rev Genet,* 5**,** 396-400.

BARTON, T. S., ROBAIRE, B. & HALES, B. F. (2007) DNA damage recognition in the rat zygote following chronic paternal cyclophosphamide exposure. *Toxicol Sci,* 100**,** 495-503.

BASSING, C. H. & ALT, F. W. (2004) The cellular response to general and programmed DNA double strand breaks. *DNA Repair (Amst),* 3**,** 781-96.

BAUMANN, P. & WEST, S. C. (1997) The human Rad51 protein: polarity of strand transfer and stimulation by hRP-A. *EMBO J,* 16**,** 5198-206.

BEAUJEAN, N., HARTSHORNE, G., CAVILLA, J., TAYLOR, J., GARDNER, J., WILMUT, I., MEEHAN, R. & YOUNG, L. (2004a) Non-conservation of mammalian preimplantation methylation dynamics. *Curr Biol,* 14**,** R266-7.

BEAUJEAN, N., TAYLOR, J., GARDNER, J., WILMUT, I., MEEHAN, R. & YOUNG, L. (2004b) Effect of limited DNA methylation reprogramming in the normal sheep embryo on somatic cell nuclear transfer. *Biol Reprod,* 71**,** 185-93.

BELETSKII, A. & BHAGWAT, A. S. (1996) Transcription-induced mutations: increase in C to T mutations in the nontranscribed strand during transcription in Escherichia coli. *Proc Natl Acad Sci U S A,* 93**,** 13919-24.

BELL, C. E., CALDER, M. D. & WATSON, A. J. (2008) Genomic RNA profiling and the programme controlling preimplantation mammalian development. *Mol Hum Reprod,* 14**,** 691-701.

BEREZIKOV, E., CHUNG, W. J., WILLIS, J., CUPPEN, E. & LAI, E. C. (2007) Mammalian mirtron genes. *Mol Cell,* 28**,** 328-36.

BERNSTEIN, E., KIM, S. Y., CARMELL, M. A., MURCHISON, E. P., ALCORN, H., LI, M. Z., MILLS, A. A., ELLEDGE, S. J., ANDERSON, K. V. & HANNON, G. J. (2003) Dicer is essential for mouse development. *Nat Genet,* 35**,** 215-7.

BIGGAR, K. K. & STOREY, K. B. (2010) The emerging roles of microRNAs in the molecular responses of metabolic rate depression. *J Mol Cell Biol,* 3**,** 167-75.

BILL, C. A., DURAN, W. A., MISELIS, N. R. & NICKOLOFF, J. A. (1998) Efficient repair of all types of single-base mismatches in recombination intermediates in Chinese hamster ovary cells. Competition between long-patch and G-T glycosylase-mediated repair of G-T mismatches. *Genetics,* 149**,** 1935-43.

BISHOP, D. K. & KOLODNER, R. D. (1986) Repair of heteroduplex plasmid DNA after transformation into Saccharomyces cerevisiae. *Mol Cell Biol,* 6**,** 3401-9.

BOGLIOLO, M. & SURRALLES, J. (2010) The Fanconi Anemia/BRCA Pathway: FANCD2 at the Crossroad between Repair and Checkpoint Responses to DNA Damage. IN BALAJEE, A. (Ed.) *DNA Repair and Human Disease.* 2005 ed. Georgetown, Landes Bioscience/Eurekah.

BONCI, D., COPPOLA, V., MUSUMECI, M., ADDARIO, A., GIUFFRIDA, R., MEMEO, L., D'URSO, L., PAGLIUCA, A., BIFFONI, M., LABBAYE, C., BARTUCCI, M., MUTO, G., PESCHLE, C. & DE MARIA, R. (2008) The miR-15a-miR-16-1 cluster controls prostate cancer by targeting multiple oncogenic activities. *Nat Med,* 14**,** 1271-7.

BOOMINATHAN, L. (2010) The guardians of the genome (p53, TA-p73, and TA-p63) are regulators of tumor suppressor miRNAs network. *Cancer Metastasis Rev,* 29**,** 613-39.

BOUWMAN, P. & JONKERS, J. (2012) The effects of deregulated DNA damage signalling on cancer chemotherapy response and resistance. *Nat Rev Cancer,* 12**,** 587-98.

BRANZEI, D. & FOIANI, M. (2008) Regulation of DNA repair throughout the cell cycle. *Nat Rev Mol Cell Biol,* 9**,** 297-308.

BRAUDE, P., BOLTON, V. & MOORE, S. (1988) Human gene expression first occurs between the four- and eight-cell stages of preimplantation development. *Nature,* 332**,** 459-61.

BRAUN, C. J., ZHANG, X., SAVELYEVA, I., WOLFF, S., MOLL, U. M., SCHEPELER, T., ÃˇRNTOFT, T. F., ANDERSEN, C. L. & DOBBELSTEIN, M. (2008) p53-Responsive MicroRNAs 192 and 215 Are Capable of Inducing Cell Cycle Arrest. *Cancer Research,* 68**,** 10094-10104.

BRISON, D. R., HOLLYWOOD, K., ARNESEN, R. & GOODACRE, R. (2007) Predicting human embryo viability: the road to non-invasive analysis of the secretome using metabolic footprinting. *Reprod Biomed Online,* 15**,** 296-302.

BROWN, T. C. & JIRICNY, J. (1988) Different base/base mispairs are corrected with different efficiencies and specificities in monkey kidney cells. *Cell,* 54**,** 705-11.

BRYANT, H. E., PETERMANN, E., SCHULTZ, N., JEMTH, A. S., LOSEVA, O., ISSAEVA, N., JOHANSSON, F., FERNANDEZ, S., MCGLYNN, P. & HELLEDAY, T. (2009) PARP is activated at stalled forks to mediate Mre11-dependent replication restart and recombination. *EMBO J,* 28**,** 2601-15.

BUENO, M. J. & MALUMBRES, M. (2011) MicroRNAs and the cell cycle. *Biochim Biophys Acta,* 1812**,** 592-601.

BUERMEYER, A. B., DESCHENES, S. M., BAKER, S. M. & LISKAY, R. M. (1999) Mammalian DNA mismatch repair. *Annu Rev Genet,* 33**,** 533-64.

CALDECOTT, K. W. (2008) Single-strand break repair and genetic disease. *Nat Rev Genet,* 9**,** 619-31.

CANNELL, I. G., KONG, Y. W., JOHNSTON, S. J., CHEN, M. L., COLLINS, H. M., DOBBYN, H. C., ELIA, A., KRESS, T. R., DICKENS, M., CLEMENS, M. J.,

HEERY, D. M., GAESTEL, M., EILERS, M., WILLIS, A. E. & BUSHELL, M. (2010) p38 MAPK/MK2-mediated induction of miR-34c following DNA damage prevents Myc-dependent DNA replication. *Proceedings of the National Academy of Sciences,* 107**,** 5375-5380.

CARETHERS, J. M., HAWN, M. T., CHAUHAN, D. P., LUCE, M. C., MARRA, G., KOI, M. & BOLAND, C. R. (1996) Competency in mismatch repair prohibits clonal expansion of cancer cells treated with N-methyl-N'-nitro-N-nitrosoguanidine. *J Clin Invest,* 98**,** 199-206.

CARLSON, L. L., PAGE, A. W. & BESTOR, T. H. (1992) Properties and localization of DNA methyltransferase in preimplantation mouse embryos: implications for genomic imprinting. *Genes Dev,* 6**,** 2536-41.

CARRAWAY, M. & MARINUS, M. G. (1993) Repair of heteroduplex DNA molecules with multibase loops in Escherichia coli. *J Bacteriol,* 175**,** 3972-80.

CARROLL, A. P., TRAN, N., TOONEY, P. A. & CAIRNS, M. J. (2012) Alternative mRNA fates identified in microRNA-associated transcriptome analysis. *BMC Genomics,* 13**,** 561.

CAUX-MONCOUTIER, V., PAGES-BERHOUET, S., MICHAUX, D., ASSELAIN, B., CASTERA, L., DE PAUW, A., BUECHER, B., GAUTHIER-VILLARS, M., STOPPA-LYONNET, D. & HOUDAYER, C. (2009) Impact of BRCA1 and BRCA2 variants on splicing: clues from an allelic imbalance study. *Eur J Hum Genet,* 17**,** 1471-80.

CAZALLA, D., YARIO, T. & STEITZ, J. A. (2010) Down-regulation of a host microRNA by a Herpesvirus saimiri noncoding RNA. *Science,* 328**,** 1563-6.

CHAUDHRY, M. A., SACHDEVA, H. & OMARUDDIN, R. A. (2010) Radiation-induced micro-RNA modulation in glioblastoma cells differing in DNA-repair pathways. *DNA Cell Biol,* 9**,** 553- 561.

CHEN, Y., GELFOND, J. A., MCMANUS, L. M. & SHIREMAN, P. K. (2009) Reproducibility of quantitative RT-PCR array in miRNA expression profiling and comparison with microarray analysis. *BMC Genomics,* 10**,** 407.

CHRISTMANN, M., TOMICIC, M. T., ROOS, W. P. & KAINA, B. (2003) Mechanisms of human DNA repair: an update. *Toxicology,* 193**,** 3-34.

CROMIE, G. A., CONNELLY, J. C. & LEACH, D. R. (2001) Recombination at double-strand breaks and DNA ends: conserved mechanisms from phage to humans. *Mol Cell,* 8**,** 1163–1174.

CROSBY, M. E., KULSHRESHTHA, R., IVAN, M. & GLAZER, P. M. (2009) MicroRNA Regulation of DNA Repair Gene Expression in Hypoxic Stress. *Cancer Research,* 69**,** 1221-1229.

CZECH, B. & HANNON, G. J. (2011) Small RNA sorting: matchmaking for Argonautes. *Nature Reviews, Genetics,* 12**,** 19-31.

DANTZER, F., DE LA RUBIA, G., MENISSIER-DE MURCIA, J., HOSTOMSKY, Z., DE MURCIA, G. & SCHREIBER, V. (2000) Base excision repair is impaired in mammalian cells lacking Poly(ADP-ribose) polymerase-1. *Biochemistry,* 39**,** 7559-69.

DANTZER, F., SCHREIBER, V., NIEDERGANG, C., TRUCCO, C., FLATTER, E., DE LA RUBIA, G., OLIVER, J., ROLLI, V., MENISSIER-DE MURCIA, J. & DE MURCIA, G. (1999) Involvement of poly(ADP-ribose) polymerase in base excision repair. *Biochimie,* 81**,** 69-75.

DAVIS, T. L., YANG, G. J., MCCARREY, M. S. & BARTOLOMEI, M. S. (2000) The H19 methylation imprint is erased and re-established differentially on the parental alleles during male germ cell development. *Hum Mol Genet,* 9**,** 2885-94.

DE VOS, M., HAYWARD, B., BONTHRON, D. T. & SHERIDAN, E. (2005) Phenotype associated with recessively inherited mutations in DNA mismatch repair (MMR) genes. *Biochem Soc Trans,* 33**,** 718-20.

DE VOS, M., SCHREIBER, V. & DANTZER, F. (2012) The diverse roles and clinical relevance of PARPs in DNA damage repair: current state of the art. *Biochem Pharmacol,* 84**,** 137-46.

DE VRIES, S. S., BAART, E. B., DEKKER, M., SIEZEN, A., DE ROOIJ, D. G., DE BOER, P. & TE RIELE, H. (1999) Mouse MutS-like protein Msh5 is required for proper chromosome synapsis in male and female meiosis. *Genes Dev,* 13**,** 523-31.

DEAN, W., LUCIFERO, D. & SANTOS, F. (2005) DNA methylation in mammalian development and disease. *Birth Defects Res C Embryo Today,* 75**,** 98-111.

DEAN, W., SANTOS, F. & REIK, W. (2003) Epigenetic reprogramming in early mammalian development and following somatic nuclear transfer. *Semin Cell Dev Biol,* 14**,** 93-100.

DEAN, W., SANTOS, F., STOJKOVIC, M., ZAKHARTCHENKO, V., WALTER, J., WOLF, E. & REIK, W. (2001) Conservation of methylation reprogramming in mammalian development: aberrant reprogramming in cloned embryos. *Proc Natl Acad Sci U S A,* 98**,** 13734-8.

DEANS, A. J. & WEST, S. C. (2011) DNA interstrand crosslink repair and cancer. *Nat Rev Cancer,* 11**,** 467-80.

DEWEESE, T. L., SHIPMAN, J. M., LARRIER, N. A., BUCKLEY, N. M., KIDD, L. R., GROOPMAN, J. D., CUTLER, R. G., TE RIELE, H. & NELSON, W. G. (1998) Mouse embryonic stem cells carrying one or two defective Msh2 alleles respond abnormally to oxidative stress inflicted by low-level radiation. *Proc Natl Acad Sci U S A,* 95**,** 11915-20.

DIANOV, G., BISCHOFF, C., PIOTROWSKI, J. & BOHR, V. A. (1998) Repair pathways for processing of 8-oxoguanine in DNA by mammalian cell extracts. *J Biol Chem,* 273**,** 33811-6.

DIEDERICHS, S. & HABER, D. A. (2007) Dual role for argonautes in microRNA processing and posttranscriptional regulation of microRNA expression. *Cell,* 131**,** 1097-108.

DIKOMEY, E., DAHM-DAPHI, J., BRAMMER, I., MARTENSEN, R. & KAINA, B. (1998) Correlation between cellular radiosensitivity and non-repaired double-strand breaks studied in nine mammalian cell lines. *Int J Radiat Biol,* 73**,** 269-78.

DOMINGUEZ, F., GADEA, B., ESTEBAN, F. J., HORCAJADAS, J. A., PELLICER, A. & SIMON, C. (2008) Comparative protein-profile analysis of implanted versus non-implanted human blastocysts. *Hum Reprod,* 23**,** 1993-2000.

DRONKERT, M. L., BEVERLOO, H. B., JOHNSON, R. D., HOEIJMAKERS, J. H., JASIN, M. & KANAAR, R. (2000) Mouse RAD54 affects DNA double-strand break repair and sister chromatid exchange. *Mol Cell Biol,* 20**,** 3147-56.

DROST, J. B. & LEE, W. R. (1995) Biological basis of germline mutation: comparisons of spontaneous germline mutation rates among drosophila, mouse, and human. *Environ Mol Mutagen,* 25 Suppl 26**,** 48-64.

DUFTNER, N., LARKINS-FORD, J., LEGENDRE, M. & HOFMANN, H. A. (2008) Efficacy of RNA amplification is dependent on sequence characteristics: implications for gene expression profiling using a cDNA microarray. *Genomics,* 91**,** 108-17.

DYRKHEEVA, N. S., KHODYREVA, S. N. & LAVRIK, O. I. (2008) Interaction of APE1 and other repair proteins with DNA duplexes imitating intermediates of DNA repair and replication. *Biochemistry (Mosc),* 73**,** 261-72.

EARLE, J. S., LUTHRA, R., ROMANS, A., ABRAHAM, R., ENSOR, J., YAO, H. & HAMILTON, S. R. (2010) Association of microRNA expression with microsatellite instability status in colorectal adenocarcinoma. *J Mol Diagn,* 12**,** 433-40.

ECKERT, K. A. & HILE, S. E. (2009) Every microsatellite is different: Intrinsic DNA features dictate mutagenesis of common microsatellites present in the human genome. *Mol Carcinog,* 48**,** 379-88.

EDELMANN, W., COHEN, P. E., KANE, M., LAU, K., MORROW, B., BENNETT, S., UMAR, A., KUNKEL, T., CATTORETTI, G., CHAGANTI, R., POLLARD, J. W., KOLODNER, R. D. & KUCHERLAPATI, R. (1996) Meiotic pachytene arrest in MLH1-deficient mice. *Cell,* 85**,** 1125-34.

EDELMANN, W., COHEN, P. E., KNEITZ, B., WINAND, N., LIA, M., HEYER, J., KOLODNER, R., POLLARD, J. W. & KUCHERLAPATI, R. (1999) Mammalian MutS homologue 5 is required for chromosome pairing in meiosis. *Nat Genet,* 21**,** 123-7.

EGGERT, A. & SCHULTE, J. H. (2010) A small kiss of death for cancer. *Nat Med,* 16**,** 1079-81.

ESTELLER, M., SILVA, J. M., DOMINGUEZ, G., BONILLA, F., MATIAS-GUIU, X., LERMA, E., BUSSAGLIA, E., PRAT, J., HARKES, I. C., REPASKY, E. A., GABRIELSON, E., SCHUTTE, M., BAYLIN, S. B. & HERMAN, J. G. (2000) Promoter hypermethylation and BRCA1 inactivation in sporadic breast and ovarian tumors. *J Natl Cancer Inst,* 92**,** 564-9.

FAIR, T., CARTER, F., PARK, S., EVANS, A. C. & LONERGAN, P. (2007) Global gene expression analysis during bovine oocyte in vitro maturation. *Theriogenology,* 68 Suppl 1**,** S91-7.

FANG, W. H. & MODRICH, P. (1993) Human strand-specific mismatch repair occurs by a bidirectional mechanism similar to that of the bacterial reaction. *J Biol Chem,* 268**,** 11838-44.

FEBER, A., XI, L., LUKETICH, J. D., PENNATHUR, A., LANDRENEAU, R. J., WU, M., SWANSON, S. J., GODFREY, T. E. & LITLE, V. R. (2008) MicroRNA expression profiles of esophageal cancer. *J Thorac Cardiovasc Surg,* 135**,** 255-60; discussion 260.

FELDMANN, E., SCHMIEMANN, V., GOEDECKE, W., REICHENBERGER, S. & PFEIFFER, P. (2000) DNA double-strand break repair in cell-free extracts from Ku80-deficient cells: implications for Ku serving as an alignment factor in non-homologous DNA end joining. *Nucleic Acids Res,* 28**,** 2585-96.

FENG, S., CONG, S., ZHANG, X., BAO, X., WANG, W., LI, H., WANG, Z., WANG, G., XU, J., DU, B., QU, D., XIONG, W., YIN, M., REN, X., WANG, F., HE, J. & ZHANG, B. (2011) MicroRNA-192 targeting retinoblastoma 1 inhibits cell proliferation and induces cell apoptosis in lung cancer cells. *Nucleic Acids Res,* 39**,** 6669-78.

FERGUSON-SMITH, A. C., SASAKI, H., CATTANACH, B. M. & SURANI, M. A. (1993) Parental-origin-specific epigenetic modification of the mouse H19 gene. *Nature,* 362**,** 751-5.

FERNANDEZ-GONZALEZ, R., MOREIRA, P. N., PEREZ-CRESPO, M., SANCHEZ-MARTIN, M., RAMIREZ, M. A., PERICUESTA, E., BILBAO, A., BERMEJO-ALVAREZ, P., DE DIOS HOURCADE, J., DE FONSECA, F. R. & GUTIERREZ-ADAN, A. (2008) Long-term effects of mouse intracytoplasmic sperm injection with DNA-fragmented sperm on health and behavior of adult offspring. *Biol Reprod,* 78**,** 761-72.

FILIPOWICZ, W., BHATTACHARYYA, S. N. & SONENBERG, N. (2008) Mechanisms of post-transcriptional regulation by microRNAs: are the answers in sight? *Nat Rev Genet,* 9**,** 102-14.

FLACH, G., JOHNSON, M. H., BRAUDE, P. R., TAYLOR, R. A. & BOLTON, V. N. (1982) The transition from maternal to embryonic control in the 2-cell mouse embryo. *EMBO J,* 1**,** 681-6.

FLORES-ROZAS, H. & KOLODNER, R. D. (1998) The Saccharomyces cerevisiae MLH3 gene functions in MSH3-dependent suppression of frameshift mutations. *Proc Natl Acad Sci U S A,* 95**,** 12404-9.

FOLGER, K. R., THOMAS, K. & CAPECCHI, M. R. (1985) Efficient correction of mismatched bases in plasmid heteroduplexes injected into cultured mammalian cell nuclei. *Mol Cell Biol,* 5**,** 70-4.

FORTINI, P., PASCUCCI, B., PARLANTI, E., D'ERRICO, M., SIMONELLI, V. & DOGLIOTTI, E. (2003) The base excision repair: mechanisms and its relevance for cancer susceptibility. *Biochimie,* 85**,** 1053-71.

FRAGOULI, E. & WELLS, D. (2012) Aneuploidy screening for embryo selection. *Semin Reprod Med,* 30**,** 289-301.

FRANCO-ZORRILLA, J. M., VALLI, A., TODESCO, M., MATEOS, I., PUGA, M. I., RUBIO-SOMOZA, I., LEYVA, A., WEIGEL, D., GARCIA, J. A. & PAZ-ARES, J. (2007) Target mimicry provides a new mechanism for regulation of microRNA activity. *Nat Genet,* 39**,** 1033-7.

FRIEDBERG, E. C., BOND, J. P., BURNS, D. K., CHEO, D. L., GREENBLATT, M. S., MEIRA, L. B., NAHARI, D. & REIS, A. M. (2000) Defective nucleotide excision repair in xpc mutant mice and its association with cancer predisposition. *Mutat Res,* 459**,** 99-108.

FRIEDBERG, E. C. & MEIRA, L. B. (2000) Database of mouse strains carrying targeted mutations in genes affecting cellular responses to DNA damage. Version 4. *Mutat Res,* 459**,** 243-74.

FROUIN, I., MAGA, G., DENEGRI, M., RIVA, F., SAVIO, M., SPADARI, S., PROSPERI, E. & SCOVASSI, A. I. (2003) Human proliferating cell nuclear antigen, poly(ADP-ribose) polymerase-1, and p21waf1/cip1. A dynamic exchange of partners. *J Biol Chem,* 278**,** 39265-8.

FUKS, F., HURD, P. J., WOLF, D., NAN, X., BIRD, A. P. & KOUZARIDES, T. (2003) The methyl-CpG-binding protein MeCP2 links DNA methylation to histone methylation. *J Biol Chem,* 278**,** 4035-40.

FULKA, H., MRAZEK, M., TEPLA, O. & FULKA, J., JR. (2004) DNA methylation pattern in human zygotes and developing embryos. *Reproduction,* 128**,** 703-8.

GENSCHEL, J., BAZEMORE, L. R. & MODRICH, P. (2002) Human exonuclease I is required for 5' and 3' mismatch repair. *J Biol Chem,* 277**,** 13302-11.

GEORGES, S. A., BIERY, M. C., KIM, S.-Y., SCHELTER, J. M., GUO, J., CHANG, A. N., JACKSON, A. L., CARLETON, M. O., LINSLEY, P. S., CLEARY, M. A. & CHAU, B. N. (2008) Coordinated Regulation of Cell Cycle Transcripts by p53-Inducible microRNAs, miR-192 and miR-215. *Cancer Research,* 68**,** 10105-10112.

GIRALDEZ, A. J., CINALLI, R. M., GLASNER, M. E., ENRIGHT, A. J., THOMSON, J. M., BASKERVILLE, S., HAMMOND, S. M., BARTEL, D. P. & SCHIER, A. F. (2005) MicroRNAs regulate brain morphogenesis in zebrafish. *Science,* 308**,** 833-8.

GIRALDEZ, A. J., MISHIMA, Y., RIHEL, J., GROCOCK, R. J., VAN DONGEN, S., INOUE, K., ENRIGHT, A. J. & SCHIER, A. F. (2006) Zebrafish MiR-430 promotes deadenylation and clearance of maternal mRNAs. *Science,* 312**,** 75-9.

GOTTLIEB, T. M. & JACKSON, S. P. (1993) The DNA-dependent protein kinase: requirement for DNA ends and association with Ku antigen. *Cell,* 72**,** 131-42.

GRADIA, S., ACHARYA, S. & FISHEL, R. (1997) The human mismatch recognition complex hMSH2-hMSH6 functions as a novel molecular switch. *Cell,* 91**,** 995-1005.

GREALY, M., DISKIN, M. G. & SREENAN, J. M. (1996) Protein content of cattle oocytes and embryos from the two-cell to the elongated blastocyst stage at day 16. *J Reprod Fertil,* 107**,** 229-33.

GREGORY, R. I., YAN, K. P., AMUTHAN, G., CHENDRIMADA, T., DORATOTAJ, B., COOCH, N. & SHIEKHATTAR, R. (2004) The Microprocessor complex mediates the genesis of microRNAs. *Nature,* 432**,** 235-40.

GRIFFITHS-JONES, S., GROCOCK, R. J., VAN DONGEN, S., BATEMAN, A. & ENRIGHT, A. J. (2006) miRBase: microRNA sequences, targets and gene nomenclature. *Nucleic Acids Res,* 34**,** D140-4.

GRILLEY, M., HOLMES, J., YASHAR, B. & MODRICH, P. (1990) Mechanisms of DNA-mismatch correction. *Mutat Res,* 236**,** 253-67.

GU, T. P., GUO, F., YANG, H., WU, H. P., XU, G. F., LIU, W., XIE, Z. G., SHI, L., HE, X., JIN, S. G., IQBAL, K., SHI, Y. G., DENG, Z., SZABO, P. E., PFEIFER, G. P., LI, J. & XU, G. L. (2011) The role of Tet3 DNA dioxygenase in epigenetic reprogramming by oocytes. *Nature,* 477**,** 606-10.

GUNARATNE, P. H. (2009) Embryonic stem cell microRNAs: defining factors in induced pluripotent (iPS) and cancer (CSC) stem cells? *Curr Stem Cell Res Ther,* 4**,** 168-77.

GURTU, V. E., VERMA, S., GROSSMANN, A. H., LISKAY, R. M., SKARNES, W. C. & BAKER, S. M. (2002) Maternal effect for DNA mismatch repair in the mouse. *Genetics,* 160**,** 271-7.

HABER, J. E. (2000) Partners and pathwaysrepairing a double-strand break. *Trends GENET,* 16**,** 259–264.

HAMMARSTEN, O., DEFAZIO, L. G. & CHU, G. (2000) Activation of DNA-dependent protein kinase by single-stranded DNA ends. *J Biol Chem,* 275**,** 1541-50.

HANSEN, T. B., JENSEN, T. I., CLAUSEN, B. H., BRAMSEN, J. B., FINSEN, B., DAMGAARD, C. K. & KJEMS, J. (2013) Natural RNA circles function as efficient microRNA sponges. *Nature,* 495**,** 384-8.

HANSEN, T. B., WIKLUND, E. D., BRAMSEN, J. B., VILLADSEN, S. B., STATHAM, A. L., CLARK, S. J. & KJEMS, J. (2011) miRNA-dependent gene silencing involving Ago2-mediated cleavage of a circular antisense RNA. *EMBO J,* 30**,** 4414-22.

HARE, J. & TAYLOR, J. H. (1985a) Methylation directed strand discrimination in mismatch repair. *Prog Clin Biol Res,* 198**,** 37-44.

HARE, J. T. & TAYLOR, J. H. (1985b) One role for DNA methylation in vertebrate cells is strand discrimination in mismatch repair. *Proc Natl Acad Sci U S A,* 82**,** 7350-4.

HARFE, B. D. (2005) MicroRNAs in vertebrate development. *Curr Opin Genet Dev,* 15**,** 410-5.

HARFE, B. D. & JINKS-ROBERTSON, S. (2000) DNA polymerase zeta introduces multiple mutations when bypassing spontaneous DNA damage in Saccharomyces cerevisiae. *Mol Cell,* 6**,** 1491-9.

HARFE, B. D., MCMANUS, M. T., MANSFIELD, J. H., HORNSTEIN, E. & TABIN, C. J. (2005) The RNaseIII enzyme Dicer is required for morphogenesis but not patterning of the vertebrate limb. *Proc Natl Acad Sci U S A,* 102**,** 10898-903.

HARRIS, J. L., JAKOB, B., TAUCHER-SCHOLZ, G., DIANOV, G. L., BECHEREL, O. J. & LAVIN, M. F. (2009) Aprataxin, poly-ADP ribose polymerase 1 (PARP-1)

and apurinic endonuclease 1 (APE1) function together to protect the genome against oxidative damage. *Hum Mol Genet,* 18**,** 4102-17.

HARTLEY, K. O., GELL, D., SMITH, G. C., ZHANG, H., DIVECHA, N., CONNELLY, M. A., ADMON, A., LEES-MILLER, S. P., ANDERSON, C. W. & JACKSON, S. P. (1995) DNA-dependent protein kinase catalytic subunit: a relative of phosphatidylinositol 3-kinase and the ataxia telangiectasia gene product. *Cell,* 82**,** 849-56.

HASHIMOTO, Y., RAY CHAUDHURI, A., LOPES, M. & COSTANZO, V. (2010) Rad51 protects nascent DNA from Mre11-dependent degradation and promotes continuous DNA synthesis. *Nat Struct Mol Biol,* 17**,** 1305-11.

HATFIELD, S. D., SHCHERBATA, H. R., FISCHER, K. A., NAKAHARA, K., CARTHEW, R. W. & RUOHOLA-BAKER, H. (2005) Stem cell division is regulated by the microRNA pathway. *Nature,* 435**,** 974-8.

HAWN, M. T., UMAR, A., CARETHERS, J. M., MARRA, G., KUNKEL, T. A., BOLAND, C. R. & KOI, M. (1995) Evidence for a connection between the mismatch repair system and the G2 cell cycle checkpoint. *Cancer Res,* 55**,** 3721-5.

HAYASHI, K., CHUVA DE SOUSA LOPES, S. M., KANEDA, M., TANG, F., HAJKOVA, P., LAO, K., O'CARROLL, D., DAS, P. P., TARAKHOVSKY, A., MISKA, E. A. & SURANI, M. A. (2008) MicroRNA biogenesis is required for mouse primordial germ cell development and spermatogenesis. *PLoS One,* 3**,** e1738.

HAYS, J. B., HOFFMAN, P. D. & WANG, H. (2005) Discrimination and versatility in mismatch repair. *DNA Repair (Amst),* 4**,** 1463-74.

HE, L., HE, X., LIM, L. P., DE STANCHINA, E., XUAN, Z., LIANG, Y., XUE, W., ZENDER, L., MAGNUS, J., RIDZON, D., JACKSON, A. L., LINSLEY, P. S., CHEN, C., LOWE, S. W., CLEARY, M. A. & HANNON, G. J. (2007) A microRNA component of the p53 tumour suppressor network. *Nature,* 447**,** 1130-4.

HEALE, J. T., BALL, A. R., JR., SCHMIESING, J. A., KIM, J. S., KONG, X., ZHOU, S., HUDSON, D. F., EARNSHAW, W. C. & YOKOMORI, K. (2006) Condensin I interacts with the PARP-1-XRCC1 complex and functions in DNA single-strand break repair. *Mol Cell,* 21**,** 837-48.

HEITZ, F., HARTER, P., EWALD-RIEGLER, N., PAPSDORF, M., KOMMOSS, S. & DU BOIS, A. (2010) Poly(ADP-ribosyl)ation polymerases: mechanism and new target of anticancer therapy. *Expert Rev Anticancer Ther,* 10**,** 1125-36.

HENDRICKSON, D. G., HOGAN, D. J., MCCULLOUGH, H. L., MYERS, J. W., HERSCHLAG, D., FERRELL, J. E. & BROWN, P. O. (2009) Concordant regulation of translation and mRNA abundance for hundreds of targets of a human microRNA. *PLoS Biol,* 7**,** e1000238.

HENRIQUE BARRETA, M., GARZIERA GASPERIN, B., BRAGA RISSI, V., DE CESARO, M. P., FERREIRA, R., DE OLIVEIRA, J. F., GONCALVES, P. B. & BORDIGNON, V. (2012) Homologous recombination and non-homologous end-joining repair pathways in bovine embryos with different developmental competence. *Exp Cell Res,* 318**,** 2049-58.

HERMEKING, H. (2012) MicroRNAs in the p53 network: micromanagement of tumour suppression. *Nat Rev Cancer,* 12**,** 613-26.

HEYWOOD, L. A. & BURKE, J. F. (1990a) Mismatch repair in mammalian cells. *Bioessays,* 12**,** 473-7.

HEYWOOD, L. A. & BURKE, J. F. (1990b) Repair of single nucleotide DNA mismatches transfected into mammalian cells can occur by short-patch excision. *Mutat Res,* 236**,** 59-66.

HOCHEGGER, H., DEJSUPHONG, D., FUKUSHIMA, T., MORRISON, C., SONODA, E., SCHREIBER, V., ZHAO, G. Y., SABERI, A., MASUTANI, M., ADACHI, N.,

KOYAMA, H., DE MURCIA, G. & TAKEDA, S. (2006) Parp-1 protects homologous recombination from interference by Ku and Ligase IV in vertebrate cells. *EMBO J,* 25**,** 1305-14.

HOLMES, J., JR., CLARK, S. & MODRICH, P. (1990) Strand-specific mismatch correction in nuclear extracts of human and Drosophila melanogaster cell lines. *Proc Natl Acad Sci U S A,* 87**,** 5837-41.

HOWELL, C. Y., BESTOR, T. H., DING, F., LATHAM, K. E., MERTINEIT, C., TRASLER, J. M. & CHAILLET, J. R. (2001) Genomic imprinting disrupted by a maternal effect mutation in the Dnmt1 gene. *Cell,* 104**,** 829-38.

HOWLETT, S. K. & REIK, W. (1991) Methylation levels of maternal and paternal genomes during preimplantation development. *Development,* 113**,** 119-27.

HSIA, K. T., MILLAR, M. R., KING, S., SELFRIDGE, J., REDHEAD, N. J., MELTON, D. W. & SAUNDERS, P. T. (2003) DNA repair gene Ercc1 is essential for normal spermatogenesis and oogenesis and for functional integrity of germ cell DNA in the mouse. *Development,* 130**,** 369-78.

HU, H., DU, L., NAGABAYASHI, G., SEEGER, R. C. & GATTI, R. A. (2010) ATM is down-regulated by N-Myc regulated microRNA-421. *Proceedings of the National Academy of Sciences,* 107**,** 1506-1511.

HU, H. & GATTI, R. A. (2010) MicroRNAs: new players in the DNA damage response. *J Mol Cell Biol,* 3**,** 151-8.

HUANG, J. C., HSU, D. S., KAZANTSEV, A. & SANCAR, A. (1994) Substrate spectrum of human excinuclease: repair of abasic sites, methylated bases, mismatches, and bulky adducts. *Proc Natl Acad Sci U S A,* 91**,** 12213-7.

HUANG, Y., NAYAK, S., JANKOWITZ, R., DAVIDSON, N. E. & OESTERREICH, S. (2011) Epigenetics in breast cancer: what's new? *Breast Cancer Res,* 13**,** 225.

HUNTRISS, J., DANIELS, R., BOLTON, V. & MONK, M. (1998) Imprinted expression of SNRPN in human preimplantation embryos. *Am J Hum Genet,* 63**,** 1009-14.

HURST, L. D. & ELLEGREN, H. (1998) Sex biases in the mutation rate. *Trends Genet,* 14**,** 446-52.

HUTTLEY, G. A., JAKOBSEN, I. B., WILSON, S. R. & EASTEAL, S. (2000) How important is DNA replication for mutagenesis? *Mol Biol Evol,* 17**,** 929-37.

IBALA-ROMDHANE, S., AL-KHTIB, M., KHOUEIRY, R., BLACHERE, T., GUERIN, J. F. & LEFEVRE, A. (2011) Analysis of H19 methylation in control and abnormal human embryos, sperm and oocytes. *Eur J Hum Genet,* 19**,** 1138-43.

ISSABEKOVA, A., BERILLO, O., REGNIER, M. & ANATOLY, I. (2011) Interactions of intergenic microRNAs with mRNAs of genes involved in carcinogenesis. *Bioinformation,* 8**,** 513-8.

JACKSON, J. P., LINDROTH, A. M., CAO, X. & JACOBSEN, S. E. (2002) Control of CpNpG DNA methylation by the KRYPTONITE histone H3 methyltransferase. *Nature,* 416**,** 556-60.

JACKSON, S. P. & BARTEK, J. (2009) The DNA-damage response in human biology and disease. *Nature,* 461**,** 1071-8.

JAROUDI, S., KAKOUROU, G., CAWOOD, S., DOSHI, A., RANIERI, D. M., SERHAL, P., HARPER, J. C. & SENGUPTA, S. B. (2009) Expression profiling of DNA repair genes in human oocytes and blastocysts using microarrays. *Hum Reprod,* 24**,** 2649-55.

JAROUDI, S. & SENGUPTA, S. (2007) DNA repair in mammalian embryos. *Mutat Res,* 635**,** 53-77.

JEGGO, P., SINGLETON, B., BEAMISH, H. & PRIESTLEY, A. (1999) Double strand break rejoining by the Ku-dependent mechanism of non-homologous end-joining. *C R Acad Sci III,* 322**,** 109-12.

JEONG-YU, S. J. & CARROLL, D. (1992) Test of the double-strand-break repair model of recombination in Xenopus laevis oocytes. *Mol Cell Biol,* 12**,** 112-9.

JIANG, J., GUSEV, Y., ADERCA, I., METTLER, T. A., NAGORNEY, D. M., BRACKETT, D. J., ROBERTS, L. R. & SCHMITTGEN, T. D. (2008) Association of MicroRNA expression in hepatocellular carcinomas with hepatitis infection, cirrhosis, and patient survival. *Clin Cancer Res,* 14**,** 419-27.

JIRICNY, J. & NYSTROM-LAHTI, M. (2000) Mismatch repair defects in cancer. *Curr Opin Genet Dev,* 10**,** 157-61.

JOHNSON, R. D. & JASIN, M. (2000) Sister chromatid gene conversion is a prominent double-strand break repair pathway in mammalian cells. *EMBO J,* 19**,** 3398–3407.

JONES, S., EMMERSON, P., MAYNARD, J., BEST, J. M., JORDAN, S., WILLIAMS, G. T., SAMPSON, J. R. & CHEADLE, J. P. (2002) Biallelic germline mutations in MYH predispose to multiple colorectal adenoma and somatic G:C-->T:A mutations. *Hum Mol Genet,* 11**,** 2961-7.

JURADO, J. O., PASQUINELLI, V., ALVAREZ, I. B., PENA, D., ROVETTA, A. I., TATEOSIAN, N. L., ROMEO, H. E., MUSELLA, R. M., PALMERO, D., CHULUYAN, H. E. & GARCIA, V. E. (2012) IL-17 and IFN-gamma expression in lymphocytes from patients with active tuberculosis correlates with the severity of the disease. *J Leukoc Biol,* 91**,** 991-1002.

JURISICOVA, A., LATHAM, K. E., CASPER, R. F. & VARMUZA, S. L. (1998) Expression and regulation of genes associated with cell death during murine preimplantation embryo development. *Mol Reprod Dev,* 51**,** 243-53.

KADYROV, F. A., GENSCHEL, J., FANG, Y., PENLAND, E., EDELMANN, W. & MODRICH, P. (2009) A possible mechanism for exonuclease 1-independent eukaryotic mismatch repair. *Proc Natl Acad Sci U S A,* 106**,** 8495-500.

KAGAWA, W., KURUMIZAKA, H., IKAWA, S., YOKOYAMA, S. & SHIBATA, T. (2001) Homologous pairing promoted by the human Rad52 protein. *J Biol Chem,* 276**,** 35201-8.

KAKOUROU, G., JAROUDI, S., TULAY, P., HEATH, C., SERHAL, P., HARPER, J. C. & SENGUPTA, S. B. (2012) Investigation of gene expression profiles before and after embryonic genome activation and assessment of functional pathways at the human metaphase II oocyte and blastocyst stage. *Fertil Steril,* 99**,** 803-814.

KASPAREK, T. R. & HUMPHREY, T. C. (2011) DNA double-strand break repair pathways, chromosomal rearrangements and cancer. *Semin Cell Dev Biol,* 22**,** 886-97.

KATZ-JAFFE, M. G., MCREYNOLDS, S., GARDNER, D. K. & SCHOOLCRAFT, W. B. (2009) The role of proteomics in defining the human embryonic secretome. *Mol Hum Reprod,* 15**,** 271-7.

KHOUEIRY, R., IBALA-ROMDHANE, S., AL-KHTIB, M., BLACHERE, T., LORNAGE, J., GUERIN, J. F. & LEFEVRE, A. (2012) Abnormal methylation of KCNQ1OT1 and differential methylation of H19 imprinting control regions in human ICSI embryos. *Zygote***,** 1-10.

KIM, V. N. (2008) Cell cycle micromanagement in embryonic stem cells. *Nat Genet,* 40**,** 1391-2.

KNEITZ, B., COHEN, P. E., AVDIEVICH, E., ZHU, L., KANE, M. F., HOU, H., JR., KOLODNER, R. D., KUCHERLAPATI, R., POLLARD, J. W. & EDELMANN, W. (2000) MutS homolog 4 localization to meiotic chromosomes is required for chromosome pairing during meiosis in male and female mice. *Genes Dev,* 14**,** 1085-97.

KREJCI, L., ALTMANNOVA, V., SPIREK, M. & ZHAO, X. (2012) Homologous recombination and its regulation. *Nucleic Acids Res,* 40**,** 5795-818.

KRICHEVSKY, A. M. & GABRIELY, G. (2009) miR-21: a small multi-faceted RNA. *Journal of Cellular and Molecular Medicine,* 13**,** 39-53.

KUNKEL, T. A. & ERIE, D. A. (2005) DNA mismatch repair. *Annu Rev Biochem,* 74**,** 681-710.

LABHART, P. (1999) Ku-dependent nonhomologous DNA end joining in Xenopus egg extracts. *Mol Cell Biol,* 19**,** 2585-93.

LAGERWERF, S., VROUWE, M. G., OVERMEER, R. M., FOUSTERI, M. I. & MULLENDERS, L. H. (2011) DNA damage response and transcription. *DNA Repair (Amst),* 10**,** 743-50.

LAGHI, L., BIANCHI, P. & MALESCI, A. (2008) Differences and evolution of the methods for the assessment of microsatellite instability. *Oncogene,* 27**,** 6313-21.

LATHAM, K. E., GARRELS, J. I., CHANG, C. & SOLTER, D. (1992) Analysis of embryonic mouse development: construction of a high-resolution, two-dimensional gel protein database. *Appl Theor Electrophor,* 2**,** 163-70.

LEBER, R., WISE, T. W., MIZUTA, R. & MEEK, K. (1998) The XRCC4 gene product is a target for and interacts with the DNA-dependent protein kinase. *J Biol Chem,* 273**,** 1794-801.

LEE, D. Y., SHATSEVA, T., JEYAPALAN, Z., DU, W. W., DENG, Z. & YANG, B. B. (2009) A 3'-untranslated region (3'UTR) induces organ adhesion by regulating miR-199a* functions. *PLoS One,* 4**,** e4527.

LEE, R. C. & AMBROS, V. (2001) An extensive class of small RNAs in Caenorhabditis elegans. *Science,* 294**,** 862-4.

LEE, R. C., FEINBAUM, R. L. & AMBROS, V. (1993) The C. elegans heterochronic gene lin-4 encodes small RNAs with antisense complementarity to lin-14. *Cell,* 75**,** 843-54.

LEHMANN, A. R. (2003) DNA repair-deficient diseases, xeroderma pigmentosum, Cockayne syndrome and trichothiodystrophy. *Biochimie,* 85**,** 1101-11.

LEI, X., ZHU, Y., TOMKINSON, A. & SUN, L. (2004) Measurement of DNA mismatch repair activity in live cells. *Nucleic Acids Res,* 32**,** e100.

LI, J., BHAT, A. & XIAO, W. (2011) Regulation of nucleotide excision repair through ubiquitination. *Acta Biochim Biophys Sin (Shanghai),* 43**,** 919-29.

LI, M., LIU, G. H. & IZPISUA BELMONTE, J. C. (2012) Navigating the epigenetic landscape of pluripotent stem cells. *Nat Rev Mol Cell Biol,* 13**,** 524-35.

LIANG, L. H. & HE, X. H. (2011) Macro-management of microRNAs in cell cycle progression of tumor cells and its implications in anti-cancer therapy. *Acta Pharmacol Sin,* 32**,** 1311-20.

LIGHTEN, A. D., HARDY, K., WINSTON, R. M. & MOORE, G. E. (1997) IGF2 is parentally imprinted in human preimplantation embryos. *Nat Genet,* 15**,** 122-3.

LIN, Y., CHEN, Y., YANG, X., XU, D. & LIANG, S. (2009) Proteome analysis of a single zebrafish embryo using three different digestion strategies coupled with liquid chromatography-tandem mass spectrometry. *Anal Biochem,* 394**,** 177-85.

LIN, Y., YU, F., GAO, N., SHENG, J., QIU, J. & HU, B. (2011) microRNA-143 Protects Cells from DNA Damage-Induced Killing by Downregulating FHIT Expression. *Cancer Biotherapy & Radiopharmaceuticals,* 26**,** 365- 372.

LINDAHL, T. & BARNES, D. E. (2000) Repair of endogenous DNA damage. *Cold Spring Harb Symp Quant Biol,* 65**,** 127-33.

LINDAHL, T. & NYBERG, B. (1972) Rate of depurination of native deoxyribonucleic acid. *Biochemistry,* 11**,** 3610-8.

LIPKIN, S. M., MOENS, P. B., WANG, V., LENZI, M., SHANMUGARAJAH, D., GILGEOUS, A., THOMAS, J., CHENG, J., TOUCHMAN, J. W., GREEN, E. D., SCHWARTZBERG, P., COLLINS, F. S. & COHEN, P. E. (2002) Meiotic arrest and aneuploidy in MLH3-deficient mice. *Nat Genet,* 31**,** 385-90.

LIPKIN, S. M., WANG, V., JACOBY, R., BANERJEE-BASU, S., BAXEVANIS, A. D., LYNCH, H. T., ELLIOTT, R. M. & COLLINS, F. S. (2000) MLH3: a DNA mismatch repair gene associated with mammalian microsatellite instability. *Nat Genet,* 24**,** 27-35.

LIPTON, L., HALFORD, S. E., JOHNSON, V., NOVELLI, M. R., JONES, A., CUMMINGS, C., BARCLAY, E., SIEBER, O., SADAT, A., BISGAARD, M. L., HODGSON, S. V., AALTONEN, L. A., THOMAS, H. J. & TOMLINSON, I. P. (2003) Carcinogenesis in MYH-associated polyposis follows a distinct genetic pathway. *Cancer Res,* 63**,** 7595-9.

LITTMAN, S. J., FANG, W. H. & MODRICH, P. (1999) Repair of large insertion/deletion heterologies in human nuclear extracts is directed by a 5' single-strand break and is independent of the mismatch repair system. *J Biol Chem,* 274**,** 7474-81.

LIU, J., CARMELL, M. A., RIVAS, F. V., MARSDEN, C. G., THOMSON, J. M., SONG, J. J., HAMMOND, S. M., JOSHUA-TOR, L. & HANNON, G. J. (2004) Argonaute2 is the catalytic engine of mammalian RNAi. *Science,* 305**,** 1437-41.

LIU, J., VALENCIA-SANCHEZ, M. A., HANNON, G. J. & PARKER, R. (2005) MicroRNA-dependent localization of targeted mRNAs to mammalian P-bodies. *Nat Cell Biol,* 7**,** 719-23.

LIU, Y. & LU, X. (2012) Non-coding RNAs in DNA damage response. *Am J Cancer Res,* 2**,** 658-75.

LIXIA, M., ZHIJIAN, C., CHAO, S., CHAOJIANG, G. & CONGYI, Z. (2007) Alternative splicing of breast cancer associated gene BRCA1 from breast cancer cell line. *J Biochem Mol Biol,* 40**,** 15-21.

LOMONOSOV, M., ANAND, S., SANGRITHI, M., DAVIES, R. & VENKITARAMAN, A. R. (2003) Stabilization of stalled DNA replication forks by the BRCA2 breast cancer susceptibility protein. *Genes Dev,* 17**,** 3017-22.

LUDWIG, T., CHAPMAN, D. L., PAPAIOANNOU, V. E. & EFSTRATIADIS, A. (1997) Targeted mutations of breast cancer susceptibility gene homologs in mice: lethal phenotypes of Brca1, Brca2, Brca1/Brca2, Brca1/p53, and Brca2/p53 nullizygous embryos. *Genes Dev,* 11**,** 1226-41.

LUKAS, J., LUKAS, C. & BARTEK, J. (2004) Mammalian cell cycle checkpoints: signalling pathways and their organization in space and time. *DNA Repair (Amst),* 3**,** 997-1007.

LUND, E., GUTTINGER, S., CALADO, A., DAHLBERG, J. E. & KUTAY, U. (2004) Nuclear export of microRNA precursors. *Science,* 303**,** 95-8.

LUND, E., LIU, M., HARTLEY, R. S., SHEETS, M. D. & DAHLBERG, J. E. (2009) Deadenylation of maternal mRNAs mediated by miR-427 in Xenopus laevis embryos. *RNA,* 15**,** 2351-63.

MAATOUK, D. M., LOVELAND, K. L., MCMANUS, M. T., MOORE, K. & HARFE, B. D. (2008) Dicer1 is required for differentiation of the mouse male germline. *Biol Reprod,* 79**,** 696-703.

MAC AULEY, A., WERB, Z. & MIRKES, P. E. (1993) Characterization of the unusually rapid cell cycles during rat gastrulation. *Development,* 117**,** 873-83.

MACKEY, Z. B., RAMOS, W., LEVIN, D. S., WALTER, C. A., MCCARREY, J. R. & TOMKINSON, A. E. (1997) An alternative splicing event which occurs in mouse pachytene spermatocytes generates a form of DNA ligase III with distinct biochemical properties that may function in meiotic recombination. *Mol Cell Biol,* 17**,** 989-98.

MAKRIDAKIS, N. M., CALDAS FERRAZ, L. F. & REICHARDT, J. K. (2009) Genomic analysis of cancer tissue reveals that somatic mutations commonly occur in a specific motif. *Hum Mutat,* 30**,** 39-48.

MALUMBRES, M. (2012) miRNAs versus oncogenes: the power of social networking. *Mol Syst Biol,* 8**,** 569.

MAMO, S., GAL, A. B., BODO, S. & DINNYES, A. (2007) Quantitative evaluation and selection of reference genes in mouse oocytes and embryos cultured in vivo and in vitro. *BMC Dev Biol,* 7**,** 14.

MANSOUR, W. Y., RHEIN, T. & DAHM-DAPHI, J. (2010) The alternative end-joining pathway for repair of DNA double-strand breaks requires PARP1 but is not dependent upon microhomologies. *Nucleic Acids Res,* 38**,** 6065-77.

MARANGOS, P. & CARROLL, J. (2012) Oocytes progress beyond prophase in the presence of DNA damage. *Curr Biol,* 22**,** 989-94.

MARQUEZ, N., CHAPPELL, S. C., SANSOM, O. J., CLARKE, A. R., COURT, J., ERRINGTON, R. J. & SMITH, P. J. (2003) Single cell tracking reveals that Msh2 is a key component of an early-acting DNA damage-activated G2 checkpoint. *Oncogene,* 22**,** 7642-8.

MARSISCHKY, G. T., FILOSI, N., KANE, M. F. & KOLODNER, R. (1996) Redundancy of Saccharomyces cerevisiae MSH3 and MSH6 in MSH2-dependent mismatch repair. *Genes Dev,* 10**,** 407-20.

MARTENSSON, S. & HAMMARSTEN, O. (2002) DNA-dependent protein kinase catalytic subunit. Structural requirements for kinase activation by DNA ends. *J Biol Chem,* 277**,** 3020-9.

MARTORELL, L., JOHNSON, K., BOUCHER, C. A. & BAIGET, M. (1997) Somatic instability of the myotonic dystrophy (CTG)n repeat during human fetal development. *Hum Mol Genet,* 6**,** 877-80.

MARYON, E. & CARROLL, D. (1989) Degradation of linear DNA by a strand-specific exonuclease activity in Xenopus laevis oocytes. *Mol Cell Biol,* 9**,** 4862-71.

MASER, R. S., MONSEN, K. J., NELMS, B. E. & PETRINI, J. H. (1997) hMre11 and hRad50 nuclear foci are induced during the normal cellular response to DNA double-strand breaks. *Mol Cell Biol,* 17**,** 6087-96.

MASSIRER, K. B., PEREZ, S. G., MONDOL, V. & PASQUINELLI, A. E. (2012) The miR-35-41 family of microRNAs regulates RNAi sensitivity in Caenorhabditis elegans. *PLoS Genet,* 8**,** e1002536.

MATHESON, E. C. & HALL, A. G. (2003) Assessment of mismatch repair function in leukaemic cell lines and blasts from children with acute lymphoblastic leukaemia. *Carcinogenesis,* 24**,** 31-8.

MAY, A., KIRCHNER, R., MULLER, H., HARTMANN, P., EL HAJJ, N., TRESCH, A., ZECHNER, U., MANN, W. & HAAF, T. (2009) Multiplex rt-PCR expression analysis of developmentally important genes in individual mouse preimplantation embryos and blastomeres. *Biol Reprod,* 80**,** 194-202.

MAYER, W., NIVELEAU, A., WALTER, J., FUNDELE, R. & HAAF, T. (2000) Demethylation of the zygotic paternal genome. *Nature,* 403**,** 501-502.

MCCALLIE, B., SCHOOLCRAFT, W. B. & KATZ-JAFFE, M. G. (2009) Aberration of blastocyst microRNA expression is associated with human infertility. *Fertil Steril,* 93**,** 2374-2382.

MCCLAY, D. W. & CLARKE, H. J. (2003) Remodelling the paternal chromatin at fertilisation in mammals. *Reproduction,* 125**,** 625-33.

MCCULLOCH, S. D., GU, L. & LI, G. M. (2003) Bi-directional processing of DNA loops by mismatch repair-dependent and -independent pathways in human cells. *J Biol Chem,* 278**,** 3891-6.

MCPHEE, F., FRIBORG, J., LEVINE, S., CHEN, C., FALK, P., YU, F., HERNANDEZ, D., LEE, M., CHANIEWSKI, S., SHEAFFER, A. K. & PASQUINELLI, C. (2012) Resistance Analysis of the Hepatitis C Virus NS3 Protease Inhibitor Asunaprevir. *Antimicrob Agents Chemother*.

MEDINA, P. P. & SLACK, F. J. (2008) microRNAs and cancer: an overview. *Cell Cycle,* 7**,** 2485-92.

MEMCZAK, S., JENS, M., ELEFSINIOTI, A., TORTI, F., KRUEGER, J., RYBAK, A., MAIER, L., MACKOWIAK, S. D., GREGERSEN, L. H., MUNSCHAUER, M., LOEWER, A., ZIEBOLD, U., LANDTHALER, M., KOCKS, C., LE NOBLE, F. & RAJEWSKY, N. (2013) Circular RNAs are a large class of animal RNAs with regulatory potency. *Nature,* 495**,** 333-8.

MENEZO, Y., JR., RUSSO, G., TOSTI, E., EL MOUATASSIM, S. & BENKHALIFA, M. (2007) Expression profile of genes coding for DNA repair in human oocytes using pangenomic microarrays, with a special focus on ROS linked decays. *J Assist Reprod Genet,* 24**,** 513-20.

MESTDAGH, P., FEYS, T., BERNARD, N., GUENTHER, S., CHEN, C., SPELEMAN, F. & VANDESOMPELE, J. (2008) High-throughput stem-loop RT-qPCR miRNA expression profiling using minute amounts of input RNA. *Nucleic Acids Res,* 36**,** e143.

MILLER, E. M., HOUGH, H. L., CHO, J. W. & NICKOLOFF, J. A. (1997) Mismatch repair by efficient nick-directed, and less efficient mismatch-specific, mechanisms in homologous recombination intermediates in Chinese hamster ovary cells. *Genetics,* 147**,** 743-53.

MIRANDA, K. C., HUYNH, T., TAY, Y., ANG, Y. S., TAM, W. L., THOMSON, A. M., LIM, B. & RIGOUTSOS, I. (2006) A pattern-based method for the identification of MicroRNA binding sites and their corresponding heteroduplexes. *Cell,* 126**,** 1203-17.

MISHIMA, Y., GIRALDEZ, A. J., TAKEDA, Y., FUJIWARA, T., SAKAMOTO, H., SCHIER, A. F. & INOUE, K. (2006) Differential regulation of germline mRNAs in soma and germ cells by zebrafish miR-430. *Curr Biol,* 16**,** 2135-42.

MISHRA, P. J., SONG, B., WANG, Y., HUMENIUK, R., BANERJEE, D., MERLINO, G., JU, J. & BERTINO, J. R. (2009) MiR-24 tumor suppressor activity is regulated independent of p53 and through a target site polymorphism. *PLoS One,* 4**,** e8445.

MODRICH, P. (1987) DNA mismatch correction. *Annu Rev Biochem,* 56**,** 435-66.

MODRICH, P. & LAHUE, R. (1996) Mismatch repair in replication fidelity, genetic recombination, and cancer biology. *Annu Rev Biochem,* 65**,** 101-33.

MONDOU, E., DUFORT, I., GOHIN, M., FOURNIER, E. & SIRARD, M. A. (2012) Analysis of microRNAs and their precursors in bovine early embryonic development. *Mol Hum Reprod,* 18**,** 425-434.

MONK, M., BOUBELIK, M. & LEHNERT, S. (1987) Temporal and regional changes in DNA methylation in the embryonic, extraembryonic and germ cell lineages during mouse embryo development. *Development,* 99**,** 371-82.

MONK, M. & SALPEKAR, A. (2001) Expression of imprinted genes in human preimplantation development. *Mol Cell Endocrinol,* 183 Suppl 1**,** S35-40.

MOORE, K., PERSAUD, T.V.N. (1998) *The Developing Human*.

MOSKWA, P., BUFFA, F. M., PAN, Y., PANCHAKSHARI, R., GOTTIPATI, P., MUSCHEL, R. J., BEECH, J., KULSHRESTHA, R., ABDELMOHSEN, K., WEINSTOCK, D. M., GOROSPE, M., HARRIS, A. L., HELLEDAY, T. & CHOWDHURY, D. (2010) miR-182-Mediated Downregulation of BRCA1 Impacts DNA Repair and Sensitivity to PARP Inhibitors. *Molecular cell,* 41**,** 210-220.

MUELLER, A. C., SUN, D. & DUTTA, A. (2012) The miR-99 family regulates the DNA damage response through its target SNF2H. *Oncogene,* 32**,** 1164-1672.

MUGAL, C. F., VON GRUNBERG, H. H. & PEIFER, M. (2009) Transcription-induced mutational strand bias and its effect on substitution rates in human genes. *Mol Biol Evol,* 26**,** 131-42.

MURCHISON, E. P., STEIN, P., XUAN, Z., PAN, H., ZHANG, M. Q., SCHULTZ, R. M. & HANNON, G. J. (2007) Critical roles for Dicer in the female germline. *Genes & Development,* 21**,** 682-693.

NAKAMURA, J., WALKER, V. E., UPTON, P. B., CHIANG, S. Y., KOW, Y. W. & SWENBERG, J. A. (1998) Highly sensitive apurinic/apyrimidinic site assay can detect spontaneous and chemically induced depurination under physiological conditions. *Cancer Res,* 58**,** 222-5.

NAVARRO, A., GAYA, A., MARTINEZ, A., URBANO-ISPIZUA, A., PONS, A., BALAGUE, O., GEL, B., ABRISQUETA, P., LOPEZ-GUILLERMO, A., ARTELLS, R., MONTSERRAT, E. & MONZO, M. (2008) MicroRNA expression profiling in classic Hodgkin lymphoma. *Blood,* 111**,** 2825-32.

NELMS, B. E., MASER, R. S., MACKAY, J. F., LAGALLY, M. G. & PETRINI, J. H. (1998) In situ visualization of DNA double-strand break repair in human fibroblasts. *Science,* 280**,** 590-2.

NIWA, R. & SLACK, F. J. (2007) The evolution of animal microRNA function. *Curr Opin Genet Dev,* 17**,** 145-50.

NOREN HOOTEN, N., KOMPANIEZ, K., BARNES, J., LOHANI, A. & EVANS, M. K. (2011) Poly(ADP-ribose) polymerase 1 (PARP-1) binds to 8-oxoguanine-DNA glycosylase (OGG1). *J Biol Chem,* 286**,** 44679-90.

NOTO, J. M. & PEEK, R. M. (2012) The Role of microRNAs in Helicobacter pylori Pathogenesis and Gastric Carcinogenesis. *Front Cell Infect Microbiol,* 1**,** 21.

O'CARROLL, D., MECKLENBRAUKER, I., DAS, P. P., SANTANA, A., KOENIG, U., ENRIGHT, A. J., MISKA, E. A. & TARAKHOVSKY, A. (2007) A Slicer-independent role for Argonaute 2 in hematopoiesis and the microRNA pathway. *Genes Dev,* 21**,** 1999-2004.

O'REGAN, N. E., BRANCH, P., MACPHERSON, P. & KARRAN, P. (1996) hMSH2-independent DNA mismatch recognition by human proteins. *J Biol Chem,* 271**,** 1789-96.

ODA, N., SAXENA, J. K., JENKINS, T. M., PRASAD, R., WILSON, S. H. & ACKERMAN, E. J. (1996) DNA polymerases alpha and beta are required for DNA repair in an efficient nuclear extract from Xenopus oocytes. *J Biol Chem,* 271**,** 13816-20.

OIKAWA, A., TOHDA, H., KANAI, M., MIWA, M. & SUGIMURA, T. (1980) Inhibitors of poly(adenosine diphosphate ribose) polymerase induce sister chromatid exchanges. *Biochem Biophys Res Commun,* 97**,** 1311-6.

OKAMURA, K., HAGEN, J. W., DUAN, H., TYLER, D. M. & LAI, E. C. (2007) The mirtron pathway generates microRNA-class regulatory RNAs in Drosophila. Cell. *Cell,* 130**,** 89-100.

OLEK, A. & WALTER, J. (1997) The pre-implantation ontogeny of the H19 methylation imprint. *Nat Genet,* 17**,** 275-6.

OLSEN, A. K., BJORTUFT, H., WIGER, R., HOLME, J., SEEBERG, E., BJORAS, M. & BRUNBORG, G. (2001) Highly efficient base excision repair (BER) in human and rat male germ cells. *Nucleic Acids Res,* 29**,** 1781-90.

ORBAN, T. I. & OLAH, E. (2003) Emerging roles of BRCA1 alternative splicing. *Mol Pathol,* 56**,** 191-7.

OSWALD, J., ENGEMANN, S., LANE, N., MAYER, W., OLEK, A., FUNDELE, R., DEAN, W., REIK, W. & WALTER, J. (2000) Active demethylation of the paternal genome in the mouse zygote. *Curr Biol,* 10**,** 475-8.

PACE, P., MOSEDALE, G., HODSKINSON, M. R., ROSADO, I. V., SIVASUBRAMANIAM, M. & PATEL, K. J. (2010) Ku70 corrupts DNA repair in the absence of the Fanconi anemia pathway. *Science,* 329**,** 219-23.

PARK, J. K., HENRY, J. C., JIANG, J., ESAU, C., GUSEV, Y., LERNER, M. R., POSTIER, R. G., BRACKETT, D. J. & SCHMITTGEN, T. D. (2011) miR-132 and miR-212 are increased in pancreatic cancer and target the retinoblastoma tumor suppressor. *Biochem Biophys Res Commun,* 406**,** 518-23.

PARK, M. S., LUDWIG, D. L., STIGGER, E. & LEE, S. H. (1996) Physical interaction between human RAD52 and RPA is required for homologous recombination in mammalian cells. *J Biol Chem,* 271**,** 18996-9000.

PARK, Y. & GERSON, S. L. (2005) DNA repair defects in stem cell function and aging. *Annu Rev Med,* 56**,** 495-508.

PATEL, O. V., SUCHYTA, S. P., SIPKOVSKY, S. S., YAO, J., IRELAND, J. J., COUSSENS, P. M. & SMITH, G. W. (2005) Validation and application of a high fidelity mRNA linear amplification procedure for profiling gene expression. *Vet Immunol Immunopathol,* 105**,** 331-42.

PAULI, A., RINN, J. L. & SCHIER, A. F. (2011) Non-coding RNAs as regulators of embryogenesis. *Nature Reviews, Genetics,* 12**,** 136-149.

PETRANOVIC, M., VLAHOVIC, K., ZAHRADKA, D., DZIDIC, S. & RADMAN, M. (2000) Mismatch repair in xenopus egg extracts is not strand-directed by DNA methylation. *Neoplasma,* 47**,** 375-81.

PFEIFFER, P., GOEDECKE, W. & OBE, G. (2000) Mechanisms of DNA double-strand break repair and their potential to induce chromosomal aberrations. *Mutagenesis,* 15**,** 289-302.

PICHIORRI, F., SUH, S.-S., ROCCI, A., DE LUCA, L., TACCIOLI, C., SANTHANAM, R., ZHOU, W., BENSON, D. M., HOFMAINSTER, C., ALDER, H., GAROFALO, M., DI LEVA, G., VOLINIA, S., LIN, H.-J., PERROTTI, D., KUEHL, M., AQEILAN, R. I., PALUMBO, A. & CROCE, C. M. (2010) Downregulation of p53-inducible microRNAs 192, 194, and 215 Impairs the p53/MDM2 Autoregulatory Loop in Multiple Myeloma Development. *Cancer Cell,* 18**,** 367-381.

POLISENO, L., SALMENA, L., ZHANG, J., CARVER, B., HAVEMAN, W. J. & PANDOLFI, P. P. (2010) A coding-independent function of gene and pseudogene mRNAs regulates tumour biology. *Nature,* 465**,** 1033-8.

RAZIN, A., SZYF, M., KAFRI, T., ROLL, M., GILOH, H., SCARPA, S., CAROTTI, D. & CANTONI, G. L. (1986) Replacement of 5-methylcytosine by cytosine: a possible mechanism for transient DNA demethylation during differentiation. *Proc Natl Acad Sci U S A,* 83**,** 2827-31.

REEVES, W. H., STHOEGER, Z. M. & LAHITA, R. G. (1989) Role of antigen selectivity in autoimmune responses to the Ku (p70/p80) antigen. *J Clin Invest,* 84**,** 562-7.

REIK, W., DEAN, W. & WALTER, J. (2001) Epigenetic reprogramming in mammalian development. *Science,* 293**,** 1089-1093.

REVEL, A., ACHACHE, H., STEVENS, J., SMITH, Y. & REICH, R. (2011) MicroRNAs are associated with human embryo implantation defects. *Human Reproduction***,** 1-11.

RICH, T., ALLEN, R. L. & WYLLIE, A. H. (2000) Defying death after DNA damage. *Nature,* 407**,** 777-83.

RICHARDSON, L. L., PEDIGO, C. & ANN HANDEL, M. (2000) Expression of deoxyribonucleic acid repair enzymes during spermatogenesis in mice. *Biol Reprod,* 62**,** 789-96.

RIEDL, T., HANAOKA, F. & EGLY, J. M. (2003) The comings and goings of nucleotide excision repair factors on damaged DNA. *EMBO J,* 22**,** 5293-303.

RIGGS, A. D. & JONES, P. A. (1983) 5-methylcytosine, gene regulation, and cancer. *Adv Cancer Res,* 40**,** 1-30.

RIIS, B., RISOM, L., LOFT, S. & POULSEN, H. E. (2002) OGG1 mRNA expression and incision activity in rats are higher in foetal tissue than in adult liver tissue while 8-oxo-2'-deoxyguanosine levels are unchanged. *DNA Repair (Amst),* 1**,** 709-17.

RO, S., PARK, C., SANDERS, K. M., MCCARREY, J. R. & YAN, W. (2007) Cloning and expression profiling of testis-expressed microRNAs. *Dev Biol,* 311**,** 592-602.

ROBERTSON, A. B., KLUNGLAND, A., ROGNES, T. & LEIROS, I. (2009) DNA repair in mammalian cells: Base excision repair: the long and short of it. *Cell Mol Life Sci,* 66**,** 981-93.

RODRIGUE, A., COULOMBE, Y., JACQUET, K., GAGNE, J. P., ROQUES, C., GOBEIL, S., POIRIER, G. & MASSON, J. Y. (2012) The RAD51 paralogs ensure cellular protection against mitotic defects and aneuploidy. *J Cell Sci,* 126**,** 348-359.

ROIG, I., LIEBE, B., EGOZCUE, J., CABERO, L., GARCIA, M. & SCHERTHAN, H. (2004) Female-specific features of recombinational double-stranded DNA repair in relation to synapsis and telomere dynamics in human oocytes. *Chromosoma,* 113**,** 22-33.

RONEN, A. & GLICKMAN, B. W. (2001) Human DNA repair genes. *Environ Mol Mutagen,* 37**,** 241-83.

ROSENBLUTH, E. M., SHELTON, D. N., SPARKS, A. E., DEVOR, E., CHRISTENSON, L. & VAN VOORHIS, B. J. (2012) MicroRNA expression in the human blastocyst. *Fertil Steril,* 99**,** 855-861.

ROUGIER, N., BOURC'HIS, D., GOMES, D. M., NIVELEAU, A., PLACHOT, M., PALDI, A. & VIEGAS-PEQUIGNOT, E. (1998) Chromosome methylation patterns during mammalian preimplantation development. *Genes Dev,* 12**,** 2108-13.

RUBY, J. G., JAN, C. H. & BARTEL, D. P. (2007) Intronic microRNA precursors that bypass Drosha processing. *Nature,* 448**,** 83-86.

RYAZANSKY, S. S. & GVOZDEV, V. A. (2008) Small RNAs and cancerogenesis. *Biochemistry (Mosc),* 73**,** 514-27.

SABERI, A., HOCHEGGER, H., SZUTS, D., LAN, L., YASUI, A., SALE, J. E., TANIGUCHI, Y., MURAKAWA, Y., ZENG, W., YOKOMORI, K., HELLEDAY, T., TERAOKA, H., ARAKAWA, H., BUERSTEDDE, J. M. & TAKEDA, S. (2007) RAD18 and poly(ADP-ribose) polymerase independently suppress the access of nonhomologous end joining to double-strand breaks and facilitate homologous recombination-mediated repair. *Mol Cell Biol,* 27**,** 2562-71.

SALMENA, L., POLISENO, L., TAY, Y., KATS, L. & PANDOLFI, P. P. (2011) A ceRNA hypothesis: the Rosetta Stone of a hidden RNA language? *Cell,* 146**,** 353-8.

SAMPSON, J. R., JONES, S., DOLWANI, S. & CHEADLE, J. P. (2005) MutYH (MYH) and colorectal cancer. *Biochem Soc Trans,* 33**,** 679-83.

SANTOS, F. & DEAN, W. (2004) Epigenetic reprogramming during early development in mammals. *Reproduction,* 127**,** 643-51.

SANTOS, F., HENDRICH, B., REIK, W. & DEAN, W. (2002) Dynamic reprogramming of DNA methylation in the early mouse embryo. *Dev Biol,* 241**,** 172-82.

SANTOS, F., ZAKHARTCHENKO, V., STOJKOVIC, M., PETERS, A., JENUWEIN, T., WOLF, E., REIK, W. & DEAN, W. (2003) Epigenetic marking correlates with

developmental potential in cloned bovine preimplantation embryos. *Curr Biol,* 13**,** 1116-21.

SANTUCCI-DARMANIN, S. & PAQUIS-FLUCKLINGER, V. (2003) [Homologs of MutS and MutL during mammalian meiosis]. *Med Sci (Paris),* 19**,** 85-91.

SARVER, A. L., FRENCH, A. J., BORRALHO, P. M., THAYANITHY, V., OBERG, A. L., SILVERSTEIN, K. A., MORLAN, B. W., RISKA, S. M., BOARDMAN, L. A., CUNNINGHAM, J. M., SUBRAMANIAN, S., WANG, L., SMYRK, T. C., RODRIGUES, C. M., THIBODEAU, S. N. & STEER, C. J. (2009) Human colon cancer profiles show differential microRNA expression depending on mismatch repair status and are characteristic of undifferentiated proliferative states. *BMC Cancer,* 9**,** 401.

SASAKI, M. S. (1975) Is Fanconi's anaemia defective in a process essential to the repair of DNA cross links? *Nature,* 257**,** 501-3.

SCHEPELER, T., REINERT, J. T., OSTENFELD, M. S., CHRISTENSEN, L. L., SILAHTAROGLU, A. N., DYRSKJOT, L., WIUF, C., SORENSEN, F. J., KRUHOFFER, M., LAURBERG, S., KAUPPINEN, S., ORNTOFT, T. F. & ANDERSEN, C. L. (2008) Diagnostic and prognostic microRNAs in stage II colon cancer. *Cancer Res,* 68**,** 6416-24.

SCHLACHER, K., CHRIST, N., SIAUD, N., EGASHIRA, A., WU, H. & JASIN, M. (2011) Double-strand break repair-independent role for BRCA2 in blocking stalled replication fork degradation by MRE11. *Cell,* 145**,** 529-42.

SCHLACHER, K., WU, H. & JASIN, M. (2012) A distinct replication fork protection pathway connects Fanconi anemia tumor suppressors to RAD51-BRCA1/2. *Cancer Cell,* 22**,** 106-16.

SCHLISSEL, M., CONSTANTINESCU, A., MORROW, T., BAXTER, M. & PENG, A. (1993) Double-strand signal sequence breaks in V(D)J recombination are blunt, 5'-phosphorylated, RAG-dependent, and cell cycle regulated. *Genes Dev,* 7**,** 2520-32.

SCHROEDER, A., MUELLER, O., STOCKER, S., SALOWSKY, R., LEIBER, M., GASSMANN, M., LIGHTFOOT, S., MENZEL, W., GRANZOW, M. & RAGG, T. (2006) The RIN: an RNA integrity number for assigning integrity values to RNA measurements. *BMC Mol Biol,* 7**,** 3.

SEITZ, H. (2009) Redefining microRNA targets. *Curr Biol,* 19**,** 870-3.

SEKI, Y., HAYASHI, K., ITOH, K., MIZUGAKI, M., SAITOU, M. & MATSUI, Y. (2005) Extensive and orderly reprogramming of genome-wide chromatin modifications associated with specification and early development of germ cells in mice. *Dev Biol,* 278**,** 440-58.

SHANNON, M., LAMERDIN, J. E., RICHARDSON, L., MCCUTCHEN-MALONEY, S. L., HWANG, M. H., HANDEL, M. A., STUBBS, L. & THELEN, M. P. (1999) Characterization of the mouse Xpf DNA repair gene and differential expression during spermatogenesis. *Genomics,* 62**,** 427-35.

SHI, C. Z., COLLINS, H. W., GARSIDE, W. T., BUETTGER, C. W., MATSCHINSKY, F. M. & HEYNER, S. (1994) Protein databases for compacted eight-cell and blastocyst-stage mouse embryos. *Mol Reprod Dev,* 37**,** 34-47.

SHIBATA, S., SASAKI, M., MIKI, T., SHIMAMOTO, A., FURUICHI, Y., KATAHIRA, J. & YONEDA, Y. (2006) Exportin-5 orthologues are functionally divergent among species. *Nucleic Acids Res,* 34**,** 4711-21.

SHUCK, S. C., SHORT, E. A. & TURCHI, J. J. (2008) Eukaryotic nucleotide excision repair: from understanding mechanisms to influencing biology. *Cell Res,* 18**,** 64-72.

SINGLETON, M. R., WENTZELL, L. M., LIU, Y., WEST, S. C. & WIGLEY, D. B. (2002) Structure of the single-strand annealing domain of human RAD52 protein. *Proc Natl Acad Sci U S A,* 99**,** 13492-7.

SIPLEY, J. D., MENNINGER, J. C., HARTLEY, K. O., WARD, D. C., JACKSON, S. P. & ANDERSON, C. W. (1995) Gene for the catalytic subunit of the human DNA-activated protein kinase maps to the site of the XRCC7 gene on chromosome 8. *Proc Natl Acad Sci U S A,* 92**,** 7515-9.

SMALLWOOD, S. A. & KELSEY, G. (2012) De novo DNA methylation: a germ cell perspective. *Trends Genet,* 28**,** 33-42.

SMITH, G. C. & JACKSON, S. P. (1999) The DNA-dependent protein kinase. *Genes Dev,* 13**,** 916-34.

SMITH, Z. D., CHAN, M. M., MIKKELSEN, T. S., GU, H., GNIRKE, A., REGEV, A. & MEISSNER, A. (2012) A unique regulatory phase of DNA methylation in the early mammalian embryo. *Nature,* 484**,** 339-44.

SOHAIL, A., LIEB, M., DAR, M. & BHAGWAT, A. S. (1990) A gene required for very short patch repair in Escherichia coli is adjacent to the DNA cytosine methylase gene. *J Bacteriol,* 172**,** 4214-21.

SONG, J. H. & MELTZER, S. J. (2012) MicroRNAs in pathogenesis, diagnosis, and treatment of gastroesophageal cancers. *Gastroenterology,* 143**,** 35-47 e2.

SONODA, E., TAKATA, M., YAMASHITA, Y. M., MORRISON, C. & TAKEDA, S. (2001) Homologous DNA recombination in vertebrate cells. *Proc Natl Acad Sci U S A,* 98**,** 8388-94.

STASIAK, A. Z., LARQUET, E., STASIAK, A., MULLER, S., ENGEL, A., VAN DYCK, E., WEST, S. C. & EGELMAN, E. H. (2000) The human Rad52 protein exists as a heptameric ring. *Curr Biol,* 10**,** 337-40.

STRACKER, T. H., WILLIAMS, B. R., DERIANO, L., THEUNISSEN, J. W., ADELMAN, C. A., ROTH, D. B. & PETRINI, J. H. (2009) Artemis and nonhomologous end joining-independent influence of DNA-dependent protein kinase catalytic subunit on chromosome stability. *Mol Cell Biol,* 29**,** 503-14.

STRAND, M., EARLEY, M. C., CROUSE, G. F. & PETES, T. D. (1995) Mutations in the MSH3 gene preferentially lead to deletions within tracts of simple repetitive DNA in Saccharomyces cerevisiae. *Proc Natl Acad Sci U S A,* 92**,** 10418-21.

SUBRAMANIAN, S., MISHRA, R. K. & SINGH, L. (2003) Genome-wide analysis of microsatellite repeats in humans: their abundance and density in specific genomic regions. *Genome Biol,* 4**,** R13.

SUH, N. & BLELLOCH, R. (2011) Small RNAs in early mammalian development: from gametes to gastrulation. *Development,* 138**,** 1653-1661.

SUHASINI, A. N., SOMMERS, J. A., MUNIANDY, P. A., COULOMBE, Y., CANTOR, S. B., MASSON, J. Y., SEIDMAN, M. M. & BROSH, R. M., JR. (2013) Fanconi Anemia Group J Helicase and MRE11 Nuclease Interact to Facilitate the DNA Damage Response. *Mol Cell Biol,* 33**,** 2212-2227.

SUNG, J. S., DEMOTT, M. S. & DEMPLE, B. (2005) Long-patch base excision DNA repair of 2-deoxyribonolactone prevents the formation of DNA-protein cross-links with DNA polymerase beta. *J Biol Chem,* 280**,** 39095-103.

SUSSE, S., SCHOLZ, C. J., BURKLE, A. & WIESMULLER, L. (2004) Poly(ADP-ribose) polymerase (PARP-1) and p53 independently function in regulating double-strand break repair in primate cells. *Nucleic Acids Res,* 32**,** 669-80.

SUZUKI, H. I., YAMAGATA, K., SUGIMOTO, K., IWAMOTO, T., KATO, S. & MIYAZONO, K. (2009) Modulation of microRNA processing by p53. *Nature,* 460**,** 529-533.

SZABO, P. E. & MANN, J. R. (1995) Allele-specific expression and total expression levels of imprinted genes during early mouse development: implications for imprinting mechanisms. *Genes Dev,* 9**,** 3097-108.

TAGHIAN, D. G., HOUGH, H. & NICKOLOFF, J. A. (1998) Biased short tract repair of palindromic loop mismatches in mammalian cells. *Genetics,* 148**,** 1257-68.

TAKAI, H., TOMINAGA, K., MOTOYAMA, N., MINAMISHIMA, Y. A., NAGAHAMA, H., TSUKIYAMA, T., IKEDA, K., NAKAYAMA, K. & NAKANISHI, M. (2000) Aberrant cell cycle checkpoint function and early embryonic death in Chk1(-/-) mice. *Genes Dev,* 14**,** 1439-47.

TAMARU, H. & SELKER, E. U. (2001) A histone H3 methyltransferase controls DNA methylation in Neurospora crassa. *Nature,* 414**,** 277-83.

TAMMARO, C., RAPONI, M., WILSON, D. I. & BARALLE, D. (2012) BRCA1 exon 11 alternative splicing, multiple functions and the association with cancer. *Biochem Soc Trans,* 40**,** 768-72.

TANG, F., KANEDA, M., O'CARROLL, D., HAJKOVA, P., BARTON, S. C., SUN, Y. A., LEE, C., TARAKHOVSKY, A., LAO, K. & SURANI, M. A. (2007) Maternal microRNAs are essential for mouse zygotic development. *Genes Dev,* 21**,** 644-8.

TANIC, M., ZAJAC, M., GOMEZ-LOPEZ, G., BENITEZ, J. & MARTINEZ-DELGADO, B. (2011) Integration of BRCA1-mediated miRNA and mRNA profiles reveals microRNA regulation of TRAF2 and NFkappaB pathway. *Breast Cancer Res Treat,* 134**,** 41-51.

TELFORD, N. A., WATSON, A. J. & SCHULTZ, G. A. (1990) Transition from maternal to embryonic control in early mammalian development: a comparison of several species. *Mol Reprod Dev,* 26**,** 90-100.

TESARIK, J., KOPECNY, V., PLACHOT, M. & MANDELBAUM, J. (1988) Early morphological signs of embryonic genome expression in human preimplantation development as revealed by quantitative electron microscopy. *Dev Biol,* 128**,** 15-20.

TESFAYE, D., WORKU, D., RINGS, F., PHATSARA, C., THOLEN, E., SCHELLANDER, K. & HOELKER, M. (2009) Identification and expression profiling of microRNAs during bovine oocyte maturation using heterologous approach. *Mol Reprod Dev,* 76**,** 665-77.

THOMAS, D. C., ROBERTS, J. D. & KUNKEL, T. A. (1991) Heteroduplex repair in extracts of human HeLa cells. *J Biol Chem,* 266**,** 3744-51.

THOMPSON, J. G., SHERMAN, A. N., ALLEN, N. W., MCGOWAN, L. T. & TERVIT, H. R. (1998) Total protein content and protein synthesis within pre-elongation stage bovine embryos. *Mol Reprod Dev,* 50**,** 139-45.

TICHY, E. D. & STAMBROOK, P. J. (2008) DNA repair in murine embryonic stem cells and differentiated cells. *Exp Cell Res,* 314**,** 1929-36.

TOMINAGA, Y., LI, C., WANG, R. H. & DENG, C. X. (2006) Murine Wee1 plays a critical role in cell cycle regulation and pre-implantation stages of embryonic development. *Int J Biol Sci,* 2**,** 161-70.

TOMKINSON, A. E., STARR, R. & SCHULTZ, R. A. (1993) DNA ligase III is the major high molecular weight DNA joining activity in SV40-transformed human fibroblasts: normal levels of DNA ligase III activity in Bloom syndrome cells. *Nucleic Acids Res,* 21**,** 5425-30.

TRABUCCHI, M., BRIATA, P., GARCIA-MAYORAL, M., HAASE, A. D., FILIPOWICZ, W., RAMOS, A., GHERZI, R. & ROSENFELD, M. G. (2009) The RNA-binding protein KSRP promotes the biogenesis of a subset of microRNAs. *Nature,* 459**,** 1010-4.

TSAI-WU, J. J., SU, H. T., FANG, W. H. & WU, C. H. (1999) Preparation of heteroduplex DNA containing a mismatch base pair with magnetic beads. *Anal Biochem,* 275**,** 127-9.

UMAR, A., BOYER, J. C., THOMAS, D. C., NGUYEN, D. C., RISINGER, J. I., BOYD, J., IONOV, Y., PERUCHO, M. & KUNKEL, T. A. (1994) Defective mismatch repair in extracts of colorectal and endometrial cancer cell lines exhibiting microsatellite instability. *J Biol Chem,* 269**,** 14367-70.

UMAR, A., BUERMEYER, A. B., SIMON, J. A., THOMAS, D. C., CLARK, A. B., LISKAY, R. M. & KUNKEL, T. A. (1996) Requirement for PCNA in DNA mismatch repair at a step preceding DNA resynthesis. *Cell,* 87**,** 65-73.

VALERI, N., GASPARINIA, P., BRACONIB, C., PAONEA, A., LOVATA, F., FABBRIA, M., SUMANIA, K. M., ALDERA, H., AMADORIE, D., PATELB, T., NUOVOF, G. J., FISHELA, R. & CROCEA, C. M. (2010) MicroRNA-21 induces resistance to 5-fluorouracil by down-regulating human DNA MutS homolog 2 (hMSH2). *PNAS,* 107**,** 21098-21103.

VALERIE, K. & POVIRK, L. F. (2003) Regulation and mechanisms of mammalian double-strand break repair. *Oncogene,* 22**,** 5792-812.

VAN BRABANT, A. J., STAN, R. & ELLIS, N. A. (2000) DNA helicases, genomic instability, and human genetic disease. *Annu Rev Genomics Hum Genet,* 1**,** 409-59.

VAN DE VRUGT, H. J., EATON, L., HANLON NEWELL, A., AL-DHALIMY, M., LISKAY, R. M., OLSON, S. B. & GROMPE, M. (2009) Embryonic lethality after combined inactivation of Fancd2 and Mlh1 in mice. *Cancer Res,* 69**,** 9431-8.

VAN DYCK, E., STASIAK, A. Z., STASIAK, A. & WEST, S. C. (2001) Visualization of recombination intermediates produced by RAD52-mediated single-strand annealing. *EMBO Rep,* 2**,** 905-9.

VARLET, I., CANARD, B., BROOKS, P., CEROVIC, G. & RADMAN, M. (1996) Mismatch repair in Xenopus egg extracts: DNA strand breaks act as signals rather than excision points. *Proc Natl Acad Sci U S A,* 93**,** 10156-61.

VASUDEVAN, S., TONG, Y. & STEITZ, J. A. (2007) Switching from repression to activation: microRNAs can up-regulate translation. *Science,* 318**,** 1931-4.

VEECK, L. L., BODINE, R., CLARKE, R. N., BERRIOS, R., LIBRARO, J., MOSCHINI, R. M., ZANINOVIC, N. & ROSENWAKS, Z. (2004) High pregnancy rates can be achieved after freezing and thawing human blastocysts. *Fertil Steril,* 82**,** 1418-27.

VINSON, R. K. & HALES, B. F. (2002) DNA repair during organogenesis. *Mutat Res,* 509**,** 79-91.

VOLINIA, S., GALASSO, M., SANA, M. E., WISE, T. F., PALATINI, J., HUEBNER, K. & CROCE, C. M. (2012) Breast cancer signatures for invasiveness and prognosis defined by deep sequencing of microRNA. *Proc Natl Acad Sci U S A,* 109**,** 3024-9.

WALTER, C. A., INTANO, G. W., MCCARREY, J. R., MCMAHAN, C. A. & WALTER, R. B. (1998) Mutation frequency declines during spermatogenesis in young mice but increases in old mice. *Proc Natl Acad Sci U S A,* 95**,** 10015-9.

WALTER, C. A., TROLIAN, D. A., MCFARLAND, M. B., STREET, K. A., GURRAM, G. R. & MCCARREY, J. R. (1996) Xrcc-1 expression during male meiosis in the mouse. *Biol Reprod,* 55**,** 630-5.

WANG, H. & HAYS, J. B. (2002) Mismatch repair in human nuclear extracts. Quantitative analyses of excision of nicked circular mismatched DNA substrates, constructed by a new technique employing synthetic oligonucleotides. *J Biol Chem,* 277**,** 26136-42.

WANG, H. & HAYS, J. B. (2003) Mismatch repair in human nuclear extracts: effects of internal DNA-hairpin structures between mismatches and excision-initiation nicks on mismatch correction and mismatch-provoked excision. *J Biol Chem,* 278**,** 28686-93.

WANG, H. & HAYS, J. B. (2007) Human DNA mismatch repair: coupling of mismatch recognition to strand-specific excision. *Nucleic Acids Res,* 35**,** 6727-39.

WANG, P., ZOU, F., ZHANG, X., LI, H., DULAK, A., TOMKO, R. J., LAZO, J. S., WANG, Z., ZHANG, L. & YU, J. (2009) microRNA-21 Negatively Regulates Cdc25A and Cell Cycle Progression in Colon Cancer Cells. *Cancer Research,* 69**,** 8157-8165.

WANG, Q. T., PIOTROWSKA, K., CIEMERYCH, M. A., MILENKOVIC, L., SCOTT, M. P., DAVIS, R. W. & ZERNICKA-GOETZ, M. (2004) A genome-wide study of gene activity reveals developmental signaling pathways in the preimplantation mouse embryo. *Dev Cell,* 6**,** 133-44.

WANG, T. F., KLECKNER, N. & HUNTER, N. (1999) Functional specificity of MutL homologs in yeast: evidence for three Mlh1-based heterocomplexes with distinct roles during meiosis in recombination and mismatch correction. *Proc Natl Acad Sci U S A,* 96**,** 13914-9.

WANG, Y., HUANG, J. W., LI, M., CAVENEE, W. K., MITCHELL, P. S., ZHOU, X., TEWARI, M., FURNARI, F. B. & TANIGUCHI, T. (2011) MicroRNA-138 modulates DNA damage response by repressing histone H2AX expression. *Mol Cancer Res,* 9**,** 1100-11.

WANG, Y., MEDVID, R., MELTON, C., JAENISCH, R. & BLELLOCH, R. (2007) DGCR8 is essential for microRNA biogenesis and silencing of embryonic stem cell self-renewal. *Nat Genet,* 39**,** 380-5.

WANG, Z., WANG, F., TANG, T. & GUO, C. (2012) The role of PARP1 in the DNA damage response and its application in tumor therapy. *Front Med,* 6**,** 156-64.

WANG, Z. Q., STINGL, L., MORRISON, C., JANTSCH, M., LOS, M., SCHULZE-OSTHOFF, K. & WAGNER, E. F. (1997) PARP is important for genomic stability but dispensable in apoptosis. *Genes Dev,* 11**,** 2347-58.

WATERS, S. B. & AKMAN, S. A. (2001) A new assay to quantify in vivo repair of G:T mispairs by base excision repair. *Mutat Res,* 487**,** 109-19.

WEI, K., CLARK, A. B., WONG, E., KANE, M. F., MAZUR, D. J., PARRIS, T., KOLAS, N. K., RUSSELL, R., HOU, H., JR., KNEITZ, B., YANG, G., KUNKEL, T. A., KOLODNER, R. D., COHEN, P. E. & EDELMANN, W. (2003) Inactivation of Exonuclease 1 in mice results in DNA mismatch repair defects, increased cancer susceptibility, and male and female sterility. *Genes Dev,* 17**,** 603-14.

WEIDHAAS, J. B., BABAR, I., NALLUR, S. M., TRANG, P., ROUSH, S., BOEHM, M., GILLESPIE, E. & SLACK, F. J. (2007) MicroRNAs as Potential Agents to Alter Resistance to Cytotoxic Anticancer Therapy. *Cancer Research,* 67**,** 11111-11116.

WEISS, A., KESHET, I., RAZIN, A. & CEDAR, H. (1996) DNA demethylation in vitro: involvement of RNA. *Cell,* 86**,** 709-18.

WELLS, D., BERMUDEZ, M. G., STEUERWALD, N., THORNHILL, A. R., WALKER, D. L., MALTER, H., DELHANTY, J. D. & COHEN, J. (2005) Expression of genes regulating chromosome segregation, the cell cycle and apoptosis during human preimplantation development. *Hum Reprod,* 20**,** 1339-48.

WENG, Y. S. & NICKOLOFF, J. A. (1998) Evidence for independent mismatch repair processing on opposite sides of a double-strand break in Saccharomyces cerevisiae. *Genetics,* 148**,** 59-70.

WHITE, P. J., BORTS, R. H. & HIRST, M. C. (1999) Stability of the human fragile X (CGG)(n) triplet repeat array in Saccharomyces cerevisiae deficient in aspects of DNA metabolism. *Mol Cell Biol,* 19**,** 5675-84.

WIEBAUER, K. & JIRICNY, J. (1989) In vitro correction of G.T mispairs to G.C pairs in nuclear extracts from human cells. *Nature,* 339**,** 234-6.

WIEBAUER, K. & JIRICNY, J. (1990) Mismatch-specific thymine DNA glycosylase and DNA polymerase beta mediate the correction of G.T mispairs in nuclear extracts from human cells. *Proc Natl Acad Sci U S A,* 87**,** 5842-5.

WIENHOLDS, E., KLOOSTERMAN, W. P., MISKA, E., ALVAREZ-SAAVEDRA, E., BEREZIKOV, E., DE BRUIJN, E., HORVITZ, H. R., KAUPPINEN, S. & PLASTERK, R. H. (2005) MicroRNA expression in zebrafish embryonic development. *Science,* 309**,** 310-1.

WILSON, C. A., PAYTON, M. N., ELLIOTT, G. S., BUAAS, F. W., CAJULIS, E. E., GROSSHANS, D., RAMOS, L., REESE, D. M., SLAMON, D. J. & CALZONE, F. J. (1997) Differential subcellular localization, expression and biological toxicity of BRCA1 and the splice variant BRCA1-delta11b. *Oncogene,* 14**,** 1-16.

WILUSZ, C. J., WORMINGTON, M. & PELTZ, S. W. (2001) The cap-to-tail guide to mRNA turnover. *Nat Rev Mol Cell Biol,* 2**,** 237-46.

WILUSZ, J. E. & SHARP, P. A. (2013) Molecular biology. A circuitous route to noncoding RNA. *Science,* 340**,** 440-1.

WIRTHNER, R., WRANN, S., BALAMURUGAN, K., WENGER, R. H. & STIEHL, D. P. (2008) Impaired DNA double-strand break repair contributes to chemoresistance in HIF-1 alpha-deficient mouse embryonic fibroblasts. *Carcinogenesis,* 29**,** 2306-16.

WONG, M. L. & MEDRANO, J. F. (2005) Real-time PCR for mRNA quantitation. *Biotechniques,* 39**,** 75-85.

WRIGHT, S. J. (1999) Sperm nuclear activation during fertilization. *Curr Top Dev Biol,* 46**,** 133-78.

XIE, D., CHEN, C. C., PTASZEK, L. M., XIAO, S., CAO, X., FANG, F., NG, H. H., LEWIN, H. A., COWAN, C. & ZHONG, S. (2010) Rewirable gene regulatory networks in the preimplantation embryonic development of three mammalian species. *Genome Res,* 20**,** 804-15.

XIE, Q. H., HE, X. X., CHANG, Y., SUN, S. Z., JIANG, X., LI, P. Y. & LIN, J. S. (2011) MiR-192 inhibits nucleotide excision repair by targeting ERCC3 and ERCC4 in HepG2.2.15 cells. *Biochem Biophys Res Commun,* 410**,** 440-5.

XU, G., SPIVAK, G., MITCHELL, D. L., MORI, T., MCCARREY, J. R., MCMAHAN, C. A., WALTER, R. B., HANAWALT, P. C. & WALTER, C. A. (2005) Nucleotide excision repair activity varies among murine spermatogenic cell types. *Biol Reprod,* 73**,** 123-30.

XU, Y. W., WANG, B., DING, C. H., LI, T., GU, F. & ZHOU, C. (2011) Differentially expressed micoRNAs in human oocytes. *J Assist Reprod Genet,* 28**,** 559-66.

YAN, D., NG, W. L., ZHANG, X., WANG, P., ZHANG, Z., MO, Y. Y., MAO, H., HAO, C., OLSON, J. J., CURRAN, W. J. & WANG, Y. (2010) Targeting DNA-PKcs and ATM with miR-101 sensitizes tumors to radiation. *PLoS One,* 5**,** e11397.

YAN, H.-L., XUE, G., MEI, Q., WANG, Y.-Z., DING, F.-X., LIU, M.-F., LU, M.-H., TANG, Y., YU, H.-Y. & SUN, S.-H. (2009) Repression of the miR-17-92 cluster by p53 has an important function in hypoxia-induced apoptosis. *EMBO J,* 28**,** 2719-2732.

YAN, L. X., HUANG, X. F., SHAO, Q., HUANG, M. Y., DENG, L., WU, Q. L., ZENG, Y. X. & SHAO, J. Y. (2008) MicroRNA miR-21 overexpression in human breast cancer is associated with advanced clinical stage, lymph node metastasis and patient poor prognosis. *RNA,* 14**,** 2348-60.

YANG, G. H., WANG, F., YU, J., WANG, X. S., YUAN, J. Y. & ZHANG, J. W. (2009) MicroRNAs are involved in erythroid differentiation control. *J Cell Biochem,* 107**,** 548-56.

YANG, Y., BAI, W., ZHANG, L., YIN, G., WANG, X., WANG, J., ZHAO, H., HAN, Y. & YAO, Y. Q. (2008) Determination of microRNAs in mouse preimplantation embryos by microarray. *Dev Dyn,* 237**,** 2315-27.

YI, R., DOEHLE, B. P., QIN, Y., MACARA, I. G. & CULLEN, B. R. (2005) Overexpression of exportin 5 enhances RNA interference mediated by short hairpin RNAs and microRNAs. *RNA,* 11**,** 220-6.

YI, R., QIN, Y., MACARA, I. G. & CULLEN, B. R. (2003) Exportin-5 mediates the nuclear export of pre-microRNAs and short hairpin RNAs. *Genes Dev,* 17**,** 3011-6.

YU, Z., JIAN, Z., SHEN, S. H., PURISIMA, E. & WANG, E. (2007) Global analysis of microRNA target gene expression reveals that miRNA targets are lower expressed in mature mouse and Drosophila tissues than in the embryos. *Nucleic Acids Res,* 35**,** 152-64.

ZHANG, H., LI, Y. & LAI, M. (2010a) The microRNA network and tumor metastasis. *Oncogene,* 29**,** 937-48.

ZHANG, Q. M. & DIANOV, G. L. (2005) DNA repair fidelity of base excision repair pathways in human cell extracts. *DNA Repair (Amst),* 4**,** 263-70.

ZHANG, X., WAN, G., BERGER, F. G., HE, X. & LU, X. (2011) The ATM kinase induces microRNA biogenesis in the DNA damage response. *Mol Cell,* 41**,** 371-83.

ZHANG, X., WAN, G., MLOTSHWA, S., VANCE, V., BERGER, F. G., CHEN, H. & LU, X. (2010b) Oncogenic Wip1 phosphatase is inhibited by miR-16 in the DNA damage signaling pathway. *Cancer Res,* 70**,** 7176-86.

ZHAO, C., SUN, G., LI, S. & SHI, Y. (2009) A feedback regulatory loop involving microRNA-9 and nuclear receptor TLX in neural stem cell fate determination. *Nat Struct Mol Biol,* 16**,** 365-71.

ZHAO, Y., SAMAL, E. & SRIVASTAVA, D. (2005) Serum response factor regulates a muscle-specific microRNA that targets Hand2 during cardiogenesis. *Nature,* 436**,** 214-20.

ZHENG, P., SCHRAMM, R. D. & LATHAM, K. E. (2005) Developmental regulation and in vitro culture effects on expression of DNA repair and cell cycle checkpoint control genes in rhesus monkey oocytes and embryos. *Biol Reprod,* 72**,** 1359-69.

7. Appendix

7.1 Appendix to introduction

7.1.1 Potential correlation analysis between miRNA and their target repair transcripts in human oocytes and preimplantation embryos

MiRNAs expressed in gametes and preimplantation embryos in mouse, human and bovine and list of their target genes including repair pathways they are associated with are shown in this table. The expression of miRNA in gametes and preimplantation embryo development is represented by "✓". If the expression level of miRNA compared to the previous stage of the development is increased (i.e. increased level at the 4-cell stage than the 2-cell stage), this increased expression level is represented by "↑". If the expression level of miRNA compared to the previous stage of the development is decreased, this reduced expression level is represented by ↓. If there has not been any studies analysing the expression of a miRNA at that particular stage of preimplantation embryo development, this was shown as blank (Yang *et al.*, 2009, Tang *et al.*, 2007, Amanai *et al.*, 2006, McCallie *et al.*, 2009, Mondou *et al.*, 2012, Ro *et al.*, 2007, Xu *et al.*, 2011, Rosenbluth *et al.*, 2012).

a) Expression profiles of miRNAs in gametes and embryos and their target base excision repair genes.

miRNA	Target repair mRNA	Species	Oocyte	Sperm	Zygote	2-cell	4-cell	8-cell	Morula	Blastocyst
miR-22	*UNG,MDC1*	Mouse			✓	↑	↑	↑		
miR-96	*MBD4*	Mouse			✓	↓	↑	↑		
miR-98	*ERCC6, DCLRE1B, RAD9A*	Mouse			✓	↓	↓	↓		
		Bovine	✓							
miR-101a	*TDG, FANCM, POLH,REV3L, UBE2A*	Mouse			✓	↓	↑	↑		
miR-101b	*TDG, NEIL1, FANCM,POLH, REV3L*	Mouse			✓	↓	↑	↑		
miR-103	*NEIL1, TDG -103-a,POLH-103-as*	Mouse	✓	✓	✓	↓	↑	↑	↑	
miR-107	*TDG, NEIL1*	Mouse	✓	✓	✓	↓	↑	↓		
		Bovine	✓							
miR-204	*UNG- 5p,POLH, POLK*	Mouse			✓	↓	↓	↑	↑	↑
miR-211	*UNG,POLH, POLK*	Mouse			✓	↓	↑	↓	↑	↓
miR-223	*PARP1*	Mouse	✓	✓	✓	↓	↑	↓		
		Bovine	✓							
miR-296	*MBD4*	Mouse			✓	↓	↑	↑		
miR-298	*OGG1*									
	TDP1	Mouse	✓	✓	✓	↑	↓	↑		

b) Expression profiles of miRNAs in gametes and embryos and their target nucleotide excision repair genes.

miRNA	Target repair mRNA	Species	Oocyte	Sperm	Zygote	2-cell	4-cell	8-cell	Morula	Blastocyst
miR-10a	*GTF2H1*	Mouse	✓	✓	✓	↓	↓	↓		
		Bovine	✓							
miR-10b	*GTF2H1*	Mouse	✓	✓	✓	↑	↑	↑		
		Bovine	✓							
miR-15b	*ERCC6, RAD23B, DDB2 (LHX3),CHEK1*	Mouse	✓	✓			✓	✓	↑	↑
		Bovine	✓							
miR-16	*RAD23B,CHEK1,Wip1*	Mouse	✓	✓	✓	↓	↓	↓		
		Bovine	✓							
		Human	✓							
miR-20b	*RPA2b,CHAF1A,UBE2,FANCD2,POLQ, POLH*	Bovine	✓							
miR-23a	*CCNH, RAD23B,RAD1,DCLRE1A, UBE2V2,POLH, FANCD2*	Mouse	✓	✓	✓	↓	↓	↓		
miR-23b	*CCNH, RAD23B,H2AX,RAD1, DCLRE1A, POLH, FANCD1*	Mouse	✓	✓	✓	↓	↓	↓		
		Bovine	✓							
miR-130a	*ERCC4, GTF2H1, FANCA*	Mouse			✓	↓	↑	↑		
		Bovine	✓							
miR-134	*ERCC6, RAD18*	Mouse	✓	✓	✓	✓	↑	↑		
miR-144	*GTF2H2*	Mouse			✓	✓	✓	✓		
miR-152	*GTF2H1*	Mouse			✓	↑	↓	↑		
miR-181c	*RAD23B,POLI, POLQ, ATM, FANCM*	Mouse			✓	↓	↑	↑		
		Bovine	✓							
miR-192	*ERCC3, ERCC4*	Mouse			✓	↑	↓	✓		
		Bovine	✓							
		Human								✓
miR-199a-5p	*RAD23B*	Mouse			✓	↑	↑	↓		
		Bovine	✓							
miR-199b-5p	*RAD23B*	Mouse			✓	↓	↑	↓		
miR-215	*ERCC4 (XPF)*	Mouse			✓	✓	✓	✓		
miR-218	*CETN2,RAD1*	Mouse			✓	↓	↑	↓		
miR-221	*ERCC4 (XPF),RRM2B, FANCD2*	Mouse	✓	✓	✓	↓	↑	↓		
miR-222	*ERCC4 (XPF),RRM2B, FANCD2*	Mouse	✓	✓	✓	↓	↓	↓		
miR-323	*DDB1*	Mouse			✓	↑	↓	↑		
miR-324-3p	*RPA1*	Mouse				↓	↑	↑		
miR-345	*RPA1*	Mouse			✓					
miR-33	*ERCC4(XPF)-33a, ERCC6*	Mouse			✓	✓	✓	✓		
miR-342	*MMS19L (MMS19) - 3P*	Mouse	✓	✓	✓	↓	↓	↑		
		Bovine	✓							
miR-345	*RPA1*	Mouse			✓	↑	↑	↓		
miR-372	*ERCC4 (XPF), POLK,RAD18, UBE2B*	Human								✓
		Bovine	✓							
miR-373	*ERCC4, POLK,UBE2B, RAD18*	Bovine	✓							
		Human								✓
miR-381	*GTF2H1,TP53*	Mouse			✓	↑	↓	↓		
		Bovine	✓							
miR-423	*DDB2 (LHX3)- 423-5p*	Bovine	✓							
miR-424	*ERCC6, RAD23B, DDB2(LHX3)*	Mouse					↓			
		Bovine	✓							
miR-450	*ERCC4 (XPF), GTF2H1- b-5b,UBE2A-b-5p, POLQ-b-3p*	Mouse			✓	↑	↑	↑		
miR-454	*GTF2H1, ERCC4,FANCA*	Human								✓
miR-483	*GTF2H1*	Bovine	✓							
miR-512-3p	*ERCC4,POLK*	Human								✓
miR-888	*GTF2H2,TDP1*	Human	✓							
miR-1260	*DDB1,RAD18, FANCC*	Bovine	✓							

c) Expression profiles of miRNAs in gametes and embryos and their target double strand break repair genes.

miRNA	Target repair mRNA	Species	Oocyte	Sperm	Zygote	2-cell	4-cell	8-cell	Morula	Blastocyst
miR-1	*BRCA1, TDP1*	Mouse			✓	↓	↑	↓		
miR-9	*MRE11A, PRKDC, POLE, POLI*	Mouse			✓	↓	↓	↑		
miR-18	*RBBP8, DCLRE1C, ATM*	Mouse		✓	✓	↓	↑	↑		
miR-24	*H2AX,*	Mouse	✓	✓	✓	↓	↓	↓		
	H2AFX	Human	✓							↓
miR-34a	*EME1*	Mouse				↑	↑	↑	↑	
miR-34b	*XRCC2*	Mouse			✓	✓	↑	↑	↓	
	FANCF	Human	✓							✓
miR-34c	*EME1- 5p*	Mouse	✓	✓	✓	✓	↑	↑		
		Bovine	✓							
miR-125a	*BRCA1- 3p*	Mouse	✓	✓	✓	↑	↑	↑	↑	↑
	MDC1- 5p	Bovine	✓			↑	↓	↑	↓	↓
miR-128a	*RAD52*	Mouse			✓	✓	✓	↑		
	UBE2N	Bovine	✓							
miR-128b	*RAD52*	Mouse			✓	✓	✓	↑		
	UBE2N	Bovine	✓							
miR-138	*H2AX*	Mouse			✓	↑	↓	↓		
		Bovine	✓							
miR-139	*EME1- 5p*	Mouse			✓	↓	↑	↓		
miR-140	*Artemis*	Mouse	✓	✓	✓	↑	↑	↑	↓	↓
		Bovine	✓							
miR-143	*EME1- 3p*	Bovine	✓							
	POLH									
miR-148a	*GTF2H1*	Mouse			✓	↑	↓	↑		
		Bovine	✓							
miR-148b	*GTF2H1*	Mouse			✓	↑	↓	↑		
miR-150	*PRKDC,POLH*	Mouse			✓	↓	↑	↓		
miR-151	*LIG4- 3p*	Mouse			✓	↓	↑	↓		
	FANCA- 5p	Human								✓
miR-153	*BRCA1*	Mouse			✓	✓	✓	✓		
		Bovine	✓							
miR-154	*MRE11,PCNA, UBE2A,TDP1,LIG4*	Mouse			✓	✓	✓	✓		
miR-190	*BRCA1*	Mouse			✓	↓	↓	✓		
	POLI	Bovine	✓							
miR-193	*RAD51L1- 193a*	Mouse			✓	↓	↑	↑	↓	
	DCLRE1C(193a-5p)	Human	✓(a-5p)							✓(b)
miR-198	*RAD51*	Bovine	✓							
	FANCL									
miR-203	*DCLRE1B,RAD18,RAD51,ATM,POLI*	Mouse			✓	↓	↑	↑		
miR-224	*BRCA1, RAD51L1,TDP*	Mouse			✓	↑	↑	↓		
miR-299	*DMC1- 3p*	Mouse				↑	↑	↑		
miR-363	*RAD21*	Bovine	✓							
	REV3L, POLK									
miR-377	*LIG4*	Mouse			✓	✓	✓	✓		
miR-383	*Artemis,UBE2N, ATR,EXO1*	Mouse			✓	↓	✓	✓		
		Bovine	✓							
miR-384	*MRE11A*	Mouse			✓	✓	✓	✓		
	FANCM	Bovine	✓							
miR-412	*RAD51L1*	Mouse			✓	✓	✓	✓		
		Bovine	✓							
miR-449	*EME1-449a*	Mouse			✓	↑	↓	✓		
miR-625	*NBN (NBS1)*	Human	✓							
miR-765	*RAD52B*	Bovine	✓							
miR-1224-5p	*RAD50*	Bovine	✓							

d) Expression profiles of miRNAs in gametes and embryos and their target mismatch repair genes.

miRNA	Target repair mRNA	Species	Oocyte	Sperm	Zygote	2-cell	4-cell	8-cell	Morula	Blastocyst
miR-26a	*POLH,ATM, FANCD2, MSH3 (5p)*	Mouse	✓	✓	✓	↓	↑	↓		
		Bovine	✓							
miR-26b	*MSH3-5p,POLH, ATM, FANCD2*	Mouse			✓	↓	↑	↓		
miR-149	*MLH3*	Mouse			✓	↑	↓	↑		
		Bovine	✓							
miR-155	*MSH2, MSH6, MLH1, FANCD2, FANCF, CHAF1A, DCLRE1A*	Mouse			✓	↓	↑	↓		
		Bovine	✓							
miR-219	*MLH3- hsa-miR-219-2-3p,UBE2N - 5p, DUT- 1-3p*	Mouse			✓	↓	↓	↓		
miR-291-3p	*MSH2*	Mouse			✓	↑	↑	↑		
miR-340	*MLH3,NBN (NBS1), RAD50, Artemis, RRM2B, POLI, REV3L, HEL308*	Mouse			✓	↓	↓	↓		
miR-370	*MLH3*	Mouse			✓	↑	↓	↓		

e) Expression profiles of miRNAs in gametes and embryos and their target double strand break repair and nucleotide excision repair genes.

miRNA	DNA repair pathways	Target repair mRNA	Species	Oocyte	Sperm	Zygote	2-cell	4-cell	8-cell	Morula	Blastocyst
let-7a	NER	*ERCC6 (CSB)*	Mouse	✓	✓	✓	↓	↓	↓		
	DSBR (NHEJ)	*DCLRE1B*	Human	✓							↓
			Bovine	✓							
let-7b	NER	*ERCC6 (CSB)*	Mouse	✓	✓	✓	↓	↓	↓		
			Bovine	✓							
	DSBR (NHEJ)	*DCLRE1B*	Human	✓							✓
let-7c	NER	*ERCC6 (CSB)*	Mouse	✓	✓	✓	↓	↓	↓		
			Bovine	✓							
	DSBR (NHEJ)	*DCLRE1B*	Human	✓							✓
let-7d	NER	*ERCC6 (CSB)*	Mouse	✓	✓	✓	↓	↓	↓		
	DSBR (NHEJ)	*DCLRE1B*	Bovine	✓							
let-7e	NER	*ERCC6 (CSB)*	Mouse	✓	✓	✓	↓	↓	↓		
	DSBR (NHEJ)	*DCLRE1B*									
let-7f	NER	*ERCC6 (CSB)*	Mouse	✓	✓		↓	↓	↓		
	DSBR (NHEJ)	*DCLRE1B*	Bovine	✓							
let-7g	NER	*ERCC6 (CSB)*	Mouse			✓	↓	↓	↓		
	DSBR (NHEJ)	*DCLRE1B*	Human	✓							↑
let-7i	NER	*ERCC6 (CSB)*	Mouse			✓	↓	↓	↓		
	DSBR (NHEJ)	*DCLRE1B*									
miR-15a	NER	*ERCC6, GTF2H1, RAD23B, DDB2 (LHX3)*	Mouse			✓	↓	↑	↑		
	DSBR (HR)	*RAD50*	Bovine	✓							
	Damage response	*CHEK1*	Human	✓							
miR-19a	NER	*ERCC4*	Mouse			✓	↓	↑	↑		
	DSBR (HR)	*RAD51L1, RBBP8*	Human	✓							✓
miR-19b	NER	*ERCC4*	Mouse	✓	✓	✓	↓	↑	↑		
	DSBR (HR)	*RBBP8*	Bovine	✓							
			Human	✓							↓
miR-28	NER	*ERCC4 (XPF) - 3p*	Mouse			✓	✓	✓	↑		
	RAD6 pathway	*UBE2V2- 3p*									
	DSBR (NHEJ)	*DCLRE1C- 3p*									
miR-127	DSBR (HR)	*BRCA1*	Mouse			✓	↓	↑	↑	↑	↑
	NER	*GTF2H1-5p*	Bovine	✓			↑	↑	↑	↑	
miR-145	NER	*RAD23B*	Mouse	✓	✓	✓	✓	↑	↓		
	DSBR sensor	*H2AX*									
	DSBR (HR)	*RAD51L1*									
	DSBR (NHEJ)	*PRKDC*									
	DNA polymerases	*REV3L*									
	RAD6 pathway	*RAD18*	Bovine	✓			↑	↑	↑	↑	
	Chromatin Structure	*H2AFX*									

miRNA	DNA repair pathways	Target repair mRNA	Species	Oocyte	Sperm	Zygote	2-cell	4-cell	8-cell	Morula	Blastocyst
miR-146	NER	*RAD23B- b-3p*	Mouse			✓	↓	↓	↑		
	DSBR (HR)	*BRCA1, BRCA2- a and b-5p*									
	Suspected DNA repair function	*RECQL5 a and b-5p*	Human (miR-146b-5p)								✓
miR-183	NER	*GTF2H1*	Mouse			✓	↓	↑	↑		
	DSBR (HR)	*RAD50*									
	Suspected DNA repair function	*NEIL3*									
miR-185	DSBR (HR)	*NBN (NBS1)*									
	NER	*ERCC6 (CSB)*	Mouse			✓	↓	↓	↑		
miR-188	NER	*RAD23B- 188-3p*	Mouse	✓	✓	✓	↓	↑	↓		
	DSBR (NHEJ)	*XRCC5- 5p*									
	DNA polymerases	*POLH*	Bovine	✓							
	Damage response	*MDC1- 188-5p*									
miR-195	NER	*ERCC6 (CSB), RAD23B, DDB2 (LHX3)*	Mouse			✓	↓	↑	↓		
	DSBR (HR)	*RAD50*									
	Cell cycle checkpoint control	*Wee1*									
miR-301	NER	*GTF2H1(a, b), ERCC4 (XPF)*	Human			✓	↓	↑	↑		
	DSBR (HR)	*RAD51L1- 301a and b*									
	Genes defective and sensitivity to DNA damaging agents	*ERCC4, FANCA- a&b*									
miR-328	NER	*DDB2 (LHX3)*	Mouse			✓	↓	↓	↓		
	DSBR (HR)	*RAD51L1*									
miR-338	NER	*ERCC6- 5P, GTF2H1- 3P*	Mouse			✓	✓	↑	↑		
	DSBR (HR)	*MRE11A- 5p*									
	Chromatin Structure	*CHAF1A- 3P*									
	Suspected DNA repair function	*DCLRE1B- 5P*									
	Genes defective and sensitivity to DNA damaging agents	*BLM, FANCC- 3P, FANCM- 5P*									
miR-371-5p	HR	*PARP1, RAD51B- 3p*	Bovine	✓							
	NER	*GTF2H2*									
	Cell cycle checkpoint control	*CDK14*									
	RAD6 pathway	*UBE2A*									
miR-410	NER	*RAD23B*	Mouse			✓	✓	✓	✓		
	DSBR (HR)	*NBN (NBS1)*									
	Damage response	*RAD17*	Bovine	✓							
miR-519	DSBR	*RAD51B, ATM (miR-519-a)*	Bovine (miR-519e)	✓							
	NER	*ERCC4 (miR-519-a)*	Human (miR-519a)								✓
	DNA polymerases	*POLH, POLQ (miR-519-a)*									
miR-520	RAD6 pathway	*UBE2B, RAD18*	Human (miR-520c-3p, d-3p)								✓
	DNA polymerases	*POLK*									
	NER	*ERCC4*									
	DSBR	*RBBP7*									
miR-1246	NER	*ERCC4*	Bovine	✓							
	HR	*RAD50*									
	Rad6 Pathway	*UBE2A, UBE2H*									

f) Expression profiles of miRNAs in gametes and embryos and their target nucleotide excision repair and base excision repair genes.

miRNA	DNA repair pathways	Target repair mRNA	Species	Oocyte	Sperm	Zygote	2-cell	4-cell	8-cell	Morula	Blastocyst
miR-30a-3p	NER	*GTF2H1, RAD23B*	Mouse			✓	↓	↓	↑		
	BER	*NEIL2*									
	RAD6 pathway	*UBE2V2*	Human	✓							
miR-30a-5p	NER	*GTF2H1, RAD23B*	Mouse			✓	↓	↓	↓		
	BER	*NEIL2*	Human	✓							
	RAD6 pathway	*UBE2V2*	Bovine	✓							
miR-30b	NER	*GTF2H1, RAD23B*	Mouse	✓	✓	✓	↓	↓	↓		
	BER	*NEIL2*	Bovine	✓							
	RAD6 pathway	*UBE2V2*	Human	✓							
miR-30c	NER	*GTF2H1, RAD23B*	Mouse	✓	✓	✓	↑	↑	↑	↑	
	RAD6 pathway	*UBE2V2*	Bovine	✓							
			Human	✓							✓
miR-30d	NER	*GTF2H1, RAD23B*	Mouse	✓	✓	✓	↓	↓	↓		
	BER	*NEIL2*	Bovine	✓							
	RAD6 pathway	*UBE2V2*	Human	✓							
miR-30e	NER	*GTF2H1, RAD23B*	Mouse			✓	↓	↑	↓		
	BER	*NEIL2*									
	RAD6 pathway	*UBE2V2*	Human	✓							
miR-130b	NER	*ERCC4, GTF2H1*	Mouse			✓	↑	↑	↑		
	BER	*PARP1*									
	Genes defective and sensitivity to DNA damaging agents	*FANCA*	Bovine	✓							
miR-132	NER	*GTF2H1*	Mouse			✓	↑	↑	↑		
	BER	*NEIL2*									
miR-141	NER	*XPC*	Mouse			✓	↓	↑	↓		
	BER	*PARP2*	Human	✓							

g) Expression profiles of miRNAs in gametes and embryos and their target base excision repair and double strand break repair genes.

miRNA	DNA repair pathways	Target repair mRNA	Species	Oocyte	Sperm	Zygote	2-cell	4-cell	8-cell	Morula	Blastocyst
miR-186	BER	*SMUG1*	Mouse			✓	↓	↑	↑		
	DSBR (HR)	*NBN (NBS1), RAD50, BRCA1*									
	DNA polymerases	*POLI*									
miR-216	DSBR (HR)	*BRCA1- 216b, DMC1- 216b*	Mouse			✓	↑	↓	↑		
	BER	*MBD4*									
	RAD6 pathway	*UBE2V2*									
miR-320	BER	*TDG*	Human								✓
	DSBR (HR)	*MRE11A- 320a*									
	DSBR (NHEJ)	*XRCC5 (a-d)*									
	Repair of DNA-protein crosslinks	*TDP1 (a-d)*									
	Genes with suspected DNA repair function	*APTX*									
	Genes defective and sensitivity to DNA damaging agents	*FANCF (a-d)*	Mouse	✓	✓	✓	↓	↑	↓		
miR-331	BER	*TDG- 5p*	Mouse			✓	↓	↑	↓		
	DSBR (HR)	*DMC1- 5p, RAD50- 5p*									
	Damage response genes	*CHEK1- 5P*									
	Suspected DNA repair function	*DCLRE1B- 3P*									
miR-335	BER	*PARP1*	Mouse				↓	↑	↓		
	DSBR (HR)	*MRE11A*									
	Suspected DNA repair function	*RECQL5*									
miR-496	DSBR (HR)	*RAD51L3*	Bovine	✓			↑			↑	↓
	BER	*PARP1*	Human								

h) Expression profiles of miRNAs in gametes and embryos and their target mismatch repair, double strand break repair and nucleotide excision repair genes.

miRNA	DNA repair pathways	Target repair mRNA	Species	Oocyte	Sperm	Zygote	2-cell	4-cell	8-cell	Morula	Blastocyst
miR-21	MMR	*MSH2*	Mouse			✓	↓	↑	↑		
	DSBR (HR)	*RAD51L3*	Bovine	✓							
	NER	*RPA2*	Human	✓							✓
miR-129-5p	MMR	*MLH3*	Mouse			✓	↑	↑	↑		
	DSBR (HR)	*RAD51L1, XRCC2*									
	NER	*GTF2H1*									
miR-142-3p	MMR	*MLH3, MSH6*	Mouse			✓	✓	✓	✓		
	NER	*CCNH*									
	DSBR (HR)	*NBN (NBS1), RAD50, RBBP8*									
miR-337	NER	*GTF2H3- 3P*	Mouse			✓	✓	↑	↑		
	DSBR (NHEJ)	*LIG4- 3P*									
	DSBR (HR)	*NBN (NBS1)- 3P*									
	MMR	*MSH3- 5P*									
miR-380-3p	NER	*ERCC6*	Mouse				✓	✓	✓		
	MMR	*MSH4*									
	DSBR (NHEJ)	*XRCC4*									
	RAD6 pathway	*UBE2B*									
	Suspected DNA repair function	*DCLRE1B*									
	Genes defective and sensitivity to DNA damaging agents	*FANCF*									
miR-380-5p	MMR	*MSH4*	Mouse			✓	✓	✓	✓		
	NER	*ERCC6*									
	DSBR (NHEJ)	*XRCC4*									
	RAD6 pathway	*UBE2B*									
	Suspected DNA repair function	*DCLRE1B*									
	Genes defective and sensitivity to DNA damaging agents	*FANCF*	Bovine	✓							

i) Expression profiles of miRNAs in gametes and embryos and their target nucleotide excision repair, base excision repair and double strand break repair genes.

miRNA	DNA repair pathways	Target repair mRNA	Species	Oocyte	Sperm	Zygote	2-cell	4-cell	8-cell	Morula	Blastocyst
miR-29a	NER	*ERCC6*	Mouse			✓	↓	↓	↓		
	BER	*TDG*									
	DSBR (HR)	*MRE11A*									
	Damage response genes	*RAD1*									
miR-29b	NER	*ERCC6*	Mouse			✓	↓	↓	↓		
	DSBR (HR)	*MRE11A*									
	BER	*TDG*	Bovine	✓							
	Damage response genes	*RAD1*									
miR-29c	NER	*ERCC6*	Mouse			✓	↑	↑	↑	↑	
	BER	*TDG*									
	DSBR (HR)	*MRE11A*									
	Damage response genes	*RAD1*									
miR-124a	NER	*RAD23B*	Mouse	✓	✓	✓	↑	↓	↑		
	BER	*APEX2*									
	DSBR (HR)	*RAD51- 124a and b*									
	Damage response genes	*RAD17*	Bovine	✓							
miR-200a	NER	*XPC*	Mouse			✓	↓	↓	↓		
	BER	*PARP2*									
	DSBR (HR)	*BRCA1*									
	Suspected DNA repair function	*RECQL5, XPC*									
	Genes defective and sensitivity to DNA damaging agents	*ATM*									
miR-212	DSBR (HR)	*RAD50, BRCA1*	Mouse			✓	✓	↑	↑		
	NER	*GTF2H1*	Human	✓							
	BER	*NEIL2*									
miR-217	NER	*ERCC6 (CSB), GTF2H2*	Mouse			✓	↑	↓	✓		
	BER	*TDG*									
	DSBR (HR)	*MRE11A*									
	DNA polymerases	*POLH, PCNA*									
	Genes defective and sensitivity to DNA damaging agents	*ATM*									
miR-330	NER	*GTF2H1- 3P*	Mouse			✓	✓	↑	↓		
	BER	*TDG- 3P*									
	DSBR (NHEJ)	*LIF4- 3P*									

j) Expression profiles of miRNAs in gametes and embryos and their target genes involved in all repair pathways; mismatch repair, double strand break repair, nucleotide excision repair and base excision repair genes.

miRNA	DNA repair pathways	Target repair mRNA	Species	Oocyte	Sperm	Zygote	2-cell	4-cell	8-cell	Morula	Blastocyst
	MMR	*MSH3*									
	DSBR (HR)	*RAD51L1*									
miR-136	DNA polymerases	*POLH*	Mouse			✓	✓	✓	✓	↑	↑
	MMR	*MS2*									
miR-210	DSBR (HR)	*RAD52*	Mouse	✓	✓		↑	↑	↓		
	MMR	*MSH4*	Mouse	✓	✓	✓	↓	↓	↑		
miR-182	NER	*ERCC8 (CSA)*	Bovine	✓							
	NER	*ERCC4 (XPF) - 3p*									
	MMR	*MSH6- 3p*									
miR-409	Suspected DNA repair function	*DCLRE1B-3P*	Mouse			✓	↓	↓	↓		
	MMR	*MSH3*									
miR-7	BER	*PARP1*	Mouse			✓	✓	↑	↓		
	DSBR (NHEJ)	*XRCC5*									
miR-31	BER	*PARP1*	Mouse			✓	↓	↓	↓		

k) Expression profiles of miRNAs in gametes and embryos that are not involved in DNA repair.

miRNA	Expression of miRNAs in gametes and preimplantation embryo development								
	Species	Oocyte	Sperm	Zygote	2-cell	4-cell	8-cell	Morula	Blastocyst
miR-7b	Mouse			✓	✓	✓	✓		
miR-16-5p	Mouse			✓					
miR-17	Human								✓
miR-30	Human	✓							
	Bovine	✓							
miR-99a	Mouse	✓	✓	✓	✓	✓	↑		
	Bovine	✓							
miR-99b	Mouse	✓	✓	✓	↑	↑	↑		
miR-122a	Mouse			✓	↑	↑	↓		
	Bovine	✓							
miR-126	Bovine	✓							
miR-126-3p	Mouse			✓	↓	↑	↑		
miR-126-5p	Mouse			✓	↑	↑	↓		
miR-133a	Mouse	✓	✓	✓	↑	↑	↑		
miR-133b	Mouse			✓	✓	✓	↑		
miR-184	Mouse	✓	✓	✓	↓	↓	↑		
miR-187	Mouse			✓	↑	↑	↓		
miR-189	Mouse			✓	✓	✓	✓		
miR-196a	Mouse			✓	↓	↑	↑		
miR-196b	Mouse			✓	✓	↑	↑		
miR-201	Mouse			✓	✓	✓	✓		
miR-202	Mouse			✓	↑	↓	↑		
miR-202-5p	Bovine	✓							
miR-205	Mouse			✓	↓	↓	↑		
	Bovine	✓							
miR-206c	Mouse	✓	✓	✓	↓	↓	↑		
	Bovine	✓							
miR-207	Mouse			✓	↓	↑	↓		
	Bovine	✓							
miR-213	Mouse			✓	✓	✓	✓		
miR-214	Mouse	✓	✓	✓	↓	↓	↓		
	Bovine	✓							
miR-290	Mouse			✓	↓	↑	↑	↑	↑
miR-290-5p	Bovine	✓							
miR-291-5p	Mouse				↑	↑	↑		
miR-292-3p	Mouse			✓	↓	↑	↑		
	Bovine	✓							
miR-292-5p	Mouse			✓	↑	↑	↑	↑	
miR-293	Mouse			✓	↓	↑	↑		
miR-294	Mouse			✓	↓	↑	↑		
miR-295	Mouse			✓	↓	↑	↑		
miR-322-3p	Mouse			✓	↑	↓	↑		
miR-322-5p	Mouse			✓	↑	↑	↑		
miR-324-5p	Mouse			✓	↓	↑	↓		
miR-325	Mouse				✓	✓	✓		
miR-326	Mouse			✓	↓	↑	↑		
miR-329	Mouse	✓	✓	✓	↑	↓	↑		
	Bovine	✓							

miRNA	Expression of miRNAs in gametes and preimplantation embryo development								
	Species	Oocyte	Sperm	Zygote	2-cell	4-cell	8-cell	Morula	Blastocyst
miR-339	Mouse			✓	↓	↑	↑		
	Bovine	✓							
miR-339-5p	Human	✓							
miR-344	Mouse			✓	✓	↑	↑		
miR-346	Mouse			✓	↑	↓	↓		
miR-350	Mouse			✓	↑	↑	↓		
miR-351	Mouse			✓	↑	↑	↑		
miR-371-3p	Human								✓
miR-374	Human								✓
miR-375	Mouse		✓	✓	✓	✓	✓		
	Bovine	✓							
miR-411	Mouse			✓	↓	↓	✓		
	Bovine	✓							
miR-455-3p	Bovine	✓							
miR-467a	Bovine	✓							
miR-470	Bovine	✓							
miR-484	Bovine	✓							
	Human								✓
miR-486-5p	Human	✓							
miR-512-5p	Bovine	✓							
miR-517	Human								✓
miR-518b	Bovine	✓							
miR-541	Bovine	✓							
miR-542-5p	Bovine	✓							
miR-547	Bovine	✓							
miR-602	Human	✓							
miR-638	Bovine	✓							
miR-662	Human	✓							
miR-663	Bovine	✓							
miR-705	Bovine	✓							
miR-709	Bovine	✓							
miR-712	Bovine	✓							
miR-720	Human								✓
miR-721	Bovine	✓							✓
miR-768	Human	✓							
miR-762	Bovine	✓							✓
miR-886-3p	Human								✓
miR-923	Bovine	✓							
miR-939	Bovine	✓							
miR-1228-3p	Bovine	✓							
miR-1274	Human								✓
	Bovine	✓							
miR-1275	Bovine	✓							
	Human								✓
miR-1280	Bovine	✓							
miR-1308	Bovine	✓							
miR-1826	Bovine	✓							

7.2 Appendix to materials and methods

7.2.1 Differential gene expression in preimplantation embryos and potential relation with differential methylation

7.2.1.1 Oligonucleotides

Primer names, sequences, chromosomal locations and PCR product sizes that are used for sequencing to identify informative SNPs for differential gene expression analysis in embryos are listed. Sequences were obtained from Ensembl; *ACTB* (ENSG00000075624, Ensembl release 60), *GAPDH* (ENSG00000111640, Ensembl release 60), *SNRPN* (ENSG00000128739, Ensembl release 60), *UBE3A* (ENSG00000114062, Ensembl release 60), *IGF2* (ENSG00000167244, Ensembl release 60), *H19* (ENSG00000130600, Ensembl release 60) and *BRCA1* (ENSG00000012048, Ensembl release 60) on the Ensembl genome browser.

a) Primer information used for sequencing

Primer	Primer sequence	Chromosome : Locus	Product size (bp)
ACTBex7 F	5'-AACACTGGCTCGTGTGACAA-3'	7:5568239: 5568860	236
ACTBex7 R	5'-GGGGTGTTGAAGGTCTCAAA-3'		
ACTBex7b F	5'-GTTGCTATCCAGGCTGTGCT-3'	7:5567732: 5568351	283
ACTBex7b R	5'-CCATCTCTTGCTCGAAGTCC-3'		
ACTBex7c F	5'-CGACCAGTGTTTGCCTTTTA-3'	7:5568839: 5569758	356
ACTBex7c R	5'-AGGGCGCTTTCTCTGCAC-3'		
ACTBex8 F	5'-ATCATTGCTCCTCCTGAGC-3'	7:5566729: 5567648	495
ACTBex8 R	5'-TGTGGACTTGGGAGAGGACT-3'		
GAPDHex6 F	5'-AAGGGCCCTGACAACTCTTT-3'	12:6646936: 6647855	245
GAPDHex6 R	5'-CTTGACACAAGCCCAGCTTC-3'		
UBE3Aex9a F	5'-TCTGCTGCTGCTATGGAAGA-3'	15:25616110:25616729	326
UBE3Aex9a R	5'-GGCAAAGCCATTTCCAGATA-3'		
UBE3Aex9b F	5'-TCAATAAACCAAACTTTTTGAATG-3'	15:25618171:25619191	355
UBE3Aex9b R	5'-GAATGCAGTGGCACCATTT-3'		
UBE3Aex9c F	5'-ACATTGTATAGCCCCACAGATT-3'	15:25582800:25583423	335
UBE3Aex9c R	5'-AACAAATCATCAGGTTGATCTACAG-3'		

UBE3Aex16 F	5'-TGGCTACTGTGCCTTGTGTT-3'	15:25582163:25583382	438
UBE3Aex16 R	5'-TGCATTTTTCCTGCCAATTT-3'		
UBE3Aex16b F	5'-CCATCACGTATGCCAAAGG-3'	15:25583715:25584335	304
UBE3Aex16b R	5'-TGTAACACTTTCACGCAAAAA-3'		
SNRPNex6 F	5'-ATAATTTGTCGGGCCAACCT-3'	15:25154649:25155271	287
SNRPNex6 R	5'-TGGGGTTTGTTAAAGTTGTTAAG-3'		
SNRPNex6b F	5'- AGCACATGTAATCGGCAACA-3'	15:25154085:25155305	287
SNRPNex6b R	5'- AGGTTGGCCCGACAAATTAT-3'		
SNRPNex12 F	5'- CCTCTGCAGGCTCCATCTAC-3'	15:25219149:25219768	151
SNRPNex12 R	5'- ATTGCTGTTCCACCAAATCC-3'		
SNRPNex13 F	5'-TTGAGTATCAGCTGAAGATGAGC-3'	15:25219748:25220368	329
SNRPNex13 R	5'-TGGTGGAATCATGACCAAAA-3'		
SNRPNex17 F	5'-TGCATCGCTTTGACTGTTTC-3'	15:25222786:25223411	222
SNRPNex17 R	5'-TCTCATCAGAGATTCAAGTTCGTC-3'		
SNRPNex18 F	5'-CCACCAAGACCTTAGCATACTG-3'	15:25223502:25224126	250
SNRPNex18 R	5'-TGATTTGAATCAACTGCTTAATAGG-3'		
IGF2 F	5'-CCTTCAGCCTGCCTCAGC-3'	11:2181930:2182552	238
IGF2 R	5'-CCTGCAGGTCCTCTGCCT-3'		
IGF2ex11 F	5'-GACAACTTCCCCAGATACCC-3'	112153834:2154753	370
IGF2ex11 R	5'-GGACTGGGTCAGGAGAAGC-3'		
H19a F	5'- GTTTCCCCCGTCCCTTCT-3'	112015815:2017038	327
H19a R	5'-CAGTGTTTATTGATGATGAGTCCA-3'		
H19b F	5'-TTACTTCCTCCACGGAGTCG-3'	112016950:2017675	340
H19b R	5'-GACACGTGGGTGGGATGG-3'		
BRCA1ex9F	5'-CTCTTCAGGAGGAAAAGCACA-3'	17:41251643:41252263	287
BRCA1ex9R	5'-ACTTCCCAAAGCTGCCTACC-3'		
BRCA1ex11a F	5'-GGGTTTTGCAAACTGAAAGA-3'	17:41244732:41245353	269
BRCA1ex11a R	5'-TGGTTAACTTCATGTCCCAATG-3'		
BRCA1ex11b F	5'-AAGGCTGAATTCTGTAATAAAAGC-3'	17:41246324:41246947	250
BRCA1ex11b R	5'-TCACTTCTGGAAAACCACTCA-3'		
BRCA1ex11c F	5’-CAAAAGCACCTAAAAAGAATAGGC-3’	17:41245094:41245719	347
BRCA1ex11c R	5’-AAGTTCACTGGTATTTGAACACTTAG-3’		
BRCA1ex11d F	5’-CATTGGGACATGAAGTTAACCA-3’	17:41244430:41245653	364
BRCA1ex11d R	5'-CAAAACCTAGAGCCTCCTTTGA-3'		
BRCA1ex11e F	5'-TCAAAGGAGGCTCTAGGTTTTG-3'	17:41244039:41244860	373
BRCA1ex11e R	5'-GCTTGAATGTTTTCATCACTGG-3'		
BRCA1ex11f F	5'-TGATGGTGAAATAAAGGAAGATACT-3'	17:41243559:41244383	356

BRCA1ex11f R	5'-CCTGGTTACTGCAGTCATTTAAG-3'		
BRCA1ex12 F	5'-TCATTTAATGGAAAGCTTCTCAAAG-3'	17:41234330:41234954	290
BRCA1ex12 R	5'-AAAGGGGAAGGAAAGAATTTTG-3'		
BRCA12RNAonlyF	5'-AGCAGGAAATGGCTGAACTA-3'	17:41234126:41234745	130
BRCA12RNAonlyR	5'-TCTGATGTGCTTTGTTCTGG-3'		
BRCA1ex15 F	5'- AATTGGTGGCGATGGTTTT -3'	17:41226016:41226638	290
BRCA1ex15 R	5'- TGTTTGTTCCAATACAGCAGATG-3'		
BRCA1ex17 F	5'- AATTGGTGGCGATGGTTTT -3'	17:41222715:41223334	175
BRCA1ex17 F	5'-AATTCTGGCTTCTCCCTGCT -3'		
BRCA1ex18 F	5'-TAACTAGTATTCTGAGCTGTGTGCT-3'	17:4280654:4281875	290
BRCA1ex18 R	5'- AGTGATTCTCCTGCCTCAGC -3'		
BRCA1ex9 F	5'-CTCTTCAGGAGGAAAAGCACA-3'	17:41251643:41252263	290
BRCA1ex9 R	5'-ACTTCCCAAAGCTGCCTACC-3'		

b) Annealing sites of the primers used for determining the differential allele expression. The primer IDs as listed in table 7.2.2.1.a are shown for each region. Yellow and red coloured regions represent the primer annealing sites. Salmon-coloured regions indicate the position of exons. Highlighted letters other than the four bases (A, C, T or G) represent the SNPs. These annealing sites were obtained from Ensembl for each region with the Ensembl release: *ACTB* (ENSG00000075624, Ensembl release 60), *GAPDH* (ENSG00000111640, Ensembl release 60), *SNRPN* (ENSG00000128739, Ensembl release 60), *UBE3A* (ENSG00000114062, Ensembl release 60), *IGF2* (ENSG00000167244, Ensembl release 60), *H19* (ENSG00000130600, Ensembl release 60) and *BRCA1* (ENSG00000012048, Ensembl release 60) on the Ensembl genome browser.

ACTB (ENSG00000075624): ACTB_a in yellow, ACTB_b in red.

```
5568915 CGACATGGAGAAAATCTGGCACCACACCTTCTACAATGAGCTGCGTGKGSCKYCCSAGGA 5568856
5568855 GCACCCCGTGCTGCTGACCGAGGCCCCCCTGAACCCCAAGGCCAACCGCGAGAAGATGAC 5568796
5568795 CCAGGTGAGTGGCCCGCTAYCTCTTCTGGTGGCSGCCTCCCTCCTTCCTGGCCTCCCGGA 5568736
```

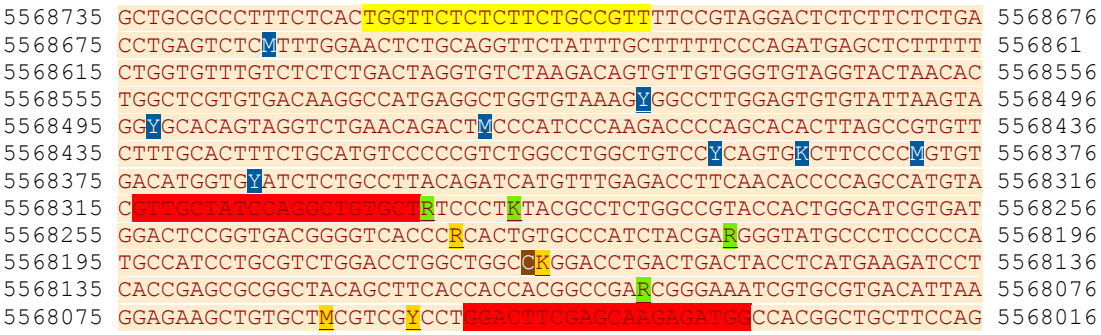

ACTB (ENSG00000075624): ACTBc

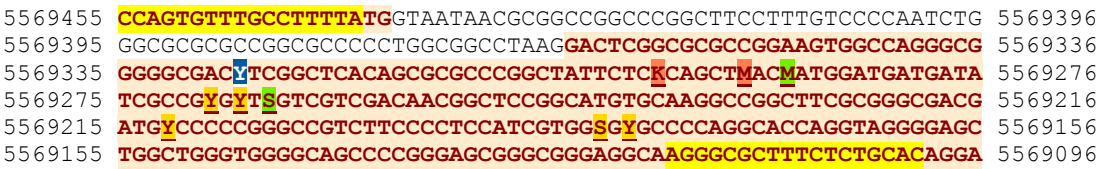

ACTB (ENSG00000075624): ACTBex8

GAPDH (ENSG00000111640): GAPDHex6

BRCA1 (ENSG00000012048): BRCA1ex9

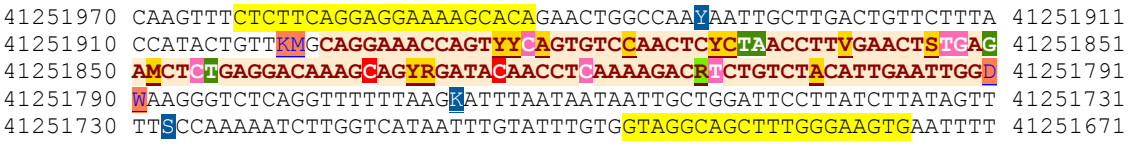

BRCA1 (ENSG00000012048): BRCA1ex11a

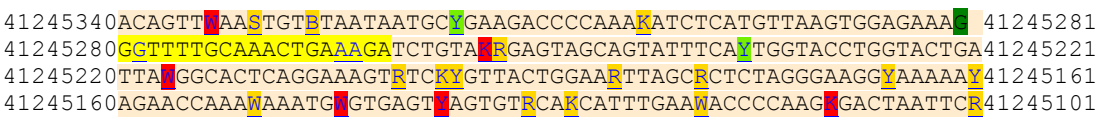

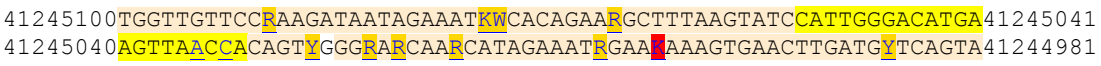

BRCA1 (ENSG00000012048): BRCA1ex11b

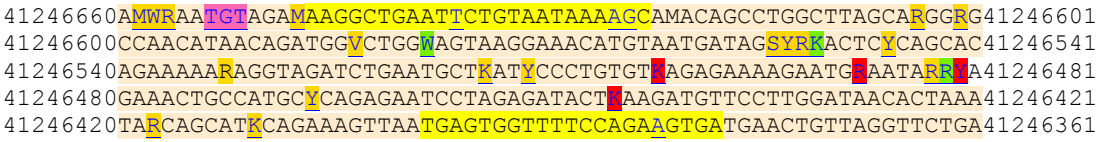

BRCA1 (ENSG00000012048): BRCA1ex11c

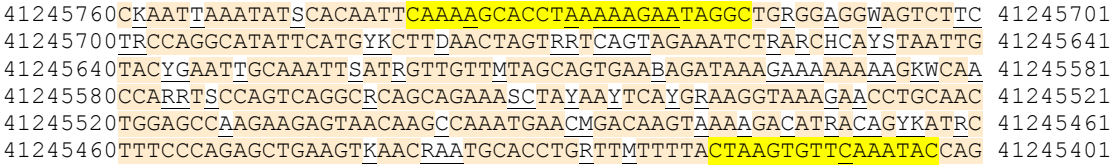

BRCA1 (ENSG00000012048): BRCA1ex11d

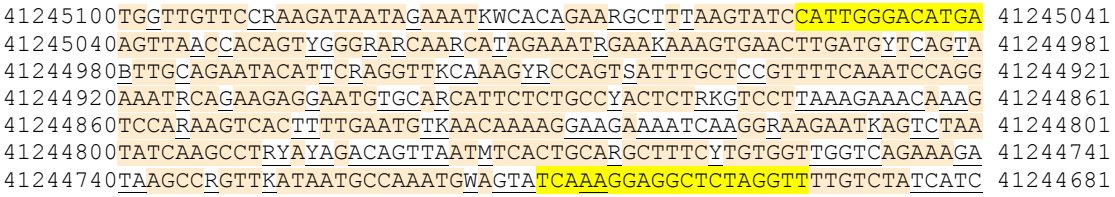

BRCA1 (ENSG00000012048): BRCA1ex11e

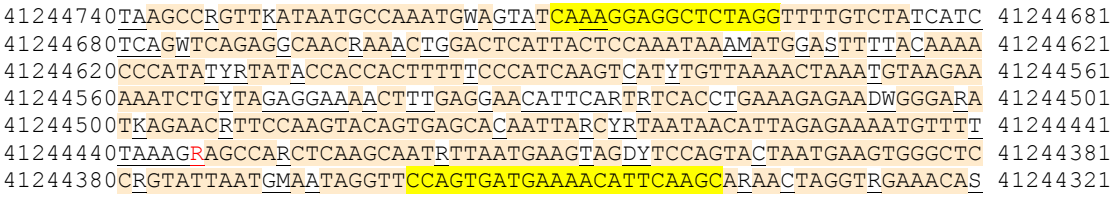

BRCA1 (ENSG00000012048): BRCA1ex11f

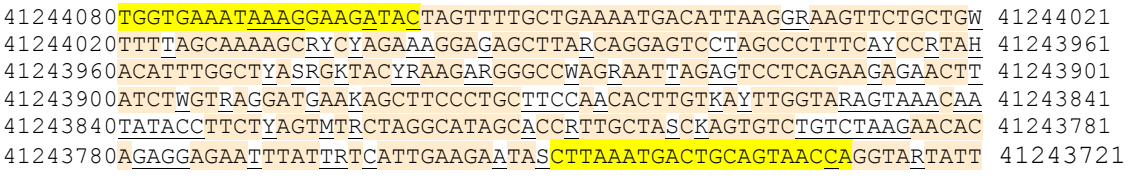

BRCA1 (ENSG00000012048): *BRCA1*ex12 in yellow and *BRCA1*ex12_RNAonly in red

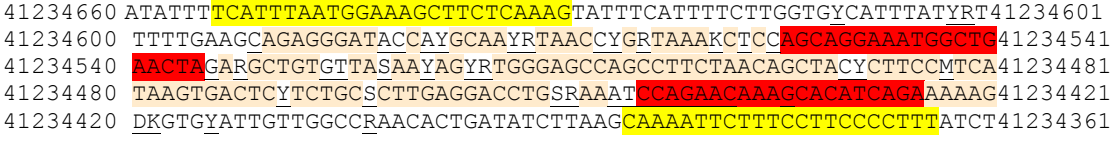

BRCA1 (ENSG00000012048): BRCA1ex15

BRCA1 (ENSG00000012048): BRCA1ex17

BRCA1 (ENSG00000012048): BRCA1ex18

SNRPN (ENSG00000128739): SNRPNex6

SNRPN (ENSG00000128739): SNRPNex6b

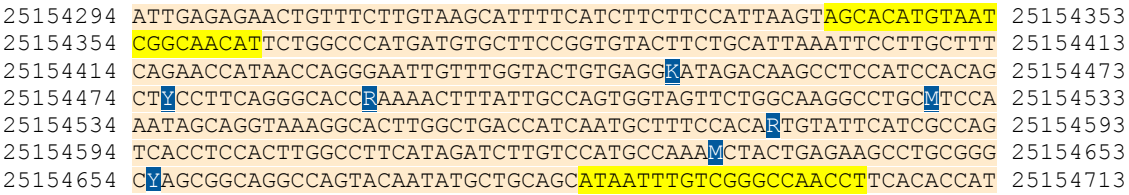

SNRPN (ENSG00000128739): SNRPNex12

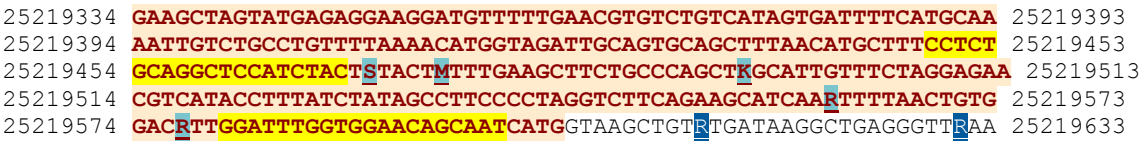

SNRPN (ENSG00000128739): SNRPNex13

SNRPN (ENSG00000128739): SNRPNex17

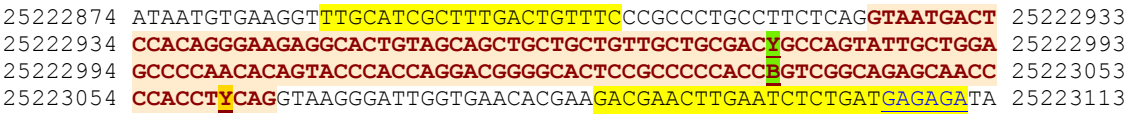

SNRPN (ENSG00000128739): SNRPNex18

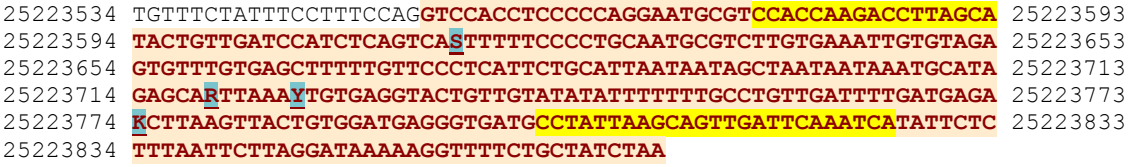

UBE3A (ENSG00000114062): UBE3Aex9a forward in yellow, a reverse and b forward in yellow and b reverse in red

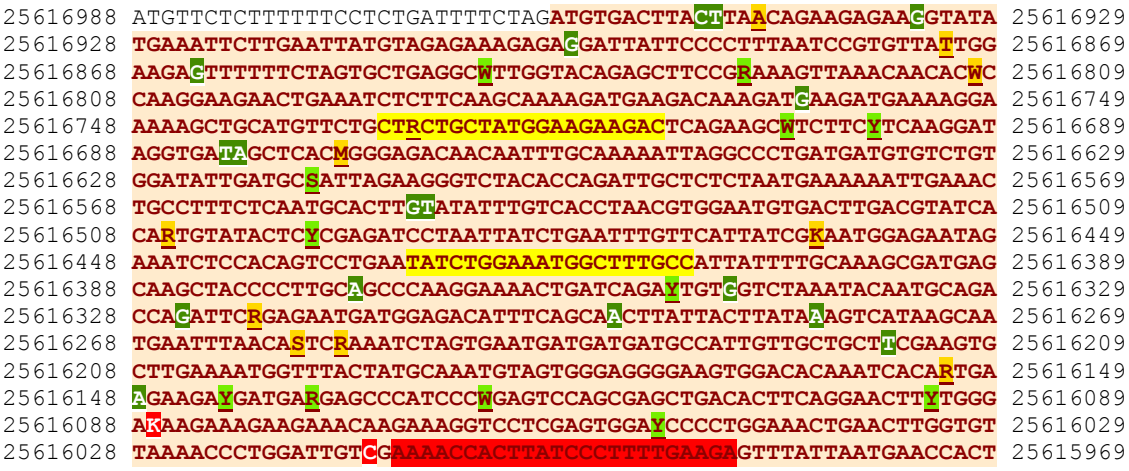

UBE3A (ENSG00000114062): UBE3Aex9c

UBE3A (ENSG00000114062): UBE3Aex16

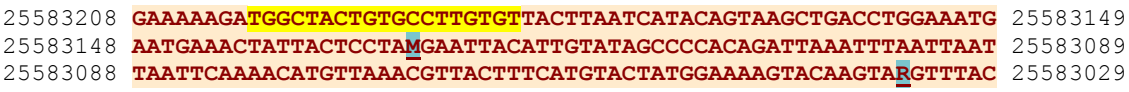

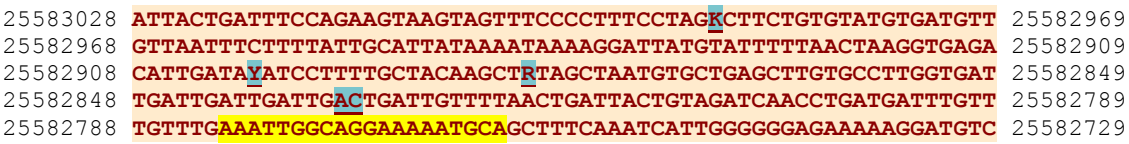

UBE3A (ENSG00000114062): UBE3Aex16b

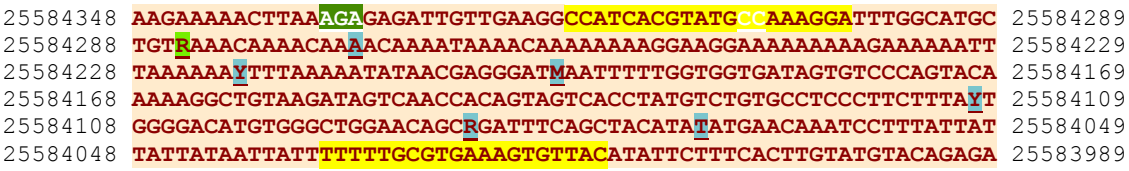

IGF2 (ENSG00000167244): IGF2

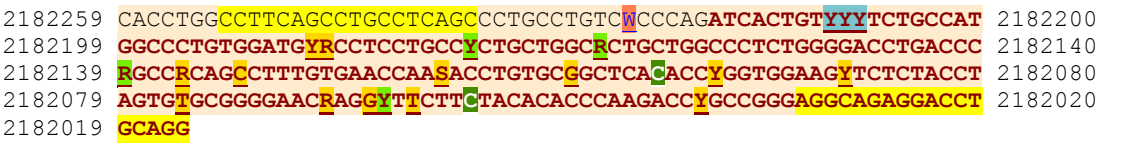

IGF2 (ENSG00000167244): IGF2ex11

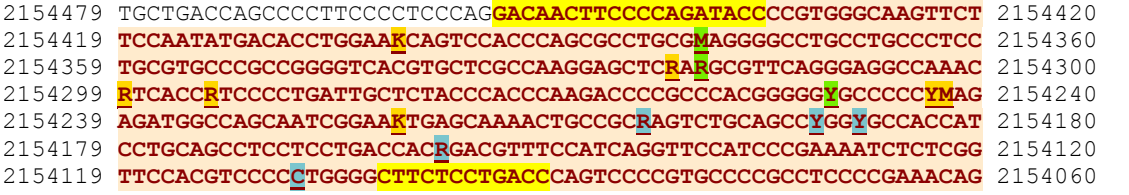

H19 (ENSG00000130600): H19a

H19 (ENSG00000130600): H19b

c) Sequences of primers used in mini-sequencing analysis to identify differential gene expression in embryos.

Primer	Chromosome	Primer sequence
MS_BRCAex11e_rs16941	17	5'-CATTAGAGAAAATGTTTTTAAAAG-3'
MS_BRCAex12_rs1060915	17	5'-CCCTTCCATCATAAGTGACTC-3'
MS_ACTBex7_rs852423	7	5'-CATTGTTTCTAGGAGAACC-3'
MS_SNRPNe12_rs75184959	15	5'-ATGATCTGTAAGGCAGAGAT-3'
MS_H19_rs11542721	11	5'-CACCTTGGCAAGTGCCTG-3'

d) Primer IDs, sequences, chromosomal locations, fluorescent labels, type of repeats and PCR product sizes that are used for aneuploidy analysis for differential gene expression study (Ensembl release dates 59). FAM stands for 6-carboxyfluorescein, YY for yakima yellow and DO for dragonfly orange.

List of informative markers used in this study:

Primer name	Primer sequence	Chromosome: Primer location on chromosome (bp)	Fluorescent label	Type of repeat	Product range (bp)
D7S2420_F D7S2420_R	CCTGTATGGAGGGCAAACTA AAATAATGACTGAGGCTCAAAACA	7: 106889627:106890251	FAM	Dinucleotide	240-292
D7S2459_F D7S2459_R	AAGAAGTGCATTGAGACTCC CCGCCTTAGTAAAACCC	7: 107331201:107331820	FAM	Dinucleotide	140 - 152
D7S486_F D7S486_R	AAAGGCCAATGGTATATCCC GCCCAGGTGATTGATAGTGC	7: 115894462:115895081	FAM	Dinucleotide	110-142
D11S1338_F D11S1338_R	GGAAAGAGTAGGAATAAGATGGTGTC TGCTACTTATTTGGAGTGTGAATTT	11: 5987706:5988331	FAM	Dinucleotide	210-224
D11S1997_F D11S1997_R	CCAATTGACAGTGGATTTTTGA CATAAAAGGGCCCGATACAA	11: 6357947:6358568	YY	Trinucleotide	176-196
D11S4174_F	ACCAGGGCCTTTTTACAC	11: 84529968:84530594	DO	Dinucleotide	227 - 249

D11S4174_R	ATCATAGACTTCAGAGTCAGGTAGA				
D15SS992_F D15S992_R	ACAGATAAACGGCAGGGAGA AGGAGGGCCACCTTGATAGT	15: 48,700,502:48,937,984	FAM	Dinucleotide	216-235
D15S123_F D15S123_R	TTTTCATGCCACCAACAAAC CTGAACCCAATGGACTCCTG	15: 48,700,502:48,937,984	FAM	Dinucleotide	182-198
D15S94_F	TGTTGGCTTAGAAACTGACTGG	15:	FAM	Dinucleotide	140-151
D15S94_R	GCTGCATTCCAGCCTAAAAG	48,700,502:48,937,984			
D17S579_F D17S579_R	CAGATCACAGAGGTGGCTGA GGCAGCAGTCCTGTAGACAA	17: 42806716:42807335	FAM	Dinucleotide	230-250
D17S1789_F D17S1789_R	GGCTCAGGAGACTCAGAGGA GAGCCAAACTGCTTTGTTCC	17: 41,196,312:41,277,387	FAM	Dinucleotide	195-239
D17S1353_F D17S1353_R	CTGAGGCACGAGAATTGCAC TACTATTCAGCCCGAGGTGC	17: 7617123:7617742	DO	Dinucleotide	200-222
D17S841_F D17S841_R	TGGACTTTCTTACATGGCAG AGGTTAGTAGTCTATGTCACAGCG	17: 27542413:27543036	DO	Dinucleotide	253-273
D19S112_F D19S112_R	GCCAGCCATTCAGTCATTTGAAG CTGAAAGACACGTCACACTGGT	19: 46378681:46379303	DO	Dinucleotide	110-130
APOC2_F	GGCTACATAGCGAGACTCCATCTCC	19:	FAM	Dinucleotide	136-156

APOC2_R	GGGAGAGGGCAAAGATCGATAAAGC	45449076:45449700

List of primers that were tested but found to be uninformative for the couples:

Primer name	Primer sequence	Chromosome: Primer location on chromosome (bp)	Fluorescent label	Type of repeat	Product range (bp)
D7S692_F	CTGATGATTGCTATAGATATTCATC	7: 108339409:108340033	DO	Dinucleotide	161-171
D7S692_R	TGTAAACACTTTTGTAGAAGAACCT				
D11S4891_F	TTTATTCCAGCCCCACTGAC	11: 5250626:5251245	FAM	Dinucleotide	160-170
D11S4891_R	TACCCAGACTAGGGCCATTC				
D11S2362_F	GGCTTTACCTTACCCCATTTC	11: 4911823: 4912443	DO	Trinucleotide	140-157
D11S2362_R	GGGGTTTCCCAGTCCTTTTA				
D11S1303_F	TGTTGGATGAAGTAATACTGG	11: 51382534: 51383154	VIC	Quadnucleotide	241-261
D11S1303_R	CTGCACTCCCATATGAACTG				
D11S1763_F	CCTTGGCCTCCCACTTACTT	11: 42861098:42861717	FAM	Di nucleotide	240-270
D11S1763_R	TCTTTAGGGGTGGTGGTGAG				
D11S1871_F	TCTGGGAAAGCATGAAGTGA	11: 5126600: 5127219	FAM	Dinucleotide	218-238
D11S1871_R	GCAGAAGAAGTTGCCCTGAT				

D11S1760_F	GGAAGAAAGAGACCCTGAGTG	11: 5384045:5384665	FAM	Dinucleotide	210-225
D11S1760_R	CTGCTGCATCATGACTTGAAA				
D11S2362_F	GGCTTTACCTTACCCCATTTC	11: 4911823:4912443	DO	Trinucleotide	140-150
D11S2362_R	GGGGTTTCCCAGTCCTTTTA				
D11S4174_F	CACCCCTTCAATACCCACTG	11: 45257828:45258447	DO	Dinucleotide	210-230
D11S4174_R	TTCCTGGCCAGCCTATCTAA				
D15S978_F	CTGGCCCCTTCTACTCACAC	15: 48,700,502:48,937,984	FAM	Dinucleotide	163-189
D15S978_R	GGAAAGTGCTGCTGACCTG				
D15S1024_F	CTCCACACTAGCCCACCTCT	15: 48,700,502: 48,937,984	FAM	Dinucleotide	202-212
D15S1024_R	AGGCTATTGTGTGGCTCCAA				
D15S1025_F	CCACGTTAACTGTTCGGTTC	15: 69403189:69403810	FAM	Dinucleotide	88-114
D15S1025_R	CCCAATGTTGCTTTAAAATTGT				
D17S250_F	GGAAGAATCAAATAGACAAT	17: 37151924:37152543	VIC	Dinucleotide	133-153
D17S250_R	GCTGGCCATATATATATTTAAACC				
D17S1307_F	AATAGACTCCAAACCAGCCTATG	17: 49297919:49298542	YY	Dinucleotide	138-150
D17S1307_R	CCTCATCTACTCCTTCAAACAGAC				

D17S1323_F D17S1323_R	TGTTCCCGATAGGAGATGGA TTGAAGCAACTTTGCAATGAG	17: 41237881:41238502	DO	Dinucleotide	142-162
D17S1327_F D17S1327_R	CTCCTCCCCTTACTCCTGCT TGAAAGACAGACTCTGGGTGA	17: 41375142:41375761	YY	Dinucleotide	100-116
D17S261_F D17S261_R	CTCCACCTAGGCACTGAAGC ACAGCCCAAATCCAAGTCAG	17: 15359531:15360150	FAM	Dinucleotide	241-255
D17S122_F D17S122_R	CAGAACCACAAAATGTCTTGC CAGACCAGGCTCTGCTCTACT	17: 15209045:15209665	FAM	Di nucleotide	150-165
D17S1802_F D17S1802_R	AAGACACATGGCCAACTTCC CGAAGGGAGTGCGAGTATGT	17: 40353097:40353716	FAM	Dinucleotide	179-199
17S1789_F D17S1789_R	GGCTCAGGAGACTCAGAGGA GAGCCAAACTGCTTTGTTCC	17: 41752716:41753336	FAM	Dinucleotide	255-270
D17S1356_F D17S1356_R	GGGTGTGGCTTTCTTATCCA CCCCTTTTCATGCAGAGTTT	17: 14894452:14895073	FAM	Dinucleotide	258-175
D17S839_F D17S839_R	CCTTGAGAGAGACCCTGGAA CTGAGCAACAACAGCGAAAC	17: 14484974:14485593	FAM	Dinucleotide	129-150
D17S1166_F	TAACAATTGTGGAACTGCAGCA ATTATT	17: 29648716:29649343	YY	Dinucleotide	189-214

D17S1166_R	CCCATACCTAGTTCTTAAAGTCTGT				
D17S1294_F	TGGCATGCAATTGTAGTCTC	17: 28382106:28382730	FAM	Dinucleotide	244-252
D17S1294_R	TTCTTTCCTTACTAAGTTGAGAACG				
D17S2229_F	CCCATTCCATAGTCATCAGA	17: 15059030:15059649	FAM	Dinucleotide	258-278
D17S2229_R	GTGTCTTTGCCATTTTACCACAAGAGG				
D17S1793_F	AAGAATCCAGCCCAAGGTTT	17: 40359098:40359717	FAM	Dinucleotide	243-260
D17S1793_R	GATCGGCCAAAAGATGAAGT				

e) Primer IDs, sequences and PCR product sizes that are used for methylation specific PCR.

Primer name	Primer sequence	Expected product size (bp)
ACTBpromoter_outer_F	GATTTGATTGATTATT TTATGAAGAT TTTT	210
ACTBpromoter_outer_R	CTCATTACCAATAATAGATAACCTA	
ACTBpromoter_methylated_F	CGCGGTTATAGTTTTATTATTACGG TCGAG	96
ACTBpromoter_methylated_R	ACCATCTCTTACTCGAAATCCAAAA CGACG	
ACTBpromoter_unmethylated_ F	TGTGGTTATA GTTTTATTAT TATGGTTGAG	120
ACTBpromoter_unmetylated_R	ACCATCAAACAACTCATAACTCTTC TCCAA	
H19promoter_outer_F	GGTTTTTAGATAGGAAAGTGGT	185
H19promoter_outer_R	AATAAAATACTAAAAAACAAAAAAA AATAC	
H19promoter_ unmethylated_F	TTGTGAATGGGATTGGGGTGTTTA GTGGTT	124
H19promoter_ unmethylated_R	CACAAACCCCCTAATAAACACAATA CC	
H19promoter_methylated_F	GATCGGGGTGTTTAGCGGTTGTGG GGATTT	134
H19promoter_ methylated_R	CGCAAACCCCCTAATAAACGCGAT ACC	
BRCA1promoter_outer_F	TTTTTTTATTTTTTGATTGTATTTTG ATTT	184
BRCA1promoter_R	TTATCTAAAAAACCCCACAACCTAT CCCCC	
BRCA1promoter_unmethylated _F	TTGGTTTTTGTGGTAATGGAAAAGT GT	86
BRCA1promoter_unmethylated _R	CAAAAAATCTCAACAAACTCACACC A	
BRCA1promoter_methylated_F	TCGTGGTAACGGAAAAGCGCGGG AATTA	75
BRCA1promoter_methylated_R	AAATCTCAACGAACTCACGCCGCG CAATCG	

7.2.1.2 Developing a functional assay for MMR

a) Chromosomal location of the synthetic oligonucleotides (A, G and T sequences) used for the formation of homo/heteroduplexes. The sequences were selected from *MSH2* gene (human chromosomes 2, 2p22-p21, Ensembl release 59) around SNP site rs1981929. The sequence of the oligonucleotides used to make the homo/heteroduplexes is highlighted in grey. Salmon-coloured regions represent the exons. The underlined, red "R" represents the SNP that the A and G alleles were substituted to create the A and G sequences, respectively. T allele was substituted to the same position of the SNP "R" within the complementary strand.

MSH2 (ENSG00000095002, Ensembl release 59)

47672468 GGGAAGCWTTGAGTGCTACATCATCTCCCTTTCTATAAAATAAATTGAGTACGAAACAAT 47672527
47672528 TTGAATTAAAACACCTGAGTAAATAGTAACTTTGGAGACCTRCTGTACTATTTGTACCTT 47672587
47672588 TTGGATCAAATGATGCTTGTTTATCTCAGTCAAAATTTTATGATTTGTATTCTGTAAAAT 47672647
47672648 GAGATCTTTTTATTTGTTTGTTTTACTACTTTCTTTTAGGAAAACACCAGAAATTATTGT 47672707

b) Annealing sites of the primers used for mini-sequencing to detect the SNP at rs1981929. The annealing sites for the primers are shown in aqua and green shades representing the "Forward A" binding to the A and G sequences and "Reverse T" binding to the T sequence, respectively.

MSH2 (ENSG00000095002, Ensembl release 59)

42961 GGGAAGCTTTGAGTGCTACATCATCTCCCTTTCTATAAAATAAATTGAGTACGAAACAAT 43020
43021 TTGAATTAAAACACCTGAGTAAATAGTAACTTTGGAGACCTRCTGTACTATTTGTACCTT 43080
43081 TTGGATCAAATGATGCTTGTTTATCTCAGTCAAAATTTTATGATTTGTATTCTGTAAAAT 43140
43141 GAGATCTTTTTATTTGTTTGTTTTACTACTTTCTTTTAGGAAAACACCAGAAATTATTGT 43200
43201 TGGCAGTTTTTGTGACTCCTCTTACTGATCTTCGTTCTGACTTCTCCAAGTTTCAGGAAA 43260
43261 TGATAGAAACAACTTTAGATATGGATCAGGTATGCAATATACTTTTTAATTTAAGCAGTA 43320

7.3 Appendix to results

7.3.1 Differential gene expression in preimplantation embryos and potential relation with differential methylation

7.3.1.1 Sequencing panels obtained from genetic analyser ABI Prism™ 3100.

Each peak represents the amplified alleles where red, green, black and blue represent T, A, G and C alleles, respectively. The informative SNPs are shown.

Sequencing panels for *ACTB*

Female partner of couple 29

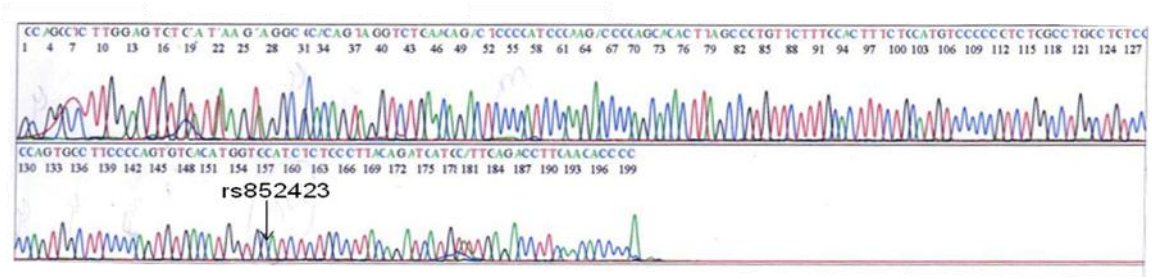

Male partner of couple 29

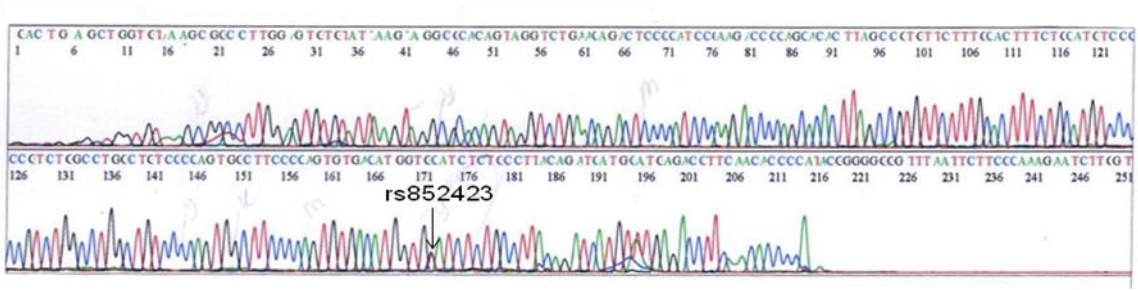

Female partner of couple 32

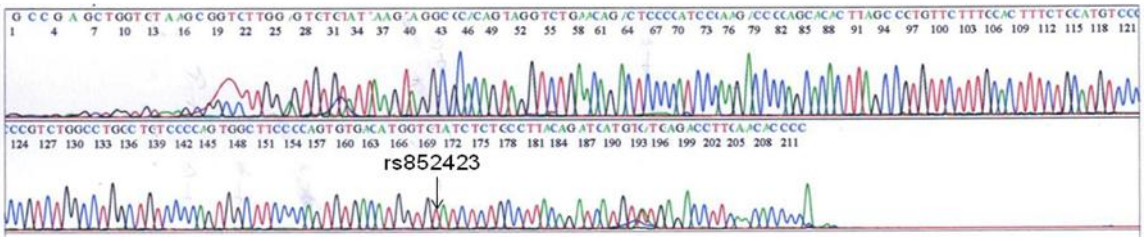

Male partner of couple 32

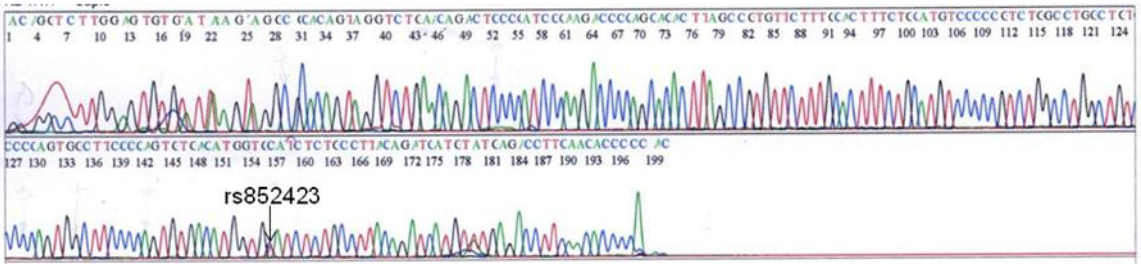

Female partner of couple 33

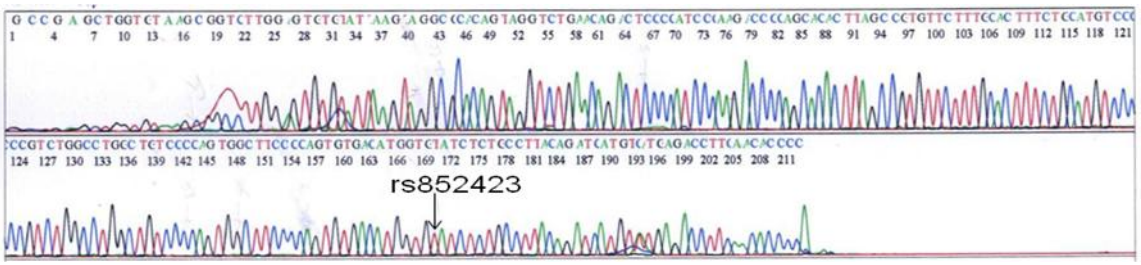

Male partner of couple 33

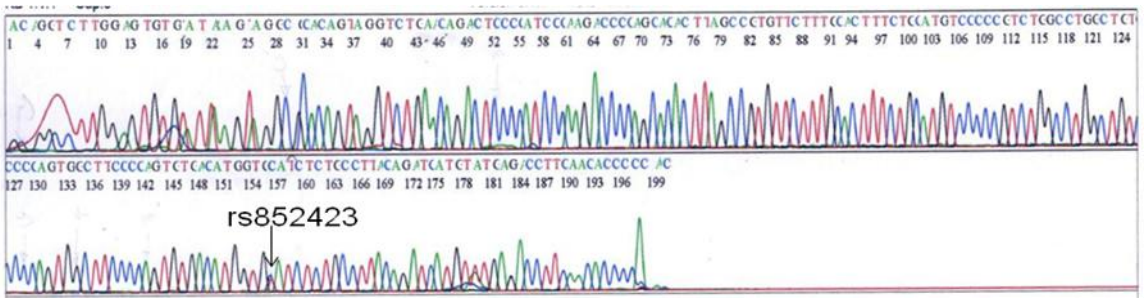

Sequencing panels for *SNRPN*

Female partner of couple 29

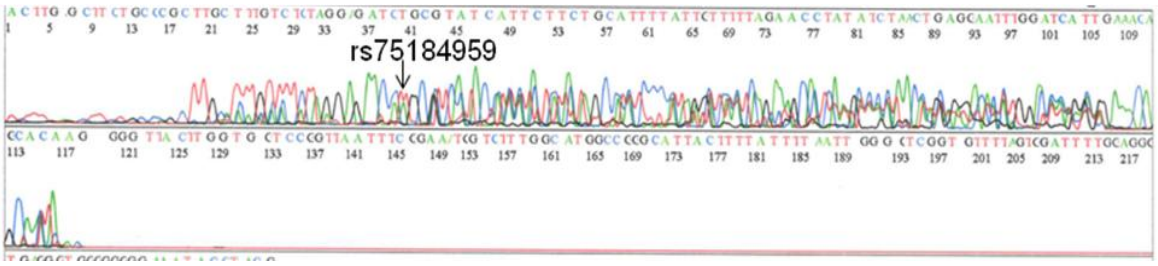

Male partner of couple 29

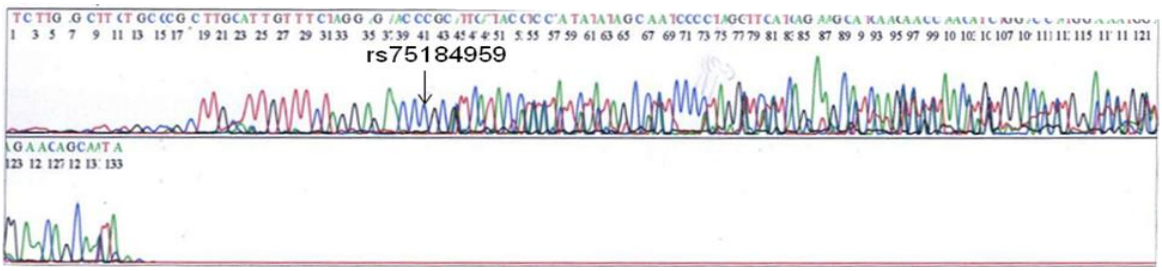

Female partner of couple 30

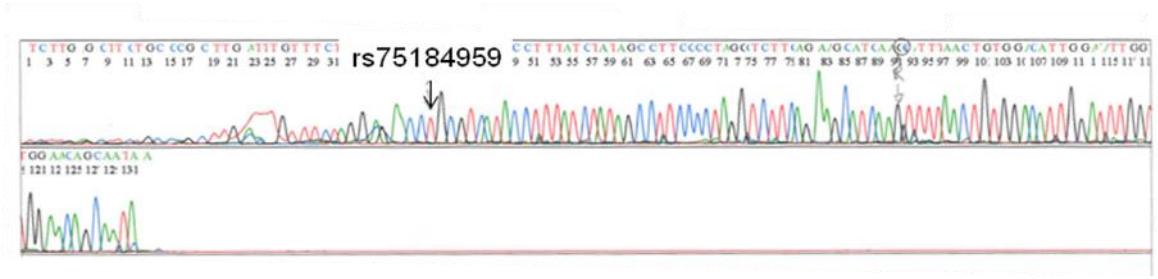

Male partner of couple 30

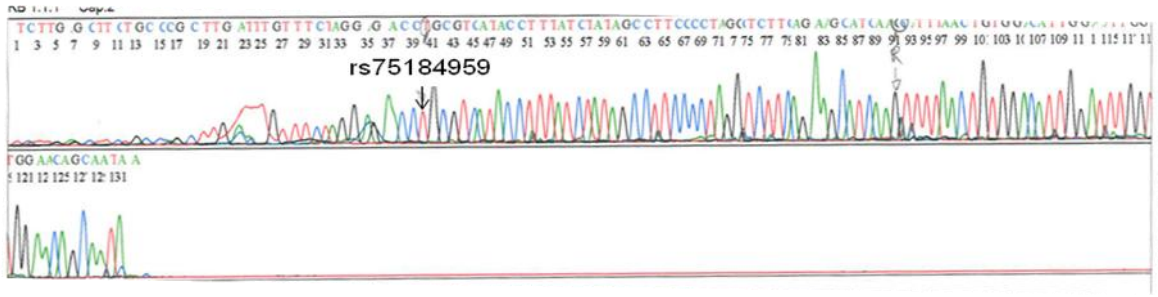

Female partner of couple 33

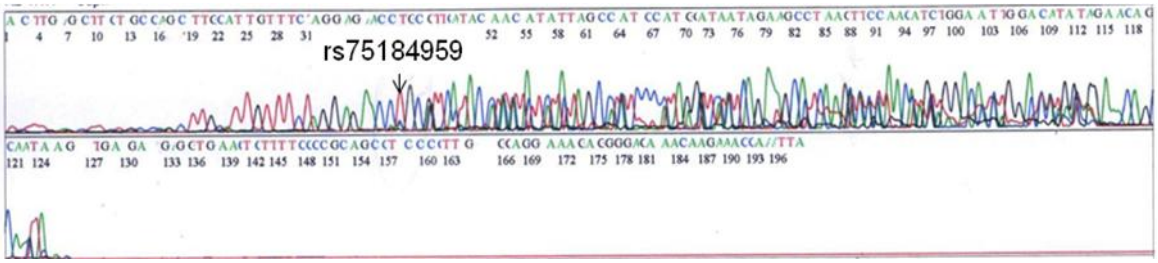

Male partner of couple 33

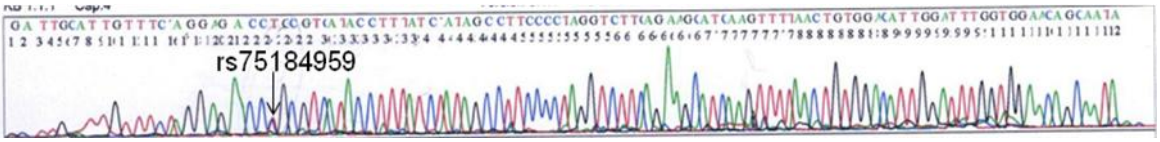

Female partner of couple 38

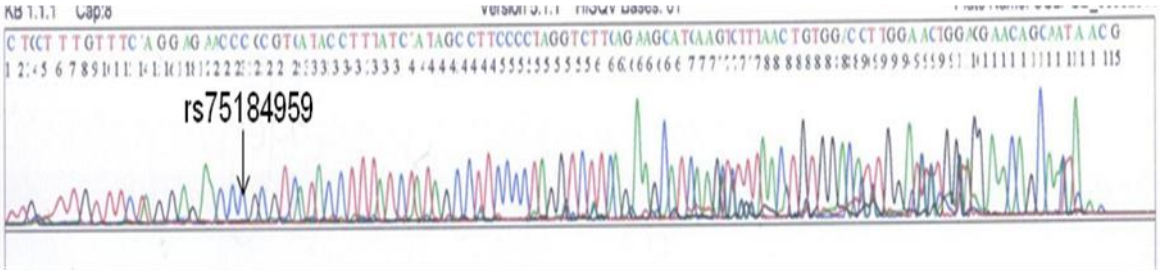

Male partner of couple 38

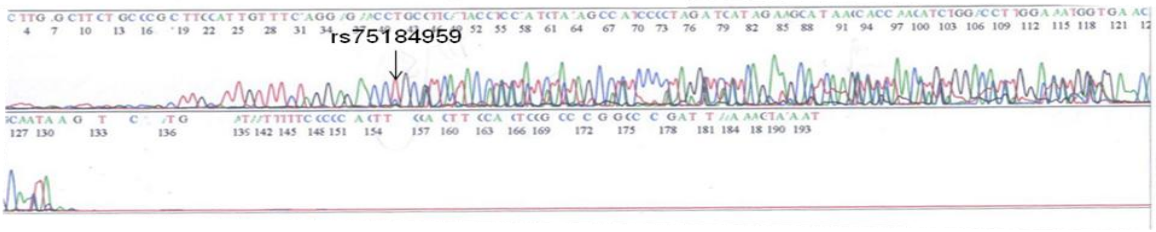

Sequencing panels for *H19*

Female partner of couple 29

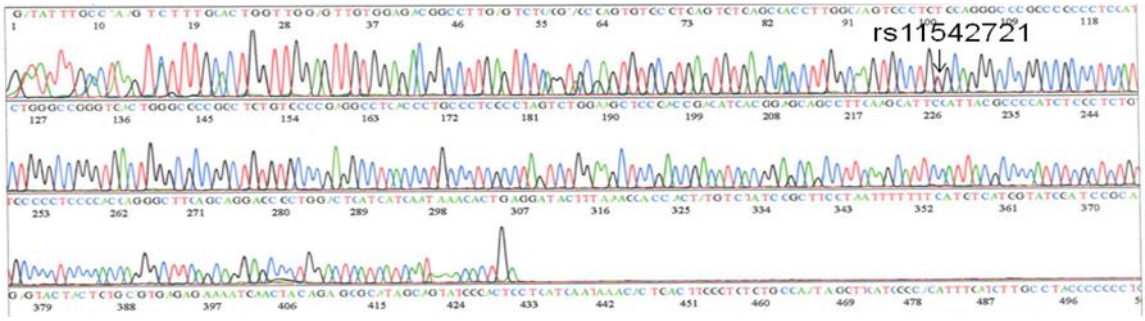

Male partner of couple 29

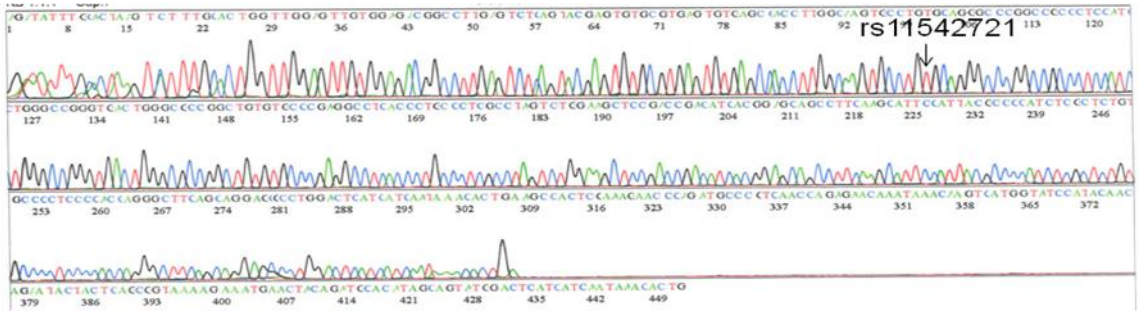

Female partner of couple 30

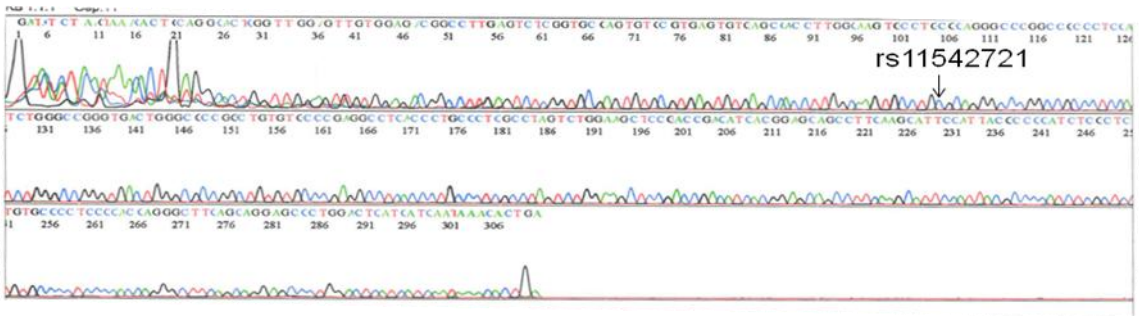

Male partner of couple 30

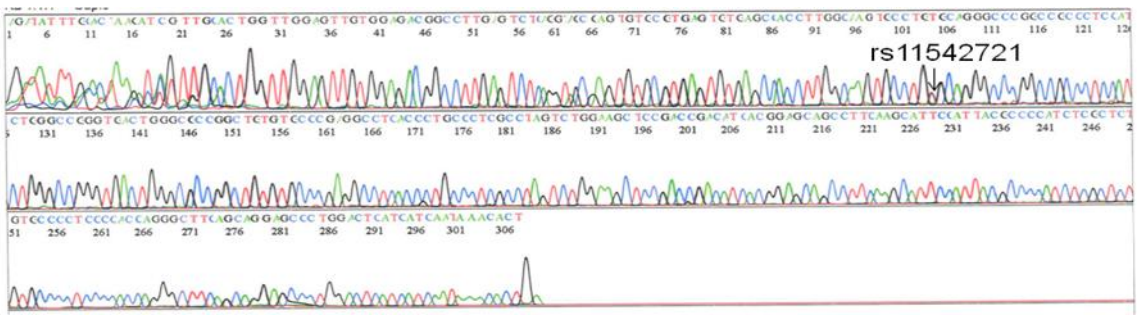

Female partner of couple 33

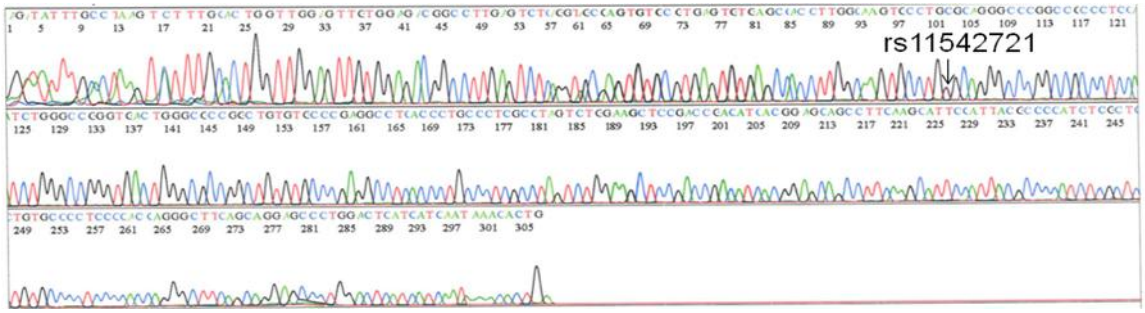

Male partner of couple 30

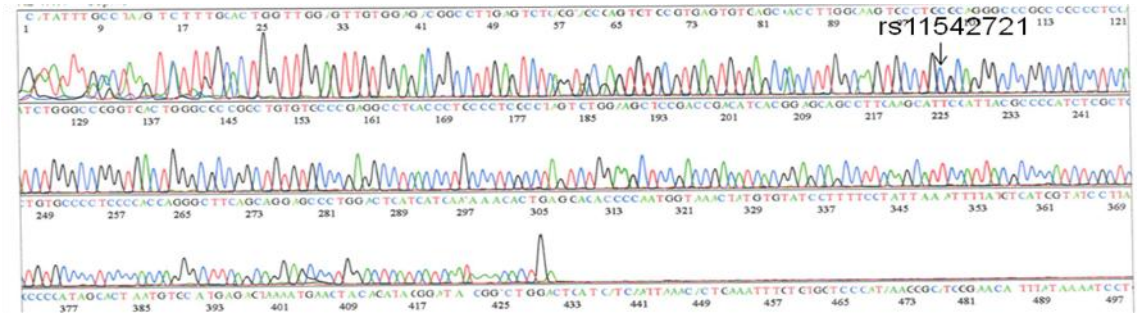

Sequencing panels for *BRCA1*

Female partner of couple 29

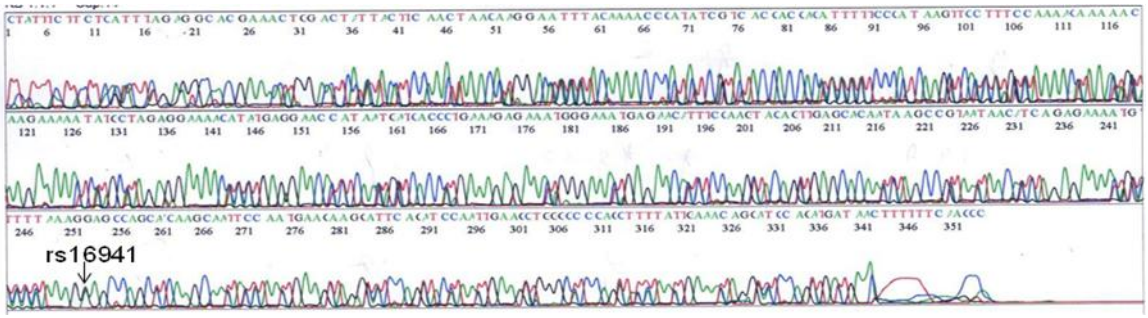

Male partner of couple 29

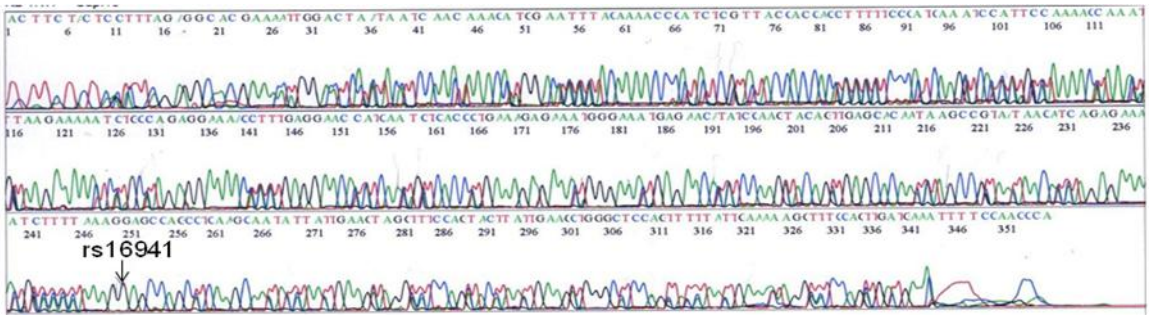

Female partner of couple 29

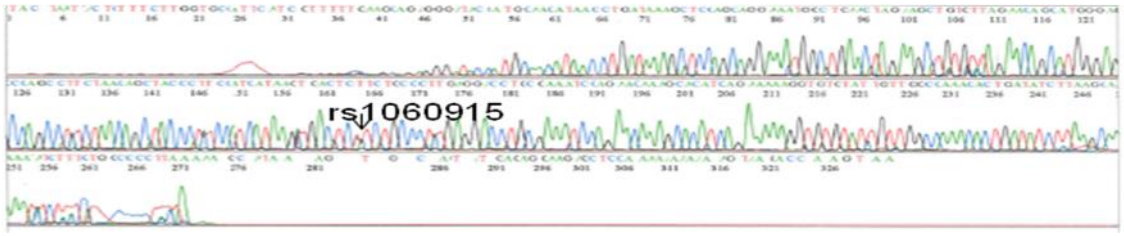

Male partner of couple 29

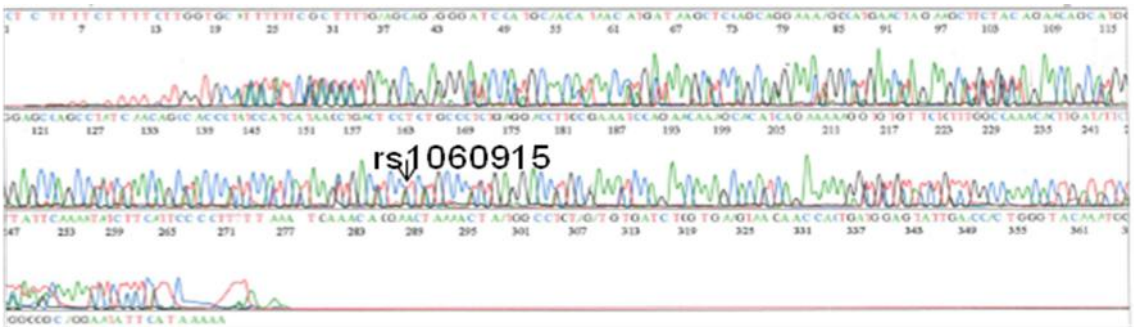

Female partner of couple 30

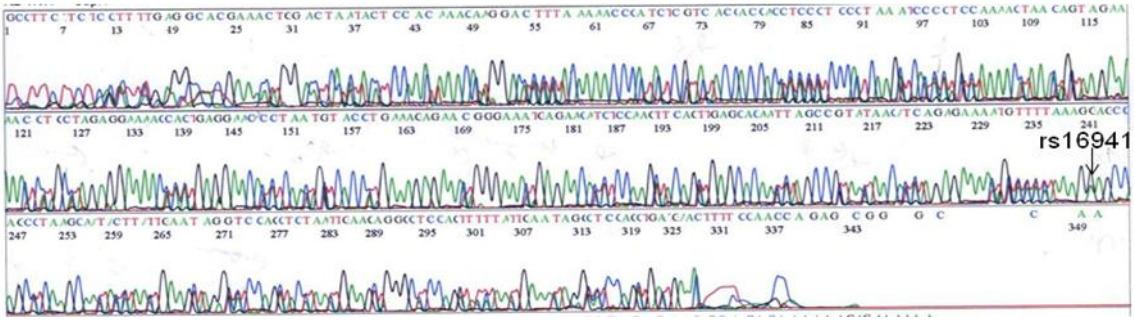

Male partner of couple 30

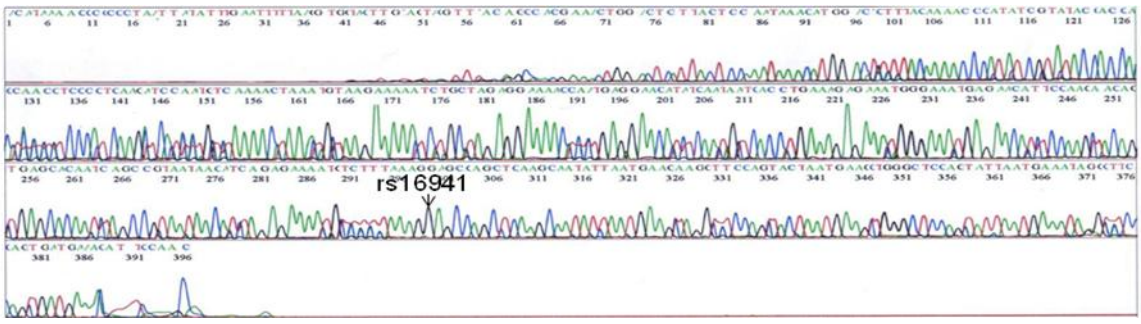

Female partner of couple 32

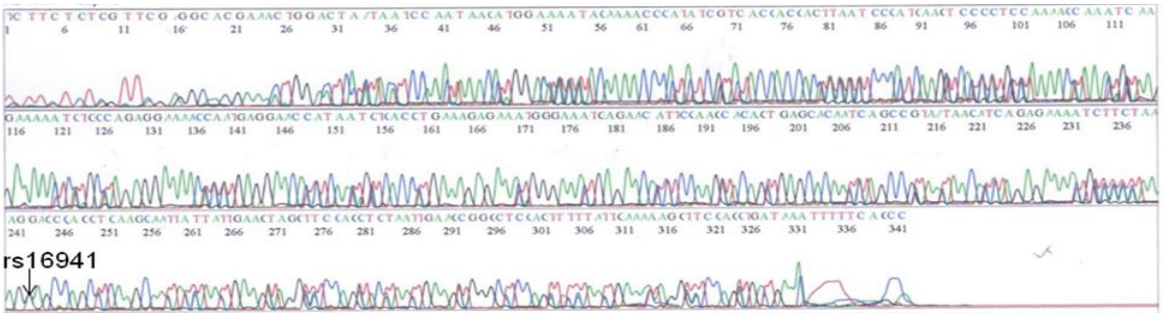

Male partner of couple 32

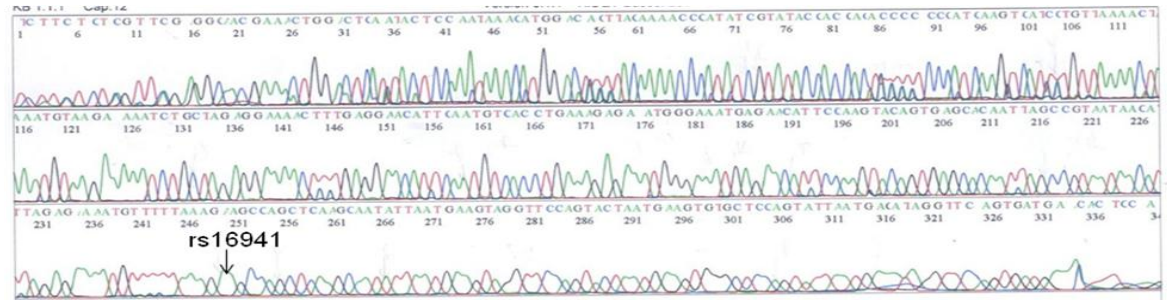

Female partner of couple 32

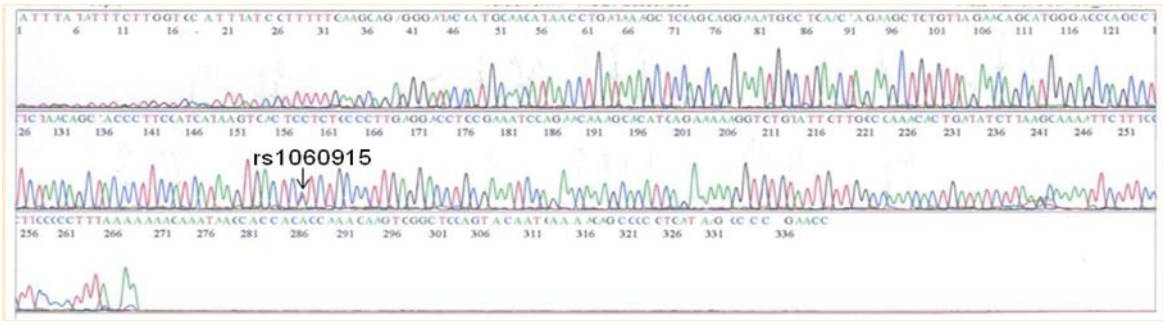

Male partner of couple 32

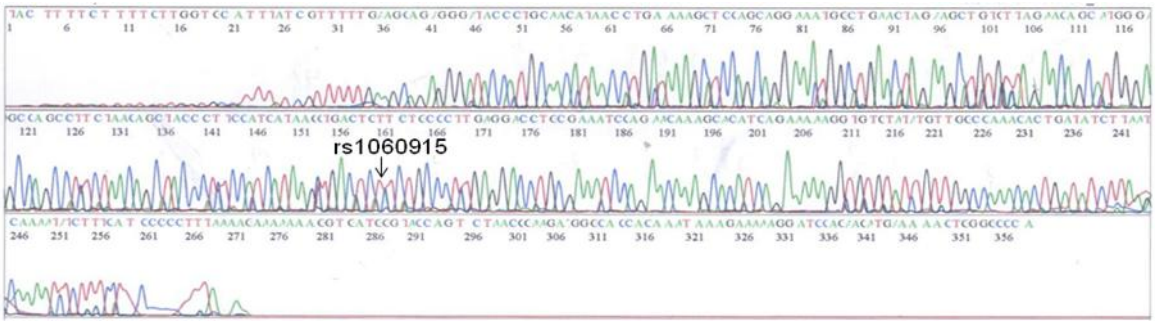

Female partner of couple 33

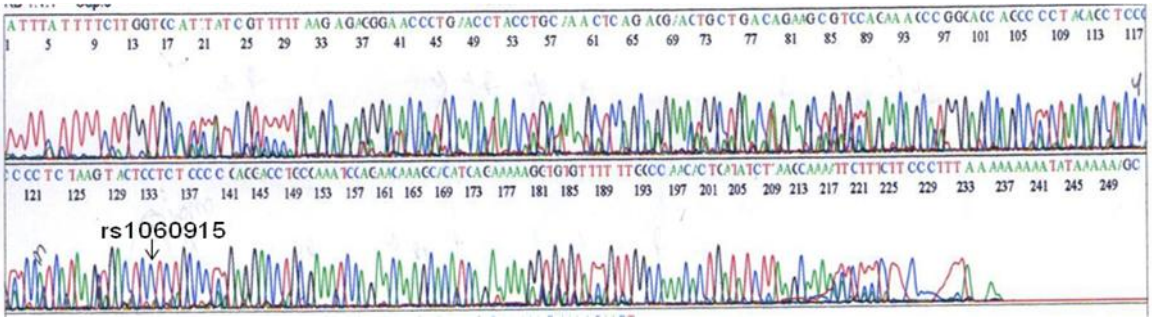

Male partner of couple 33

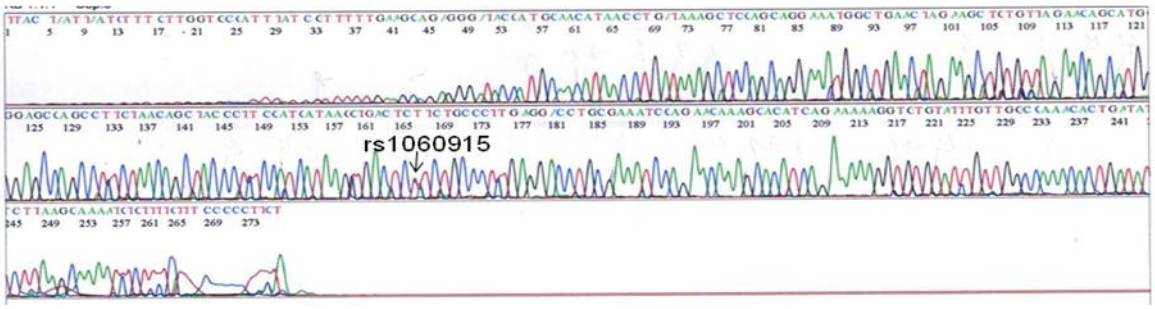

Female partner of couple 38

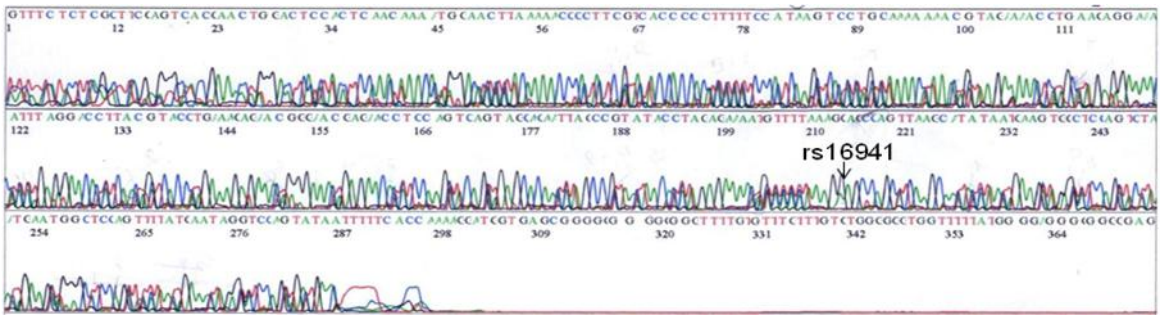

Male partner of couple 38

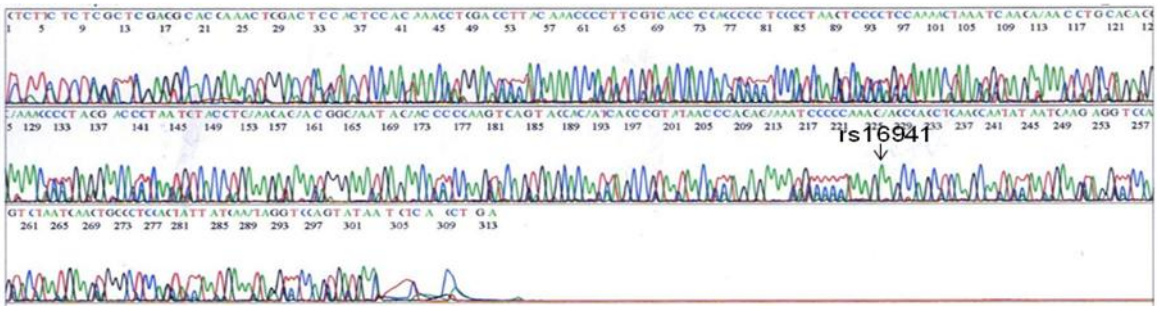

Female partner of couple 38

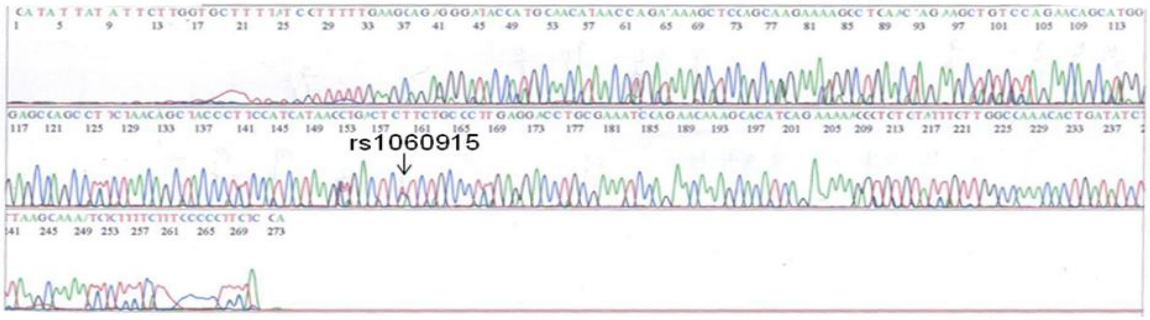

Male partner of couple 38

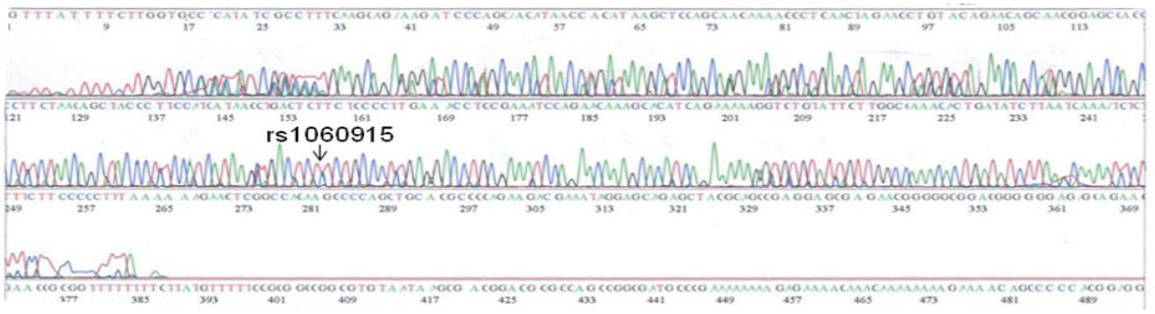

7.3.1.2 Quality and concentration of RNA and DNA extracted from human preimplantation embryos

RNA and DNA from human blastocysts were assessed using the Agilent 2100 Bioanalyzer Pico chip electrophoresis and NanoDrop technology, respectively. Sample IDs, RIN value, RNA and DNA concentrations for a) cleavage, b) morula and c) blastocyst stage embryos are shown in this table. N/A (non-applicable) indicates that this sample was not analysed for the particular subject.

a) Cleavage stage embryos

Sample ID	RIN	RNA concentration (pg/µl)	DNA concentration (ng/µl)
3	1	5460	5.5
16	N/A	213	3.2
17	N/A	221	4.5
20	2	116	7
23	N/A	422	N/A
24	N/A	N/A	3
29	1	88	1.5
32	N/A	N/A	2.3
35	6	60	22.8
36	1	55	16.7
37	N/A	N/A	2.5
38	N/A	355	50.6
39	1	66	11.7
40	2	34	12.2
43	N/A	268	0.6
44	1	29	N/A
44	8	184	N/A
45	1	61	1.7
46	N/A	N/A	2.4
48	N/A	684	N/A
55	9	291	1
57	N/A	N/A	0.6
60	N/A	N/A	2.2
61	N/A	N/A	3.4
64	N/A	167	5.8
83	N/A	451	N/A
88	2	3268	10.8
89	N/A	N/A	2.9
90	3	4818	16.9

b) Morula stage embryos

Sample ID	RIN	RNA concentration (pg/µl)	DNA concentration (ng/µl)
4	2	7232	17.9
7	N/A	369	16.1
8	5	6402	3.6
9	N/A	393	29.8
10	7	7900	38.8
11	5	19284	16.6
12	7	6400	2.4
13	4	5813	1.3
14	N/A	444	4.1
15	N/A	237	3.1
25	N/A	N/A	4.5
26	2	162	1
28	N/A	N/A	0.4
30	1	307	2.1
31	N/A	N/A	4.1
33	1	257	3.9
34	1	589	6.1
41	4	94	N/A
42	N/A	21449	N/A
47	5	2430	N/A
49	N/A	1011	0.6
50	N/A	N/A	1.9
51	N/A	277	1.4
53	3	1513	0.7
54	N/A	N/A	0.2
56	N/A	464	0.2
58	7	111	2.2
59	6	161	6.9
63	N/A	N/A	13.7
71	N/A	200	3.1
73	7	33479	5.4
79	8	449	4.2
80	8	280	10.7
81	N/A	75	4.6
82	N/A	479	27
91	2	31.3	6
92	3	254	2.5
94	N/A	393	3.8
95	N/A	268	2.6

c) Blastocyst stage embryos

Sample ID	RIN	RNA concentration (pg/µl)	DNA concentration (ng/µl)
1	6.9	12712	2.2
2	7.8	7382	12.3
19	8.4	8511	3
52	N/A	48	21.6
62	9.5	654	7.9
65	8.5	880	2.3
66	7.4	646	11.4
67	9.1	272	3.6
68	6.7	329	0.1
69	8.1	852	4
72	7.3	471	5.4
74	7.6	184	18.1
75	8.5	513	0.9
76	8.5	295	17.7
77	4.6	223	10.1
78	9.3	291	12.4
84	2.6	65	10.7
85	2.6	245	35.4
86	N/A	453	13.5
93	4.3	239	4.1

7.3.1.3 Assay sensitivity by real time PCR

Quantification for four genes analysed by real time PCR (HRM) Patient, embryo ID with Cq values are listed.

a) Cq values for *ACTB*

Patient ID	Embryo ID	Cq for *ACTB*
32	8	35
	10	38
	11	35
	12	35
	13	38
	14	35
35	51	33
36	58	34
	61	33

b) Cq values for *SNRPN*

Patient ID	Embryo ID	Cq for *SNRPN*
29	1	34
30	2	36
	3	33
	4	35
33	19	32
	20	34
	24	35
	26	36
	28	33
37	62	32
38	66	32
	67	32
	68	33
	69	33
	70	31
	71	35
41	88	34
	89	34
	90	38
42	92	37
	93	34

c) Cq values for *H19*

Patient ID	Embryo ID	Cq for *H19*
33	19	38
	21	42
34	29	44
	30	38
	33	36
	36	35
	39	35
	43	53
39	74	NR
	77	42
	78	45
	79	38
	80	41
	82	NR
	83	42

d) Cq values for *BRCA1*

Patient ID	Embryo ID	Cq for *BRCA1*	
		***BRCA* rs16941**	***BRCA* rs1060915**
29	1	37	37
30	2	37	N/A
	3	N/A	36
31	6	N/A	32
32	7	35	35
	8	N/A	38
	9	33	32
	10	N/A	35
	11	35	35
	12	35	36
	13	34	N/A
	14	N/A	36
	15	36	36
	16	N/A	36
33	19	38	33
	20	N/A	NR
	22	36	N/A
	23	37	35
	24	N/A	35
	25	36	35
	26	36	35
	28	34	N/A
34	29	37	N/A
	30	N/A	38
	31	37	N/A
	32	35	N/A
	33	35	39
	34	39	N/A
	35	N/A	35
	34	34	N/A

Patient ID	Embryo ID	Cq for *BRCA*	
		***BRCA* rs16941**	***BRCA* rs1060915**
34	37	N/A	35
	38	N/A	36
	39	N/A	37
	41	35	36
	44	33	N/A
	45	36	37
	46	33	34
35	47	N/A	32
	48	N/A	33
	49	N/A	35
	51	N/A	34
	53	N/A	36
38	65	37	N/A
	66	32	32
	67	33	32
	68	36	N/A
	69	35	33
	70	N/A	37
	71	34	35
	72	36	34
39	74	N/A	34
	76	N/A	32
	77	33	35
	78	32	33
	79	31	31
	80	32	34
	83	32	32
40	84	N/A	37
	85	N/A	36
	86	36	36

7.3.1.4 SNaPshot assay sensitivity for differential expression of parental genes

7.3.1.4.1 Haplotype analysis: Allele sizes for different STR markers identified for the all the couples.

a) Allele sizes for STR markers for chromosomes 7, 11 and 15 identified for the all the couples.

Family ID/ marker		D7S486	D7S2420	D7S692	D7S2459	D11S1338	D11D1970	D11S262	D11S4891	D11S1997	D11S2362	D11S1303	D11S4147	D11S1763	D11S1871	D15S94	D15S123	D15S992	D15S978	D15S1025	D15S978	D15S1024
29	Female	137	181/185	242/248	246/250	219/227	194	158	167	198/202	158	143	218/224	236	238	193/199	147/160	225	157/174	209	N/A	N/A
	Male	137	179/187	244/248	248/250	225/227	194/198	NR	167	193/202	158/161	131/141	224	236	237	197/201	158/160	213	157	203	N/A	N/A
30	Female	N/A				225/227	194	158	N/A	N/A	N/A	N/A	N/A	N/A	N/A	198/201	149/160	223/229	155/168	209	N/A	N/A
	Male					219/225	NR	158	N/A	N/A	N/A	N/A	N/A	N/A	N/A	NR	152/154	211/223	153/154	203/209	N/A	N/A
31	Female	N/A				N/A										N/A						
	Male																					
32	Female	137/139	178/183	248	242/248	N/A										N/A						
	Male	137	183/189	242/248	240/246																	
33	Female	N/A				215/225	185/194	158/161	167	198/202	N/A	N/A	N/A	N/A	N/A	201	158	222/224	157	209	156/157	117
	Male					225	194	155/158	167	193/223	N/A	N/A	N/A	N/A	N/A	201	152/158	212/222	155/157	209	155/157	117
34	Female	N/A				219/225	185/194	158	163/165	197	158	_	220/228	236	240	N/A						
	Male					227	NR	158/167	163	167/206	158/167	131/139	209/220	235	236							
35	Female	139/143	185/189	242/248	246/248	N/A										N/A						
	Male	130/137	183/187	244	242																	
36	Female	135/138	183/189	242	244/250	N/A										201	149/151	211/223	_	209	N/A	N/A
	Male	137/143	185/191	242/248	248/250											201/203	153/160	214	159/172	203	N/A	N/A
37	Female	135/138	183/189	242	244/250	N/A										191/201	152/160	222/223	155/157	201/209	155/157	110/118
	Male	137/143	185/191	242/248	248/250											192/199	152/158	211/225	155/157	203/209	155/157	112/118
38	Female	N/A				N/A										201/203	154/160	219/221	157/172	201/209	157/172	110/117
	Male															293/201	154	219/221	168/172	209/211	168/172	117/119
39	Female	N/A				219/225	185/194	158/161	163/165	193/202	158/167	143	218/224	N/A	N/A	**N/A**						
	Male					219/225	NR	154/158	165/166	201	158/167	148	220/222	N/A	N/A							
40	Female	N/A				221/227	187/194	158/161	165/167	198	158/161	140	220/228	N/A	N/A	**N/A**						
	Male					225/227	NR	153/161	166	198/202	155/161	143/148	218/224	N/A	N/A							
41	Female	N/A				N/A										**N/A**						
	Male																					
42	Female	N/A				N/A										199/201	149/160	220/224	159/168	203/209	N/A	N/A
	Male															201	152/163	226/227	151/155	209	N/A	N/A
Negative		Clear				Clear										Clear						

b) Allele sizes for different STR markers of chromosome 17 identified for the all the couples.

Family ID/ marker name		D17S250	D17S1307	D17S1323	D17S579	D17S1327	D17S261	D17S122	D17S1802	D17S1789	D17S1356	D17S839	D17S841	D17S1166	D17S1294	D17S2229	D17S1793	D17S1353
30	**Female**	152/157	_	167/173	239/251	111/142	N/A	N/A	N/A	N/A	N/A	N/A	N/A	N/A	N/A	N/A	N/A	N/A
	Male	NR	208	175	249/251	140/142	N/A	N/A	N/A	N/A	N/A	N/A	N/A	N/A	N/A	N/A	N/A	N/A
31	**Female**	NR	204/212	162/176	251	111/140	180	152/153	N/A	N/A	N/A	N/A	N/A	N/A	N/A	N/A	N/A	N/A
	Male	NR	204/208	173	239/249	140	180	150/152	N/A	N/A	N/A	N/A	N/A	N/A	N/A	N/A	N/A	N/A
32	**Female**	152/165	208	167/173	239/255	111/140	N/A	N/A	N/A	N/A	N/A	N/A	N/A	N/A	N/A	N/A	N/A	N/A
	Male	140/157	208	167	249/253	111	N/A	N/A	N/A	N/A	N/A	N/A	N/A	N/A	N/A	N/A	N/A	N/A
33	**Female**	152/161	208	167	251/253	106/111	N/A	N/A	N/A	N/A	N/A	N/A	N/A	N/A	N/A	N/A	N/A	N/A
	Male	150/152	200/208	162/173	243/256	111/136	N/A	N/A	N/A	N/A	N/A	N/A	N/A	N/A	N/A	N/A	N/A	N/A
34	**Female**	150/152	204/208	166/168	236/252	136/151	178/180	151/153	N/A	N/A	N/A	N/A	N/A	N/A	N/A	N/A	N/A	N/A
	Male	152	204/208	170/172	249	111*149	180	153	N/A	N/A	N/A	N/A	N/A	N/A	N/A	N/A	N/A	N/A
35	**Female**	152/157	208	166/173	236/251	111/140	180/182	152	195	192/216	198	139	260/265	189/191	252	253/264	239	165/175
	Male	152/161	208	162/166	251	112	180	145/155	195	194	198	136/139	260/267	189/191	252	253/262	239/240	179/183
38	**Female**	152	209	166/175	243/251	111/151	178	153/156	195/197	178/194	198	136/139	267	189/191	247	250/263	239	167/177
	Male	167	201/209	_	238/243	111/149	180	153	195	188/194	194/198	136	263/256	189/194	247/251	250/263	239/243	163/179
39	**Female**	157/163	208	166	247/253	112	N/A	N/A	N/A	N/A	N/A	N/A	N/A	N/A	N/A	N/A	N/A	N/A
	Male	150/163	208	166	251/253	109/132	N/A	N/A	N/A	N/A	N/A	N/A	N/A	N/A	N/A	N/A	N/A	N/A
40	**Female**	150/152	208	166	243/249	111/134	N/A	N/A	195	178/194	198/200	136/139	265/267	189/198	247	255	235/239	167/179
	Male	157/169	204/208	_	249/255	_	N/A	N/A	195/197	194	198	136/139	263/265	193/198	247/255	_	239	163/167
Negative		Clear																

7.3.1.4.2 Aneuploidy screening by aCGH

aCGH profiles of all the embryos analysed.

Embryo numbers are shown for each panel. The x-axis represents the chromosomes and the y-axis show the threshold. Any losses or gains are labelled.

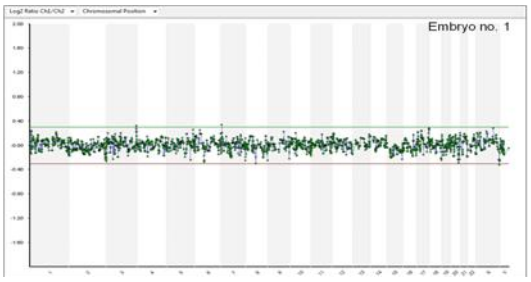

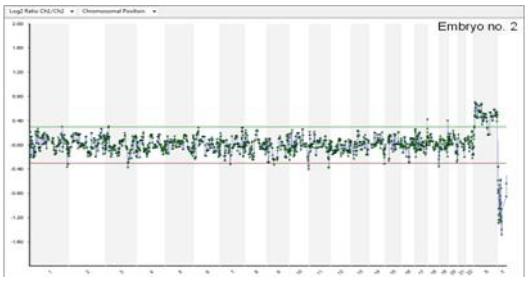

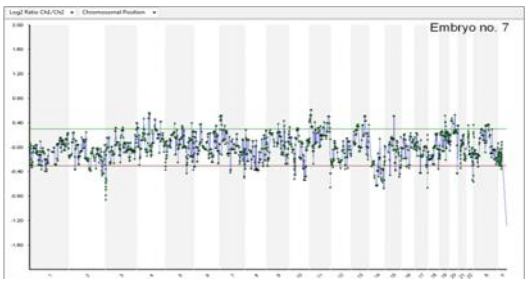

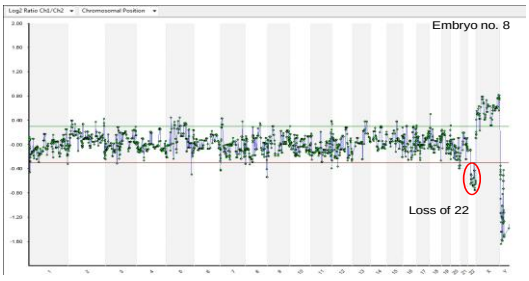

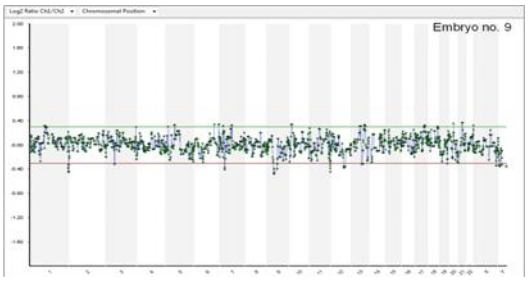

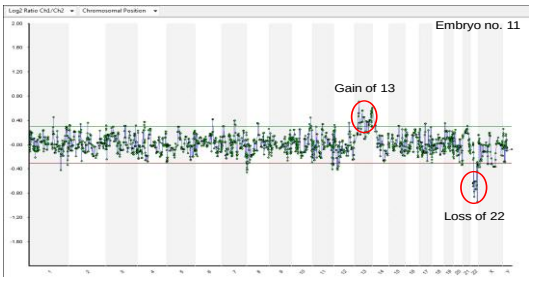

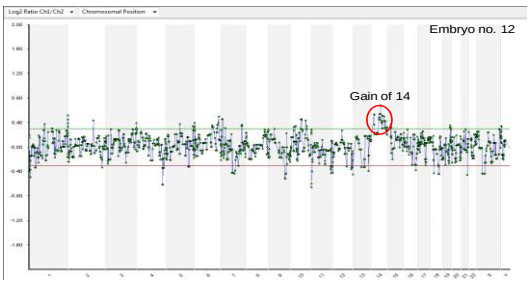

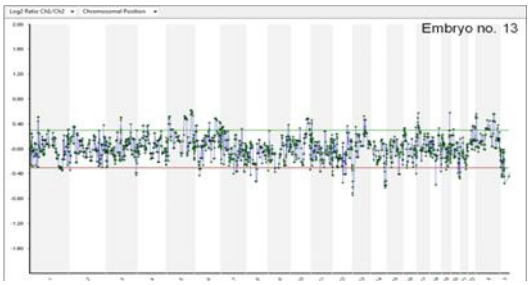

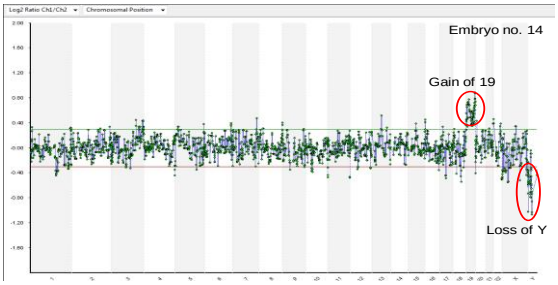
Embryo no. 14
Gain of 19
Loss of Y

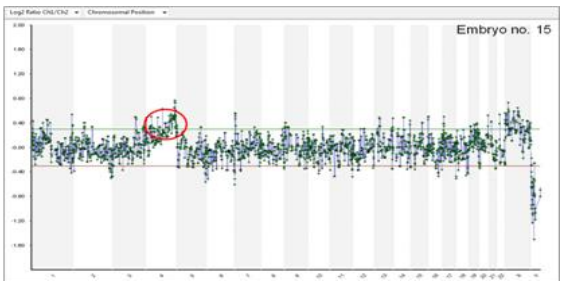
Embryo no. 15

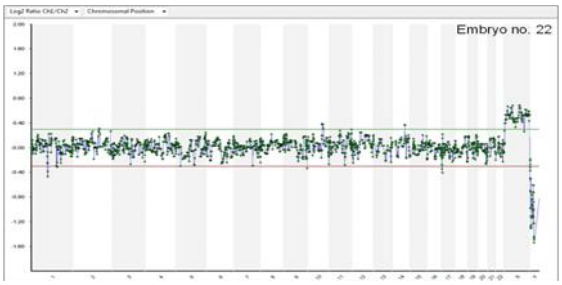
Embryo no. 22

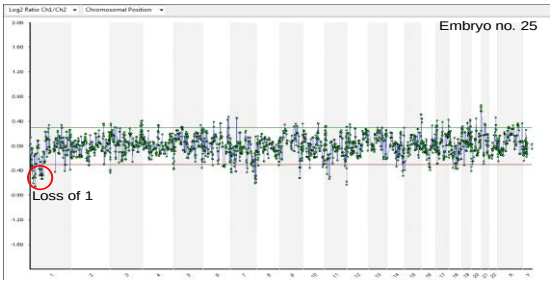
Embryo no. 25
Loss of 1

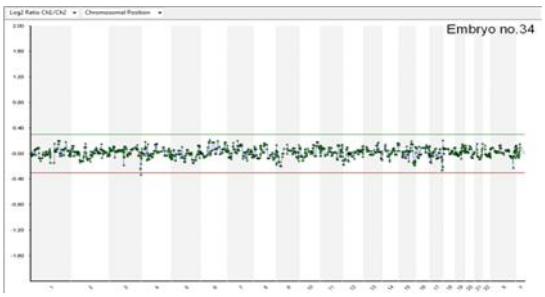
Embryo no.34

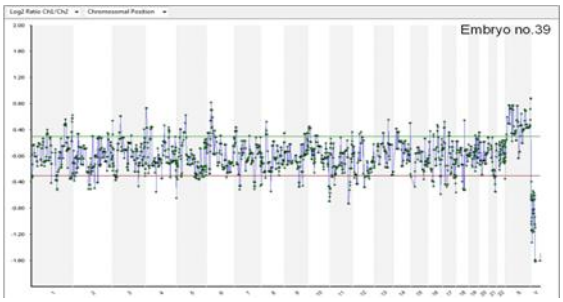
Embryo no.39

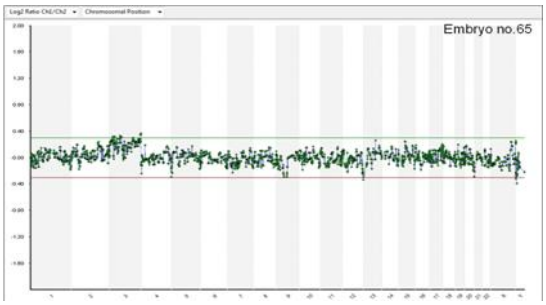
Embryo no.65

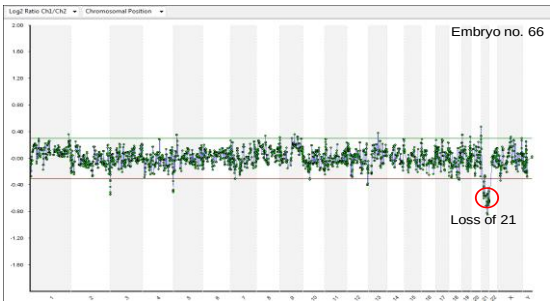
Embryo no. 66
Loss of 21

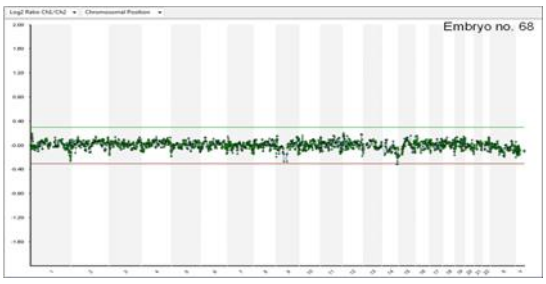
Embryo no. 68

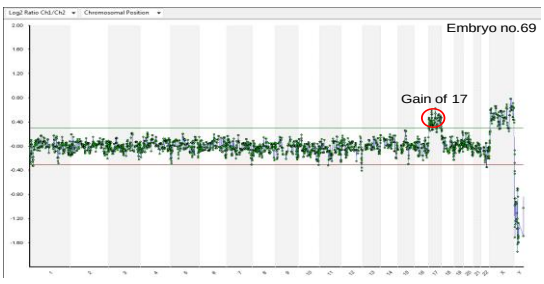
Embryo no.69
Gain of 17

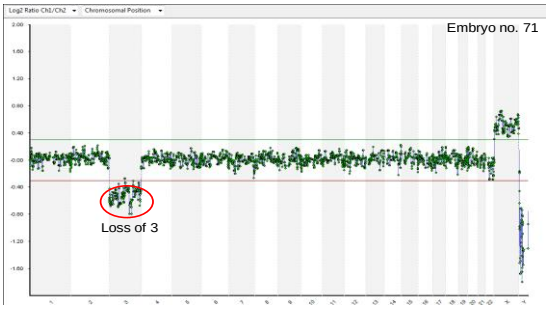
Embryo no. 71
Loss of 3

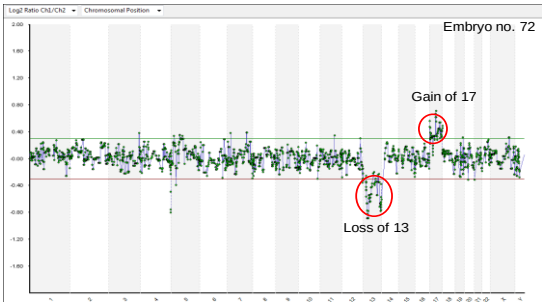
Embryo no. 72
Gain of 17
Loss of 13

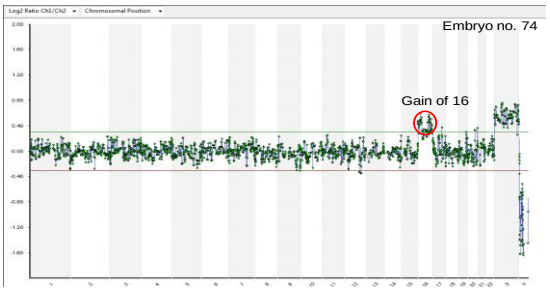
Embryo no. 74
Gain of 16

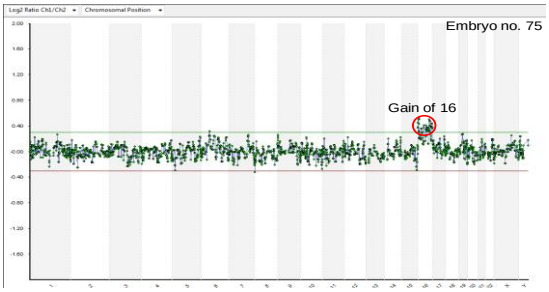
Embryo no. 75
Gain of 16

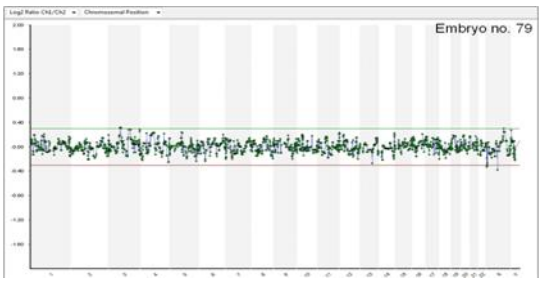
Embryo no. 79

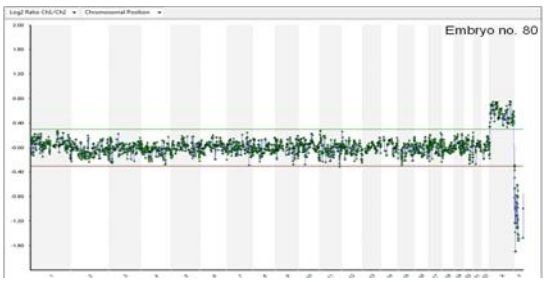
Embryo no. 80

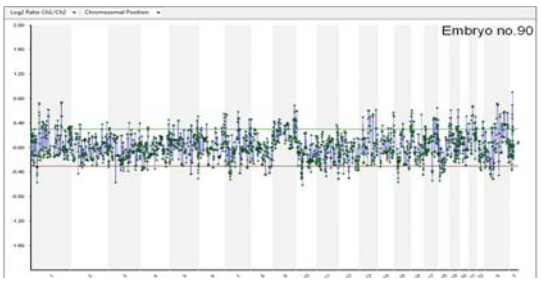
Embryo no.90

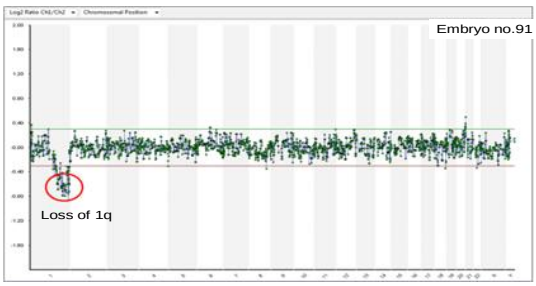
Embryo no.91
Loss of 1q

Posters and Publications from this study

Posters

- British Human Genetics Conference 2011, Warwick, UK, 17-19 September 2011

  Tulay, P., Jaroudi, S., Harper, J., & SenGupta, SB. (2011) Functional Assessment of Mismatch Repair. *Journal of Medical Genetics, 48, S51*

- 12th International Meeting on Human Genome Variation and Complex Genome Analysis, California, USA, 8-10 September 2011

  Tulay, P., SenGupta, SB. (2011) Strategy for determining the parental origin of transcripts in preimplantation embryos

- 11th International Conference on Preimplantation Genetic Diagnosis (PGDIS), Bregenz, Austria, 16-19 May 2012

  Tulay; P., Doshi; A., Serhal, P., SenGupta, SB. (2012) Determining the parental origin of transcripts in human preimplantation embryos Reproductive BioMedicine Online Volume 24, Supplement 2, Pages i-v, S27-S76

- European Society of Human Genetics Conference

  Tulay, P., Jaroudi, S., Harper, J., SenGupta, S. “DNA repair”, June 2012

- 28th Annual Meeting of European Society of Human Reproduction and Embryology (ESHRE)
  P. Tulay., R.P. Naja, O. Cascales-Roman, S. Cawood, A. Doshi, P. Serhal, S.B. SenGupta (2012) Investigation of microRNA expression with DNA repair in human oocytes and preimplantation embryos. P-459.

Publications

- **Tulay; P**., Doshi; A., Serhal, P., SenGupta, SB. (2013) Investigation of gene expression and embryo development. In process of submission.

- **Tulay; P**., Naja; RP., Doshi; A., Serhal, P., SenGupta, SB. (2013) Investigation of miRNA expression with DNA repair in human oocytes and preimplantation embryos. In preparation.

- **Tulay; P**., SenGupta, SB. (2013) MicroRNA expression and miRNA association with DNA repair in human preimplantation embryos final (Review). In process of submission.
- **Tulay; P.**, Jaroudi; S., Doshi; A., SenGupta, SB. (2013) Functional Assessment of Mismatch Repair. In preparation.